NUREG/CR-6202
IPSN 94-03
SAND 94-0485

Long-Term Aging and Loss-of-Coolant Accident (LOCA) Testing of Electrical Cables

U.S./French Cooperative Research Program

Prepared by
C. F. Nelson, SNL
G. Gauthier, CEA/IPSN
F. Carlin, M. Attal, G. Gaussens, P. Le Tutour, CEA/ORIS/CIS bio international
C. Morin, CEA/DRE/SRO

Sandia National Laboratories

Institute of Nuclear Safety and Protection (IPSN)
Commissariat à l'Energie Atomique

Prepared for
U.S. Nuclear Regulatory Commission

AVAILABILITY NOTICE

Availability of Reference Materials Cited in NRC Publications

Most documents cited in NRC publications will be available from one of the following sources:

1. The NRC Public Document Room, 2120 L Street, NW., Lower Level, Washington, DC 20555-0001

2. The Superintendent of Documents, U.S. Government Printing Office, P. O. Box 37082, Washington, DC 20402-9328

3. The National Technical Information Service, Springfield, VA 22161-0002

Although the listing that follows represents the majority of documents cited in NRC publications, it is not intended to be exhaustive.

Referenced documents available for inspection and copying for a fee from the NRC Public Document Room include NRC correspondence and internal NRC memoranda; NRC bulletins, circulars, information notices, inspection and investigation notices; licensee event reports; vendor reports and correspondence; Commission papers; and applicant and licensee documents and correspondence.

The following documents in the NUREG series are available for purchase from the Government Printing Office: formal NRC staff and contractor reports, NRC-sponsored conference proceedings, international agreement reports, grantee reports, and NRC booklets and brochures. Also available are regulatory guides, NRC regulations in the *Code of Federal Regulations,* and *Nuclear Regulatory Commission Issuances.*

Documents available from the National Technical Information Service include NUREG-series reports and technical reports prepared by other Federal agencies and reports prepared by the Atomic Energy Commission, forerunner agency to the Nuclear Regulatory Commission.

Documents available from public and special technical libraries include all open literature items, such as books, journal articles, and transactions. *Federal Register* notices, Federal and State legislation, and congressional reports can usually be obtained from these libraries.

Documents such as theses, dissertations, foreign reports and translations, and non-NRC conference proceedings are available for purchase from the organization sponsoring the publication cited.

Single copies of NRC draft reports are available free, to the extent of supply, upon written request to the Office of Administration, Distribution and Mail Services Section, U.S. Nuclear Regulatory Commission, Washington, DC 20555-0001.

Copies of industry codes and standards used in a substantive manner in the NRC regulatory process are maintained at the NRC Library, Two White Flint North, 11545 Rockville Pike, Rockville, MD 20852-2738, for use by the public. Codes and standards are usually copyrighted and may be purchased from the originating organization or, if they are American National Standards, from the American National Standards Institute, 1430 Broadway, New York, NY 10018-3308.

NUREG/CR–6202
IPSN 94–03
SAND 94–0485

Long-Term Aging and Loss-of-Coolant Accident (LOCA) Testing of Electrical Cables

U.S./French Cooperative Research Program

Manuscript Completed: July 1996
Date Published: October 1996

Prepared by
C. F. Nelson, SNL
G. Gauthier, CEA/IPSN
F. Carlin, M. Attal, G. Gaussens, P. Le Tutour, CEA/ORIS/CIS bio international
C. Morin, CEA/DRE/SRO

Sandia National Laboratories
Albuquerque, NM 87185–0742

Department of Safety Evaluation
Institute of Nuclear Safety and Protection (IPSN)
Commissariat à l'Energie Atomique
Fontenay aux Roses, FRANCE

S. Aggarwal, NRC Program Manager

Prepared for
Division of Engineering Technology
Office of Nuclear Regulatory Research
U.S. Nuclear Regulatory Commission
Washington, DC 20555–0001
NRC Job Code A1841

DISCLAIMER

Abstract

Experiments were performed to assess the aging degradation and loss-of-coolant accident (LOCA) behavior of electrical cables subjected to long-term aging exposures. Four different cable types were tested in both the U.S. and France:

1. U.S. 2 conductor with ethylene propylene rubber (EPR) insulation and a Hypalon jacket.
2. U.S. 3 conductor with cross-linked polyethylene (XLPE) insulation and a Hypalon jacket.
3. French 3 conductor with EPR insulation and a Hypalon jacket.
4. French coaxial with polyethylene (PE) insulation and a PE jacket.

The data represent up to 5 years of simultaneous aging where the cables were exposed to identical aging radiation doses at either 40°C or 70°C; however, the dose rate used for the aging irradiation was varied over a wide range (2–100 Gy/hr). Aging was followed by exposure to simulated French LOCA conditions. Several mechanical, electrical, and physical-chemical condition monitoring techniques were used to investigate the degradation behavior of the cables. All the cables, except for the French PE cable, performed acceptably during the aging and LOCA simulations. In general, cable degradation at a given dose was highest for the lowest dose rate, and the amount of degradation decreased as the dose rate was increased.

Table of Contents

List of Figures

List of Tables

Executive Summary

This report presents the results obtained during a cooperative research program between the French Commissariat à l'Energie Atomique (CEA) and the United States Nuclear Regulatory Commission (NRC) regarding the aging degradation and loss-of-coolant accident (LOCA) behavior of electrical cables and cable materials subjected to long-term aging exposures. The objective was to investigate the effect of radiation dose rate on aging degradation and LOCA survivability while also investigating the effect of temperature on the aging and whether there is synergy between the radiation and thermal aging exposures.

This program was originally designed to test control and instrumentation cables that provide safety functions under both normal and LOCA nuclear power plant environment conditions. However, the French coaxial cable was added to the program even though it is not required to remain operable under accident conditions in French nuclear power plants. Both cut and complete (electrically energized) cable specimens were tested. The four different cable types tested in the U.S. and France were:

1. U.S. 2 conductor with ethylene propylene rubber (EPR) insulation and a Hypalon jacket.
2. U.S. 3 conductor with cross-linked polyethylene (XLPE) insulation and a Hypalon jacket.
3. French 3 conductor with EPR insulation and a Hypalon jacket.
4. French coaxial with polyethylene (PE) insulation and a PE jacket.

The U.S. and French test programs exposed the cables to the same aging radiation doses and similar simulated LOCA conditions; however, the dose rate used for the aging irradiation varied over a wide range for the two test programs. The radiation aging was accompanied by simultaneous thermal aging at either 40°C or 70°C. The aging dose rates range from those of a "hot" location in a nuclear reactor containment up to those used in previous U.S. cable qualification test programs. By investigating cable material behavior under aging conditions more realistic than is typically used for environmental qualification and previous test programs, the results of this cooperative program shed new light on the use of short-term, high dose rate radiation exposures to simulate the aging degradation of electrical cables caused by the long-term, low dose rate environment of a nuclear power plant.

In the French test program, the aging exposures were:

- 14 to 210 kGy (1.4–21 Mrad) at 5, 10, and 20 Gy/hr (0.5, 1, and 2 krad/hr) and 40°C and 70°C for cut cable specimens.
- 14 to 56 kGy (1.4–5.6 Mrad) at 2 Gy/hr (0.2 krad/hr) and 40°C for cut and complete cable specimens.
- 14 to 84 kGy (1.4–8.4 Mrad) at 5, 10, and 20 Gy/hr (0.5, 1, and 2 krad/hr) and 40°C and 70°C for complete cable specimens.
- Thermal-only at 70°C for 5 years.

The aging exposures for the U.S. test program were:

- 28 to 200 kGy (2.8–20 Mrad) at 100 Gy/hr (10 krad/hr) and 40°C for cut cable specimens.
- Up to 84 kGy (8.4 Mrad) at 100 Gy/hr (10 krad/hr) and 40°C for complete cable specimens.

Following the various aging exposures, the cables were subjected to similar simulated LOCA conditions in the U.S. and France consisting of an accident radiation exposure sequentially followed by an accident steam exposure. The accident irradiations were performed at dose rates of 800 and 900 Gy/hr (80 and 90 krad/hr) at 70°C to an accident dose of 600 kGy (60 Mrad). The 14-day accident steam exposure utilized a single transient with peak conditions of approximately 159°C and 600 kPa absolute. Note that the exposures generally followed French qualification procedures, which utilize a lower peak steam temperature and substantially smaller aging and accident radiation doses than those used in typical U.S. cable test or qualification programs.

Several condition monitoring techniques were used to investigate the degradation behavior of the cables. These included mechanical measurements (density, hardness, elongation at break, and tensile strength) and physical-chemical measurements (gel fraction) of the cut cable specimens. Electrical measurements (ac leakage current, insulation resistance, dielectric strength, microbreakdown, and characteristic impedance) were performed on the complete cable specimens. Elongation at break was the most effective technique for monitoring the aging degradation of the polymeric cable materials. The electrical techniques showed very little change in electrical properties with

aging. Gel fraction measurements showed that cross-linking of the three Hypalon jacket materials increased during aging and also during the LOCA simulation.

The conclusions of this cooperative program with regard to the program objectives are addressed below.

Objective: Investigate the effect of radiation dose rate on aging degradation and LOCA behavior.

- All the cables, except for the French PE cable, performed acceptably during the aging and LOCA simulations in both the U.S. and France. The French PE cable is susceptible to radiation damage and is not suitable for accident applications.
- In general, degradation *at a given dose* was highest for the lowest dose rate, and the amount of degradation decreased as the dose rate was increased. While this effect was present, but small relative to scatter in the data, for irradiation at 40°C, the 70°C data from the French test program indicate that this effect is larger at higher temperatures; however, no 100 Gy/hr data at 70°C were available to confirm this.
- The elongation at break data for the Hypalon jackets and PE insulation were well predicted by the time-temperature-dose rate methodology of Gillen and Clough.
- The effect of dose rate becomes more pronounced as the aging dose increases.
- At 40°C, the behavior of the cable irradiated at 2 Gy/hr in a research reactor was very similar to the cable irradiated at 5 Gy/hr using cobalt-60 sources.
- All cables that functioned electrically prior to the accident steam exposure remained electrically functional through the accident steam exposure. This held true even for cables that had degraded to low residual elongation prior to the steam exposure.
- The dependence of the post-LOCA measurements on aging dose confirms that pre-aging these cables affects their post-LOCA values.
- Significant degradation in cable materials was observed after aging and the 600 kGy accident irradiation. Prior to the accident steam exposure, the elongation at break (E/E_0) was in the range of 5–15% for the U.S. XLPO cable's XLPE insulation and 20–50% for the U.S. EPR cable's FR-EPDM insulation. The accident steam exposure tended to slightly improve the elongation at break for the EPR and XLPE insulation materials, while the elongation was either unchanged or decreased slightly for the Hypalon jackets.

Objective: Investigate the effect of temperature on the aging and whether there is synergy between the radiation and thermal aging exposures.

- Except for the Hypalon jackets, all insulation and jacket materials had slight degradation or none after being exposed to 5 years of thermal-only aging at 70°C. The Hypalon jackets from the U.S. EPR and U.S. XLPO cables had lost over half of their relative elongation at the end of the 5-year thermal aging period; the French EPR cable's Hypalon jacket did slightly better.
- The EPR insulations (from the U.S. EPR and French EPR cables) exhibited unusual behavior; their elongation at break data showed greater degradation at 40°C than at 70°C during 20 Gy/hr irradiation. This "inverse temperature effect" behavior has been noted by previous researchers and may be due to a transition in material structure in this temperature range.
- There appears to be synergy between radiation and thermal aging for the three Hypalon jacket materials, which all had substantially more degradation when exposed to simultaneous 70°C thermal and 5 Gy/hr radiation exposures than for the individual thermal and radiation exposures. The two EPR insulation materials exhibited no synergistic effect between radiation and thermal aging.

Acknowledgements

U.S. Author

Because my role has consisted of data analysis, compilation, and writing this report, my appreciation is extended to all who contributed to this research effort. This joint program was begun by Larry Bustard at Sandia National Laboratories and later passed on to Mark Jacobus before finally being passed on to me. Larry and Mark set up the U.S. program, defined (with the French) test conditions and the cables to be tested, and supervised the testing. The test program was actually implemented and performed by Gary Fuehrer with help from Ed Baynes, Bob Padilla, and Mike Ramirez, who all contributed to setting up and running the tests. Special thanks goes to Bill Farmer, Milt Vagins, and Satish Aggarwal of the NRC for their support and guidance throughout this program. *C.F.N.*

French Authors

The study that took place over a period of 6 years required the successive efforts of many people. We would like to thank, first and foremost, Jacques Chénion for his effective help in setting up and following the work from 1986 to 1992, as well as Yves Moyon, William Viger, and Marc Omer, who contributed at CIS bio international to the successful testing work.

We would also like to thank Michel Baugé for his valuable assistance in the design and production of Evocable.

Finally, we would like to thank, in particular, Marcel Lemeur and Jean-Yves Henry from IPSN/DES, who succeeded one another as managers of this program and who continued to provide their advice and help through to the end of this study.

Nomenclature

Acronyms	
ac	alternating current
AFNOR	Association Française de Normalisation (French standards organization)
CEA	Commissariat à l'Energie Atomique (French government-owned research organization)
CSPE	chlorosulfonated polyethylene
dc	direct current
DRE	Département des Réacteurs Expérimentaux
EMD	electrostatic microdischarge
EPR	ethylene propylene rubber
FC	French PE cable (French coaxial)
FM	French EPR cable (French multiconductor)
FR-EPDM	flame-retardant ethylene propylene diene monomer; this is a specific type of EPR
Hypalon	trademark of DuPont's CSPE formulation
IEEE	Institute of Electrical and Electronics Engineers
IPSN	Institut de Protection et de Sureté Nucléaire (Institute of Nuclear Safety and Protection, branch of the CEA)
IR	insulation resistance
LICA	Low Intensity Cobalt Array
LOCA	loss-of-coolant accident
NIST	National Institute of Standards and Technology
NRC	United States Nuclear Regulatory Commission
ORIS	Office des Rayonnements Ionisants, subsidiary of CEA
PE	polyethylene
rms	root-mean-square, abbreviation for square *root* of the *mean* of the *square*
SRO	Service du Réacteur Osiris ("Osiris" is a French research reactor)
TLD	thermoluminescent dosimeter
UE	U.S. EPR cable
UX	U.S. XLPO cable
XLPE	cross-linked polyethylene; this is a specific type of XLPO
XLPO	cross-linked polyolefin

Symbols	
E	elongation
E_0	elongation of unaged jacket or insulation
H	hardness
H_0	hardness of unaged cable
T	tensile strength
T_0	tensile strength of unaged jacket or insulation
x	horizontal distance along the long axis of the fixture used to hold the cobalt sources and the test chamber (see Figure 2.3)
y	horizontal distance parallel to the short axis of the fixture used to hold the cobalt sources and the test chamber (see Figure 2.3)
z	vertical distance from the midpoint of the cobalt sources (see Figures 2.2 and 2.3)
Z	impedance [Ω]
ρ	density
ρ_0	density of unaged jacket or insulation
σ	standard deviation

1 Introduction and Objectives

1.1 Introduction

A formal agreement for a 6-year cooperative research program between the French Commissariat à l'Energie Atomique (CEA) and the United States Nuclear Regulatory Commission (NRC) was signed in July 1988. The purpose of the program was to investigate the long-term aging behavior of electrical cables. More precisely, the program looked at the aging caused by ionizing radiation at very low dose rates, much like those found in nuclear power plant containments. Based on the results obtained during prior studies [1] [2], this program also looked at the effect of temperature on long-term, low dose rate radiation aging and especially at whether there was any synergy between the radiation exposure and thermal environment during these low dose rate exposures.

The formal agreement included three programmatic elements:

1. French and U.S. cable specimens were irradiated at the Osiris research reactor (with an average load factor of 0.6) in France for 5 years using low dose rates [approximately 2–3 Gy/hr (200–300 rad/hr)] to achieve a total radiation dose of approximately 60 kGy (6 Mrad) after the 5-year exposure. Exposures were performed on both electrically energized cables and on cut cable specimens used for mechanical and chemical measurements. Samples were retrieved periodically from the set of cut cable specimens for tensile testing. At completion of the aging exposure, the cable specimens were subjected to a simulated loss-of-coolant accident (LOCA) consisting of an accident radiation exposure followed by an accident steam exposure.
2. French and U.S. cable specimens were irradiated at CIS bio international's[1] irradiation facilities in France. The cobalt-60 irradiations were performed on electrically energized cable at 40°C and 70°C using dose rates of approximately 5, 10, and 20 Gy/hr (0.5, 1.0, and 2.0 krad/hr) to a total dose of 84 kGy (8.4 Mrad). In addition, short cable specimens (not electrically energized) were retrieved during these exposures at doses of 14, 28, 42, 56, 70, 84, 100, 150, and 210 kGy (1.4 to 21 Mrad). After completion of the aging exposures, a simulated LOCA consisting of an accident irradiation followed by an accident steam test was performed. For comparison purposes, 70°C thermal exposures (without irradiation) were also performed on the cable specimens.
3. French and U.S. cable specimens were irradiated at Sandia National Laboratories using a dose rate of 100 Gy/hr (10 krad/hr) and a temperature of 40°C. After completion of the aging irradiation, a LOCA simulation consisting of an accident irradiation followed by an accident steam exposure was performed.

The NRC-sponsored, U.S. test program was known as the U.S.-French Cooperative Research Program on Long-Term Cable Aging Degradation. The CEA-sponsored, French test program was known as the VEILLE[2] program, which is a French acronym for the long-term irradiation aging of electrical cables.

1.2 Objectives

This report presents the results obtained during the cooperative program regarding the aging degradation and LOCA behavior of electrical cables and cable materials subjected to long-term aging exposures. The objective is to investigate the effect of radiation dose rate on aging degradation and LOCA survivability while also investigating the effect of temperature on the aging and whether there is synergy between the radiation and thermal aging exposures.

The aging dose rates investigated in this report vary by almost two orders of magnitude and range from those of a "hot" location in a nuclear reactor containment up to those used in previous U.S. cable qualification test programs [3][4][5]. By investigating cable material behavior under aging conditions more realistic than is typically used for environmental qualification and previous test programs, the results of this cooperative program can shed new light on the use of short-term, high dose rate radiation exposures

[1] CIS bio international is a subsidiary of Office des Rayonnements Ionisants (ORIS), which is a subsidiary of the CEA.

[2] Vieillissement Engendré par l'Irradiation à Long terme de Liaisons Electriques (VEILLE).

to simulate the aging degradation of electrical cables caused by the long-term, low dose rate environment of a nuclear power plant.

This report is divided into three parts. The first part presents the U.S. test program, which implements the third programmatic element of the cooperative program's formal agreement. The second part presents the French test program, which implements the first and second programmatic elements of the cooperative program's formal agreement. The third and final part takes the U.S. and French test results and compares them with one another and with previously published data.

Part I
U.S. Test Program

2 U.S. Experimental Apparatus and Technique

This section describes the tested cables, and the U.S. experimental apparatus and techniques used to perform measurements on them. This information applies only to the U.S. test activities; the French test activities are described in Section 4.

2.1 Test Facilities

All environmental exposures were performed using the Low Intensity Cobalt Array (LICA) facility and the steam system, both located in the north end of Building 867 in Technical Area 1 at Sandia National Laboratories in Albuquerque, NM.

The LICA facility consists of radioactive sources and various fixtures located at the bottom of a water pool as shown in Figure 2.1; only the large chamber cobalt fixtures were used for the current test. The pool water provides radiation shielding. The LICA facility is used to perform both accident irradiation and simultaneous radiation and thermal aging of test specimens.

Radiation is produced by cobalt-60 sources supplied by Neutron Products Inc. (Dickerson, MD). There are 32 cobalt-60 sources that can be used in the large chamber fixtures. Each source is 673.1 mm (26.5 in.) long by 15.9 mm (0.625 in.) outside diameter—cobalt is contained only in the middle 609.6 mm (24 in.) of each source. The total activity of the 32 sources was approximately 51 kCi as of January 1992.

To irradiate test samples, the cobalt-60 sources were placed in one of the two large chamber fixtures sitting at the bottom of the pool. A side view of a large chamber fixture (and a test chamber) is shown in Figure 2.2, and a top view of one of the fixtures is shown in Figure 2.3 giving the configuration of the tubes in which the cobalt-60 sources were placed. The two fixtures are identical except that one has only 16 source locations around the test chamber opening instead of the 32 locations shown in Figure 2.3. The large chamber fixtures are made of aluminum and are watertight (*i.e.*, they are filled with air) to minimize the amount of shielding between the cobalt sources and the test chamber.

Detailed drawings of the type of test chamber used for this program (also see Figure 2.2) and the test fixturing are shown in Figure 2.4. All test fixtures were mounted to the head of the test chamber; there was no attachment by either the fixturing or the test specimens to the test chamber bottom. This allowed the test chamber bottom to be removed to gain access to the test specimens without disturbing them. The specimens remained in the same fixturing for all phases of the environmental exposure; the test chamber also served as a pressure vessel when connected to the steam system. This minimized the possibility of damage to the specimens when the test chamber was moved from the LICA facility to the steam system because the test specimens did not have to be removed from one test chamber and then reinstalled in another.

Cut cable specimens were placed in a basket that hung below the test chamber head. Each cut cable specimen was placed in a hole in the basket to ensure that the specimens were in known locations and well spaced.

The complete cable specimens were wrapped around a mandrel that hung below the test chamber head. The mandrel consisted of two stainless steel rings attached to one another with eight stainless steel rods. All complete test specimens were run into and then back out of the test chamber; they entered the test chamber through a penetration in the test chamber head, then were wrapped several times around the mandrel rods, and finally exited the test chamber through another penetration in the test chamber head.

The steam system is used to perform the steam exposure for LOCA simulations. This system incorporates superheaters and a large accumulator to produce the initial temperature/pressure transients required during an accident steam exposure simulation.

2.2 Tested Cables

This program was originally designed to test control and instrumentation cables that provide safety functions under both normal and LOCA nuclear power plant environment conditions. However, the French PE (coaxial) cable was added to the program even though it is not required to remain operable under accident conditions in French nuclear power plants. Four different types of cables were tested (see Table 2.1);

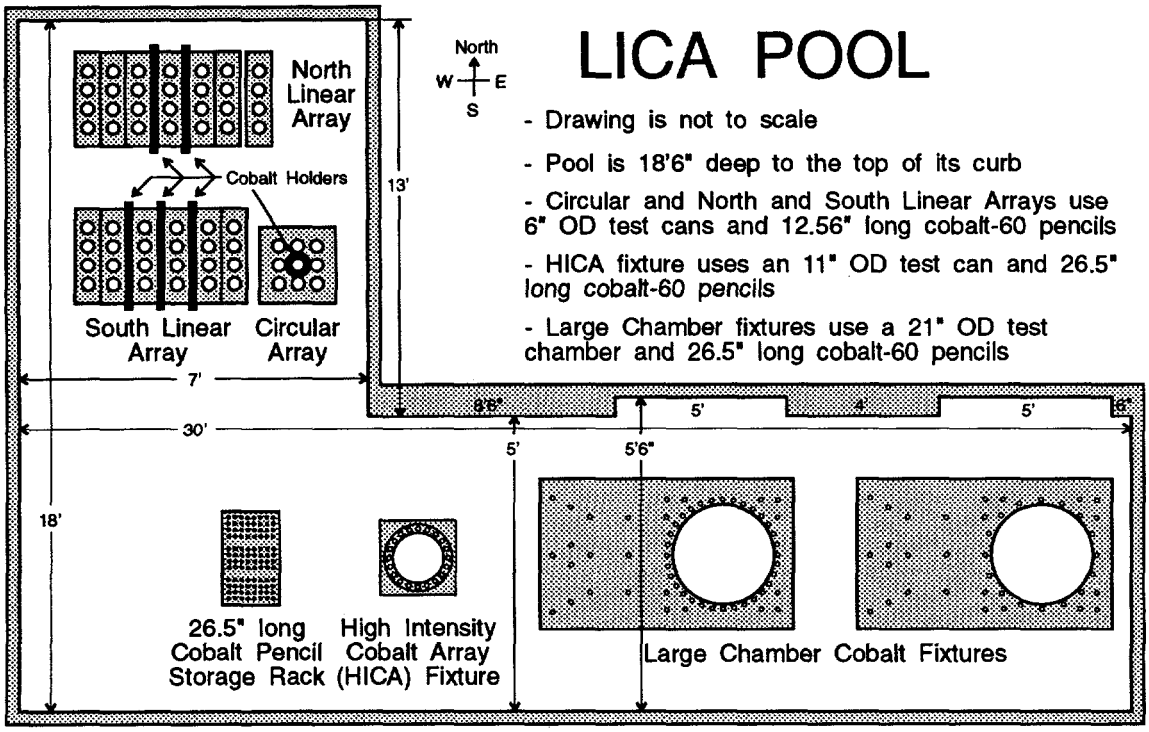

Figure 2.1: Plan view of the LICA pool and fixtures—not to scale.

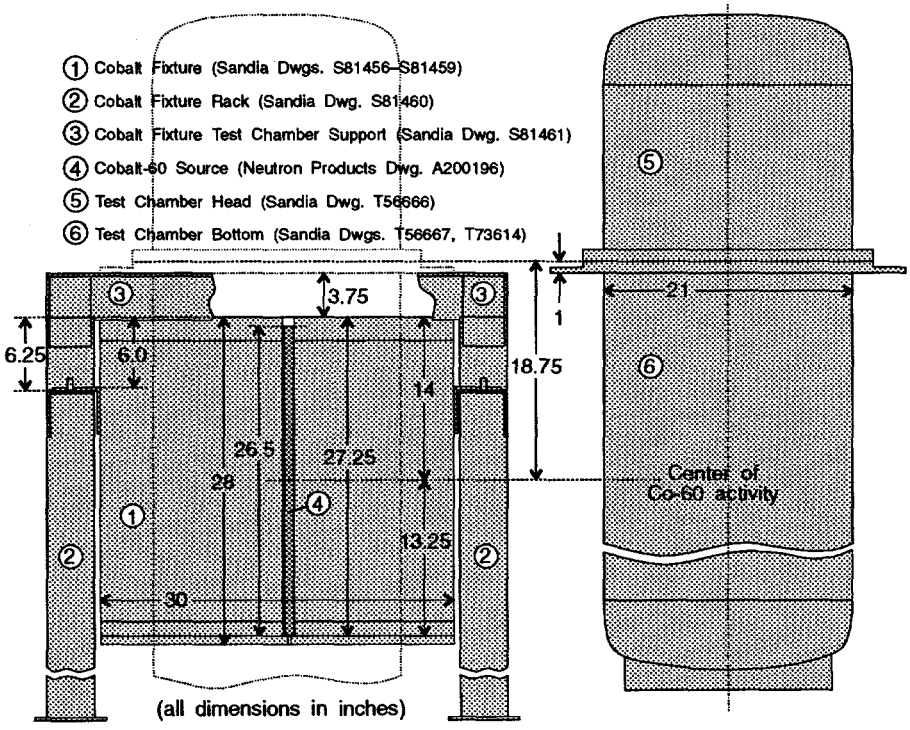

Figure 2.2: Sketch of a test chamber and large chamber cobalt fixture.

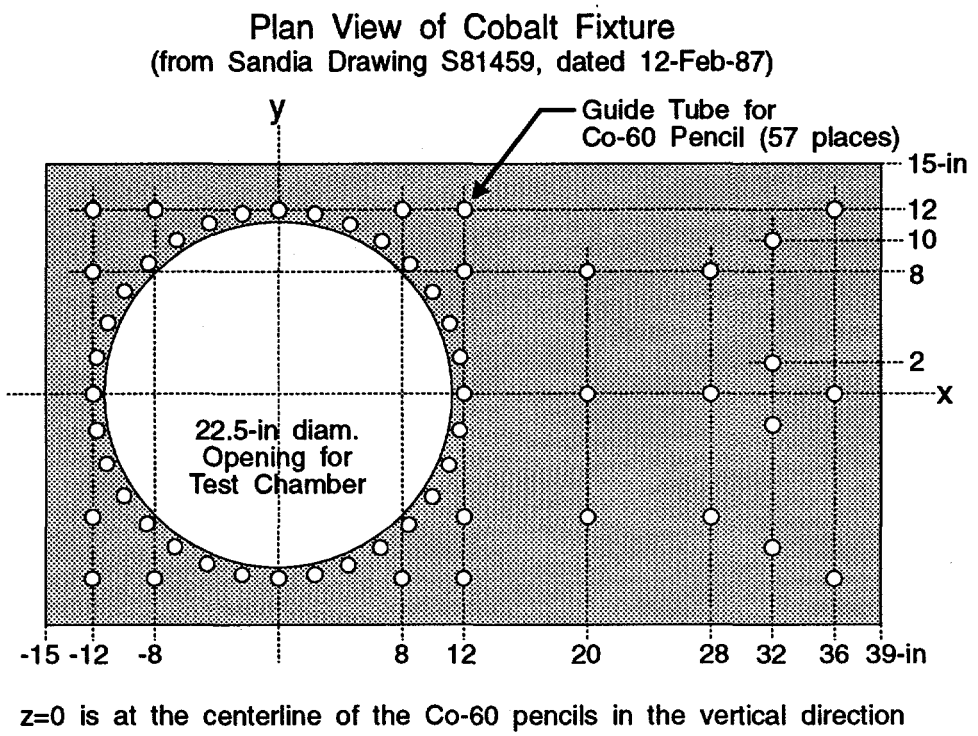

Figure 2.3: Plan view of large chamber cobalt fixture showing the fixture coordinate system and possible cobalt source locations.

both cut and complete (electrically energized) specimens were used:

1. U.S. ethylene propylene rubber (EPR) cable with flame-retardant ethylene propylene diene monomer (FR-EPDM)[1] insulation and Hypalon jacket.
2. U.S. cross-linked polyolefin (XLPO) cable with flame-retardant irradiation cross-linked polyethylene (XLPE)[2] insulation and Hypalon jacket.
3. French EPR cable with EPR insulation and Hypalon jacket.
4. French PE cable with polyethylene (PE) insulation and PE jacket. The cable jacket had no labeling; however, this cable was identified by the French as `FILECA F1203-Pro`; they also indicated that the cable's insulation and jacket are constructed of different PE formulations.

The cables tested in the U.S. and France came from the same reels.

[1]FR-EPDM is a specific type of EPR.
[2]XLPE is a specific type of XLPO.

2.2.1 Cut Cable Specimens

Cut cable specimens were used for the mechanical tests. The cables were cut into 400 mm (approx. 16 in.) lengths and Raychem heat-shrink end caps were applied to each end of the specimens. For each of the 4 cable types, there were 16 different test conditions, as indicated in Table 2.2.

2.2.2 Complete Cable Specimens

Complete cable specimens were used for the electrical tests. A total of 16 cables were tested (4 of each cable type) as indicated in Table 2.3. Each of the complete specimens was 22.86 m (75 ft) long, with approximately 3 m (9.8 ft) of that length wrapped around the mandrel in the test chamber. The remaining length was used for connection to electrical monitoring and energization equipment when the test chamber was lowered to the bottom of the LICA pool for irradiation.

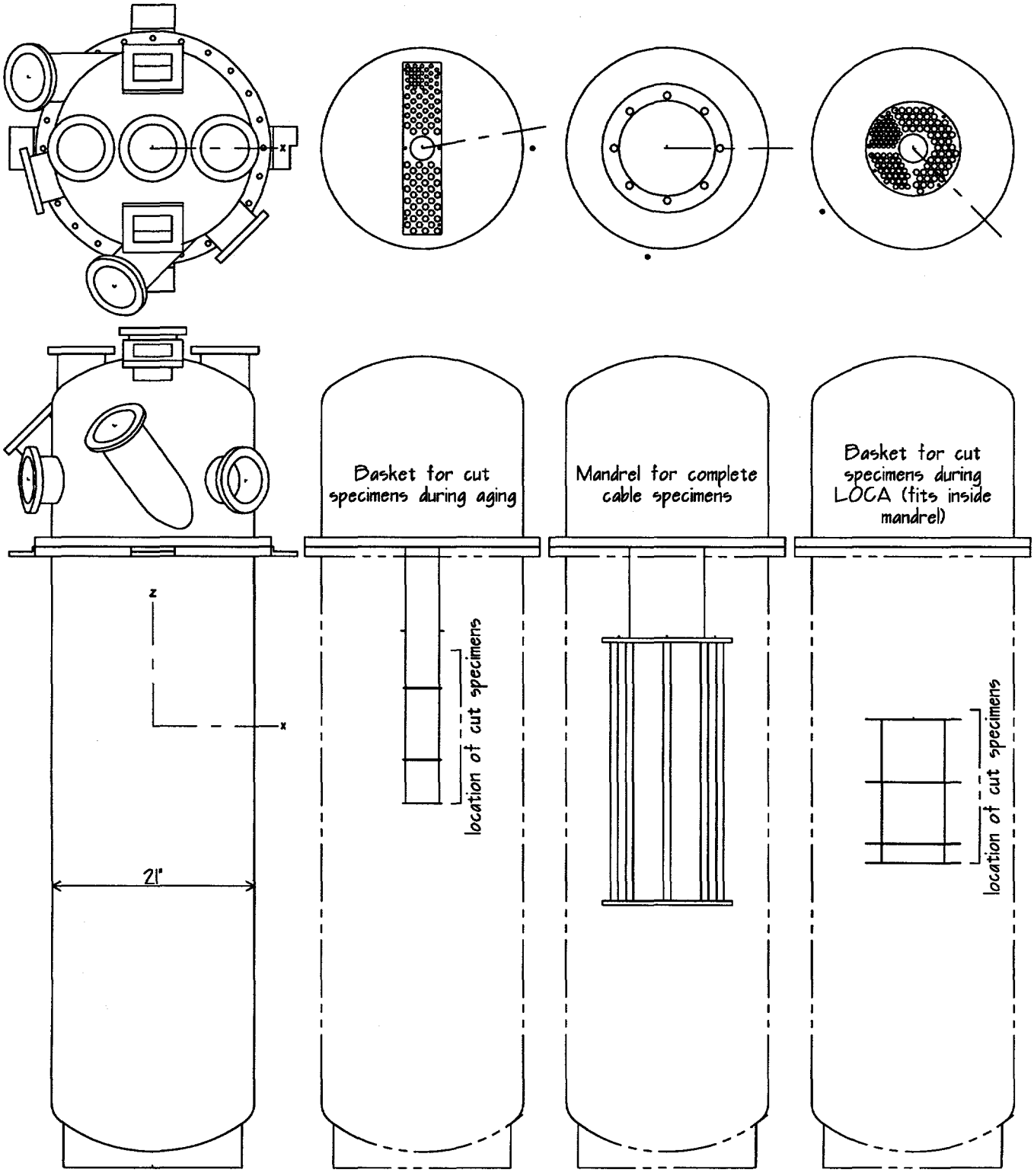

Figure 2.4: Detail of the test chamber and sketches of the two baskets used to hold cut specimens and the mandrel on which the complete specimens were mounted—drawn to scale.

Table 2.1: Cable Types Tested.

U.S. EPR (UE)	Samuel Moore Dekoron Elastoset (Part No. 1H52-68310), 2 conductors (16 AWG) plus aluminum-Mylar shield with drain wire 0.64 mm (0.025 in.) thick FR-EPDM insulation 1.14 mm (0.045 in.) thick Hypalon jacket Cable outside diameter is approximately 7.9 mm (0.31 in.) The cable jacket has the following markings, `DEKORON 2/C 16 AWG 600V SAMUEL MOORE GROUP, AURORA, OHIO`

U.S. XLPO (UX)	Rockbestos Firewall III (Part No. C52-3303), 3 conductors (12 AWG)
	0.76 mm (0.030 in.) thick flame-retardant irradiation XLPE insulation
	1.14 mm (0.045 in.) thick Hypalon jacket
	Polypropylene filler located under the cable jacket
	Cable outside diameter is approximately 11.5 mm (0.45 in.)
	The cable jacket has the following markings,
	`12 AWG 3/C ROCKBESTOS 600V FIREWALL III XHHW NEC TYPE TC (UL)`
	`K-2 COLORCODE 1987-7C 1309 COPPER FRXLPE CSPE`

French EPR (French multiconductor) (FM)	FILERGIE, 3 conductors (1.5 mm diameter) 1.15 mm (0.045 in.) thick EPR insulation 1.60 mm (0.063 in.) thick Hypalon jacket Cable outside diameter is approximately 11.5 mm (0.45 in.) The cable jacket has the following markings, `CGF-3x1,5 CU-EPR-PCS-4-209-220`
French PE (French coaxial) (FC)	FILECA F1203-Pro, coaxial (0.85 mm diameter conductor) 1.05 mm (0.040 in.) thick PE insulation 0.5 mm (0.020 in.) thick PE jacket Cable outside diameter is approximately 5.1 mm (0.20 in.) The cable jacket has no labeling.

2.3 Test Conditions

2.3.1 Aging

Two test chambers were used for the aging—one for the cut cable specimens and a second for the complete cable specimens. In each of the two test chambers, the specimens were maintained at 40°C during the aging exposure.

Aging conditions were chosen to match the temperature and total aging dose of the cables tested at CIS bio international's irradiation facilities in the French portion of the joint program. Because the aging time in the French test was much longer, the U.S. test's thermal exposure is less than that of the French test. If an equal dose, equal damage model of radiation aging is correct (*i.e.*, degradation is independent of dose rate), then the radiation aging of the U.S. test program should match that of the French test program. The data presented later in this report (see Sections 5 and 6.1), however, show that dose rate does influence the amount of degradation; thus the equal dose, equal damage model of radiation aging is not correct.

Cut Cable Specimens

The aging irradiation was performed at a dose rate of 100 Gy/hr (10 krad/hr) to doses of 28, 56, 84, 140, and 200 kGy (2.8, 5.6, 8.4, 14, and 20 Mrad) as indicated in Table 2.2. Radiation dosimetry was performed to quantify the radiation field to which the test samples were exposed. Details of the dose mapping are given in Appendix A. During aging, the test chamber was periodically brought to the surface of the LICA pool and opened to remove and replace test specimens as needed to achieve the desired total doses.

During the aging exposure, the specimens were

Table 2.2: Test Conditions for Cut Cable Specimens.

Code	Aging Dose [kGy]	Accident Dose?	Accident Steam Exposure?
0	0	No	No
0A	0	Yes	No
0L	0	Yes	Yes
28	28	No	No
28A	28	Yes	No
28L	28	Yes	Yes
56	56	No	No
56A	56	Yes	No
56L	56	Yes	Yes
84	84	No	No
84A	84	Yes	No
84L	84	Yes	Yes
14	140	No	No
20	200	No	No
20A	200	Yes	No
20L	200	Yes	Yes

maintained at 40°C. Twelve thermocouples were used to monitor the temperature inside the test chamber. Airflow of 3.3 l/sec (7 ft^3/min) or greater was supplied to the test chamber to ensure that oxygen levels were not depleted. Aging conditions (temperature and airflow) were monitored using the system shown schematically in Figure 2.5. Because cut test specimens were added and removed from the test chamber so often and the basket used to hold the cut specimens was not circularly symmetric, the test chamber was not rotated during aging; however, specimens were moved to different locations in the basket to ensure that they all received approximately the same total aging radiation dose.

Complete Cable Specimens

The aging irradiation was performed at a dose rate of 100 Gy/hr (10 krad/hr) to a total dose of 84 kGy (8.4 Mrad). Radiation dosimetry was performed to quantify the radiation field to which the test samples were exposed. Details of the dose mapping are given in Appendix A.

During the aging exposure, the specimens were maintained at 40°C. Twenty thermocouples were used to monitor the temperature inside the test chamber. As shown in Figure 2.6, the non-coaxial cable specimens were energized with 300 mA of current and the French PE cables were energized at 600 Vdc, 0 mA. One conductor from each cable (or the shield, if present) was electrically grounded during the aging as indicated in Table 2.3. Airflow of 3.3 l/sec (7 ft^3/min) or greater was supplied to the test chamber to ensure that oxygen levels were not depleted. Aging conditions (temperature, airflow, and cable excitation) were monitored using the system shown schematically in Figure 2.5. The test chamber was rotated three times during aging to help ensure a uniform radiation dose for all the tested cables.

2.3.2 Loss-of-Coolant Accident Simulation

A LOCA simulation was performed after completion of the aging exposure. The LOCA simulation consisted of an accident radiation exposure followed by an accident steam exposure.

Accident Radiation Exposure

An accident radiation exposure was performed after completion of the aging exposure. A single test chamber was used for the accident irradiation; a round

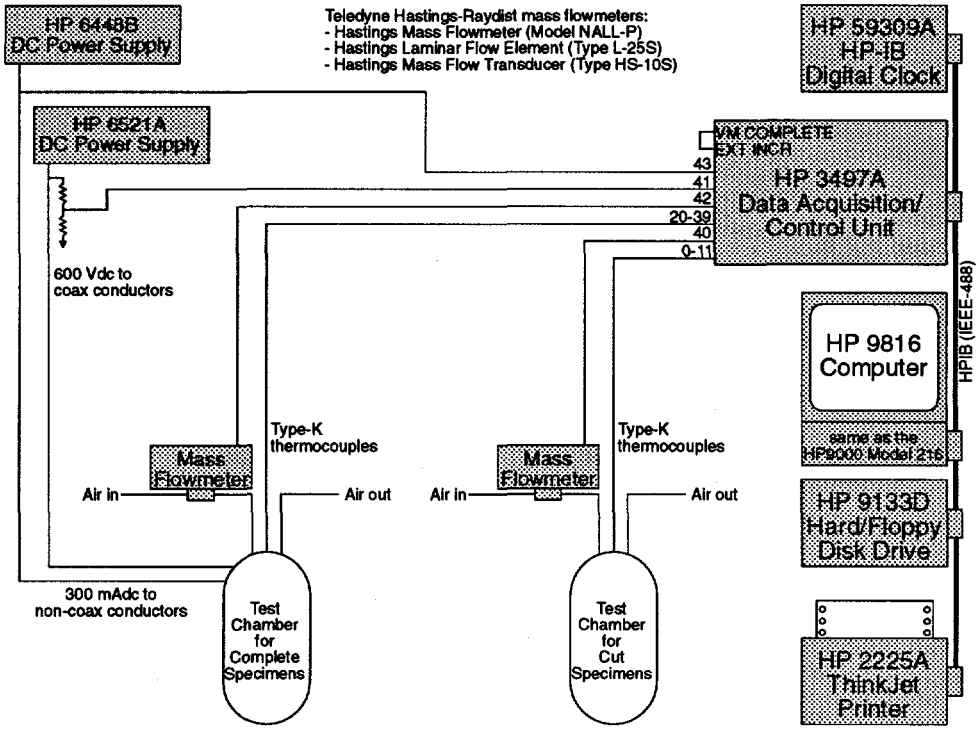

Figure 2.5: Schematic of the system used to monitor test chamber conditions during aging and accident irradiation.

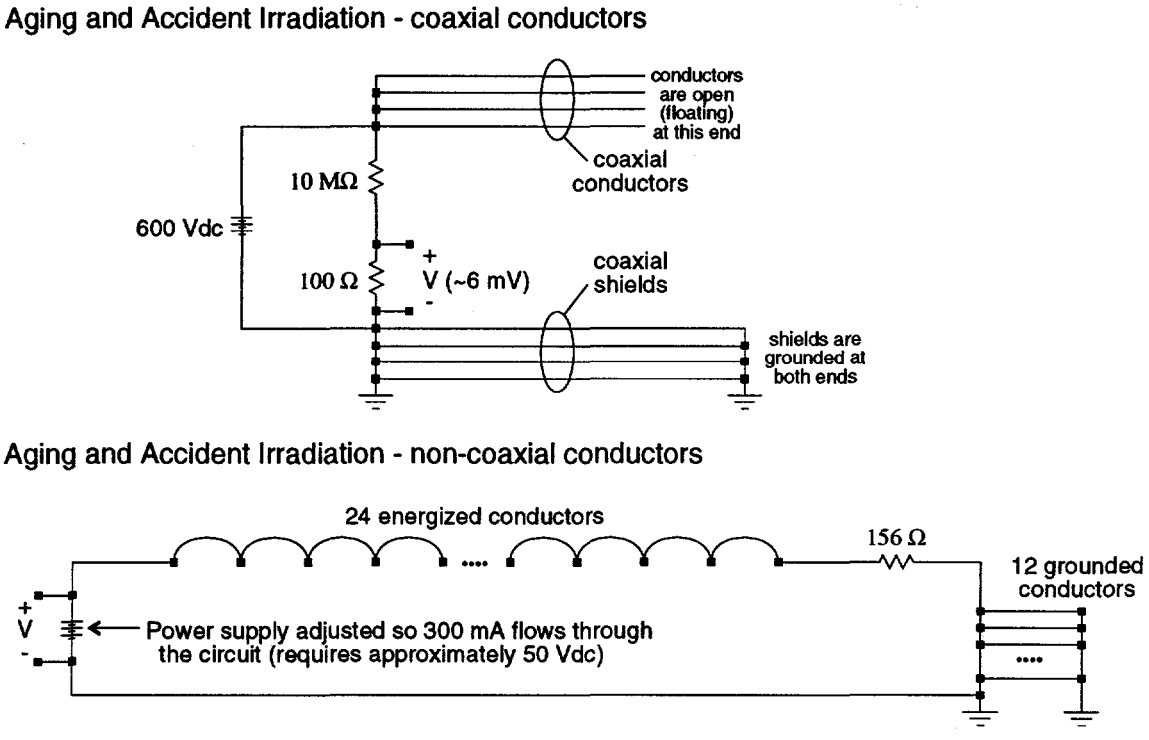

Figure 2.6: Schematic of the circuits used to electrically energize the complete cable specimens during aging and accident irradiation.

Table 2.3: Conductor Numbers for the 16 Complete Cable Specimens.

U.S. EPR			
	Conductor 1	Conductor 2	Shield
Cable 1	01	02	**37**[a]
Cable 2	03	04	**38**
Cable 3	05	06	**39**
Cable 4 (unaged)	07	08	**40**
U.S. XLPO			
	Conductor 1	Conductor 2	Conductor 3
Cable 1	09	10	**11**
Cable 2	12	13	**14**
Cable 3	15	16	**17**
Cable 4 (unaged)	18	19	**20**
French EPR			
	Conductor 1	Conductor 2	Conductor 3
Cable 1	21	22	**23**
Cable 2	24	25	**26**
Cable 3	27	28	**29**
Cable 4 (unaged)	30	31	**32**
French PE			
	Conductor	Shield	
Cable 1	33	**41**	
Cable 2	34	**42**	
Cable 3	35	**43**	
Cable 4 (unaged)	36	**44**	

[a]**Conductor numbers listed in bold were electrically grounded during aging, accident irradiation, and the accident steam exposure.**

basket of cut cable specimens was mounted inside the mandrel on which the complete cable specimens were wrapped. The complete cable specimens were not disturbed.

The accident irradiation was performed at a dose rate of 900 Gy/hr (90 krad/hr) to a total dose of 600 kGy (60 Mrad). Previous testing by Buckalew [6] has shown that accident radiation exposures are conservatively simulated by isotropic gamma ray sources such as the cobalt-60 used for this test. Radiation dosimetry was performed to quantify the accident radiation field to which the test samples were exposed. Details of the dose mapping are given in Appendix A.

The cable specimens were kept at 70°C during the accident irradiation. As shown in Figure 2.6, the non-coaxial complete cable specimens were energized with 300 mA of current and the complete French PE cables were energized at 600 Vdc, 0 mA. One conductor from each cable (or the shield, if present) was electrically grounded during the accident irradiation as indicated in Table 2.3. Airflow of 8.0 l/sec (17 ft^3/min) or greater was supplied to the test chamber to ensure that oxygen levels were not depleted and to help ensure temperature uniformity. Accident irradiation conditions (temperature, airflow, and cable excitation) were monitored using the system shown schematically in Figure 2.5. Because of the near symmetry of the radioactive cobalt sources around the test chamber, the chamber was not rotated during the accident irradiation.

Accident Steam Exposure

The accident steam exposure was performed after the accident radiation exposure. The steam exposure consisted of simulated LOCA transient temperature and pressure conditions. The same test chamber used for the accident irradiation was used for the accident steam exposure.

All the complete cable specimens, including the French PE cables, were energized at approximately 50 Vdc, 0 mA to allow for on-line measurement of insulation resistance. One conductor from each complete cable (or the shield, if present) was grounded during the accident steam exposure as indicated in Table 2.3.

The target temperature and pressure for the accident steam exposure follow the French profile shown in Table 2.4. The target test profile goes immediately to saturated steam conditions in the initial transient and remains at saturated steam conditions for the first 3 hours. After air overpressure was added to the chamber beginning at 3 hours, the test chamber environment consisted of steam, at a partial pressure equal to its saturation pressure for the test chamber temperature,[3] with air added to achieve the target pressure. The test chamber environment remained wet (*i.e.*, saturated steam conditions) even after the air overpressure began because of the continuous condensation of steam, which had to be replenished by injecting more steam into the test chamber. Previous testing by Gillen [9] [10] has shown that the presence of oxygen during a steam test can have a large effect on material performance. No chemical spray was used during the accident steam exposure.

This French test profile varies from the "generic" accident steam condition profile given in Appendix A of IEEE Std. 323-1974[4] [11, Figure A1]. The IEEE profile reaches a higher peak temperature (171.1°C versus 159°C) but a slightly lower peak pressure (583.9 kPa versus 600 kPa) than the French steam profile. The French profile has one transient with saturated steam conditions, while the IEEE profile has two transients with superheated steam conditions. The IEEE profile goes to saturated steam conditions 6 hours after the start of its second transient. The French profile includes air during the steam exposure, while the IEEE profile has a pure steam environment.

The accident steam profile was manually controlled during the first 3 hours of the test (the saturated portion of the profile). After 3 hours, the air overpressure was controlled by an automatic system which used three solenoid valves to control the steam system. These valves (test chamber vent valve, steam inlet valve, and overpressure air inlet valve) were controlled by the same computer program that performed the logging of temperature, pressure, and on-line IR data. Each control period, the program checked the following list of 5 conditions and performed only the first action that applied:

1. pressure too high—vent test chamber.
2. temperature too low—add steam to test chamber.
3. pressure too low—add overpressure air to test chamber.
4. pressure and temperature are on target but the chamber has not been vented for a long time—vent test chamber so "fresh" air and steam will be added in ensuing control periods (ensures that sufficient oxygen is present in the test chamber in spite of possible oxygen-depleting cable degradation mechanisms).
5. pressure and temperature are on target—no action required.

This simple algorithm proved sufficient to control the air overpressure conditions very accurately.

The actual and target pressure and temperature during the accident steam exposure are shown in Figure 2.7. The pressure shown in Figure 2.7 was measured using a single Heise 710B pressure transducer with a range of 0–1380 kPa gage (0–200 psig). The temperature shown in Figure 2.7 is the average value calculated from the 20 thermocouples in the test chamber. Two problems occurred during the accident steam exposure: first the drop in pressure seen for parts of days 7 and 8 was caused by the overpressure air inlet valve failing and not allowing overpressure air into the test chamber. This led to the test chamber pressure falling toward the saturated steam pressure. Second, the drop in temperature seen late in day 8 was caused by the replacement overpressure air inlet valve failing to seat correctly, which allowed air to continually flow into the chamber. Because the test chamber pressure was continually too high, steam was seldom added because the control program spent all its time venting the test chamber. As these drops persisted for approximately 1 day, the accident steam exposure was extended by 1 day to achieve the desired exposure time.

[3] Actually the presence of air alters the steam's saturation pressure by a very small amount. For a 100°C, 200 kPa air-water vapor mixture, the saturation pressure is only increased by approximately 0.06% over that for pure steam at 100°C [8, Sections 10.4 and 12.6].

[4] The newer standard, IEEE Std. 323-1983, has never been endorsed by the NRC. It also does not include a "generic" steam condition profile like that found in Appendix A of IEEE Std. 323-1974.

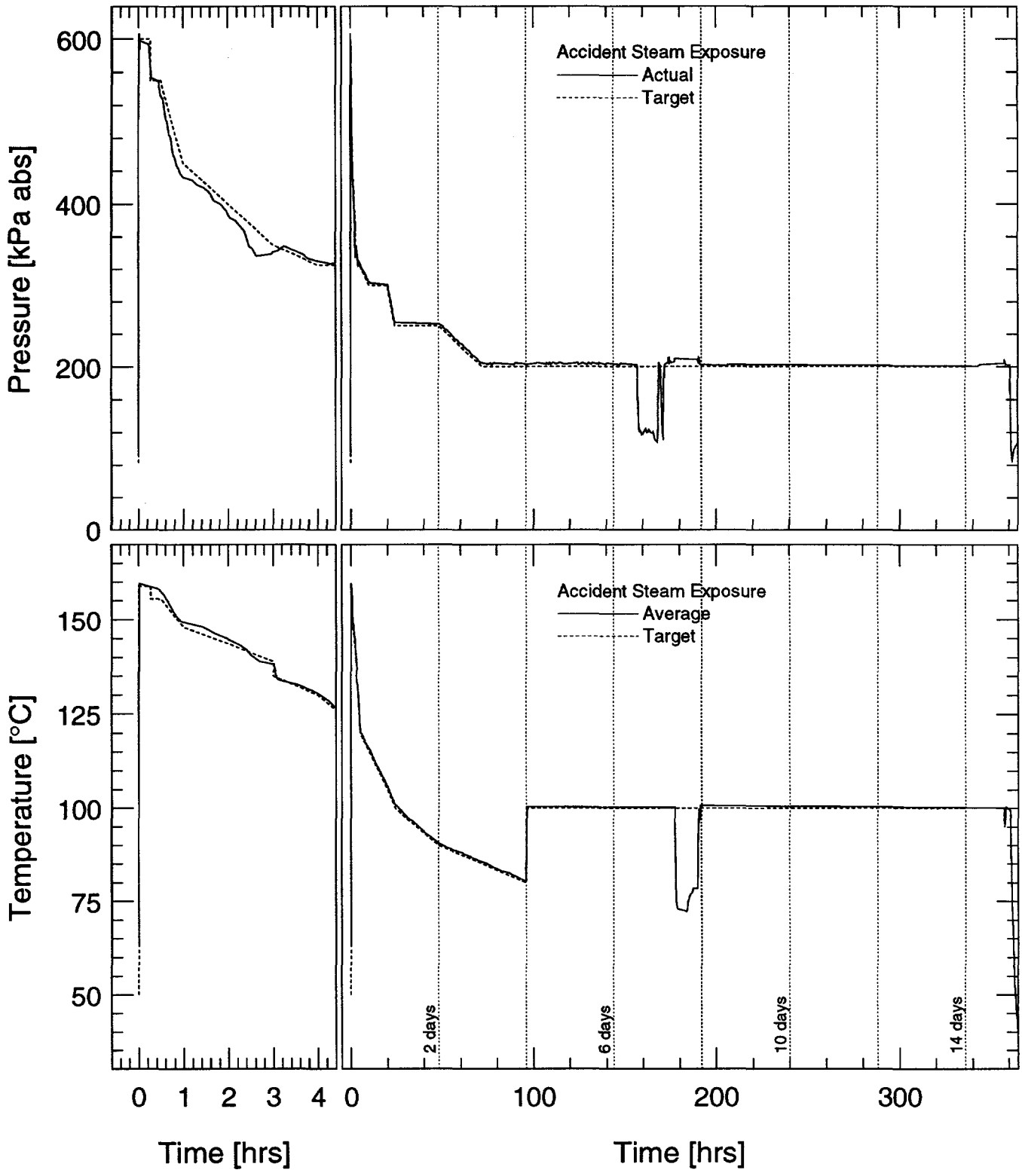

Figure 2.7: Pressure and temperature during the accident steam exposure.

Table 2.4: Target Accident Steam Exposure Test Profile (French Profile).

Time	Intended Test Profile		
	Temperature [°C]	Absolute Pressure [kPa]	Test Chamber Conditions
0–10 sec	50–159	ambient[a]–600	
10 sec–16 min	159	600	saturated steam
16–30 min	155	550	saturated steam
30 min–1 hr	155–148	550–450	saturated steam
1–2 hr	148–144	450–400	saturated steam
2–3 hr	144–139	400–350	saturated steam
3–4 hr	135–130	350–325	air overpressure
4–5 hr	130–120	325	air overpressure
5–10 hr	120–115	325–300	air overpressure
10–15 hr	115–110	300	air overpressure
15–20 hr	110–105	300	air overpressure
20–24 hr	105–100	300–250	air overpressure
1–2 days	100–90	250	air overpressure
2–3 days	90–85	250–200	air overpressure
3–4 days	85–80	200	air overpressure
4–14 days	100	200	air overpressure

[a]Note that the laboratory elevation is approximately 1646 m (5400 ft) for which the standard ambient pressure is 83.057 kPa [7, p. 121], rather than the standard sea level ambient pressure of 101.325 kPa.

2.4 Mechanical Measurement Techniques

Mechanical measurements were performed only on the cut cable specimens; no mechanical measurements were performed on the complete specimens.

2.4.1 Density

Density of the insulation and jacket samples was measured using density gradient columns. The principle of operation of the density gradient column is dependent upon the hydrostatic equilibrium between a solid specimen and a liquid of identical density. A column of liquid with an approximately linear density gradient is maintained at constant temperature. Calibrated density standards, in the form of glass floats, are introduced into the column and their position in the gradient column is recorded. These data are used to produce a calibration of density versus position in the column. When a specimen is placed into the column, it will descend until it reaches the level where the density of the liquid matches the density of the specimen. By measuring the equilibrium position of the specimen and using the calibration of position versus density, the specimen density can be determined. Small specimens were used for density measurements; one dimension was the material thickness and each of the other two dimensions were typically smaller than 6 mm (1/4 in.). At least two specimens of each cable for each test condition were used to determine the density for the type. Details of the technique used to create the density gradient columns and issues involved with density gradient column testing can be found in Ref. [12]. Special care was taken to ensure that the specimens were fully wetted (*i.e.*, had no attached air bubbles) before placing them in the gradient column.

Densities greater than 1 g/cm^3 were measured using a gradient column filled with a water-calcium nitrate solution. Densities less than 1 g/cm^3 were measured using a gradient column filled with an ethyl alcohol-water solution; pure ethyl alcohol (ethanol) was used in the solution to ensure that there were no denaturing additives in the alcohol that might have caused swelling of the French PE cable's polyethylene insulation and jacket. Water-calcium nitrate liquid systems have a density range of 1.00–1.60 g/cm^3 and

ethanol-water liquid systems have a density range of 0.79–1.00 g/cm^3 [13].

2.4.2 Hardness

The cable hardness was measured using a Shore Durometer Hardness Tester, Type "A-2" (Shore Instrument & Mfg. Co., Jamaica, NY). The instrument displays a hardness reading ranging from 0 to 100; however, any measurements above 90 are really too hard for this instrument, and the hardness should be read with the next higher-range Durometer. Hardness measurements were only taken from the outside of the cable; thus the measured value is not related solely to the hardness of the cable jacket, but is also influenced by the underlying insulation and conductors. For each cut test sample, 5 measurements were taken across the entire length of a single cut cable and the cable was turned approximately 1/5 turn between each measurement. Measurements were not taken close to the ends of the cut test samples to minimize the possibility of encountering end effects that could give misleading hardness readings.

The U.S. EPR cable does not have a smooth jacket, but is ribbed because of the underlying conductors. This can lead to scatter in the data if one hardness measurement is performed on a rib (which is directly above a metal conductor) and the next measurement is performed between ribs (where there is no metal conductor below). For this cable, all hardness measurements were taken on the ribs, not on the region between ribs. Even when this was done, the U.S. EPR cable showed the most variation in its hardness.

2.4.3 Elongation and Tensile Strength

Tensile data on the insulation and jacket samples were measured using the system shown schematically in Figure 2.8. The tensile testing was performed using an Instron Model 1000 (Instron Corporation, Canton, MA) with Instron Model 3C Pneumatic-Action Clamps to hold the specimens in place during the pull.

Test specimen extension was measured using an Instron Model XL Elastomeric Extensometer, which provides a resistance change with specimen elongation. The extensometer resistance output was read using an HP 34401A Multimeter.

The force applied to the specimen was measured using the 0.5 kN (100 lbf) capacity load cell built into the Instron Model 1000. The load cell's dc voltage output was measured using the internal voltmeter of an HP 3497A Data Acquisition/Control Unit (*i.e.*, using the Internally Connected DVM Option).

The voltage and resistance data were stored by an HP 9000 Model 216 computer using the HP Interface Bus (IEEE-488 interface) connected to the multimeter and data acquisition/control unit. The computer allowed the entire force-elongation curve of the specimen during the tensile test to be digitized and saved.

The tensile tester load cell was calibrated using a linear fit through the two data points acquired using no mass and a 5-kg mass attached to the load cell. The extensometer was calibrated using an aluminum bar machined with notches at 10, 20, 30, 40, 50, 60, 80, and 100 mm. Data were taken for each of these extensions and fit using a linear least-squares regression.

The force applied to the specimen was converted to a stress using the initial cross-sectional area of the specimen. Two types of tensile specimens were used.

- Jacket specimens were punched from the cable jacket using an H3 dumbbell-shaped punch [14] supplied by the French. The cross-sectional area of the jacket specimens was calculated by punching 5 jacket specimens from each type of unaged cable and measuring their average thickness and average width (3.95 mm). As shown in Figure 2.9, the H3 tensile specimens are approximately 50 mm (2 in.) long.
- Insulation specimens were 127-mm (5 in.) long sections of the cable insulation with the conductor removed. For each of the 4 cable types, a nominal cross-sectional area was calculated using dimensions measured on a single, unaged specimen. The conductor diameter was used as the insulation inside diameter.

The cross-sectional areas used for the various tensile specimens are tabulated in Table 2.5. All tensile strength data are based upon the original cross-sectional area of unaged samples; no attempt was made to measure the cross-sectional area of the specimens as they stretched during pulling or to measure the original cross-sectional area for each test condition.

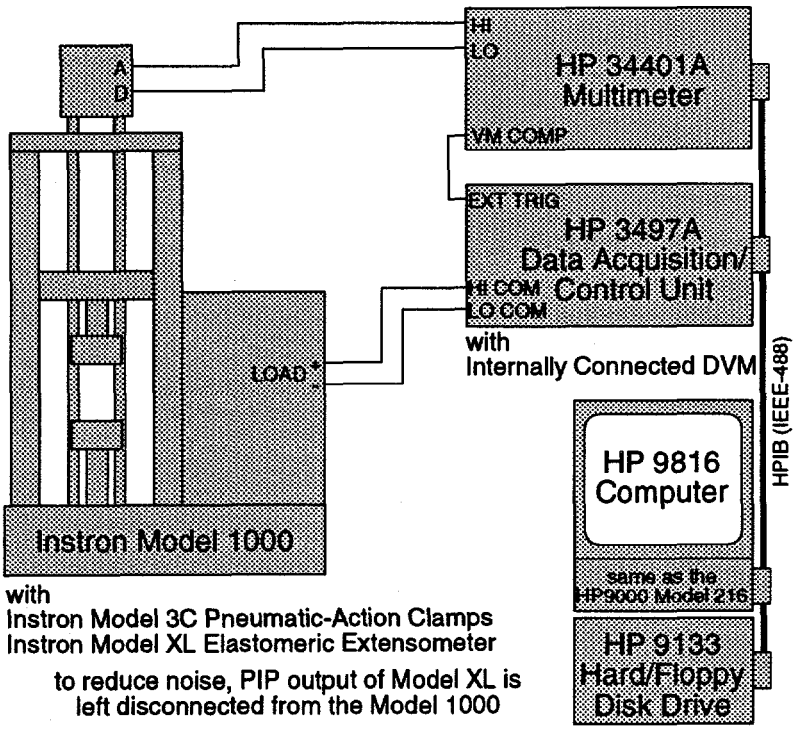

Figure 2.8: Schematic of the system used to measure tensile properties.

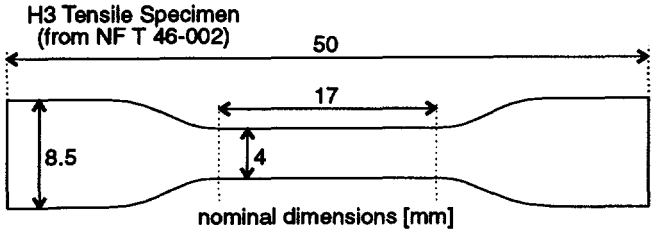

Figure 2.9: H3 tensile specimen, nominal dimensions.

Table 2.5: Cross-Sectional Areas of Tensile Specimens.

Cable	Jacket Specimens		Insulation Specimens		
	Thickness [mm]	Area [mm^2]	Outside Diam. [mm]	Inside Diam. [mm]	Area [mm^2]
French EPR	1.77	6.973	3.77	1.48	9.460
U.S. EPR	1.12	4.415	2.80	1.49	4.434
U.S. XLPO	1.38	5.468	3.97	2.18	8.644

For both types of tensile specimens, the cross-head speed of the tensile tester was run at 50.8 mm/min (2 in./min) during the pull, and the gage length (initial separation of the tensile tester jaws) was nominally 10 mm.

Note that the cut cable specimens were exposed to one of the 16 test conditions listed in Table 2.2 before the jacket was cut off to produce jacket specimens and the insulation was stripped from the conductors to produce insulation specimens. This was done to ensure that the cable exposure was as realistic as possible.

2.5 Electrical Measurement Techniques

Electrical measurements were performed only on the complete cable specimens; no electrical measurements were performed on the cut specimens.

2.5.1 High Potential

The high potential testing measured the ac charging and leakage current. When an ac voltage is applied to a cable, the resulting current is the sum of the current actually leaking from the conductor through the insulation to a ground outside the cable plus the current necessary to charge and discharge the cable's reactive impedance (at the excitation frequency of the applied ac voltage) as the applied cable voltage changes.

Using the system shown schematically in Figure 2.10, a Hipotronics Model 750-2 AC Dielectric Test Set (Hipotronics, Inc., Brewster, NY) was used to measure the ac charging and leakage current on the cables. Conductor data were acquired at 2000 Vac rms (60 Hz) and shield data were acquired at 600 Vac rms (60 Hz)[5]. The conductor (or shield) under test was connected to the dielectric test set and all other conductors (and shields) were electrically grounded before the ac voltage was applied. The opposite ends of the conductors (and shields) were allowed to float electrically.

The Hipotronics dielectric test set was modified to output dc voltages proportional to the ac excitation voltage and ac charging/leakage current. These two dc voltage outputs were acquired using the internal digital voltmeter in each of two HP 3497A Data Acquisition/Control Units, one acquired the excitation voltage and the other the current. Data acquisition utilized the following procedure:

1. Start the acquisition program; the two streams of data are acquired every half second by the DVMs and sent to the HP 9000 Model 216 computer for storage.
2. Ramp the excitation voltage up to the desired voltage using a voltage ramp rate of 500 Vac/sec.
3. Hold at the desired excitation voltage for 1 min.
4. Ramp the excitation voltage back down.
5. Stop the acquisition program.

The ac charging and leakage current data point was calculated by the program based on the acquired values during the 1-min hold at the desired excitation voltage.

2.5.2 Insulation Resistance

Insulation resistance (IR) gives a measure of the resistive component of dielectric impedance. The IR

[5]Nominal value; the shield energization voltage is actually in the range 600–800 Vac because the Hipotronics test set cannot precisely control such low ac voltages.

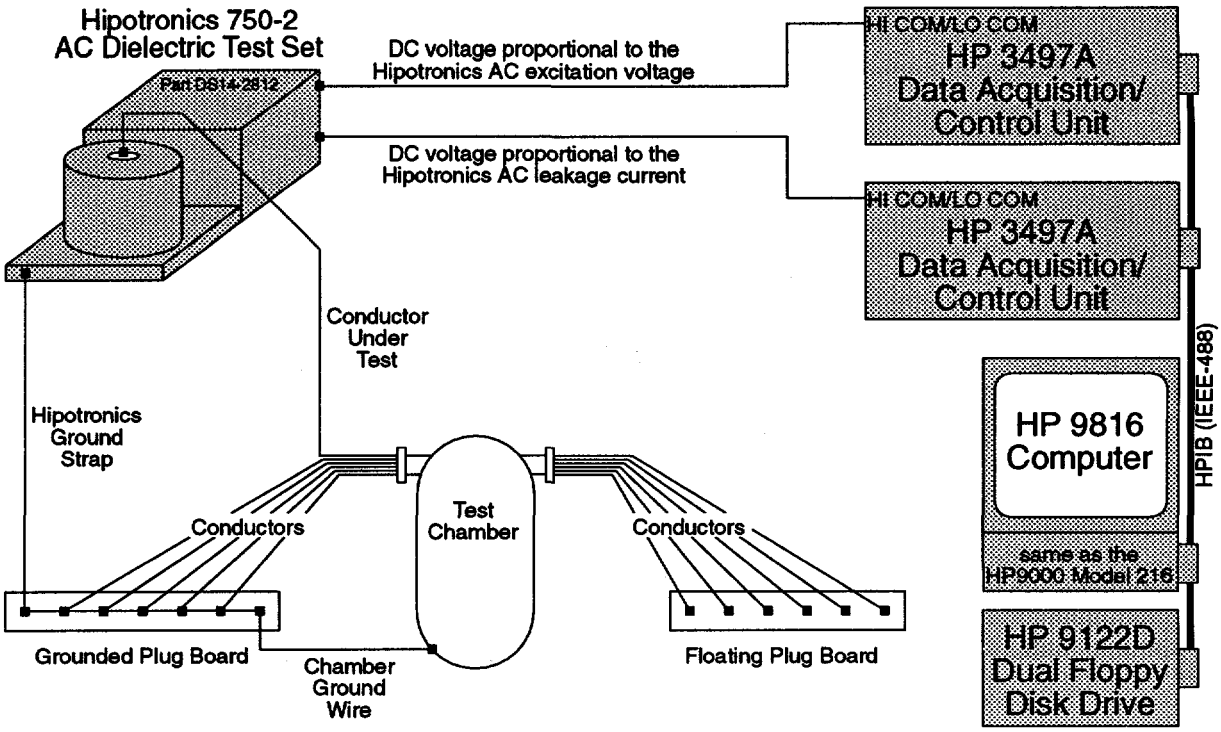

Figure 2.10: Schematic of the system used to measure ac charging and leakage currents.

value calculated from the applied dc voltage and measured current only includes resistive impedance; any initial ac effects due to the sudden application of the dc voltage are effectively gone by the time the IR measurement is taken. IR values are typically used by the utility industry as a go/no-go test of insulation; however, no technical basis is available to set an IR acceptance criteria for age-related degradation. Typically, an IR test is used to assist detection of locally damaged cable (*i.e.*, insulation windings that are wet, or a gouged cable that is "sufficiently close" to the ground plane in the test).

The IR of the complete cable samples was measured at discrete times using the system shown schematically in Figure 2.11; a detailed discussion of this system appears in Ref. [3, Section A.2]. The conductor (or shield) under test was connected to the dc power supply through a resistor[6]; all other conductors (and shields) were grounded before the dc voltage was applied. The opposite ends of all the cables were allowed to float electrically. IR measurements were performed at 3 power supply voltages: 50, 100, and 250 Vdc. A single IR measurement consisted of acquiring 15 samples of the voltage across the resistor using a Keithley 619 Electrometer at times ranging from 2 sec to 1 min after application of the power supply voltage. For each of the 15 samples, the conductor's IR was calculated using the measured voltage across the known resistance and the power supply voltage. To reduce the effect of measurement noise, the IR values were fit using a least-squares polynomial regression and the value from the fit, rather than the actual measured value, was used as the IR at 1 min.

During the accident steam exposure, IR measurements were performed using the circuit shown in Figure 2.12 in addition to the discrete IR measurements. These IRs are referred to as "continuous" IRs, even though they were not truly continuous; these measurements were performed at intervals ranging from 10 to 300 sec. The conductor numbers in the figure correspond to the numbers in Table 2.3. As indicated in Figure 2.12 and Table 2.3, one conductor or shield from each cable was connected to ground to provide a ground plane; no continuous IR measurements are available for these grounded conductors. The continuous system could measure IR values up to approximately 10^8 Ω, which is

[6]Figure 2.11 shows that a relay board is used to select one of four possible resistors; this allows the IR to be measured accurately over a wide range of values.

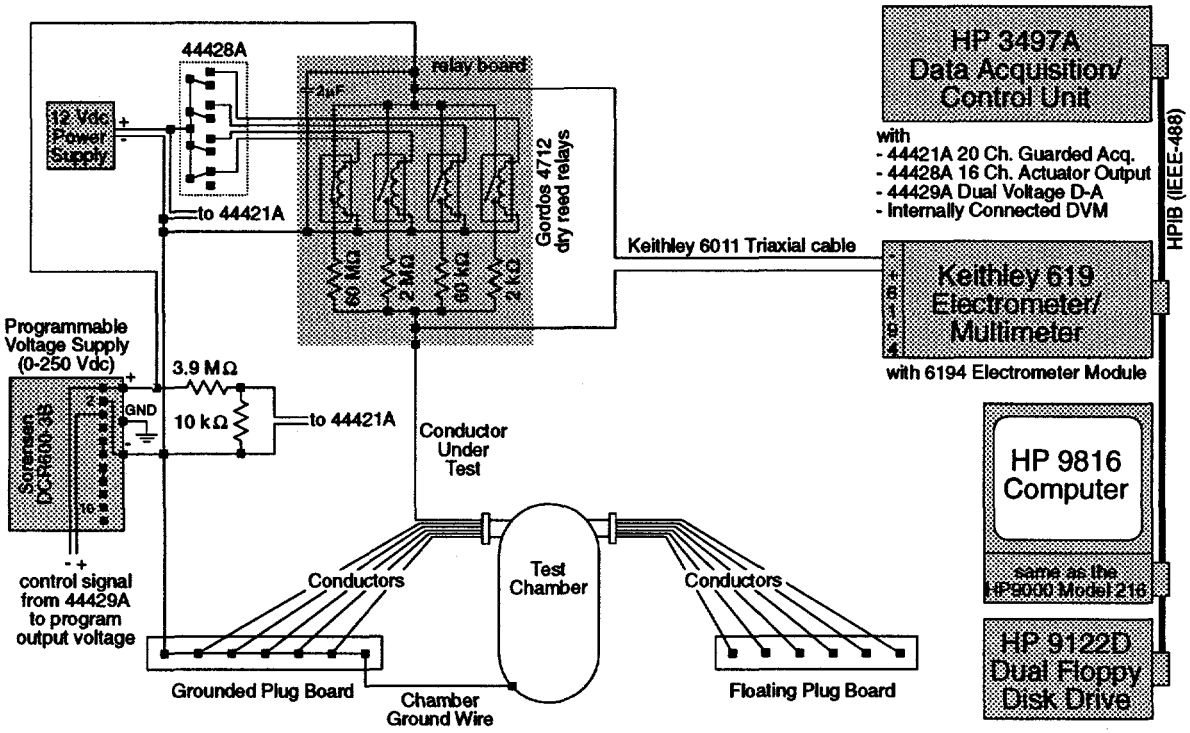

Figure 2.11: Schematic of the system used to measure insulation resistance.

several orders of magnitude less than what could be measured with the discrete IR system. The continuous IR system is most useful for identifying short-term drops in IR values, such as during the initial transient of the accident steam exposure, which would otherwise be missed by the discrete IR system. A more complete discussion of the measurement limits of the continuous IR system appears in Ref. [3, Section 2.4.3].

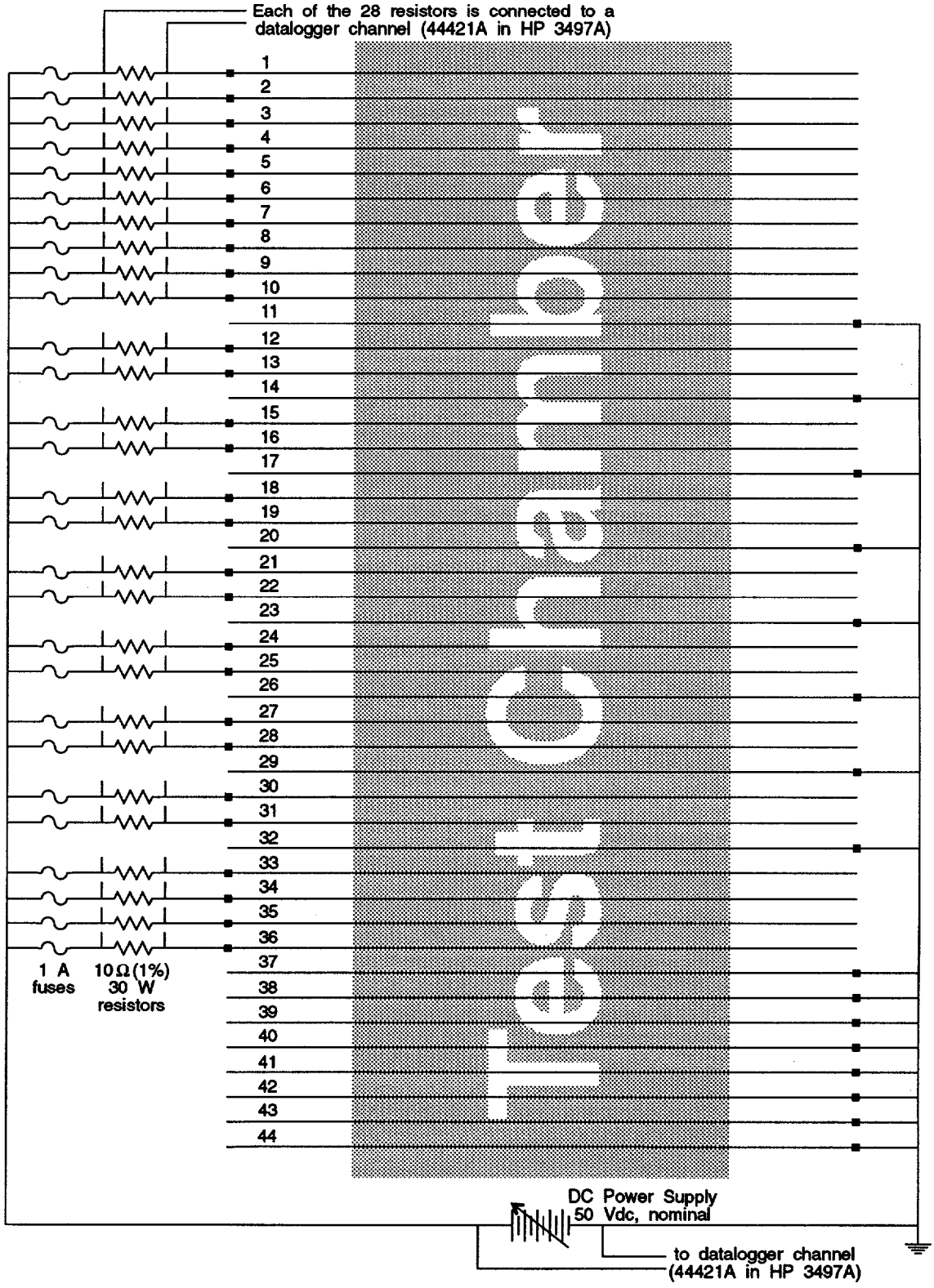

Figure 2.12: Circuitry used to measure continuous insulation resistance during the accident steam exposure.

3 U.S. Experimental Results

This section presents the experimental data[1] acquired from the four different types of cable during the U.S. test program. The results for the French test program are presented in Section 5.

3.1 Mechanical Measurement Results

The mechanical measurement data presented here are from the cut cable specimens; no mechanical measurements were performed on the complete specimens.

3.1.1 Density

Density data are tabulated for both cable insulation and jackets in Table 3.1. For each cable type, density data were acquired for four different environmental conditions:

1. unaged specimens
2. specimens aged to 200 kGy at 40°C
3. specimens aged to 200 kGy at 40°C, plus an accident irradiation of 600 kGy at 70°C
4. specimens aged to 200 kGy at 40°C, plus an accident irradiation of 600 kGy at 70°C, plus an accident steam exposure

The French EPR cable's EPR insulation was less dense than its Hypalon jacket. No statement can be made about the density behavior of the jacket because its density always remained higher than what could be measured with the density columns. The insulation density was essentially unchanged during the aging; however, it did increase during the accident irradiation. The insulation density at the completion of the accident steam exposure could not be measured precisely because of the limited range of the density gradient columns available when the measurements were performed. However, the measurements that were performed bracketed the insulation density in the range 1.29–1.31 g/cm^3; thus the insulation density probably did not change dramatically during the steam exposure.

Both the French PE cable's PE insulation and PE jacket were less dense than water. The insulation and jacket had similar behavior; their density increased during both the aging and accident irradiation, only to decrease during the accident steam exposure. The jacket's density had increased more than 5% by the end of the accident irradiation, while the insulation density increased by a much smaller percentage.

The U.S. EPR cable's FR-EPDM insulation was less dense than its Hypalon jacket. The jacket density increased slightly during aging, decreased slightly during the accident irradiation, and increased again during the accident steam exposure. The insulation density increased during both aging and the accident irradiation, but was unchanged during the accident steam exposure.

The U.S. XLPO cable's XLPE insulation was less dense than its Hypalon jacket. No statement can be made about the behavior of the jacket because its density always remained higher than what could be measured with the density columns. The insulation density decreased very slightly during aging, but increased during the accident irradiation, only to decrease during the accident steam exposure.

Even though three of the cables had Hypalon jackets, the jackets had different densities, which indicates that the Hypalon formulation was not the same in all three jackets. While the Hypalon jacket density of the French EPR and U.S. XLPO cables cannot be compared with one another in Table 3.1, the U.S. EPR Hypalon jacket is clearly less dense than the other two Hypalon jackets.

3.1.2 Hardness

Hardness data[2] for the cables are plotted versus dose in Figures 3.1–3.4. The H_0 value listed on each figure is the average hardness of unaged cable. Each plotted

[1] In addition to the figures and tables included in this section, all the raw data are available upon request from the author.

[2] All hardness measurements were performed on the outside of the cut cable specimens; thus the measured value is closely related to the hardness of the cable jacket, but is also influenced by the underlying insulation and conductors.

Table 3.1: Density Results.

Cable	Aging Dose [kGy]	600 kGy Accident Dose	Accident Steam Exposure	Jacket Specimens Number of Samples	Jacket Specimens Average $[\rho/\rho_0]$	Jacket Specimens Std. Dev. $[\sigma_\rho/\rho_0]$	Insulation Specimens Number of Samples	Insulation Specimens Average $[\rho/\rho_0]$	Insulation Specimens Std. Dev. $[\sigma_\rho/\rho_0]$
French EPR				$\rho_0 > 1.55$ g/cm^3			$\rho_0 = 1.3102$ g/cm^3		
FM0	0	No	No	2	1.0000[a]	—	4	1.0000	0.0020
FM20	200	No	No	2	—[a]	—	4	1.0016	0.0015
FM20A	200	Yes	No	2	—[a]	—	4	1.0062	0.0021
FM20L	200	Yes	Yes	2	—[a]	—	2	—[b]	—
French PE				$\rho_0 = 0.9447$ g/cm^3			$\rho_0 = 0.9357$ g/cm^3		
FC0	0	No	No	3	1.0000	0.0001	3	1.0000	0.0003
FC20	200	No	No	22	1.0255	0.0044	3	1.0055	0.0005
FC20A	200	Yes	No	6	1.0509	0.0015	3	1.0157	0.0009
FC20L	200	Yes	Yes	14	1.0216	0.0028	6	1.0100	0.0017
U.S. EPR				$\rho_0 = 1.4515$ g/cm^3			$\rho_0 = 1.2585$ g/cm^3		
UE0	0	No	No	4	1.0000	0.0136	2	1.0000	0.0006
UE20	200	No	No	2	1.0079	0.0010	2	1.0044	0.0090
UE20A	200	Yes	No	2	0.9952	0.0024	2	1.0179	0.0079
UE20L	200	Yes	Yes	2	1.0031	0.0039	2	1.0179	0.0079
U.S. XLPO				$\rho_0 > 1.55$ g/cm^3			$\rho_0 = 1.3425$ g/cm^3		
UX0	0	No	No	2	1.0000[a]	—	2	1.0000	0.0037
UX20	200	No	No	2	—[a]	—	2	0.9974	0.0032
UX20A	200	Yes	No	2	—[a]	—	2	1.0078	0.0063
UX20L	200	Yes	Yes	2	—[a]	—	2	1.0011	0.0105

[a] All density measurements were greater than 1.55 g/cm^3.
[b] All density measurements were in the range 1.29–1.31 g/cm^3 ($\rho/\rho_0 = 0.9846$–0.9998).

data point represents the average of 5 hardness measurements for the given test conditions. The bars for each plotted data point give the sample standard deviation of the 5 hardness measurements. No hardness measurements were taken during the accident irradiation; thus only data prior to and after the accident irradiation of 600 kGy are shown in the figures. This means that data for a dose of 656 kGy represent a specimen that was aged to 56 kGy and then subjected to an accident irradiation of 600 kGy.

The hardness of the French EPR cable, shown in Figure 3.1, increased by almost 60% during aging and increased further during the accident irradiation. During the accident steam exposure, samples originally unaged or aged to 28 kGy increased very slightly in hardness, samples originally aged to 56 kGy showed almost no change in hardness, and the hardness decreased for samples originally aged to higher doses.

The hardness of the French PE cable, shown in Figure 3.2, remained almost constant during the entire test. As indicated in Section 2.4.2, the hardness of unaged French PE cable ($H_0 = 90.4$) is in the region where measurements cannot be considered reliable for the particular hardness tester used. Thus, limitations in the hardness testing apparatus may account for the negligible changes in hardness seen for the French PE cable. The presence of a braided metal shield just under the thin jacket is most likely a partial cause of the high hardness values. Even though the values fall into a very narrow range, there is some indication that the accident steam exposure decreased the cable hardness slightly.

The hardness of the U.S. EPR cable, shown in Figure 3.3, changed relatively little during the test. Hardness initially increased slightly during aging, only to decrease a little for the 200 kGy measurement while remaining above H_0. The accident irradiation produced only a slight additional increase in hardness or none. After the accident irradiation, the cables initially aged to 56 kGy and less were harder than those initially aged to higher doses. The accident steam exposure decreased hardness slightly for all aging conditions except for cables initially aged to

200 kGy, which had a large (20%) decrease in hardness.

The hardness of the U.S. XLPO cable, shown in Figure 3.4, initially decreased with aging before increasing at larger aging doses; by 200 kGy the hardness had increased approximately 10% over its unaged value. The accident irradiation caused only a slight additional decrease in hardness or none for samples originally aged up to 84 kGy; however the hardness of the samples originally aged to 200 kGy increased another 10% during the accident irradiation. The accident steam exposure tended to increase the hardness of the cable except for originally unaged cable (hardness decreased during the steam exposure) and cable originally aged to 56 kGy (no hardness change during the steam exposure).

3.1.3 Elongation

Elongation data are plotted versus dose in Figures 3.5–3.7 for the cable jackets and in Figures 3.8–3.10 for the cable insulations. The e_0 value listed on each figure is the average elongation of unaged jacket or insulation. Each plotted data point represents the average of 5 elongation measurements for the given test conditions. The bars for each plotted data point show the sample standard deviation for the 5 elongation measurements. No elongation measurements were taken during the accident irradiation; thus only data prior to and after the accident irradiation of 600 kGy is shown in the figures. This means that data for a dose of 656 kGy represents a specimen that was aged to 56 kGy and then subjected to an accident irradiation of 600 kGy.

The elongation of the French EPR cable jacket, shown in Figure 3.5, decreased to approximately 70% of its unaged value with an aging dose of 200 kGy. The elongation of the U.S. EPR cable jacket, shown in Figure 3.6, decreased to approximately 60% of its unaged value with an aging dose of 200 kGy. The elongation of the U.S. XLPO cable jacket, shown in Figure 3.7, decreased to approximately 90% of its unaged value with an aging dose of 200 kGy. For all three cable jackets (all made of Hypalon), the 600 kGy accident irradiation reduced elongation by another 35% to 60% of the unaged value.[3] The accident steam exposure caused slight further decreases in elongation for all three jackets.

The elongation of the French EPR cable insulation, shown in Figure 3.8, decreased to approximately 55% of its unaged value with an aging dose of 200 kGy. The accident irradiation further decreased elongation by 25% to 50% of the unaged value, and the accident steam exposure slightly increased elongation for all samples except the initially unaged sample.

The elongation of the U.S. EPR cable insulation, shown in Figure 3.9, decreased to approximately 55% from its unaged value with an aging dose of 200 kGy. The accident irradiation further decreased elongation by 30% to 60% of the unaged value, and the accident steam exposure slightly increased elongation for all samples except those initially aged to 28 and 200 kGy.

The elongation of the U.S. XLPO cable insulation, shown in Figure 3.10, decreased to approximately 55% of its unaged value with an aging dose of 200 kGy. The accident irradiation produced substantial further decreases in elongation—all specimens exposed to the accident irradiation had less than 20% of their unaged elongation remaining. The accident steam exposure caused a noticeable recovery in elongation. This behavior has been noted previously for more severely aged XLPO cables [3, p. 54].

There are no elongation data for the French PE cable jacket or insulation because we were unable to remove the outer jacket from the braided shield for most of the test conditions without damaging the jacket. The jacket, which has a waxy look, remained flexible enough for the cable to be bent back on itself without the jacket cracking for aging doses up to 84 kGy. The cables aged to 140 kGy could be bent a little, but circumferential cracks quickly formed in the jacket when the cable was bent. The jackets of cables aged to 200 kGy were very brittle and any bending of the cable caused both longitudinal and circumferential cracks to form in the jacket. After the accident radiation exposure, all the French PE cable jackets were very brittle and any bending of the cable caused the jacket to crack; in some cases the jacket would simply flake away or crumble. The jackets of all the French PE cables exposed to the accident steam had a melted appearance—for some of the cables, the jackets

[3] If the elongation at break was $0.80e_0$ for an aging dose of 84 kGy, then the phrase "accident irradiation reduced elongation by another 35% to 60% of the unaged value" means that the same specimen would have an elongation at break of $0.20e_0$ to $0.45e_0$ at the completion of the accident dose (now with a total dose of 684 kGy).

did actually partially melt and drip off the cable during the accident steam exposure. However, even though the jackets had a melted appearance after the accident steam exposure, they remained very brittle and any bending of the cable caused the jacket to crack. Because the jacket for most of the French PE test specimens was too brittle to be removed from the cable without damage, there was no attempt to remove the shield from the outside of the insulation to provide insulation samples for testing.

3.1.4 Tensile Strength

Tensile strength data are plotted against dose in Figures 3.11–3.13 for the cable jackets and in Figures 3.14–3.16 for the cable insulations. The T_0 value listed on each figure is the average tensile strength of unaged jacket or insulation. The tensile strength data are for the same number of samples and test conditions as for the elongation data (see Section 3.1.3). For the same reason there are no French PE elongation data in Section 3.1.3, there are no tensile strength data for the French PE cable jacket or insulation.

The tensile strength of the French EPR cable jacket, shown in Figure 3.11, does not indicate any clear trend during aging because it remained relatively constant except for low values at 84 and 200 kGy. After the accident irradiation, the tensile strength was within 15% of T_0 for all initial aging values. The accident steam exposure caused essentially no change in tensile strength except for a slight decrease for jackets initially aged to 28 kGy and a more substantial decrease for jackets initially aged to 200 kGy.

The tensile strength of the U.S. EPR cable jacket, shown in Figure 3.12, increased by more than 20% for aging doses up to 84 kGy, then decreased slightly until the tensile strength at 200 kGy was 15% higher than the unaged jacket. The tensile strength was relatively unchanged by the accident irradiation, but decreased during the accident steam exposure.

The tensile strength of the U.S. XLPO cable jacket, shown in Figure 3.13, increased by more than 15% for aging doses up to 84 kGy, then decreased for larger aging doses until the tensile strength at 200 kGy was essentially the same as the unaged jacket. The tensile strength was decreased by the accident irradiation, and was further decreased during the accident steam exposure.

The U.S. EPR and U.S. XLPO cable jackets are both made of Hypalon and exhibited very similar tensile strength behavior, which might lead one to erroneously think that their Hypalon formulations are similar[4]; note, however, that the density measurements in Section 3.1.1 showed that the U.S. EPR jacket is clearly less dense than the U.S. XLPO jacket. The only real difference is that the tensile strength after aging is slightly above the unaged value for the U.S. EPR jacket and slightly below for the U.S. XLPO jacket; however, because of the difference in T_0 for the two jackets, the tensile strengths are actually very close after aging. The accident steam exposure decreased the tensile strength of both jackets from their accident irradiation values. The tensile strength of the French EPR Hypalon jacket does not closely follow the tensile strength behavior of the U.S. EPR or U.S. XLPO Hypalon jackets; however, its tensile strength values are in the same general range as the other two Hypalon jackets.

The tensile strength of the French EPR cable insulation, shown in Figure 3.14, never varied more than 5% from the unaged value during aging and was relatively unchanged by the accident irradiation. Except for the initially unaged specimen, the accident steam exposure caused a small decrease in tensile strength.

The tensile strength of the U.S. EPR cable insulation, shown in Figure 3.15, was also relatively unchanged during aging and the accident irradiation. In general, the accident steam exposure caused a slight decrease in tensile strength.

The tensile strength of the U.S. XLPO cable insulation, shown in Figure 3.16, increased almost linearly with dose during aging until it was 15% higher than the unaged insulation at 200 kGy. The tensile strength decreased during the accident irradiation and increased slightly during the accident steam exposure.

[4] When a given measurement gives different results for two specimens, then the specimens clearly have different formulations. However, the converse is not true. If a given density or tensile property measurement is identical for two specimens, this does not show that the specimens have identical formulation.

3.2 Electrical Measurement Results

The electrical measurement data presented here are from the complete cable specimens; no electrical measurements were performed on the cut specimens. Previous work has shown that electrical property measurements typically do not show significant changes with aging; mechanical measurements, most notably elongation at break, generally provide a better indication of aging degradation [3, 4, 5]. However, electrical measurements are simple to perform and can be done without destroying the cables under test.

3.2.1 High Potential

AC charging/leakage current data are plotted versus test condition for both cable conductors and shields in Figures 3.17–3.20. High potential ac measurements were performed at 11 times during the testing—the legends on Figures 3.17–3.20 describing these 11 measurement times correspond to the environmental conditions listed in Table 3.2. In these figures, a data point is plotted for each measurement taken (*i.e.*, every ac charging/leakage current measurement, not just average data, is shown). The fact that the data points tend to overlap one another at each of the 11 measurement times demonstrates the small scatter in the data.

The ac charging/leakage current of the French EPR cable is shown in Figure 3.17, the French PE cable in Figure 3.18, the U.S. EPR cable in Figure 3.19, and the U.S. XLPO cable in Figure 3.20. In all four figures, the conductor ac charging/leakage currents remained relatively constant over the entire test. The French EPR and U.S. XLPO conductors showed slightly lower charging currents for the baseline, pre-accident dose, and pre-steam measurements. This was probably due to these measurements being performed at room temperature with the test chamber removed from the LICA pool. However, for both these conductors, post-steam measurements (performed at room temperature and out of the LICA pool) did not show a similar low value for ac charging/leakage current.

The ac charging/leakage currents for the French PE and U.S. EPR shields are included in Figures 3.18 and 3.19. Because of the difference in the applied ac voltages (2000 Vac for conductors versus 600 Vac for shields), the ac charging/leakage currents were expected to be smaller for the shields than for the conductors. This was only true for measurements performed at room temperature and out of the LICA pool. For measurements performed in the LICA pool at 40°C during aging and 70°C during the accident irradiation, the shield ac charging/leakage currents were typically larger than those for the conductors. Note, however, that jacket materials are often chosen for their mechanical properties rather than their electrical properties; this could contribute to the difference in ac charging/leakage current levels seen for the shields and conductors.

The U.S. EPR shield ac charging/leakage currents increased during aging, but remained relatively constant or decreased slightly during the accident irradiation. The French PE shield ac charging/leakage currents initially increased during aging, but then remained constant for 2 weeks of aging through 1 week of the accident radiation exposure. However, the currents greatly increased for several of the shields by the fourth week of the accident irradiation. By the end of the accident radiation exposure, all of the aged French PE shields had very large ac charging/leakage currents. At the completion of the accident steam exposure, even the unaged French PE shield had very large ac charging/leakage currents.

If a typical cable is assumed to have a capacitance of roughly 98.4 pF/m (30 pF/ft) and the complete cable specimens are approximately 22.9 m (75 ft) long, then the cable impedance for 60 Hz excitation would be:

$$Z = \frac{1}{\omega C} = \frac{1}{(2\pi f)C}$$
$$= \frac{1}{(2\pi \times 60)(30 \times 10^{-12} \times 75)} = 1.18 \times 10^{6}\Omega.$$

For the 2000 Vac conductor excitation voltage, this results in a capacitive charging current of 1.7 mAac. The ac charging/leakage current measurement is the sum of the current actually leaking from the conductor through the insulation to a ground outside the cable plus the current necessary to charge and discharge the capacitance of the cable dielectric (insulation) as the applied cable voltage changes. This differs from an IR measurement, which only gives the dc leakage of current from the conductor through the insulation to a ground outside the cable (assuming the dc voltage has been applied long enough for initial transients to die off). At 2000 Vac, the cable IR must be less than

Table 3.2: Environmental Conditions for the 11 Discrete Times at which AC Charging/Leakage Current Measurements Were Performed during the Test.

Legend on	Approximate Dose		Environmental Conditions		
Figures 3.17–3.20	Aged Cable	Unaged Cable	Dose Rate	Temperature	In LICA Pool?[a]
baseline	0 Gy	—	0 Gy/hr	ambient	no
		Start of Aging Radiation Exposure			
aging 1 week	18 kGy	—	100 Gy/hr	40°C	yes
aging 2 weeks	37 kGy	—	100 Gy/hr	40°C	yes
aging 3 weeks	52 kGy	—	100 Gy/hr	40°C	yes
aging 4 weeks	71 kGy	—	100 Gy/hr	40°C	yes
aging 5 weeks	83 kGy	—	100 Gy/hr	40°C	yes
		End of Aging Radiation Exposure			
pre-acc. dose	84 kGy	0 kGy	0 Gy/hr	ambient	no
		Start of Accident Radiation Exposure			
acc. dose 1 week	191 kGy	107 kGy	900 Gy/hr	70°C	yes
acc. dose 4 weeks	662 kGy	578 kGy	900 Gy/hr	70°C	yes
		End of Accident Radiation Exposure			
pre-steam	684 kGy	600 kGy	0 Gy/hr	ambient	no
		Accident Steam Exposure			
post-steam	684 kGy	600 kGy	0 Gy/hr	ambient	no

[a] "Yes" means the test chamber was at the bottom of the LICA pool; note that the test chamber interior was never flooded and thus the portion of the cable exposed to the environmental condition was not submerged; however, the portion of the cable outside the test chamber was in direct contact with the pool water when the test chamber was in the pool.

2 MΩ before leakage through the conductor is comparable to a typical capacitive charging current. Because typical measured IRs are greater than 10^8 Ω (see Figures 3.21–3.32), the capacitive charging current accounts for a substantial portion of the ac charging/leakage current shown in Figures 3.17–3.20. Increases in the ac charging/leakage current are caused by a combination of increased cable capacitance or substantial decreases in the cable IR. The very large currents for the French PE shield in Figure 3.18 correspond to the decreased IR values in Figure 3.23. The overall cable capacitance is raised when the cable leads are surrounded by water instead of air. This is one reason why the measurements performed with the test chamber in water (see Table 3.2) tended to have a higher ac charging/leakage current than measurements in air.

The ac charging/leakage current did not change significantly with aging and thus is not a good indicator of aging degradation. Large changes in the ac charging/leakage current occur only when the cable is actually failing.

3.2.2 Insulation Resistance

Appendix B shows that measured IR values depend on the length of cable; for a given cable, the measured IR will decrease as the cable length is increased. Because of this, an IR of 500 kΩ for a 3-m long conductor is equivalent to an IR of 1.5 MΩ for a 1-m long conductor or 15 kΩ for a 100-m long conductor. Comparisons between IR values from different literature references are meaningful only after accounting for the cable length on which the measurement was performed.

Because the 23-m cable length consisted of approximately 20 m outside the test chamber and 3 m inside the test chamber (see Section 2.2.2), it is incorrect to state that the measured IR results are for a 23-m cable length because only the 3 m of cable inside the test chamber was subjected to the various environmental exposures that caused the IR changes. The development in Appendix B shows that the measured IR of the entire 23-m long cable quickly approaches the IR of the 3-m of cable in the test chamber as the measured IR decreases from its initial

value. Because of this, if an IR of 500 kΩ in Figures 3.21–3.32 is at least an order of magnitude less than the initial IR value, then it should be referred to as an IR of 500 kΩ-3 m.

The initial IR values of these cables are so high that some loss in sensitivity due to the long cable leads has no meaningful effect on the results. For instance, a typical initial IR measurement of 10^{11} Ω is not an IR of 10^{11} Ω-3 m for the 3-m section of cable in the test chamber, but is actually an IR of 10^{11} Ω-23 m ($= 7.67 \times 10^{11}$ Ω-3 m) for the entire 23-m long cable. Such initial IR values are all so high that a difference of 7.67 makes no practical difference. Only when the measured IR has decreased significantly does it become meaningful to know the actual IR value; it is precisely under these conditions that the measured IR value is equivalent to the IR of the 3 m of cable wrapped around the mandrel in the test chamber.

Because the effective length of cable for which the IR measurement was performed changed over the course of the test program, no length is reported for the IR data in Figures 3.21–3.32. However, the discussion in the previous paragraphs and in Appendix B has made the reader aware of how the cable length affects the interpretation of the IR data presented. The authors decided not to "correct" the measured IR data to calculate "3 m test section IR values" because of the additional uncertainty that would be added by attempting to compensate the already noisy IR data by using an equation developed from an idealized model of a cable system. Because of limitations in the accuracy of the measuring equipment, discrete IR measurements were cut off above 2.0×10^{12} Ω and continuous IR measurements were cut off above 1.0×10^{8} Ω.

Aging and Accident Irradiation

IR data during the aging and accident irradiation are plotted versus radiation dose for both cable conductors and shields in Figures 3.21–3.26. In these figures, each plotted point is the average and the bars show the sample standard deviation for the IR measurements. Ambient IR measurements were performed before the start of aging, after aging but prior to accident irradiation, and after completion of the accident irradiation. The ambient measurements were performed at laboratory ambient temperature with the test chamber and cable leads out of the LICA pool, and thus are typically above IR data acquired at the higher temperatures present during aging and accident irradiation. IR measurements were performed 5 times during aging (cables at 40°C) for each of the voltages; these measurements are indicated by white symbols in the figures. IR measurements were performed 3 times during the accident irradiation (cables at 70°C) for each of the voltages; these measurements are indicated by black symbols in the figures.

The conductor-to-ground IR of the French EPR cable is shown in Figure 3.21. During aging, the IR values initially fell slightly for doses out to 40 kGy, but recovered their initial values by the end of aging. The IR values were relatively constant during the accident irradiation. The IR measurements were never below 10^{10} Ω during the aging or accident irradiation.

The conductor-to-ground IR of the French PE cable is shown in Figure 3.22, and its shield-to-ground IR is shown in Figure 3.23. The conductor-to-ground IR increased with dose during aging. This trend reversed during the accident irradiation; however, the conductor-to-ground IR always remained near or above 10^{10} Ω. In contrast, the shield-to-ground IR data show that most of the French PE shields failed during the accident irradiation (as previously indicated in Figure 3.18). All the shield-to-ground IR values during aging were near or above 10^{10} Ω and, except for shield 42, remained at these levels during the accident irradiation for total doses out beyond 600 kGy. At the start of the accident irradiation, the IR of shield 42 quickly dropped to levels below 30 MΩ and fell to 250–350 kΩ at a total dose of 688 kGy. Shield 41 had a 250 Vdc IR of 8.1 MΩ at 665 kGy; however, shields 41 and 43 had completely failed by the time of the 50 and 100 Vdc IR measurements at 688 kGy. The only French PE shield to complete the accident irradiation without a substantial drop in IR was shield 44[5]; however, no measurements were performed on this shield for doses above 605 kGy. As noted in Section 3.1.3, the French PE jacket became cracked and was very brittle, which could lead to the observed large shield-to-ground IR decreases.

The shield-to-ground IR of the U.S. EPR cable is shown in Figure 3.24, and its conductor-to-ground IR is shown in Figure 3.25. During aging, the conductor-to-ground IR values initially fell slightly for doses out to 40 kGy, but recovered their initial values by the end of aging. The conductor-to-ground IR

[5]Shield 44 was the unaged French PE shield.

values were relatively constant during the accident irradiation. The conductor-to-ground IR measurements were typically around 10^{11} Ω, and were never below 10^{10} Ω during the aging or accident irradiation. The shield-to-ground IR measurements remained relatively constant throughout both the aging and accident irradiation, falling slightly with increasing dose. The shield-to-ground IR values were typically around 2×10^{9} Ω, which is almost two orders of magnitude smaller than the conductor-to-ground IR values.

The conductor-to-ground IR of the U.S. XLPO cable is shown in Figure 3.26. There was a fair amount of scatter in the aging IR data; it seemed to fall slightly for doses out to 40 kGy, but then recovered its initial values by the end of aging. The IR values fell slowly but monotonically for the duration of the accident irradiation; the final IR values were just below 10^{10} Ω.

Accident Steam Exposure

IR data during the accident steam exposure are plotted versus time from the start of the steam exposure for both cable conductors and shields in Figures 3.27–3.32. In these figures, each plotted point is the average and the bars are the sample standard deviation for the IR measurements. Black symbols in the figures indicate IR data for conductors that were irradiated with an aging dose of 84 kGy and an *accident* dose of 600 kGy before being exposed to the steam. Dotted symbols in the figures indicate IR data for conductors that were only irradiated with an accident dose of 600 kGy before being exposed to the steam (*i.e.*, they were unaged before the accident). The ambient measurements at 0 sec were performed prior to the start of the accident steam exposure, and the ambient measurements at 15 days were performed when the test chamber had cooled down after the accident steam exposure ended. The remainder of the IR measurements were acquired at the pressures and temperatures indicated in Table 2.4 and in Figure 2.7.

In general, the IR measurements inversely mirrored the environmental conditions (*i.e.*, IR decreased as temperature and pressure increased, and IR increased when temperature and pressure decreased). The IR measurements performed at laboratory ambient temperature are always greater than those acquired at the higher temperatures present during the rest of the accident steam exposure. For all cables, the IR decreased by at least two orders of magnitude during the transient at the start of the accident steam exposure.

The conductor-to-ground IR of the French EPR cable during the accident steam exposure is shown in Figure 3.27. The IR remained above 10^{9} Ω during the steam transient and then recovered back to near 10^{11} Ω. When the temperature jumped at the start of day 4, the IR decreased to approximately 4×10^{10} Ω and remained there for the duration of the accident steam exposure. There was no difference between measured IRs of aged and unaged specimens.

The conductor-to-ground IR of the French PE cable during the accident steam exposure is shown in Figure 3.28. The IR remained above 10^{10} Ω during the steam transient and then recovered back to near 10^{12} Ω. The IR was relatively unaffected by the temperature jump at the start of day 4; the IR remained near 10^{12} Ω for the duration of the accident steam exposure. The unaged specimens had slightly higher IRs than the aged specimens.

The shield-to-ground IR of the French PE cable during the accident steam exposure is shown in Figure 3.29. All of the shields had failed prior to the first set of IR measurements, which were performed approximately 80 min after the start of the accident steam exposure. This behavior was not unexpected based on the shield IR failures that occurred during the accident irradiation (see Figures 3.18 and 3.23).

The shield-to-ground IR of the U.S. EPR cable during the accident steam exposure is shown in Figure 3.30. Compared with conductor-to-ground IRs, the shield-to-ground IRs were smaller and were more influenced by temperature changes. The shield-to-ground IR fell to values as low as 500 kΩ during the steam transient before recovering back to near 100 MΩ. When the temperature jumped from 80°C to 100°C at the start of day 4, the IR immediately decreased to approximately 10 MΩ; for the remainder of the accident steam exposure, the IR decreased only slightly. The shield-to-ground IR recovered by a factor of 1000 for the IR measurement taken at ambient temperature at the end of the accident steam exposure. There was no difference between measured IRs of aged and unaged specimens.

The conductor-to-ground IR of the U.S. EPR cable during the accident steam exposure is shown in

Figure 3.31. The IR remained above 10^9 Ω during the steam transient and then recovered back to near 10^{12} Ω. When the temperature jumped from 80°C to 100°C at the start of day 4, the IR decreased to approximately 3×10^{11} Ω and remained there for the duration of the accident steam exposure. There was no difference between measured IRs of aged and unaged specimens.

The conductor-to-ground IR of the U.S. XLPO cable during the accident steam exposure is shown in Figure 3.32. The IR values fell slightly below 10^8 Ω during the steam transient before recovering back to slightly above 10^{11} Ω. The IR drop below 10^8 Ω is also shown by the continuous IR trace; this was the only cable where the IR values fell far enough that meaningful continuous IR measurements could be acquired.[6] When the temperature jumped at the start of day 4, the IR decreased to approximately 2×10^{10} Ω and remained there for the duration of the accident steam exposure. There was no difference between measured IRs of aged and unaged specimens.

3.3 Summary of Experimental Results

Sections 2 and 3 have presented the NRC-sponsored, U.S. test activities performed at Sandia National Laboratories as part of a cooperative U.S./French program to investigate the long-term aging of electrical cables. This subsection summarizes the U.S. test results; see Section 5.4 for a summary of the French test results and Section 6.3 for a summary of the comparison between the two test programs.

Mechanical measurements (density, hardness, elongation, and tensile strength) were performed on the cut cable specimens.

- In general, the density tended to increase during the aging and accident irradiation for all the cable insulations and jackets; however, the uncertainty range of the measurements was large compared with the apparent increase. There was no consistent trend during the accident steam exposure.
- The hardness measurements did not show any clear trend; they remained relatively constant except for the French EPR cable's hardness, which increased by approximately 60% during the aging and accident irradiation.
- The elongation at break data showed the most clear trend; for all cable jackets and insulations, the elongation at break decreased monotonically with increasing dose during aging and accident irradiation, typically having a residual elongation near 25% of its unaged value after the 800 kGy radiation exposure. The effect of the accident steam exposure varied among the cable products. No tensile strength or elongation data were acquired for the French PE cable because its outer jacket could not be removed from the braided shield. The jacket quickly became brittle and cracked too easily to be removed in one piece.
- The tensile strength measurements showed no clear trends.

Electrical measurements (ac leakage current and dc insulation resistance) were performed on the complete cable specimens that were electrically energized during the environmental exposures. Whether the cables were aged before the simulated accident environment had almost no effect on measured electrical properties during the accident. The electrical measurements indicated that all the cables performed well except for the shield of the French PE cable, which showed severely degraded performance beginning late in the accident irradiation. Physical inspection of the French PE jacket showed that it was cracked and very brittle, which accounts for the degraded performance.

All the cables remained functional throughout the entire test except the shield of the French PE cable, which failed almost immediately after the start of the accident steam exposure. The conductor-to-ground IRs were typically greater than 10^9 Ω throughout the entire test, which is significantly higher than what is normally measured for cables tested to U.S. standards. This indicates that the French environmental exposures used for the current test program may cause less degradation than the environmental exposures used in typical U.S. test programs.

[6] As indicated in Table 2.3, the shields of the French PE and U.S. EPR cables were grounded during the accident steam exposure and thus no continuous IR measurements were performed to measure the low shield-to-ground IR values.

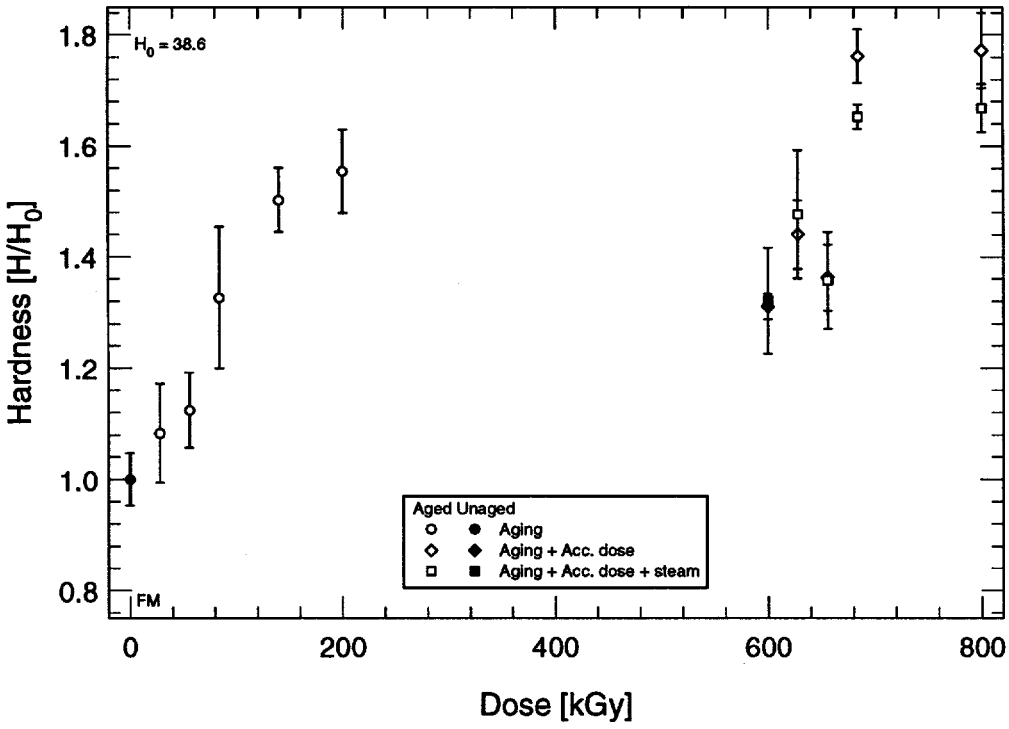

Figure 3.1: Hardness for French EPR cable.

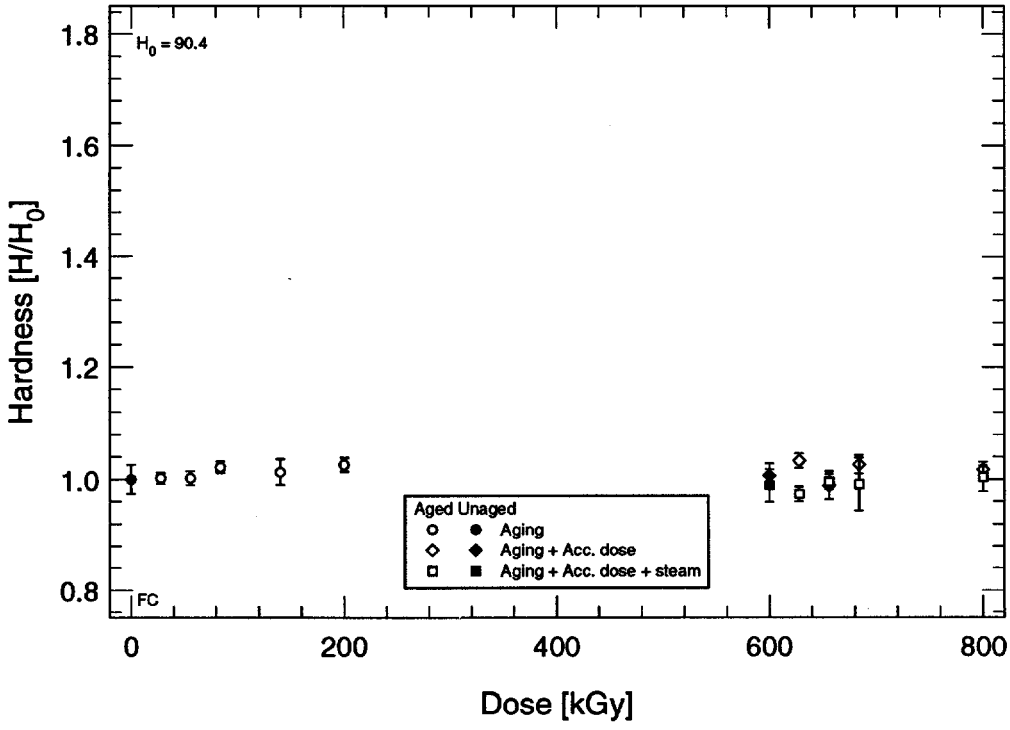

Figure 3.2: Hardness for French PE cable.

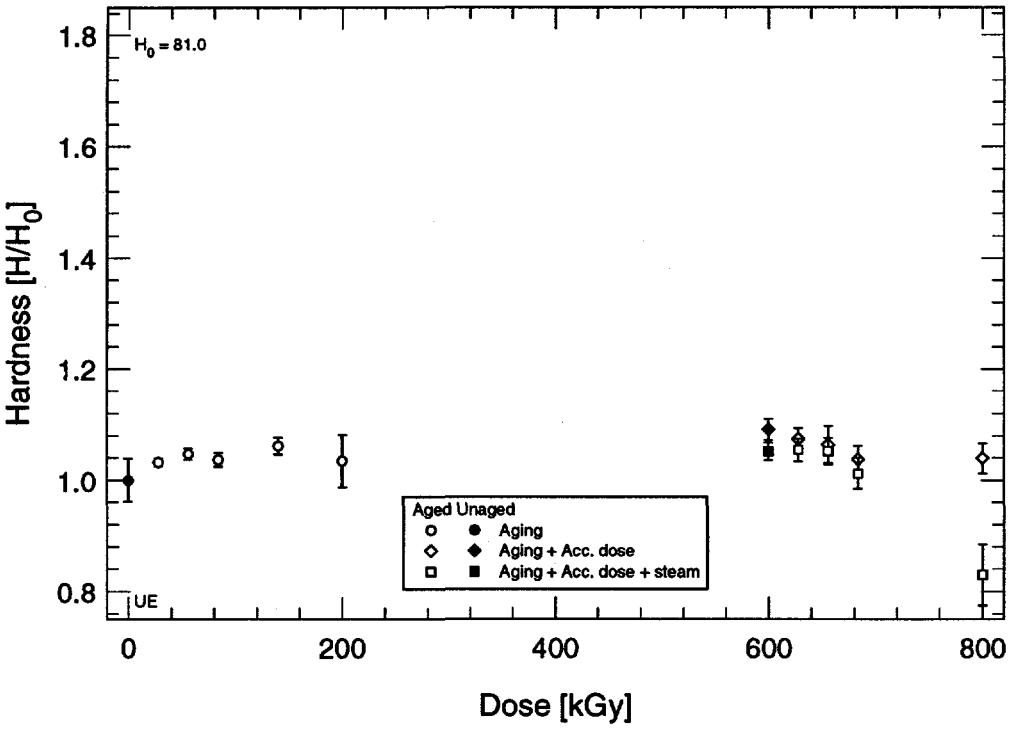

Figure 3.3: Hardness for U.S. EPR cable.

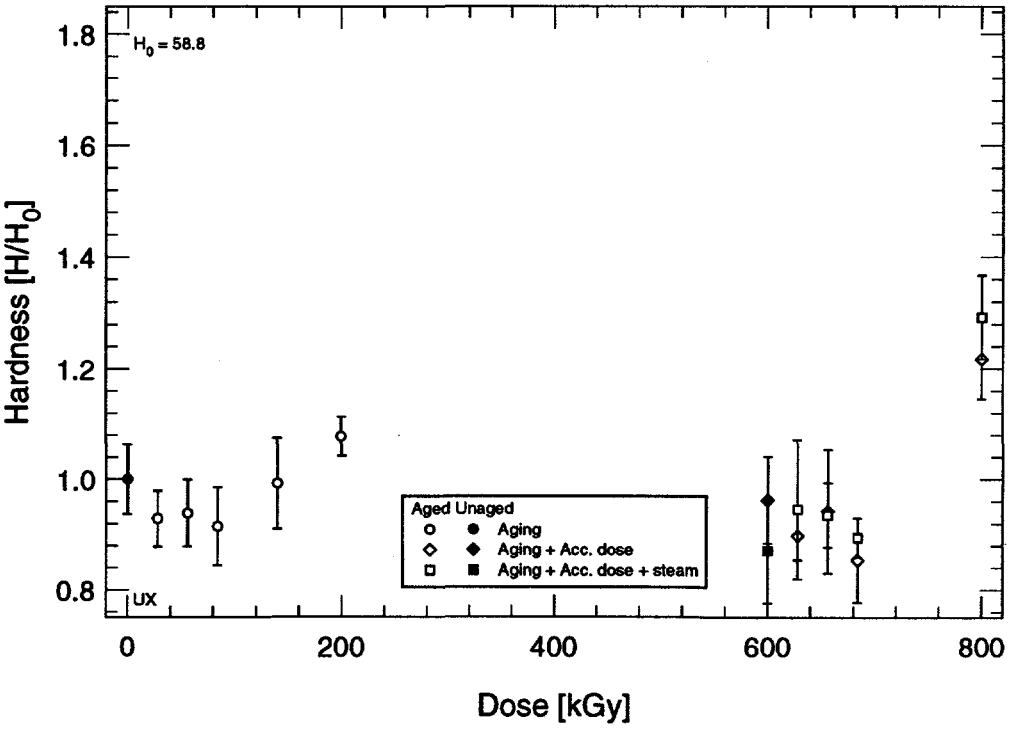

Figure 3.4: Hardness for U.S. XLPO cable.

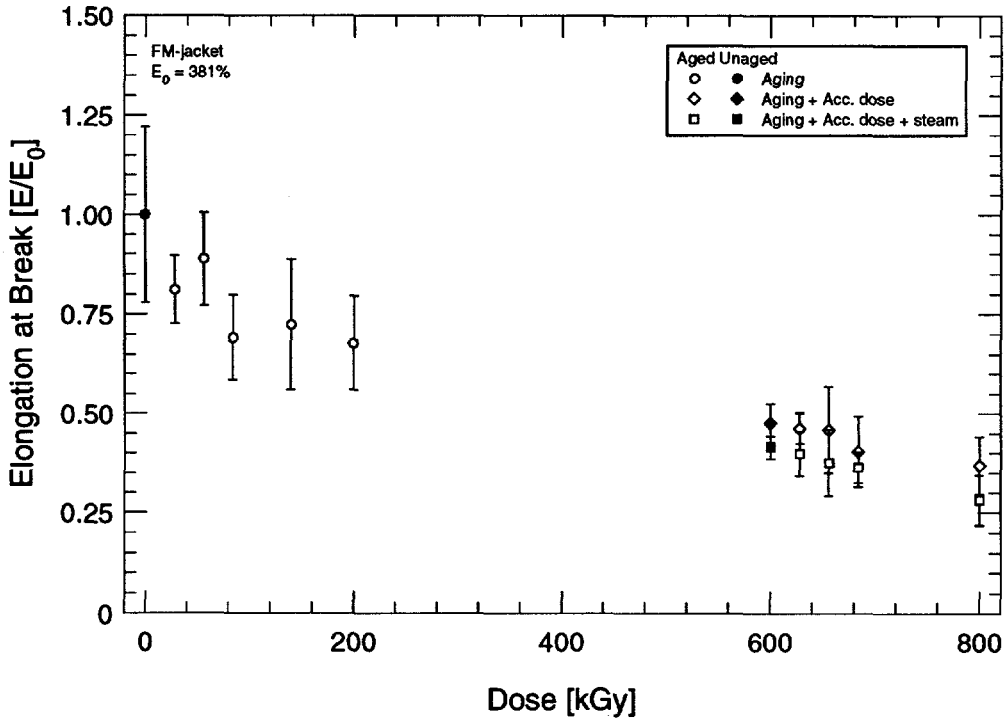

Figure 3.5: Elongation for French EPR cable—Hypalon jacket.

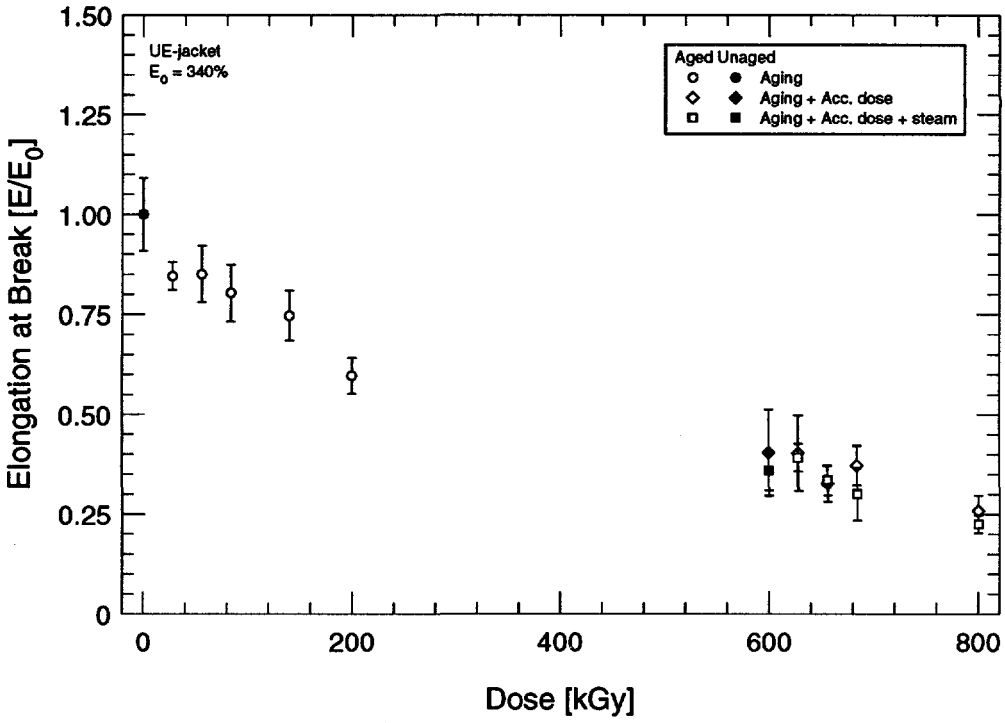

Figure 3.6: Elongation for U.S. EPR cable—Hypalon jacket.

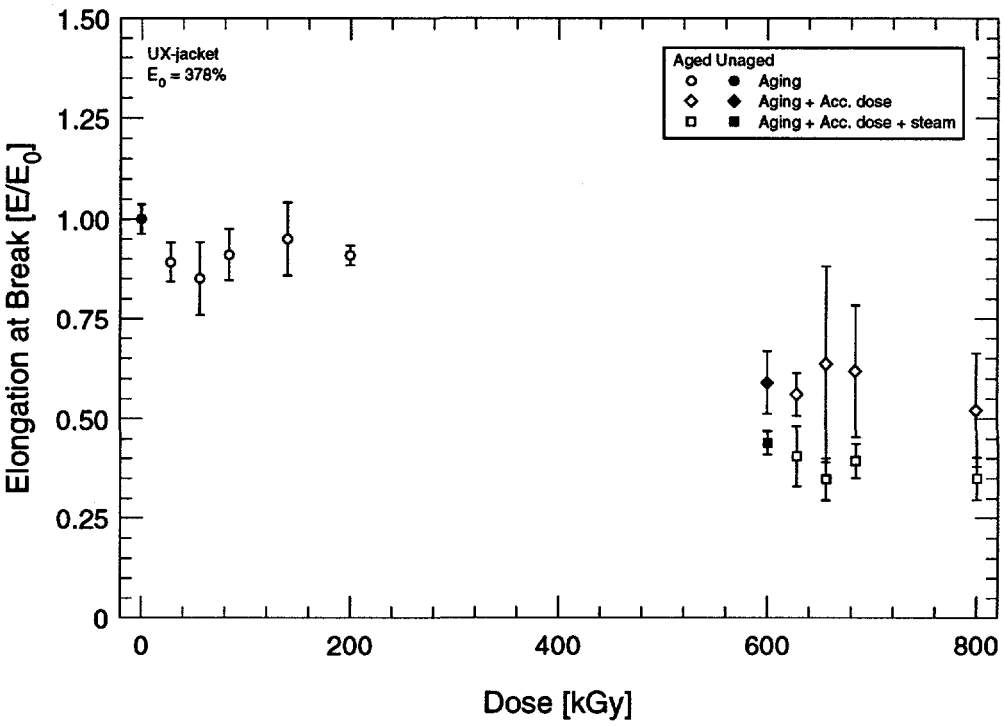

Figure 3.7: Elongation for U.S. XLPO cable—Hypalon jacket.

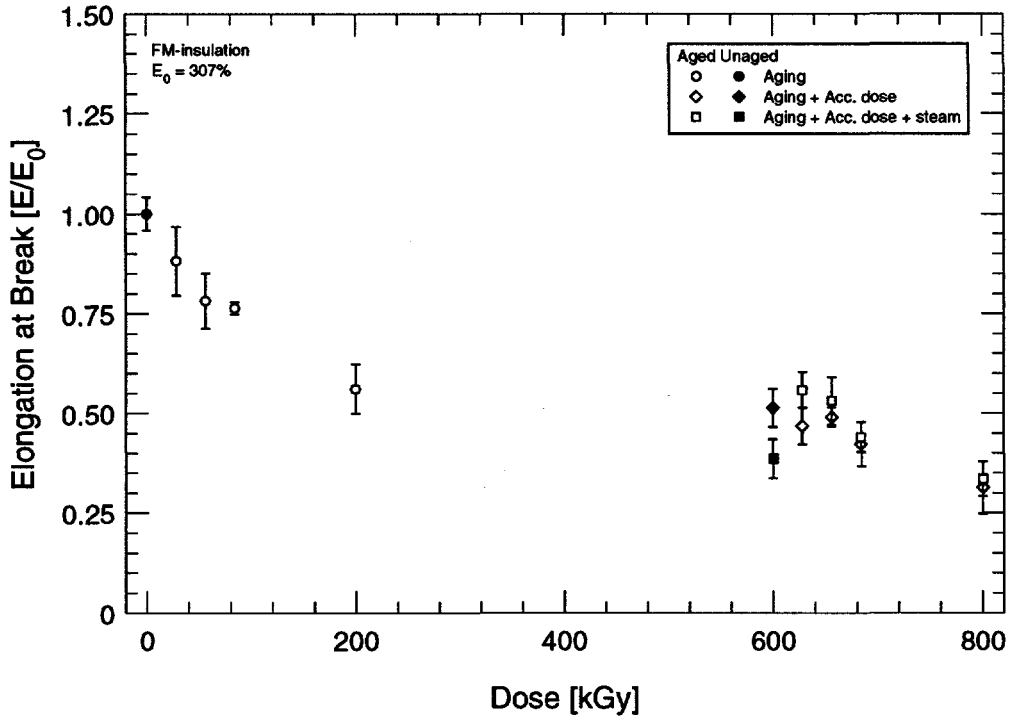

Figure 3.8: Elongation for French EPR cable—EPR insulation.

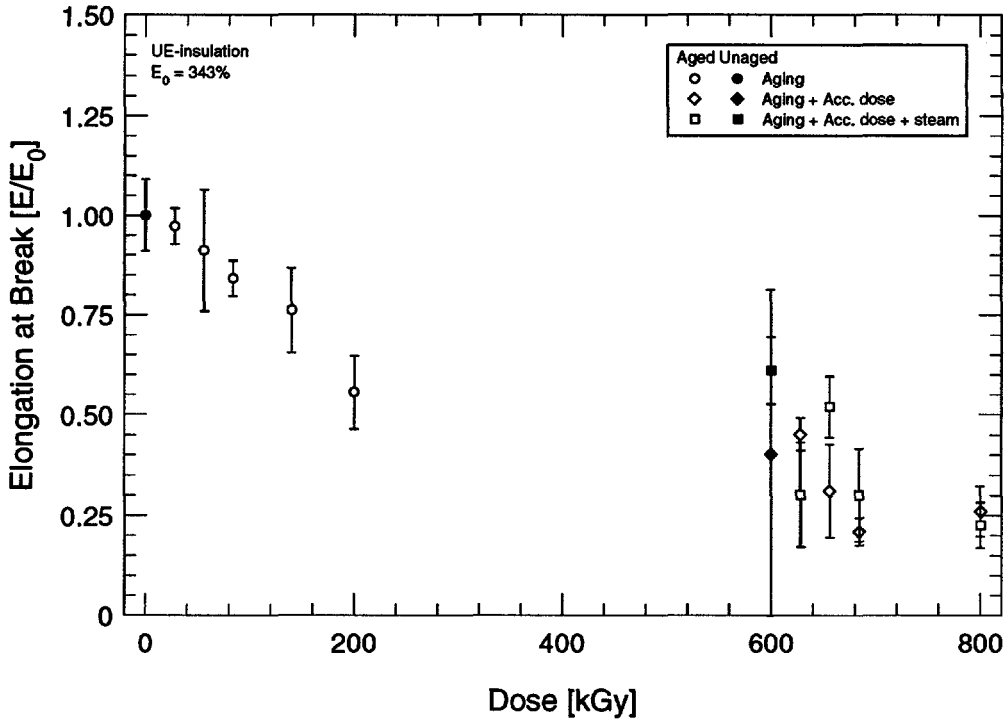

Figure 3.9: Elongation for U.S. EPR cable—FR-EPDM insulation.

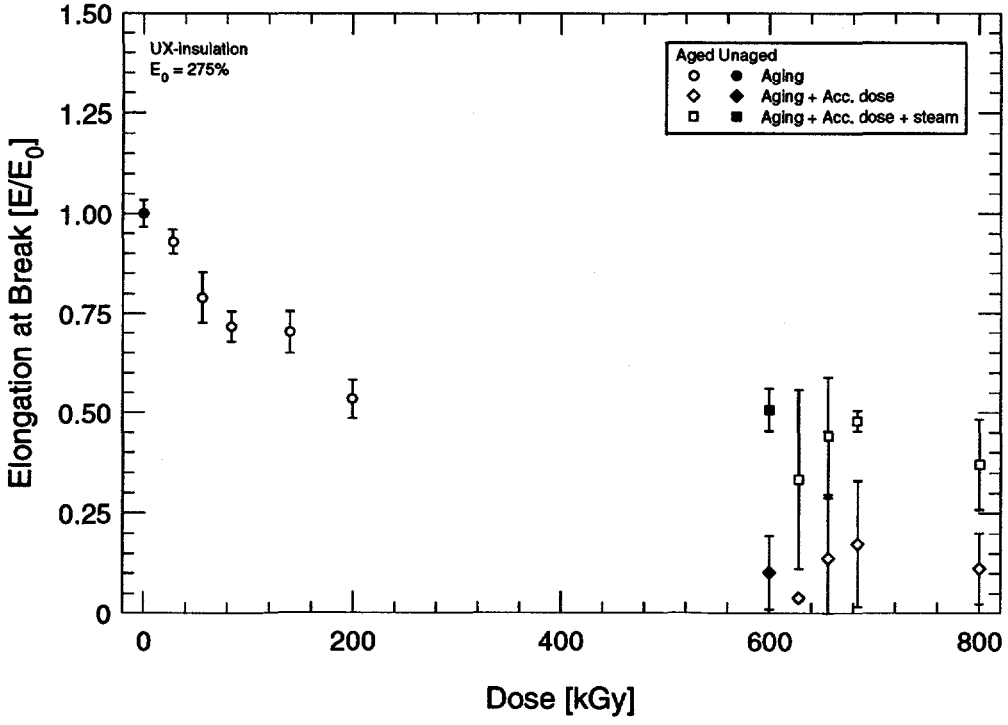

Figure 3.10: Elongation for U.S. XLPO cable—XLPE insulation.

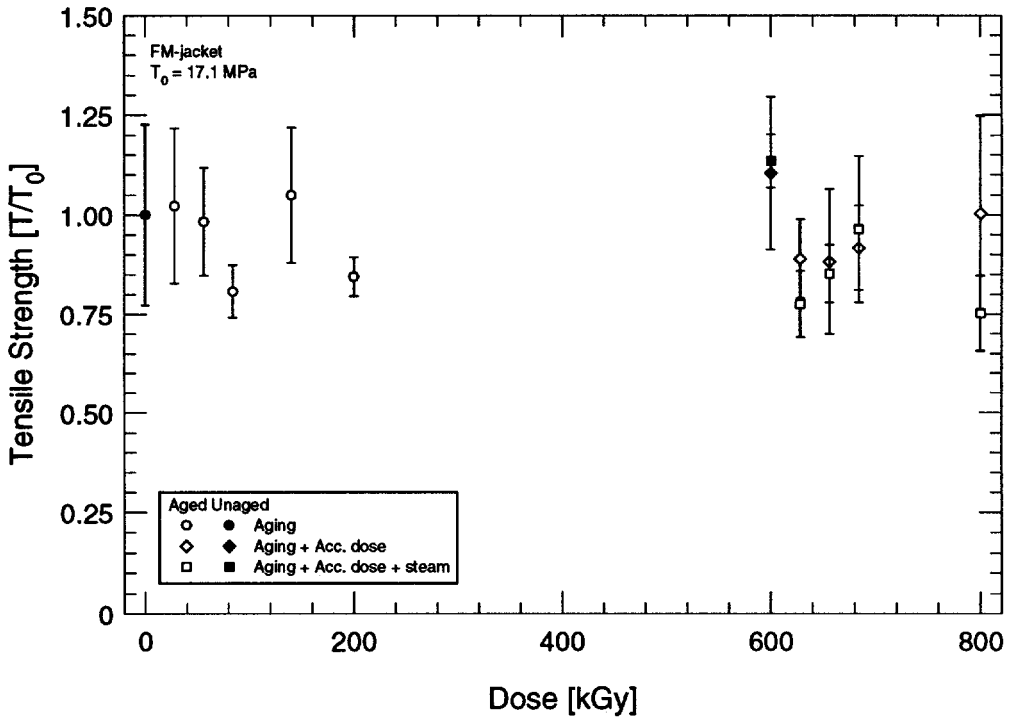

Figure 3.11: Tensile strength for French EPR cable—Hypalon jacket.

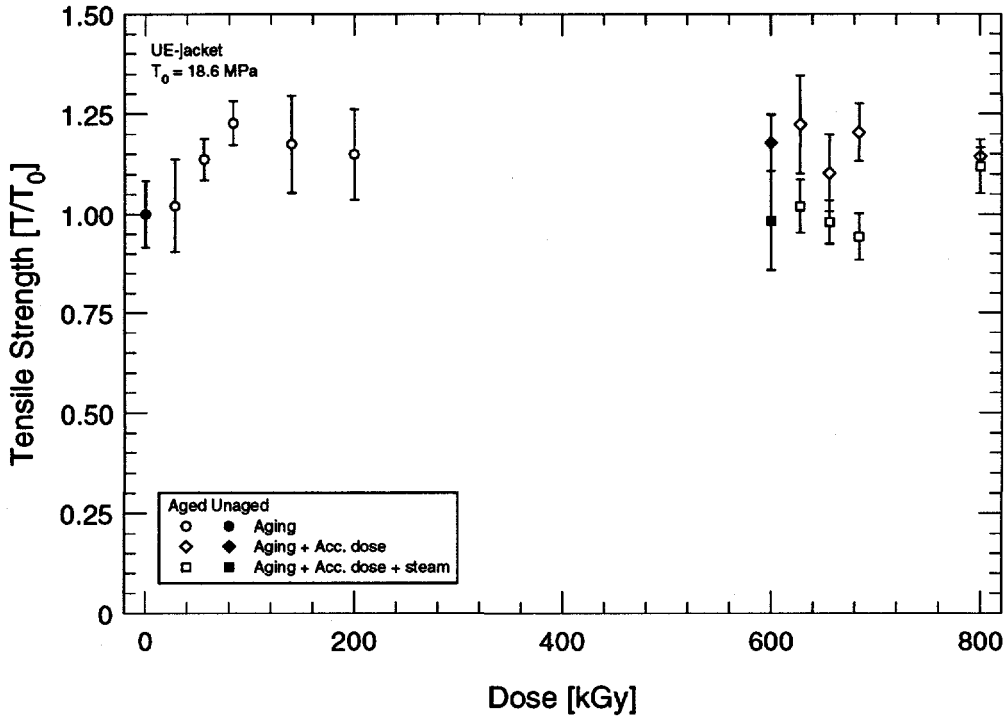

Figure 3.12: Tensile strength for U.S. EPR cable—Hypalon jacket.

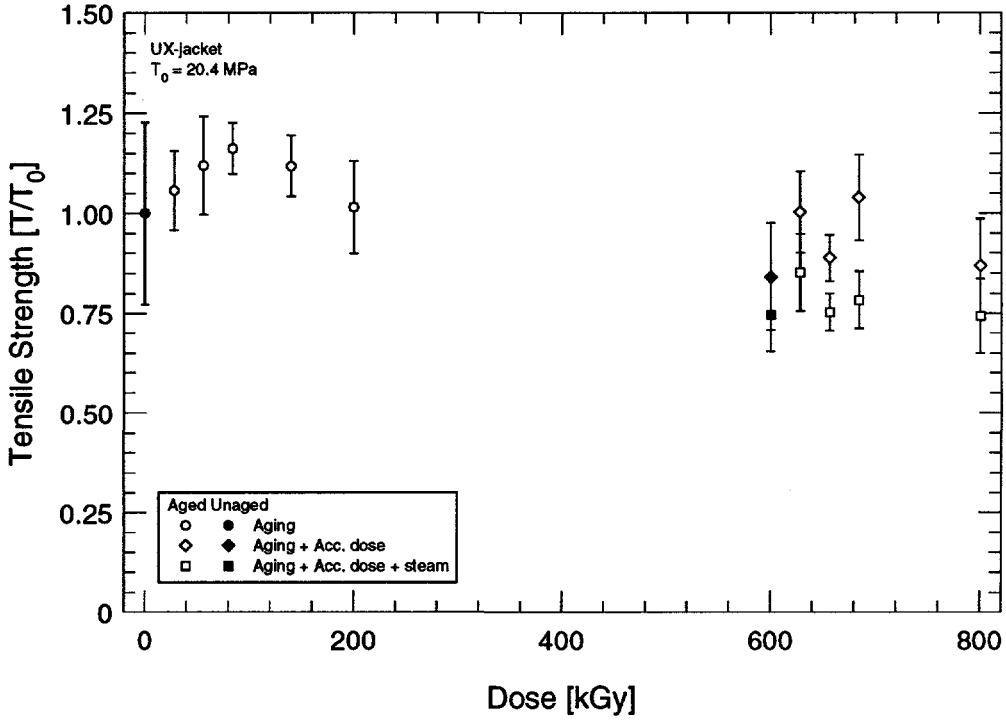

Figure 3.13: Tensile strength for U.S. XLPO cable—Hypalon jacket.

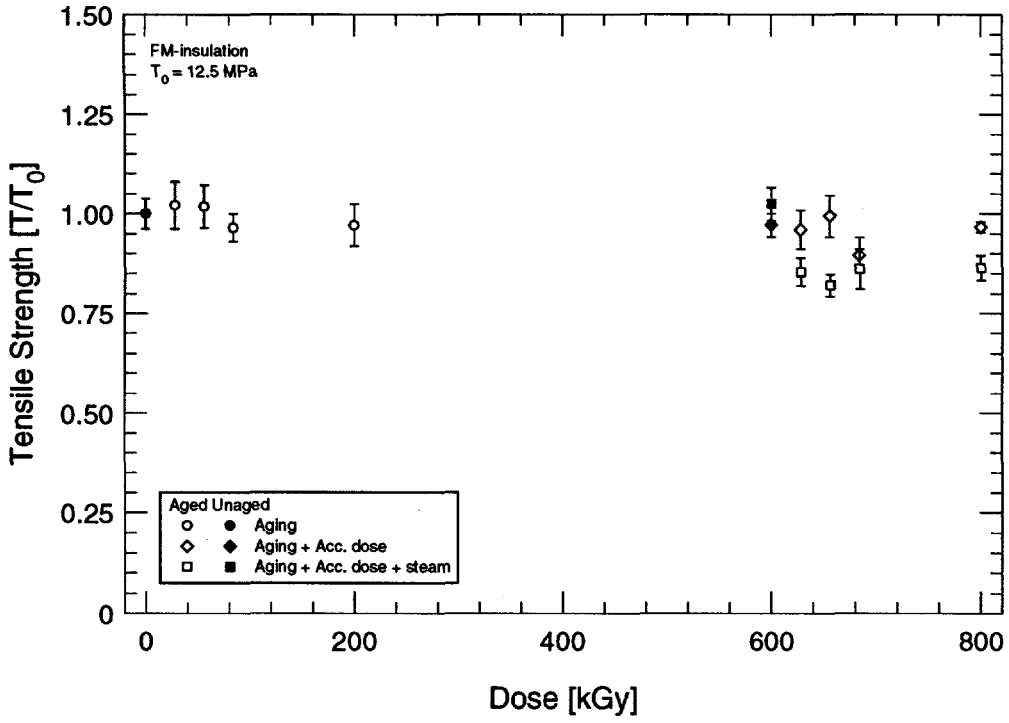

Figure 3.14: Tensile strength for French EPR cable—EPR insulation.

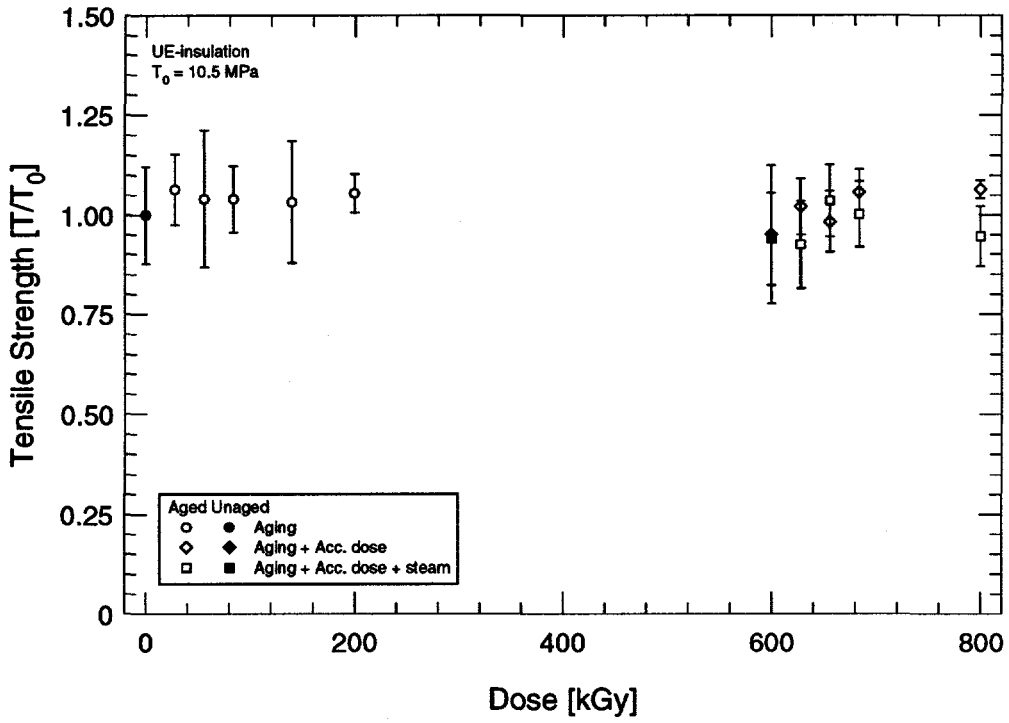

Figure 3.15: Tensile strength for U.S. EPR cable—FR-EPDM insulation.

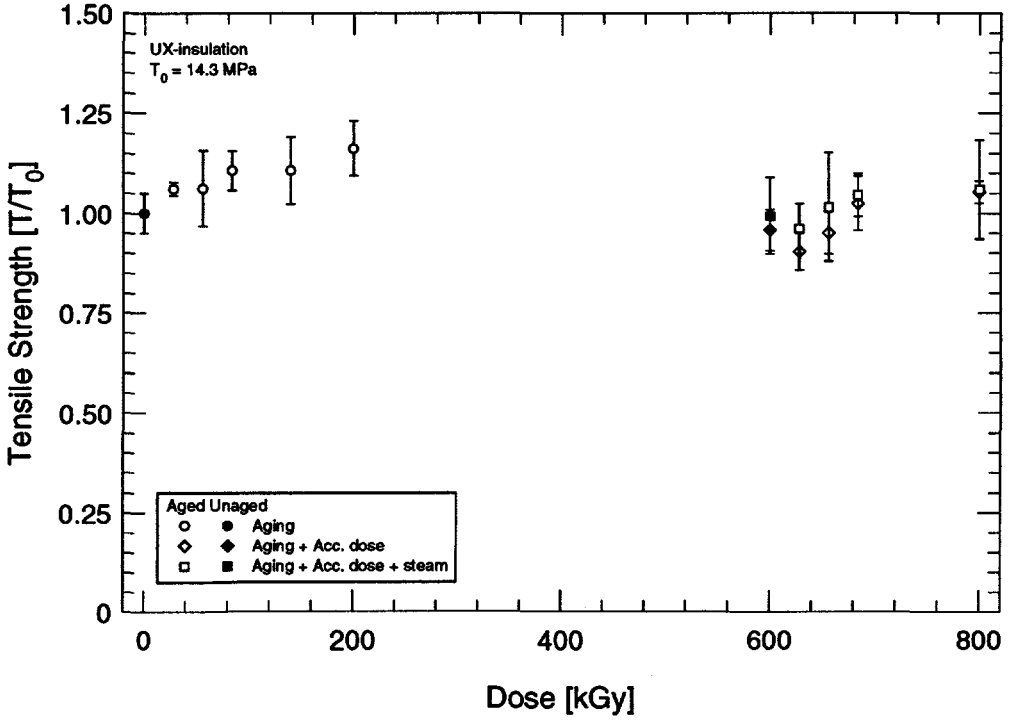

Figure 3.16: Tensile strength for U.S. XLPO cable—XLPE insulation.

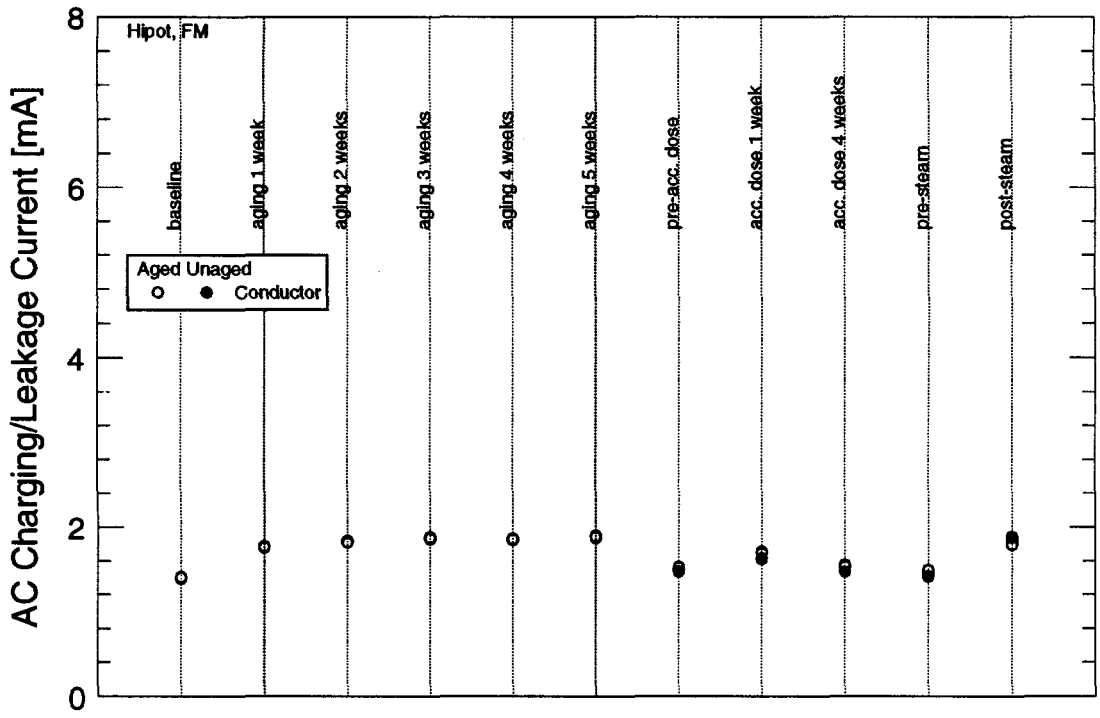

Figure 3.17: AC leakage current for French EPR cable.

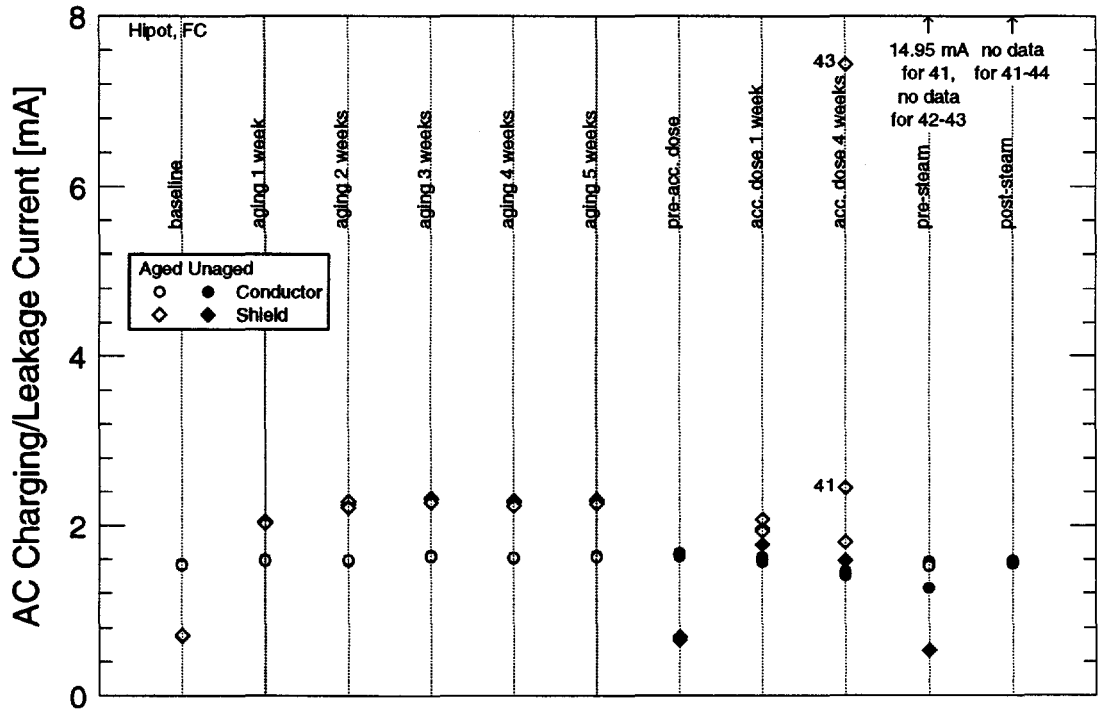

Figure 3.18: AC leakage current for French PE cable.

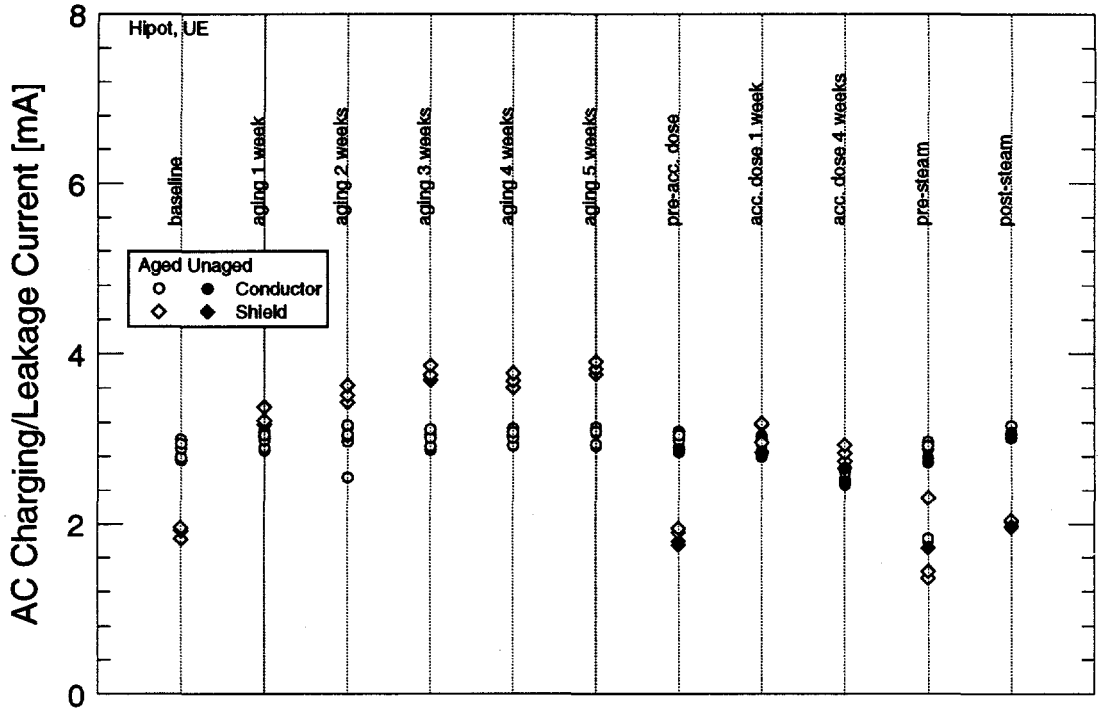

Figure 3.19: AC leakage current for U.S. EPR cable.

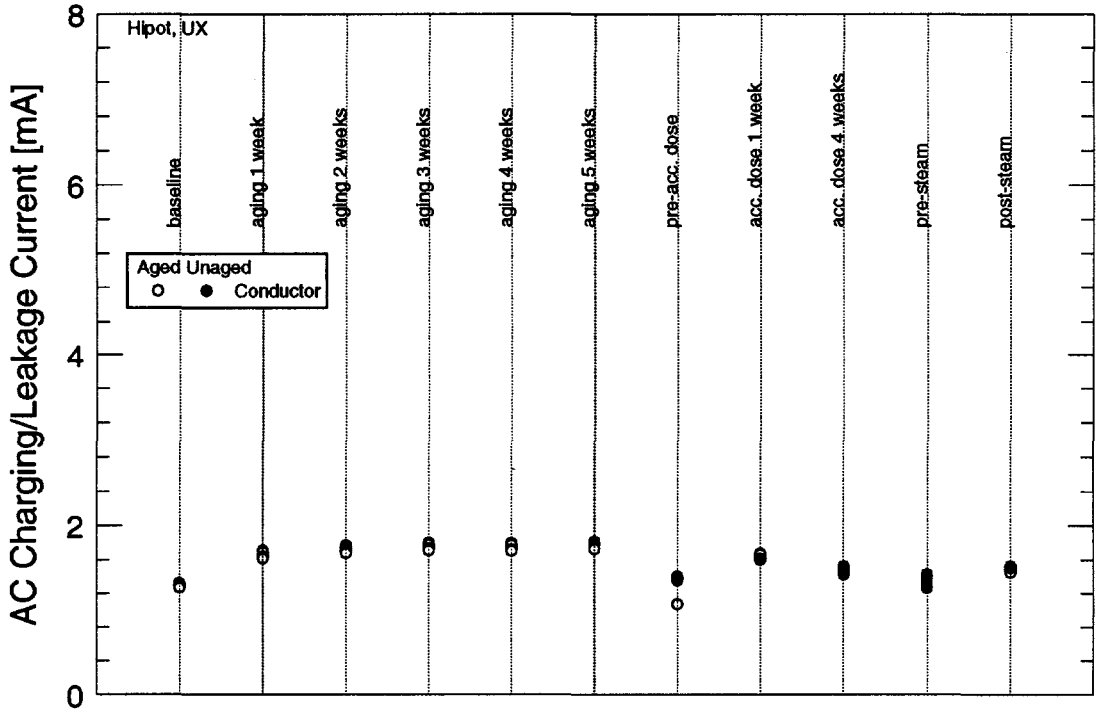

Figure 3.20: AC leakage current for U.S. XLPO cable.

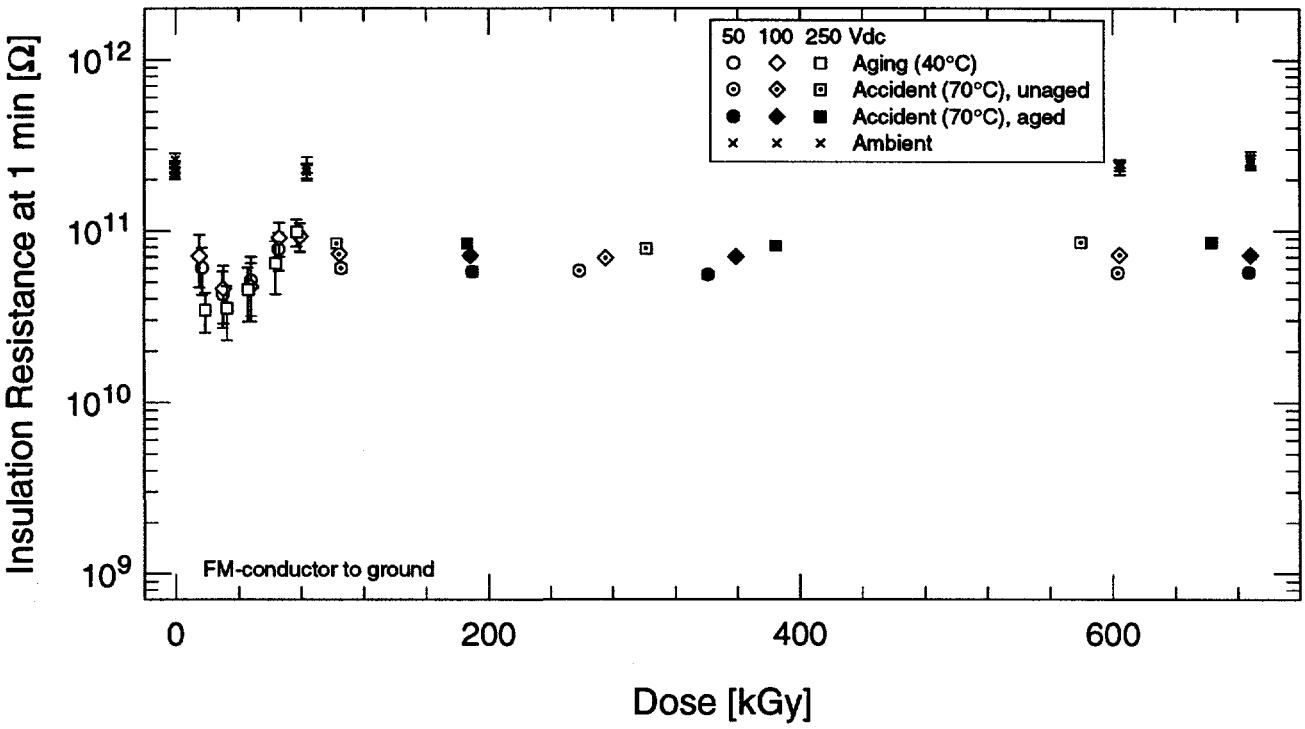

Figure 3.21: IR of French EPR cable during aging and accident irradiation—conductor to ground.

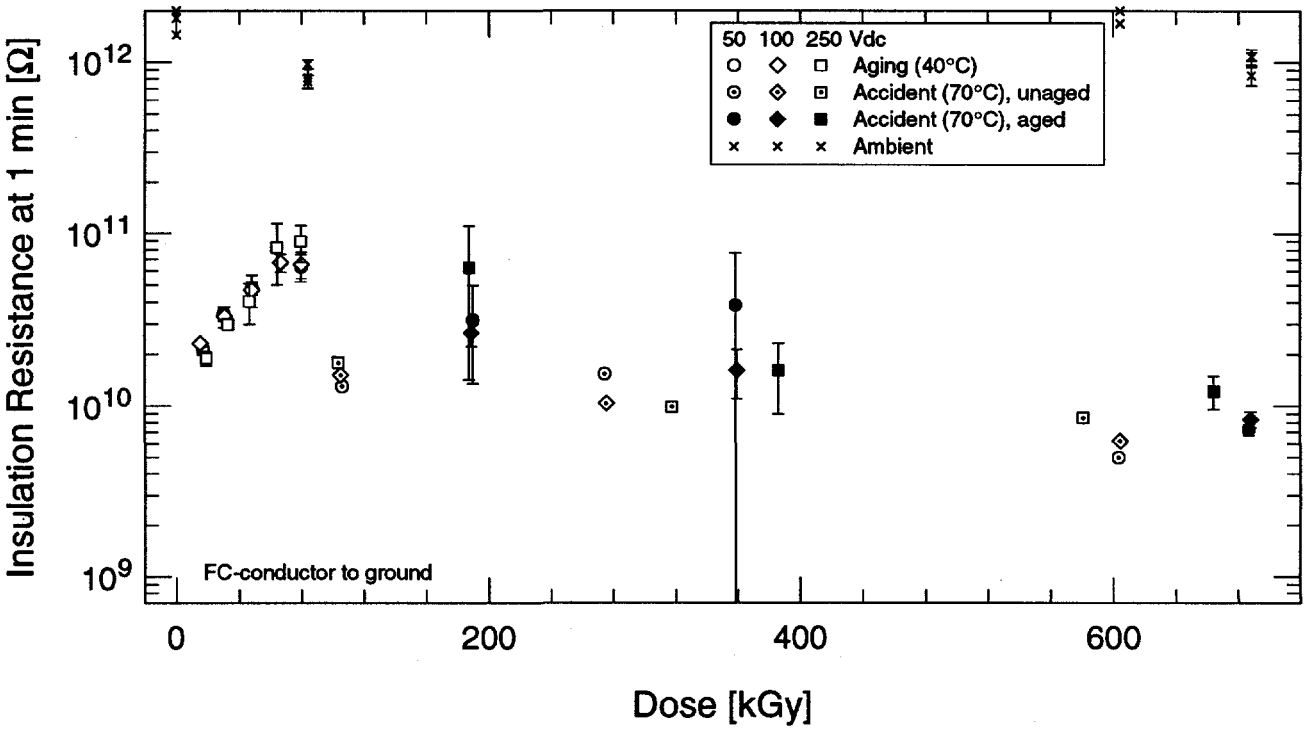

Figure 3.22: IR of French PE cable during aging and accident irradiation—conductor to ground.

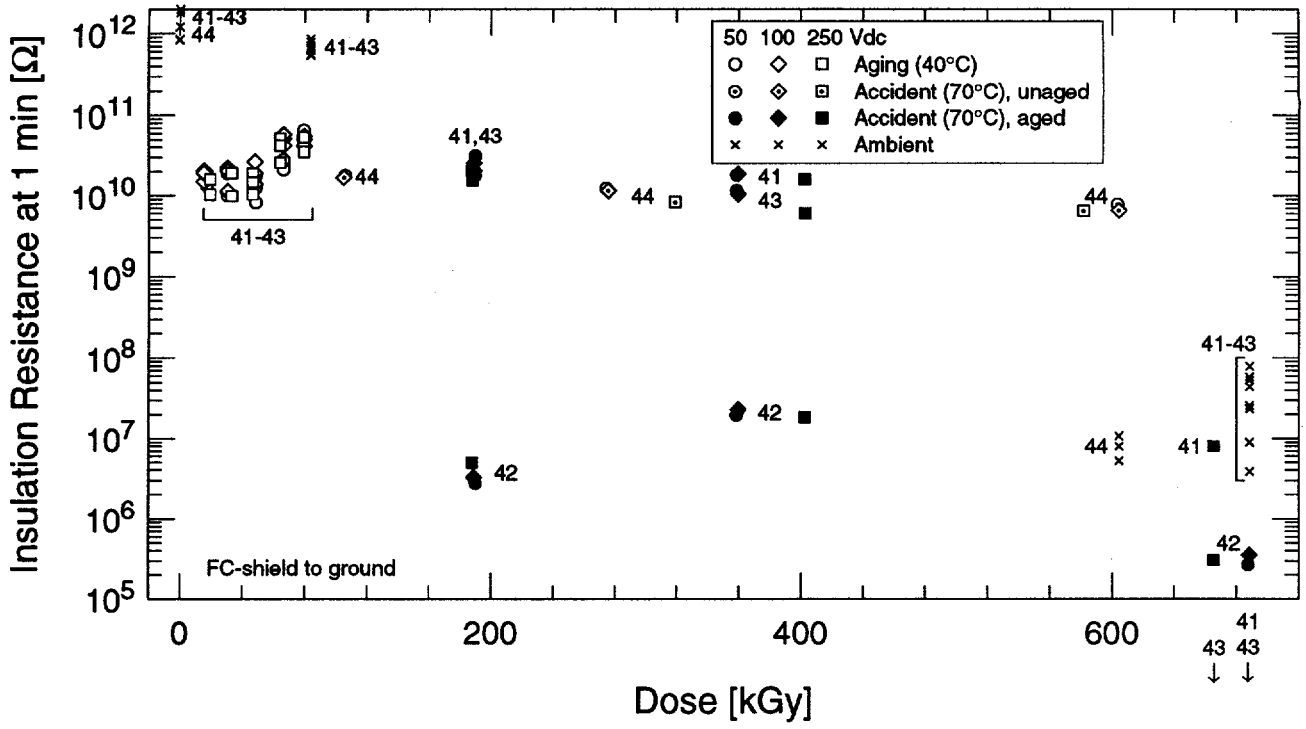

Figure 3.23: IR of French PE cable during aging and accident irradiation—shield to ground.

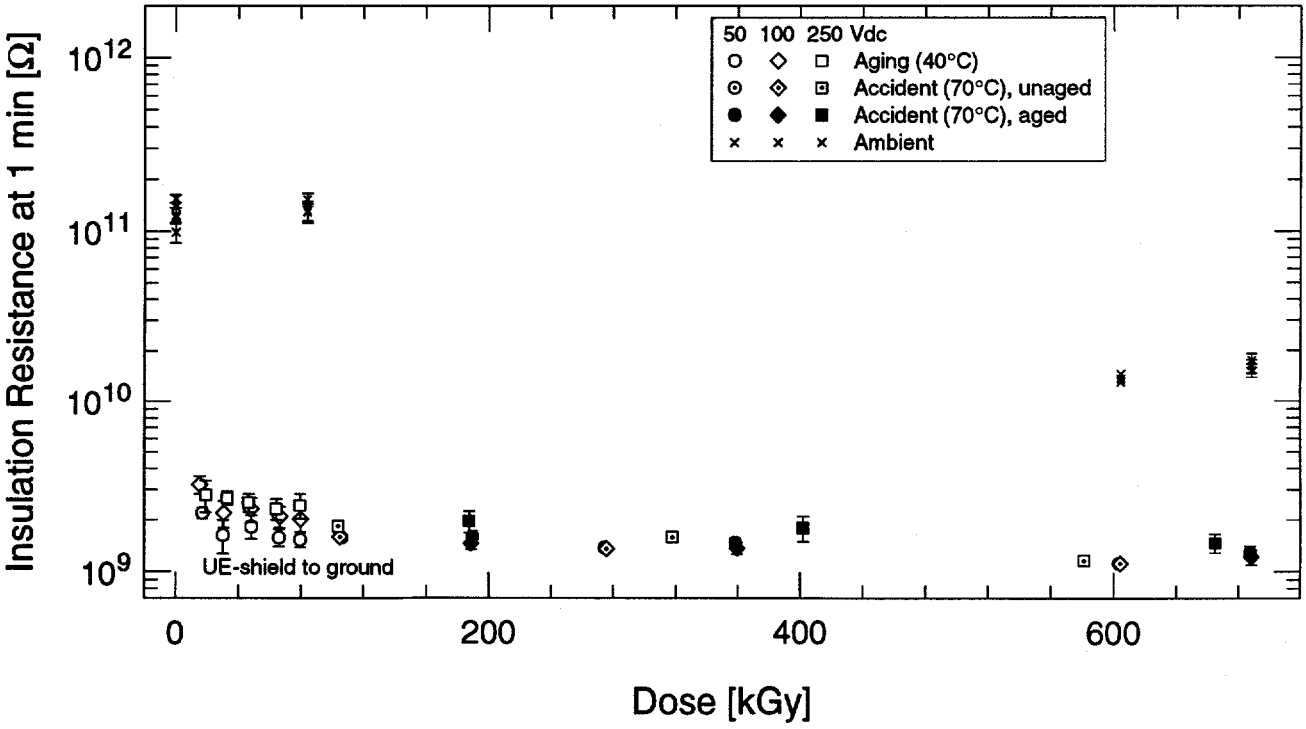

Figure 3.24: IR of U.S. EPR cable during aging and accident irradiation—shield to ground.

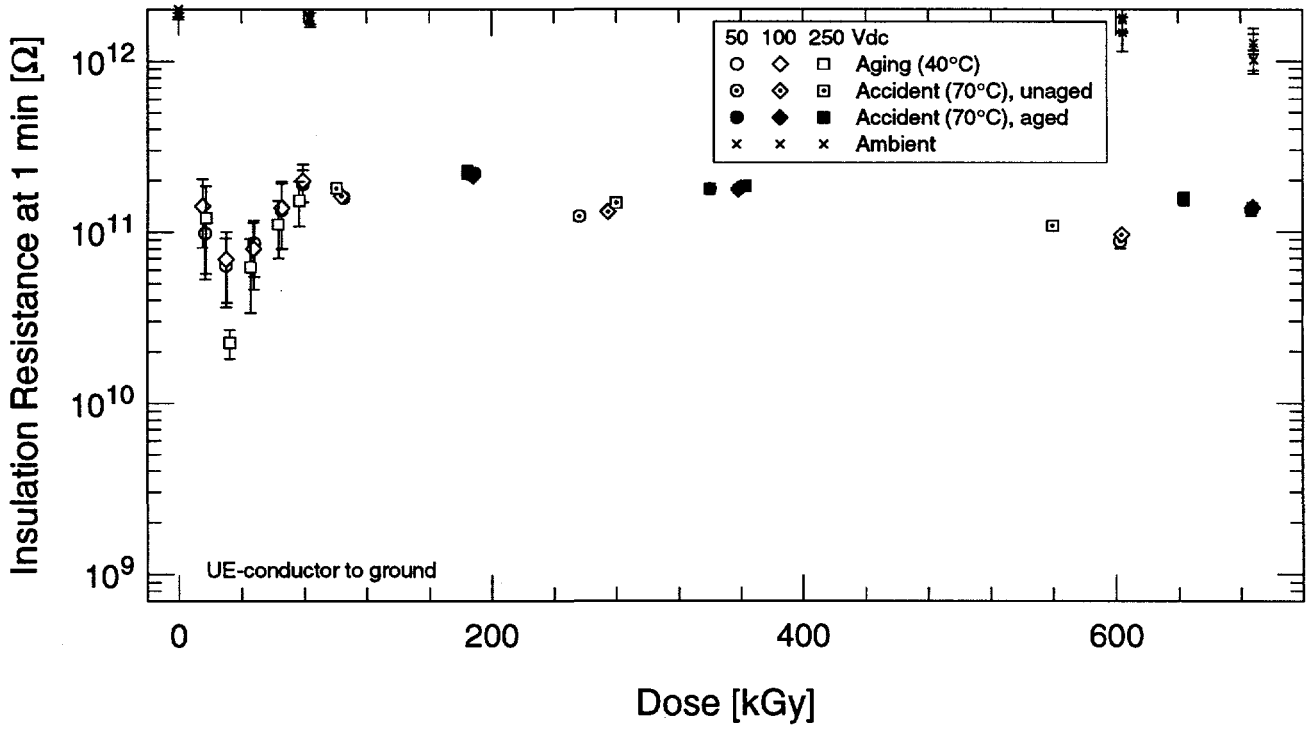

Figure 3.25: IR of U.S. EPR cable during aging and accident irradiation—conductor to ground.

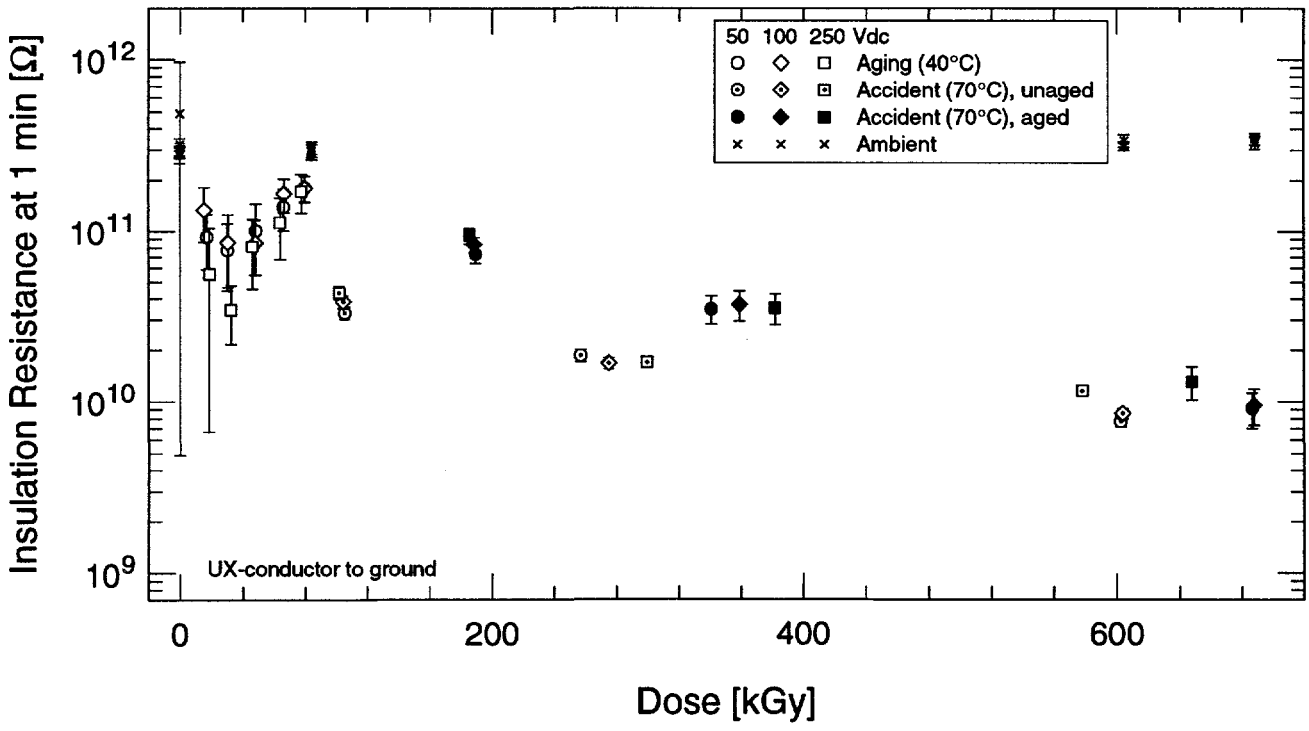

Figure 3.26: IR of U.S. XLPO cable during aging and accident irradiation—conductor to ground.

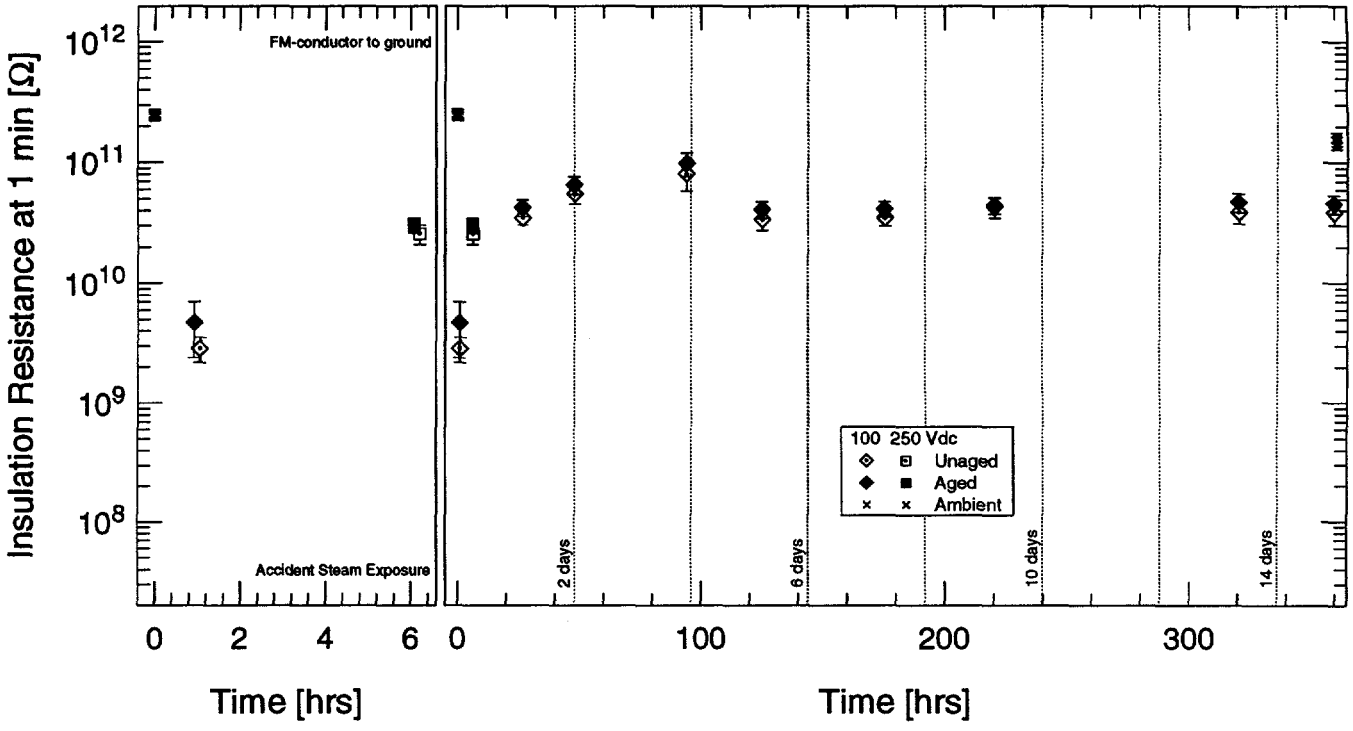

Figure 3.27: IR of French EPR cable during accident steam exposure—conductor to ground.

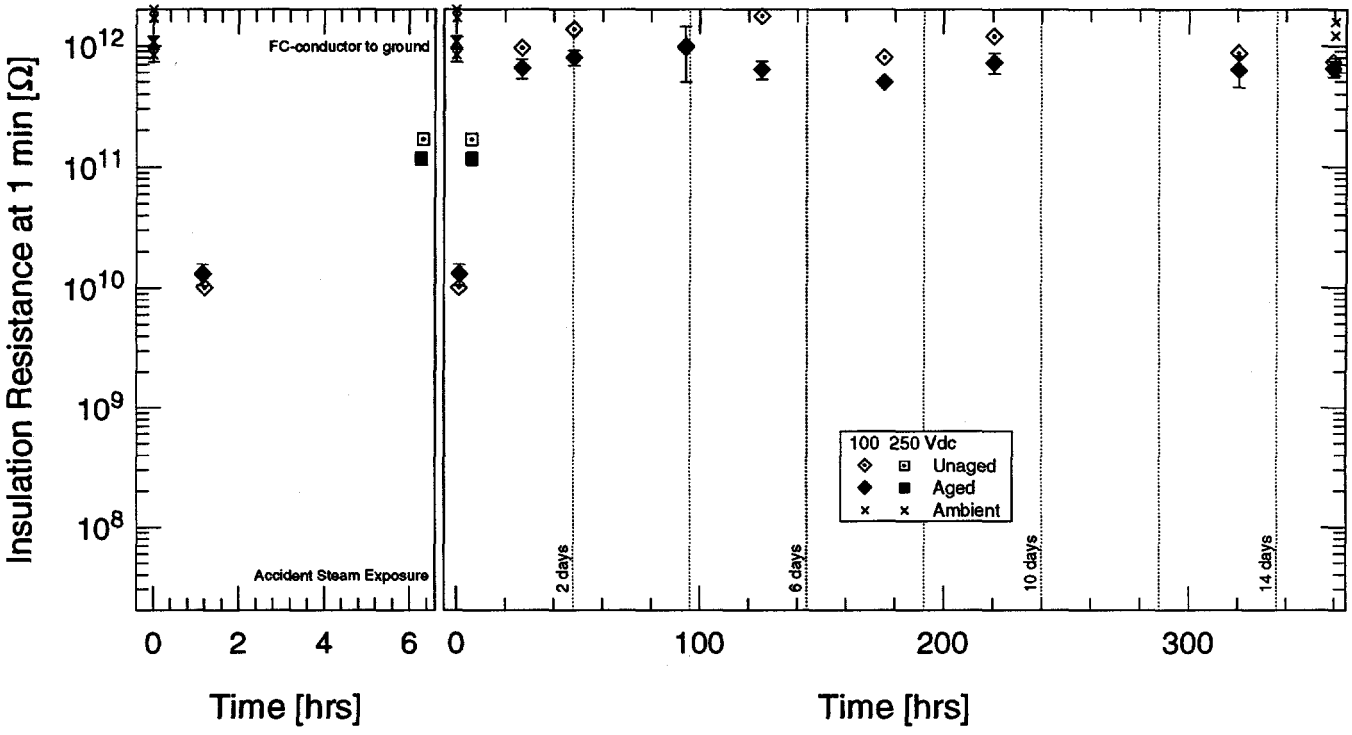

Figure 3.28: IR of French PE cable during accident steam exposure—conductor to ground.

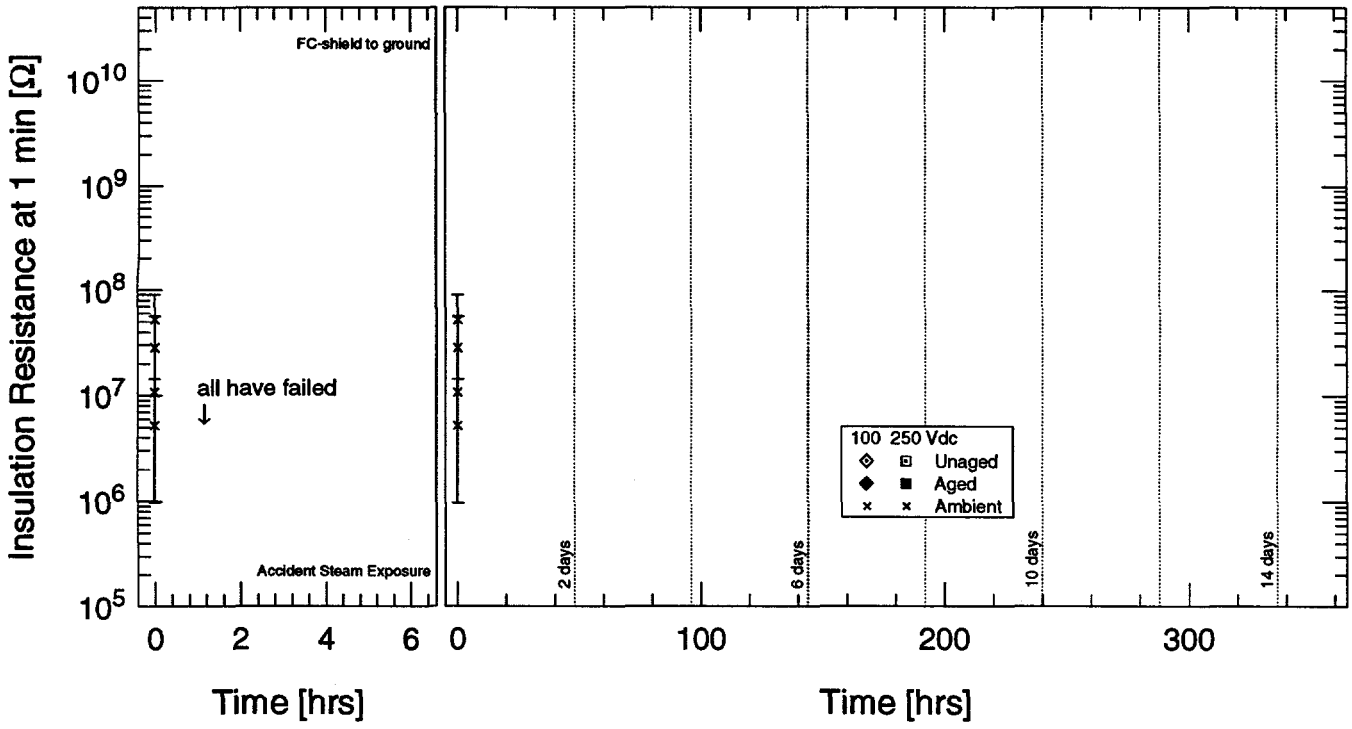

Figure 3.29: IR of French PE cable during accident steam exposure—shield to ground.

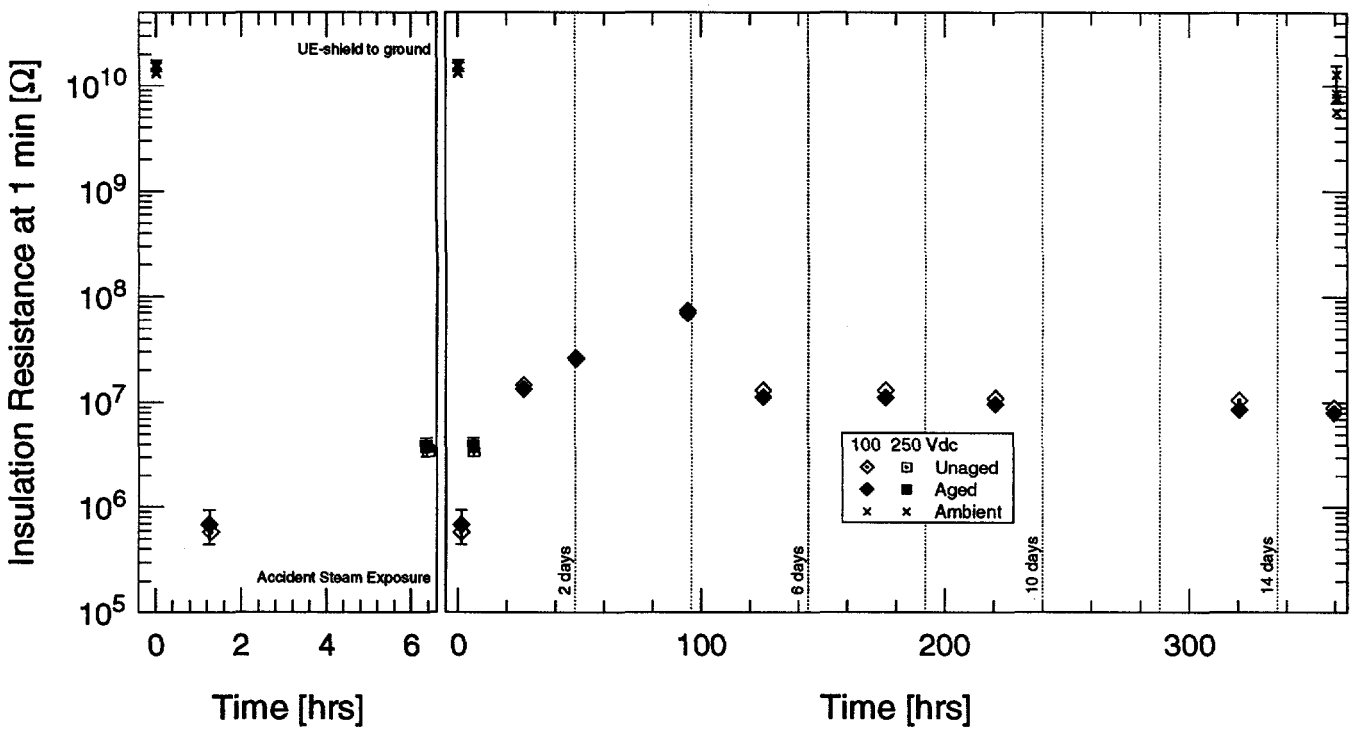

Figure 3.30: IR of U.S. EPR cable during accident steam exposure—shield to ground.

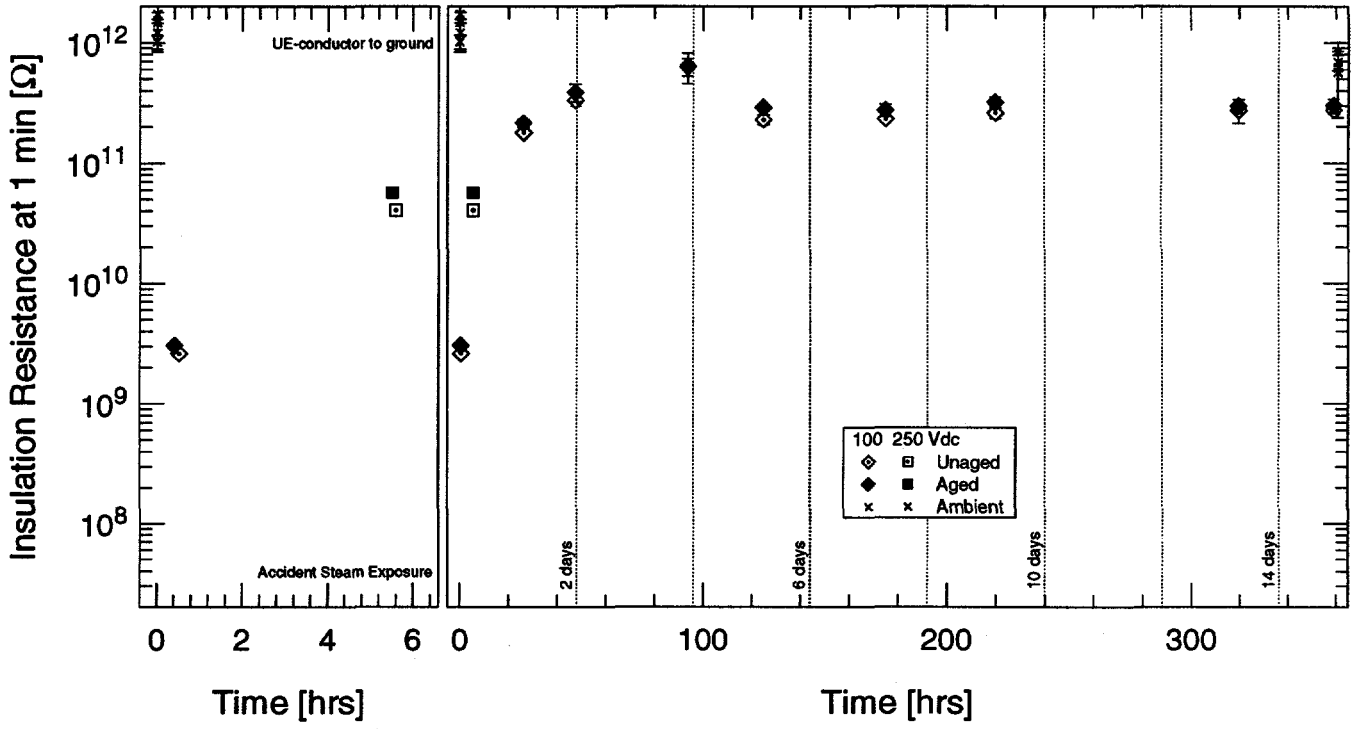

Figure 3.31: IR of U.S. EPR cable during accident steam exposure—conductor to ground.

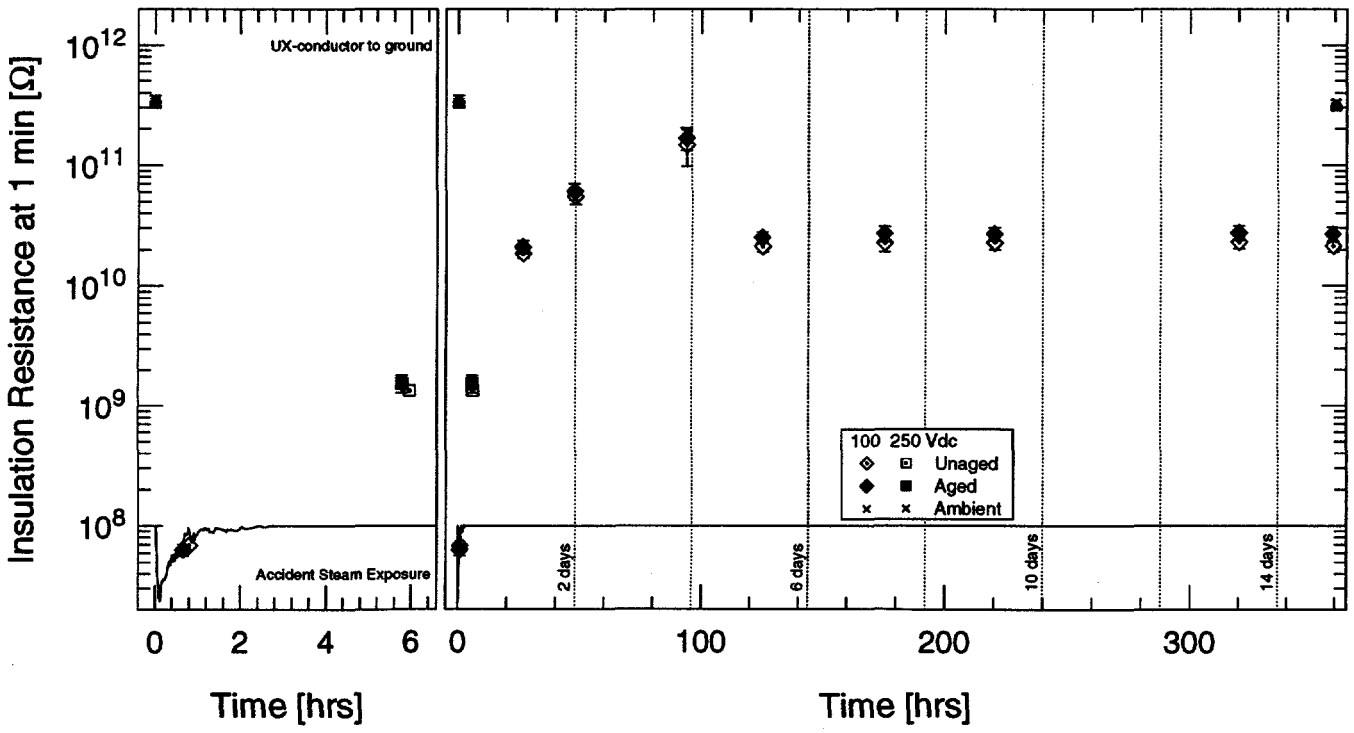

Figure 3.32: IR of U.S. XLPO cable during accident steam exposure—conductor to ground.

Part II
French Test Program

4 French Experimental Apparatus and Technique

This section describes the French experimental apparatus and techniques used to perform measurements on the cables. This information applies only to the French test activities; the U.S. test activities are described in Section 2.

4.1 Facilities

The aging tests were performed at the following four facilities at the Centre d´Études Nucléaires (Center for Nuclear Studies) in Saclay, France:

- The 5, 10, and 20 Gy/hr aging exposures were performed in CIS bio international's Kronos facility, which is immersed in the pool of the Poseidon irradiator (see Figure 4.1). Kronos consists of six boxlike housings mounted on a chassis. Each housing has its own heating and ventilation system. Sealed, 420 mm (16.5 in.) long, cobalt-60 sources were placed between the housings to obtain the desired dose rates of 5, 10, and 20 Gy/hr. A thermocouple was used to measure the temperature of each housing during irradiation. Airflow through each housing was set to provide 3 to 5 volume changes per hour.
- The 2 Gy/hr aging exposure was performed in Evocable (see Figure 4.2), which is a tubular chamber immersed in the pool of the Osiris research reactor, a CEA-DRE facility. Osiris is a light water, pool-type reactor with an open core. Its uranium oxide fuel provides 70 MW of thermal power and its operating cycles have an average duration of 3 weeks. Evocable is a 100 mm (3.9 in.) diameter, 1.5 m (59.1 in.) long tube that is mounted on the cooling pipe of the reactor core and is connected to the pool surface by two flexible tubes. Samples to be irradiated are placed inside this tube. Because of its location, the Evocable tube is exposed to radiation[1] emitted by the water in the primary cooling system of the Osiris reactor. For the 6 years of testing, the Evocable tube was irradiated for 47 operating cycles of the reactor at an average dose rate of approximately 2 Gy/hr (200 rad/hr). All Evocable system connections go to a control and instrumentation cabinet; these include test cables, the four control thermocouples installed permanently within the tube, the ventilation and electric supply system, and the ionization chamber used for dosimetry. The cable samples under test were also connected to the control and instrumentation cabinet. Sufficient airflow was supplied to the tube to provide 3 volume changes per hour.
- The accident irradiation was performed in CIS bio international's Caline facility (see Figure 4.3). This sealed, 8-m^3, box-shaped enclosure is immersed at the bottom of the Poseidon irradiator's pool. Cobalt-60 sources, having an overall activity of 250 kCi, were placed on either side of the Caline enclosure to irradiate test specimens placed in the heated and ventilated enclosure. Six thermocouples were installed in the enclosure for temperature control during testing. During irradiation, airflow was supplied to the enclosure to provide 3 to 5 volume changes per hour.
- The accident steam exposure was performed in CIS bio international's CESAR[2] facility (see Figure 4.4). This facility uses computer-controlled steam, air-admission, and exhaust valves to obtain almost any desired steam exposure profile. Simultaneous steam and cobalt-60 radiation exposures (not used for this testing) can be performed by installing the CESAR chamber in the Poseidon irradiation cell and feeding steam into CESAR via pipes passing through the cell walls.

  The steam needed to obtain the initial transient of the accident steam profile was accumulated in one of the superheaters, then abruptly released into the CESAR test chamber at the start of the test. Following these first few seconds, the test profile was controlled automatically by computer. Chemical spray was performed from the first few minutes to the end of the 4-day test.

  The cables were wrapped around a 450 mm (17.7 in.) diameter mandrel for the steam exposure. At the end of the steam exposure, the cables remained on the mandrel for electrical measurements.

[1] There was only gamma radiation at the Osiris cooling pipe location where Evocable was placed.

[2] Cellule d'Essais de Simulation d'Accident de Référence (CESAR); French acronym for reference accident simulation test cell.

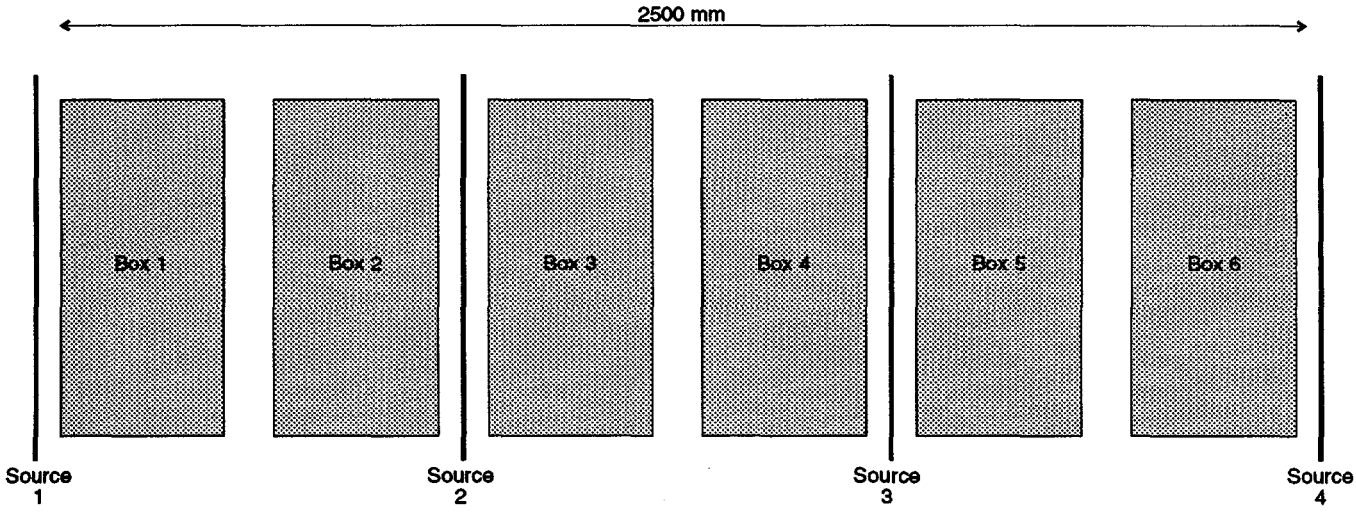

Figure 4.1: Plan view of Kronos showing its installation at the bottom of the Poseidon irradiator's pool.

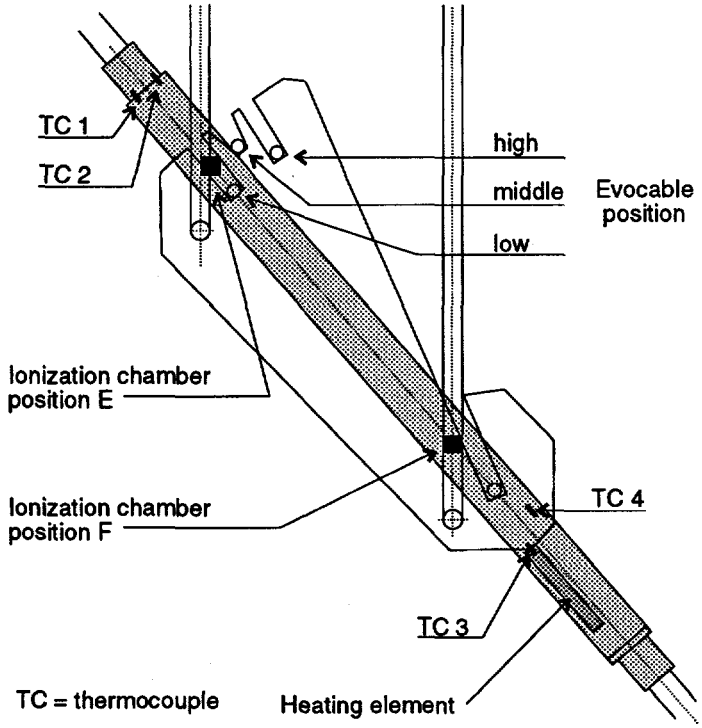

Figure 4.2: Sketch of Evocable and its mounting arrangement.

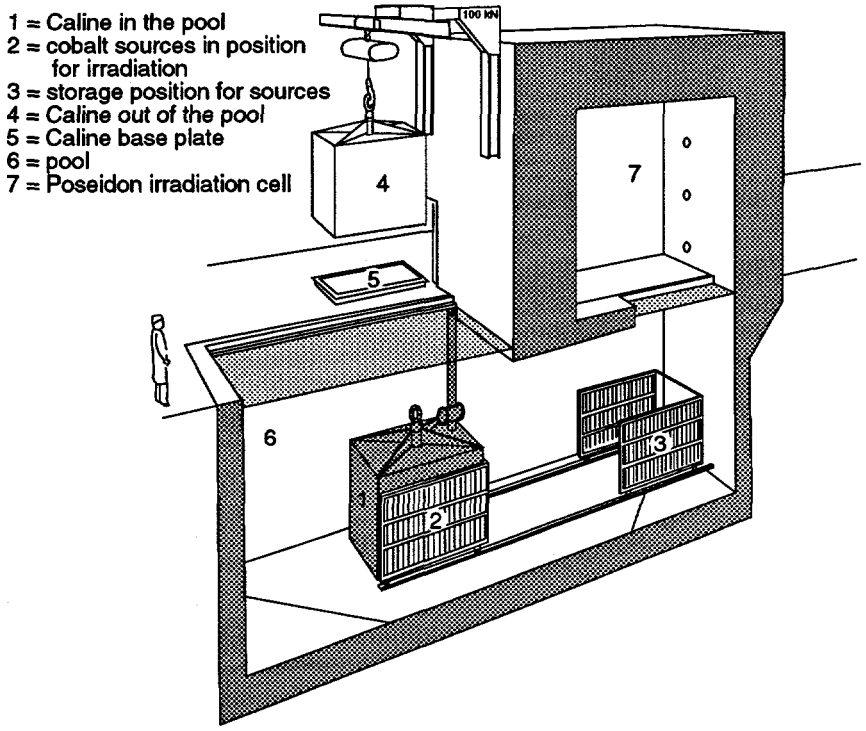

Figure 4.3: Caline facility and the Poseidon irradiator.

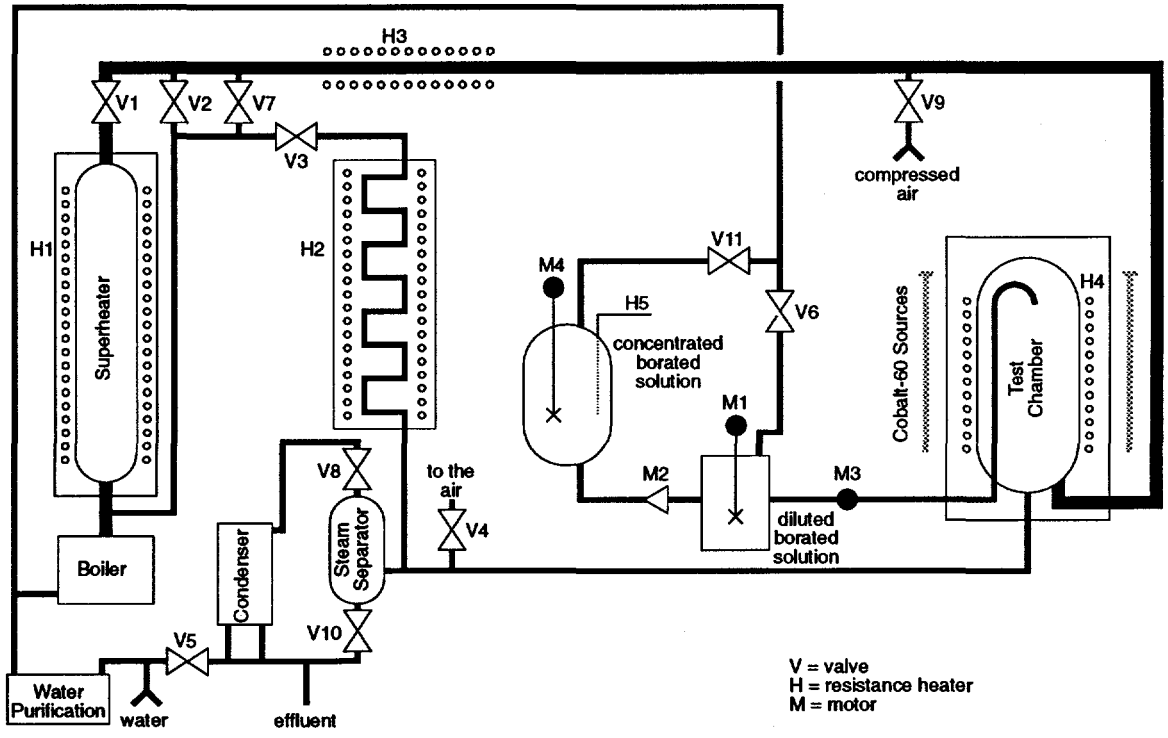

Figure 4.4: Schematic of the CESAR steam exposure facility.

Table 4.1: Test Conditions for Cut Cable Specimens Irradiated in Kronos.

Aging Temperature [°C]	Aging Dose Rate [Gy/hr]	Aging Dose [kGy]	LOCA Steam and Irradiation Exposure
ambient	0	0	No
ambient	0	0	Yes
40, 70	5, 10, 20	14	No
40, 70	5, 10, 20	28	No
40, 70	5, 10, 20	28	Yes
40, 70	5, 10, 20	42	No
40, 70	5, 10, 20	56	No
40, 70	5, 10, 20	56	Yes
40, 70	5, 10, 20	70	No
40, 70	5, 10, 20	70	Yes
40, 70	5, 10, 20	84	No
40, 70	5, 10, 20	84	Yes
40, 70	5, 10, 20	100	No
40, 70	5, 10, 20	100	Yes
40, 70	5, 10, 20	150	No
40, 70	5, 10, 20	150	Yes
40, 70	5, 10, 20	210	No
40, 70	5, 10, 20	210	Yes

4.2 Tested Cables

The French testing was performed on the same four types of instrumentation and control cables used for the U.S. testing (see Table 2.1); the cables tested in the U.S. and France came from the same reels. Both cut and complete cable specimens were tested.

4.2.1 Cut Cable Specimens

Cut cable specimens were used for mechanical tests. The cables were cut into 400 mm (approx. 16 in.) lengths and Raychem heat-shrink end caps were applied to each end of the specimen. In the Kronos housings, each of the 4 cable types were exposed to the 98 test conditions indicated in Table 4.1. In the Evocable tube, each of the 4 cable types were exposed to the 8 test conditions indicated in Table 4.2.

Table 4.2: Test Conditions for Cut Cable Specimens Irradiated in Evocable.

Aging Temperature [°C]	Aging Dose Rate [Gy/hr]	Aging Dose [kGy]	LOCA Steam and Irradiation Exposure
ambient	0	0	No
40	2	0	Yes
40	2	14	No
40	2	28	No
40	2	28	Yes
40	2	42	No
40	2	56	No
40	2	56	Yes

4.2.2 Complete Cable Specimens

Complete cable specimens were used for the electrical tests. Each of the specimens was 25 m (82 ft) long; however, the environmental exposure was applied to only a 1.2 m (3.9 ft) length in the middle of the cable; the remaining cable length was used for connections to electrical monitoring and energization equipment. One complete cable specimen of each type was tested.

In Kronos, the 1.2 m of cable was wrapped around the mandrel in the test chamber. In Evocable, the 1.2 m of cable was placed in the center of the Evocable tube.

4.3 Test Conditions

4.3.1 Aging Irradiation

The six Kronos boxes were used for the following aging irradiations:

- box 1: 20 Gy/hr (2 krad/hr) at 40°C.
- box 2: 10 Gy/hr (1 krad/hr) at 40°C.
- box 3: 5 Gy/hr (0.5 krad/hr) at 40°C.
- box 4: 5 Gy/hr (0.5 krad/hr) at 70°C.
- box 5: 10 Gy/hr (1 krad/hr) at 70°C.
- box 6: 20 Gy/hr (2 krad/hr) at 70°C.

Both the complete cables and the cut cable specimens were arranged together in the Kronos boxes. Both the complete and cut cable specimens were also arranged

together in the Evocable tube and were exposed to 2 Gy/hr (0.2 krad/hr) aging irradiation at 40°C.

Cut Cable Sections

The aging doses on the cut cable specimens irradiated in Kronos were 14, 28, 42, 56, 70, 84, 100, 150, and 210 kGy (1.4–21 Mrad). A dosimeter measurement was performed before the beginning of irradiation. After 3 years of irradiation, the sources were moved to compensate for radioactive decay and a new dosimeter measurement was performed. Details of the dosimeter measurements are given in Appendix C.

The aging doses on the cut cable specimens irradiated in Evocable were 14, 28, 42, and 56 kGy (1.4–5.6 Mrad). Prior to the first Osiris reactor operating cycle, an ionization chamber was calibrated using L-Analine dosimeters. This ionization chamber, installed in the Evocable tube, was used to measure the dose rate for all subsequent reactor operating cycles. Details of the initial dosimeter and ionization chamber measurements are given in Appendix C.

Complete Cable Specimens

Aging of the complete cable specimens was performed at the same dose rates and temperatures as for the cut cable specimens. During aging, the cables were exposed to a dose of 84 kGy (8.4 Mrad) in Kronos and 56 kGy (5.6 Mrad) in Evocable. Each complete cable had an independent electric supply and the cables were energized as shown in Figure 4.5. The voltage and current conducted through the wires were measured constantly and ammeters were checked visually.

The non-coaxial cable conductors were energized at 48 Vdc, 300 mA. Coaxial cable conductors were energized at 600 Vdc between the conductor and the metal shield, as shown in Figure 4.5. The voltage supplies were connected via HN-type connectors, and the interconnection cables were of the same type as the tested cables.

4.3.2 Thermal Aging

In parallel to the simultaneous radiation and thermal aging exposures, other cut cable specimens were being thermally aged for up to 5 years at 70 ± 2°C in ventilated ovens. Cut cable specimens were removed from the ovens for testing every 3 months.

4.3.3 Loss-of-Coolant Accident Simulation

The LOCA simulation consisted of an accident radiation exposure followed by an accident steam exposure.

Accident Radiation Exposure

An accident radiation exposure of 600 kGy (60 Mrad) was performed in the Caline installation at a dose rate of 800 Gy/hr (80 krad/hr) at 70°C. The accident irradiation was performed on the cut cable specimens after the following aging doses:

- Unaged specimens (0 kGy)
- Specimens aged to 28, 56, 70, 84, 100, 150, and 210 kGy (2.8 to 21 Mrad) in Kronos
- Specimens aged to 28 and 56 kGy (2.8 and 5.6 Mrad) in Evocable

The accident irradiation was performed on the complete cable specimens after an aging irradiation of 84 kGy (8.4 Mrad) in Kronos and 56 kGy (5.6 Mrad) in Evocable. The complete cable specimens were not electrically energized during the accident irradiation.

Accident Steam Exposure

The accident steam exposure was performed in the CESAR facility using the test profile from French Standard NF M 64-001 [15, Figure A.3] as shown in Figure 4.6. Only the second transient peak from this standard was performed—this corresponds to a sudden temperature rise to 156°C in less than 30 sec and a pressure rise to 560 kPa absolute. The 96-hr-long initial portion of the steam test profile, specified in Table 4.3, gradually decreased from its peak temperature to a final temperature of 72°C. A chemical spray of sodium borate solution was applied starting at 200 sec and continuing until the end of the 4-day initial portion of the steam exposure. The chemical solution was 1500 ppm boric acid, which was

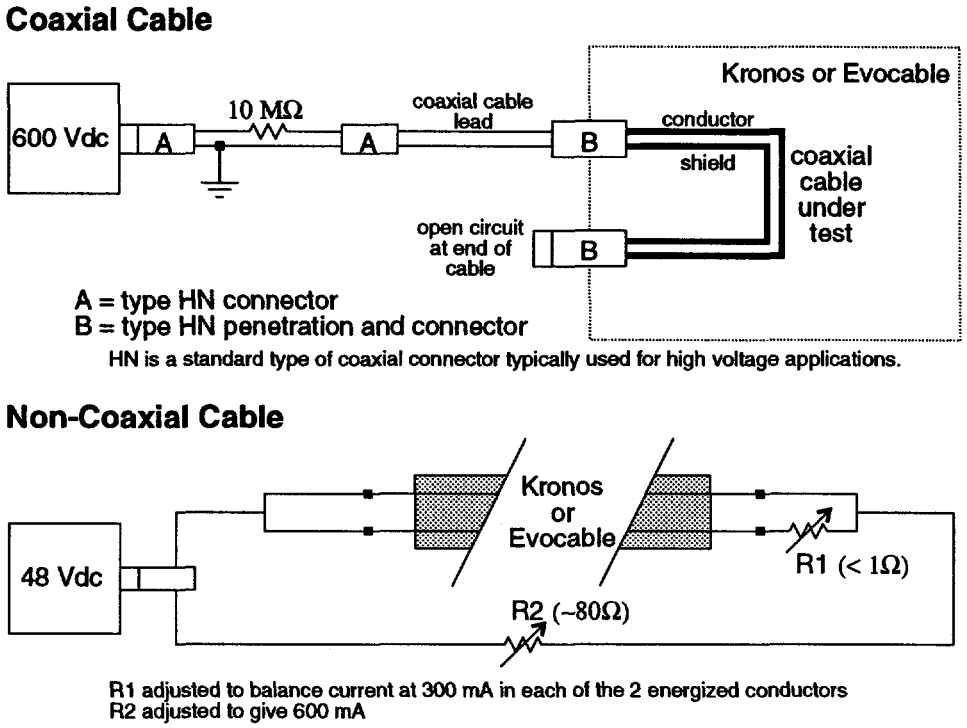

Figure 4.5: Schematic of the circuits used to electrically energize the complete cable specimens during aging.

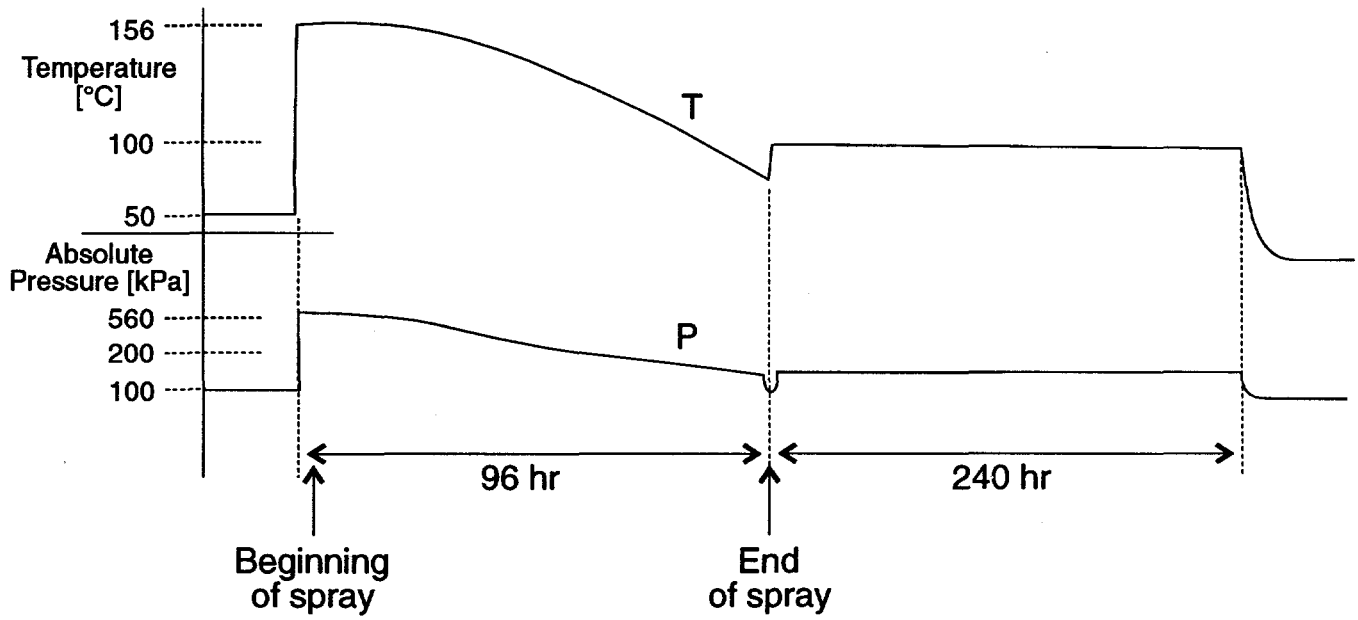

Figure 4.6: Target profile for accident steam exposure.

Table 4.3: Accident Steam Exposure Levels.

Time	Pressure [kPa absolute]	Temperature [°C]
15 sec	560	156
2 min	560	156
20 min	560	150
45 min	525	140
4 hr	350	120
18 hr	240	99
61 hr	190	79
96 hr	180	71.5

adjusted to a pH of 9 by adding sodium hydroxide (NaOH). The spray flow rate was 6.1 liters/sec (per square meter of CESAR cross sectional area[3]) from a nozzle located at the middle of CESAR's roof. During the entire accident steam exposure, the complete cable specimens were not electrically energized. The cable terminations were located outside of the CESAR enclosure.

Actual data for the initial 96 hr of the accident steam exposure are shown in Figure 4.7. After the initial 96 hr, the accident steam exposure continued for an additional 240 hr at 100°C and 200 kPa absolute.

4.4 Mechanical Measurement Techniques

Mechanical tests were performed on the cut cable specimens.

4.4.1 Elongation and Tensile Strength

The elongation and tensile strength were measured using two types of tensile specimens. Insulation specimens were 100-mm long sections of the cable insulation with the conductor removed. Jacket specimens were punched from the cable jacket using an H3 dumbbell-shaped punch (see Figure 2.9). The cut cable specimens were exposed to one of the test conditions in Table 4.1 or 4.2 before having the jacket cut off to produce jacket specimens and the insulation stripped from the conductors to produce insulation specimens.

The measurements were made using a Zwick Model 1455 tensile testing machine equipped with an optical extensometer and placed in an air-conditioned room at 20 ± 1°C. The tests were performed with an extension rate of 50 mm/min.

For each measurement point:

- 10 insulation and jacket specimens of the U.S. XLPO and U.S. EPR cables were averaged for each data point
- 6 jacket specimens and 7 insulation specimens for the French EPR and French PE cables were averaged for each data point

The average value and standard deviation were calculated for each environmental condition for which measurements were performed. If the value obtained for a tensile specimen was greater than 1.5 standard deviations from the average, it was discarded and another average was calculated.

4.4.2 Mandrel Bend Testing

Because the U.S. EPR cable's insulation adhered to the copper conductors during the accident steam exposure, tensile tests could not be performed. In order to measure the mechanical characteristics of the cable, bend tests were performed on mandrels having decreasing diameters. After each bend test, the operator inspected the cable to locate any cracking caused by the test. The test was performed for D/d values that were successively equal to 40, 20, 10, 5, 4, 3, and 1, where D is the mandrel diameter and d is the diameter of the insulation.

4.5 Physical-Chemical Measurement Techniques

Physical-chemical measurements, density and gel fraction, were performed on all the cable jackets and insulators.

[3]The CESAR test chamber is 0.70 m tall by 0.60 m diameter; thus its cross sectional area is 0.28 m^2.

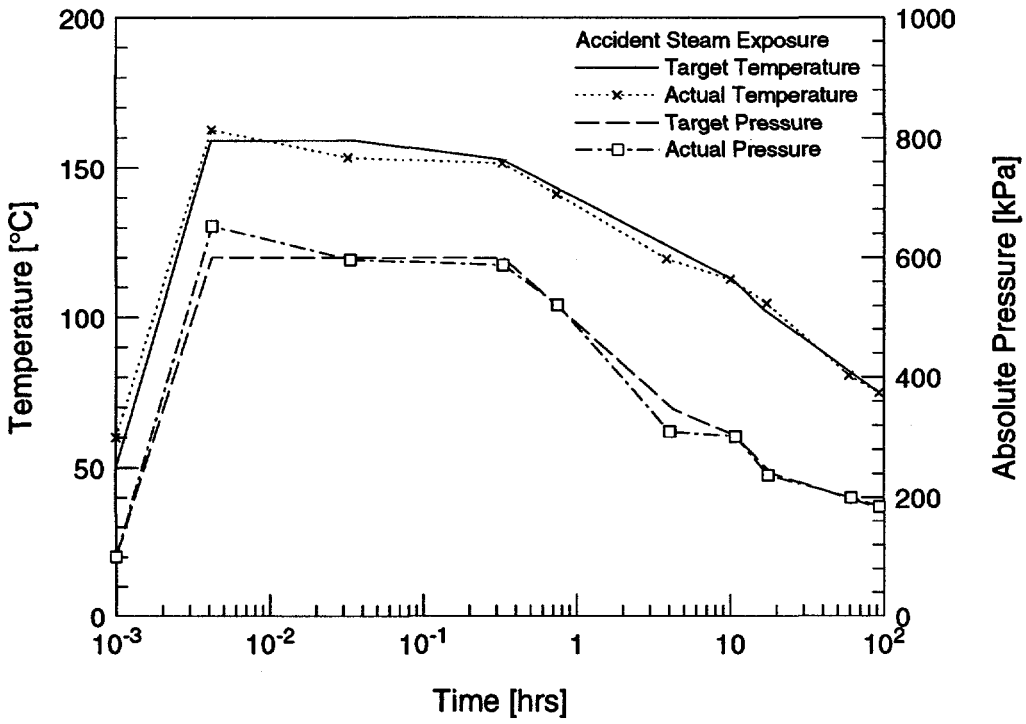

Figure 4.7: Initial 96 hr of the accident steam exposure obtained inside CESAR.

4.5.1 Density

The density[4] of the cable materials was measured using:

- a Sartorius 6080 water pycnometer for the cable jackets,
- a Quantachrome MVP1 gas pycnometer (Quantachrome Corp., Boynton Beach, FL) for the cable insulations. A gas pycnometer was used to avoid errors caused by air bubbles adsorbed at the surface of the small samples.

The pycnometer accuracy was estimated at 0.2%, however data were acquired with a resolution of 0.01.

For the cable jackets, measurements were performed on samples with a mass of approximately 1 gram. The results correspond to an average value calculated from 4 samples.

For the cable insulations, measurements were performed on samples with a mass of approximately 2 grams. The results correspond to an average value calculated from 3 samples.

[4]The specific gravity, not the density, was actually measured; however, since the values shown in the figures are normalized, this does not influence the results.

4.5.2 Gel Fraction

The gel fraction represents the fraction of the polymer material that is insoluble after extraction in a solvent. In general, gel fraction increases when a polymer material is cross-linked by irradiation, and gel fraction decreases when a polymer material is degraded by irradiation.

The gel fraction measurements were performed as follows:

1. Determination of the best solvent for each polymer material. The best solvent is that which produces the lowest gel fraction for the unaged sample.
2. Extraction for 6 hr in hot condensates of the solvent using a Soxhlet extraction apparatus.
3. Contraction of the polymer by rinsing in acetone for 4 hr in the Soxhlet extraction apparatus.

4. Drying to a constant weight.

The gel fraction is defined as GF% = $M_f/M_i \times 100$, where M_f is the final specimen mass and M_i is the initial specimen mass. The following solvents were chosen for the measurements; decahydronaphthalene (decalin) for the U.S. XLPO cable's Hypalon jacket and xylene for the other materials. The polymers were cut into small pieces taken from the full thickness of the insulation and jacket. The values shown in Figures 5.21–5.26 are the average of 2 measurements.

4.6 Electrical Measurement Techniques

Electrical measurements were performed on the complete cable specimens during aging and the LOCA tests. The cables were located in the Kronos or Evocable facilities for the measurements performed during aging. After the LOCA test, the measurements were performed with the cables mounted on the mandrel of the CESAR enclosure. In general, to correlate any variations in the electrical characteristics under atmospheric conditions, the temperature and relative humidity were measured before each measurement was performed on the irradiated cables in Kronos and Evocable.

4.6.1 Measurements Performed on Coaxial Cable

The following measurements were performed on the French PE cable:

- Electrostatic microbreakdown (EMD) measurements were performed using the MI 77 apparatus, developed at CEA, which detects extremely small, transient currents; it will measure current pulses as low as 8×10^{-7} A that last for only 10^{-8} sec. To make the measurement, the voltage was increased gradually to 1500 Vdc in 1.5 min, then held constant for 3 min. After the 3-min hold, the measurement was performed for 3 min.
- Characteristic impedance measurements were performed with a Tektronix 1502 time domain reflectometer (TDR). During the measurement, the impedance discontinuity between a standard cable connected directly to the reflectometer and the test cable was evaluated. The various levels of the reflection factors between the 2 cables were measured without taking into consideration discontinuities caused by the connections. A calibration between the reflection coefficients and the impedance was used to determine the test cable's impedance with respect to the reference cable.
- Insulation resistance was measured with a Sefelec M9900 megohmmeter at 500 Vdc. The voltage was applied between the conductor wire and the grounded metal shield. The measurement was performed after stabilization for 1 min.

4.6.2 Measurements Performed on Non-Coaxial Cables

The following measurements were performed on the 3 types of non-coaxial cables:

- Dielectric strength was measured using a Sefelec PR5M dielectric-strength tester. The voltage was increased to 2000 Vac in approximately 10 sec, and then the current was measured for 1 min at 2000 Vac. For the U.S. XLPO and French EPR cables (3 conductors), the voltage was applied between each conductor wire and the 2 others connected together; thus 3 measurements were performed for each cable. For the U.S. EPR cable (2 conductors), the voltage was applied between the two conductors.
- Insulation resistance was measured with a Sefelec M9900 megohmmeter at 500 Vdc. The resistance value displayed by a megohmmeter is calculated by measuring the current that flows when a dc voltage is applied to a conductor. For the 3-conductor cables, the voltage was applied between each conductor and the 2 others connected to ground; thus 3 measurements were performed for each cable. For the 2-conductor cable, the voltage was applied between the two conductors while one was connected to ground.

5 French Experimental Results

This section presents the experimental data[1] acquired from the four different types of cable during the French test program. The results for the U.S. test program are presented in Section 3.

5.1 Mechanical Measurement Results

The results presented here were obtained by tensile tests on the cut cable specimens. No mechanical testing was performed on the complete cable specimens.

5.1.1 Elongation at Break and Tensile Strength

Both elongation at break and tensile strength were measured. The tensile strength did not show significant effects during aging or for the post-LOCA measurements and thus these results will not be discussed.

U.S. XLPO cable—Hypalon Jacket

Elongation at break data for the U.S. XLPO cable jacket are shown in Figures 5.1 and 5.2. During the aging process (see Figure 5.1), cross-linking affects the samples according to the dose. The degradation in elongation at break of the U.S. XLPO cable jacket increases as the dose is increased. The effect of dose rate (over the range 2–20 Gy/hr) is not significant at 40°C; however, a dose-rate effect is seen at 70°C. For an equal dose, cross-linking of the material is greater when aging is at 70°C and 210 kGy, E/E_0 equals 0.16 for 5 Gy/hr, 0.50 for 10 Gy/hr, and 0.56 for 20 Gy/hr.

After the LOCA simulation (see Figure 5.1), which included accident irradiation and steam exposure, the elongation at break had decreased considerably from its pre-LOCA values. The post-LOCA values also fell with increasing dose, showing that the aging exposure affected the LOCA performance. However, the LOCA exposure is clearly much more degrading than the aging exposure for the tested conditions.

In Figure 5.2, curve fits to the data are shown. These polynomial least-squares regressions are used to determine whether there is a synergism between the radiation and thermal exposures. The solid line in Figure 5.2 is the sum of the degradation[2] from the regression fit to the 70°C exposure data and the degradation from the regression fit to the 5 Gy/hr radiation exposure[3] data. Note that this summation of the degradations was used, not because this was considered physically realistic, but because this should provide a worst-case estimate of what the degradation would be if there was no synergism between the 70°C and 5 Gy/hr exposures. A synergism exists whenever the degradation of the combined exposure is different than the combined degradations of the individual exposures; thus a synergism can be either positive or negative. For the elongation at break data, there is no physical model for how the degradations of the individual exposures should be combined; thus conclusive evidence of synergism exists only when

- degradation of the combined exposure was greater than the summed degradations of the individual exposures (positive synergism), or
- degradation of the combined exposure was less than the degradation of either individual exposure (negative synergism).

If the degradation of the combined exposure is between these two extremes, then no clear conclusion can be reached on whether synergism exists between the exposures.

In Figure 5.2, the degradation of the combined 5 Gy/hr, 70°C exposure is greater than the sum of the degradation due to the 5 Gy/hr irradiation-only exposure and the degradation due to a 70°C thermal-only exposure. This indicates synergism between the 5 Gy/hr radiation and 70°C thermal exposures.

[1] In addition to the figures and tables included in this section, all the raw data are available upon request from the author.

[2] Degradation is defined here as $1 - E/E_0$.

[3] Because 40°C is so close to "normal" ambient temperatures, the 5 Gy/hr, 40°C exposure is treated as a radiation-only exposure.

U.S. XLPO cable—XLPE Insulation

Elongation at break data for the U.S. XLPO cable insulation are shown in Tables 5.1 and 5.2. The elongation at break shows two distinct types of behaviors, and thus no figures are plotted. These two behaviors are:

- Group A, no particular anomalies
- Group B, values very low

For each group, Tables 5.1 and 5.2 specify the number of specimens put through testing.

The low values of elongation at break of group B specimens may be due, for instance, to a variation in manufacturing; however, it seems likely that this was the result of local stretching of the insulation to failure without stretching the material over its entire gage length[4]; the local E/E_0 can still be quite high, but the elongation relative to the tensile tester's gage length is low. Group B degraded quickly with increasing dose. Group A was less sensitive to irradiation, and was only slightly degraded after an exposure of 210 kGy.

After LOCA, no mechanical testing was performed because the polypropylene filler located under the cable jacket had melted and fused the insulation and jacket together.

During the thermal-only exposure (see Table 5.2), the elongation at break did not change significantly.

U.S. EPR cable—Hypalon Jacket

Elongation at break data for the U.S. EPR cable jacket are shown in Figures 5.3 and 5.4. Just as for the U.S. XLPO cable's Hypalon jacket, there was a dose-rate effect (Figure 5.3) in that the aging degradation increased as the dose rate decreased. Also, for a given dose rate and dose, there was more degradation as the temperature increased. For instance, at 70°C and 210 kGy, E/E_0 equaled 0.19 for 5 Gy/hr; 0.35 for 10 Gy/hr; and 0.49 for 20 Gy/hr. However, at 40°C, the behavior of the cable jacket was very similar when irradiated at 2 Gy/hr and 5 Gy/hr.

After LOCA (Figure 5.3), which includes accident irradiation and steam exposure, the elongation at break decreased considerably. Degradation was significant; elongation at break in some cases was less than 50% absolute (e.g., post-steam results for E, not E/E_0, after 100 kGy at 40°C).

A comparison between the 70°C thermal-only exposure and the 5 Gy/hr, 70°C exposure in Figure 5.4 shows that the irradiation increased the degradation in elongation at break. However, the heavy solid line showing the sum of the degradation due to the 5 Gy/hr irradiation-only exposure added to the degradation from the 70°C thermal-only exposure is below the simultaneous 5 Gy/hr, 70°C exposure data. Thus, no definitive conclusion can be reached on whether there was any synergism between the irradiation and 70°C thermal exposures for the U.S. EPR cable's Hypalon jacket material; this behavior may be different from the synergism seen for the U.S. XLPO cable's Hypalon jacket material in Figure 5.2.

U.S. EPR cable—FR-EPDM Insulation

Elongation at break data for the U.S. EPR cable insulation are shown in Figures 5.5 and 5.6. Elongation at break decreases with increasing dose,[5] but is independent of the dose rate. For instance, at 70°C and 210 kGy, E/E_0 equals 0.51 for 5 Gy/hr; 0.57 for 10 Gy/hr; and 0.57 for 20 Gy/hr (see Figure 5.5). The FR-EPDM insulation irradiated at 20 Gy/hr is more degraded during irradiation at 40°C than during irradiation at 70°C; this surprising behavior was also

[4] It has been hypothesized that this behavior might be due to the French use of mechanical clamps to hold specimens during tensile testing. The tube-shaped insulation specimens tend to flatten under the pressure of the clamps and also shrink in diameter as they are stretched. When a mechanical clamp is used, the high clamping pressure required to prevent slipping causes stress concentrations that can lead to localized stretching and early failure. The U.S. tensile testing utilized pneumatic jaws to clamp specimens in place. Pneumatic jaws maintain constant pressure on the specimen even as it changes shape, thereby allowing lower clamping pressures to be used. The type of clamping is not as important for the jacket specimens because their dumb-bell shape ensures that stretching occurs in the throat region of the specimen and not near the clamps.

[5] Note that the insulation initially shows increased elongation at break for low doses. This phenomenon is relatively common and is hypothesized to be the result of processing when cables are manufactured. Materials are often cured or cross-linked during manufacture to improve their properties; however, the properties are typically not improved to the maximum extent possible because of conservatism during processing and the desire not to overprocess the material, which could lead to reduced life. Thus, when exposed to thermal and radiation environments, a cable's properties often initially improve as it continues to cure or cross-link.

observed in the EPR insulation of the French EPR cable (see Figure 5.13). It should be noted that this same behavior was seen in earlier testing by Gillen and Clough [16] on this same material (EPR-B in their report), in which they found faster degradation of mechanical properties at 41°C than 61°C for dose rates of 60–70 Gy/hr. Gillen and Clough also noted that this behavior appeared in even earlier testing by Bustard and co-workers [17] on this same material (EPR 1 in their report) for 650 Gy/hr exposures at 27°C and 70°C. An explanation of this "inverse temperature effect" has been proposed by Gillen and co-workers [18] based on the semi-crystalline nature of EPR materials and the fact that these materials undergo crystalline melting and reforming over a broad temperature range from roughly room temperature up to at least 100°C.

As shown in Figure 5.6, the 70°C thermal-only exposure caused only a slight decrease in elongation at break. The specimens irradiated at 40°C and 70°C have essentially the same degradation in elongation at break; the small difference is approximately equal to the degradation caused by the 70°C thermal-only exposure. This material did not appear to exhibit any synergistic effect during the combined radiation and thermal exposure.

After the accident steam exposure, the insulation adhered to the conductor and thus mandrel bend tests, described in Section 5.1.2, were performed instead of tensile tests.

French PE cable—PE Jacket

Elongation at break data for the French PE cable jacket are shown in Figures 5.7 and 5.8. As shown in Figure 5.7, the cable jacket was entirely degraded after 56 kGy (5.6 Mrad), except for 5 Gy/hr irradiation at 70°C for which the properties remained relatively unchanged to a dose of 100 kGy (10 Mrad); thereafter the properties quickly degraded to 0% elongation at break. No difference is apparent for the 40°C irradiations at 2 Gy/hr and 5 Gy/hr. The results in Figure 5.7 show that this material's elongation at break properties are actually improved as the temperature increases from 40°C to 70°C and also as the dose rate is decreased (for the same dose). Both the temperature effect and the dose rate effect are opposite the usual polymer behavior. After the steam exposure, the jacket material had no remaining elongation at break; no figure is shown. During the 70°C thermal-only exposure (see Figure 5.8), the elongation at break was relatively constant; this indicates that the degradation seen for this material is solely due to irradiation.

French PE cable—PE Insulation

Elongation at break data for the French PE cable's insulation are shown in Figures 5.9 and 5.10. As shown in Figure 5.9, the insulation degraded very quickly during irradiation. For a given dose, the degradation in elongation at break increases with increasing temperature. At 70°C, there was no remaining elongation by a dose of 28 kGy (2.8 Mrad). After the steam exposure, the insulation material had no remaining elongation at break; no figure is shown. During the 70°C thermal-only exposure (see Figure 5.10), the elongation at break was relatively constant, this indicates that the degradation seen for this material is due solely to irradiation.

French EPR cable—Hypalon Jacket

Elongation at break data for the French EPR cable jacket are shown in Figures 5.11 and 5.12. In Figure 5.11, the elongation at break decreased with increasing dose for all dose rates and temperatures. For dose rates of 5 and 10 Gy/hr, the degradation was greater at 70°C than at 40°C. However, at 20 Gy/hr, the temperature had barely any influence on the elongation at break. In general, the degradation for a given dose increased as the dose rate was decreased; for instance, at 70°C and 210 kGy, E/E_0 equals 0.39 for 5 Gy/hr; 0.43 for 10 Gy/hr; and 0.48 for 20 Gy/hr. The 5 Gy/hr, 70°C data might indicate that there is some trend to a dose rate effect at low dose rates for 70°C. At 40°C, no difference is apparent for the irradiations at 2, 5, and 10 Gy/hr. However, note that the 20 Gy/hr, 40°C data has substantially more degradation than the data for the lower dose rates at 40°C. The reason for this unexpected behavior is unknown.

In Figure 5.11, the elongation at break values after the steam exposure had decreased considerably from their pre-LOCA values. However, the remaining elongation at break was sufficient for the cables to be handled without damaging them.

As shown in Figure 5.12, both temperature and irradiation degraded the elongation at break. In addition, the degradation of the combined 5 Gy/hr, 70°C exposure was greater than the sum of the degradations due to the 70°C thermal-only exposure added to the 5 Gy/hr irradiation-only exposure. Even though there is considerable scatter in the combined 5 Gy/hr, 70°C data, a synergy in the degradation caused by the simultaneous temperature and radiation exposure appears to be present.

French EPR cable—EPR Insulation

Elongation at break data for the French EPR cable insulation are shown in Figures 5.13 and 5.14. Figure 5.13 shows that aging degradation of the EPR insulation was relatively independent of dose rate except for the 20 Gy/hr, 40°C data, which had substantially more degradation than the lower dose rate data at 40°C. The reason for this behavior is unknown. As noted earlier for the U.S. EPR insulation, the 20 Gy/hr degradation is greater at 40°C than at 70°C. This could be because the EPR material undergoes structural changes in the 40–70°C temperature range as discussed for the FR-EPDM insulation of the U.S. EPR cable.

After the steam exposure (see Figure 5.13), there was considerable degradation of the EPR insulation material from its pre-LOCA values, especially for low doses. This effect became less pronounced at higher aging doses. In all cases, E/E_0 was less than 0.5 after the LOCA; however, the remaining elongation at break was sufficient for the cables to be handled without damaging them.

During the 70°C thermal-only exposure, shown in Figure 5.14, the elongation at break decreased slightly. Note that irradiation caused a larger decrease in elongation at break than the thermal-only exposure. No synergism between the thermal and radiation exposures was seen.

5.1.2 Mandrel Test

Mandrel bend tests were used when tensile tests were not practical. This was the case for the FR-EPDM insulation of the U.S. EPR cable, which adhered to the copper conductors during the accident steam exposure. The cable was bent around mandrels with decreasing diameters. After being bent around each mandrel, the cable was visually checked for cracks in the insulation. The FR-EPDM insulation was found to be sufficiently supple not to crack during the test, even with the smallest-diameter mandrel ($D/d = 1$).

5.2 Physical-Chemical Measurement Results

5.2.1 Density

As shown in Figures 5.15–5.20, the density of the jackets and insulators of all cables remained relatively constant during the aging. After LOCA, the densities did not vary significantly on the cable jackets or on the French EPR cable's EPR insulation, indicating that no significant amount of material was removed during accident irradiation and steam exposure. No density measurements were performed after the LOCA exposure for the insulations of the other three cables.

5.2.2 Gel Fraction

U.S. XLPO cable—Hypalon Jacket

Gel fraction data for the U.S. XLPO cable jacket are shown in Figure 5.21. The gel fraction did not change much during aging; however, the gel fraction increased slightly after LOCA for samples aged at 5 and 10 Gy/hr. This increase was possibly due to the extraction of low molecular weight components of the jacket material during the LOCA by the action of temperature and steam.

U.S. XLPO cable—XLPE Insulation

Gel fraction data for the U.S. XLPO cable insulation are shown in Figure 5.22. The gel fraction did not change significantly except for aging at 20 Gy/hr and 40°C.

The two types of material properties encountered during the tensile tests for the U.S. XLPO cable

insulation were not observed with the gel fraction data because small samples from several of the cut cable specimens were combined and one gel fraction measurement was performed. No measurements were performed after the LOCA exposure because the insulator stuck to the jacket because of the polypropylene filler.

U.S. EPR cable—Hypalon Jacket

Gel fraction data for the U.S. EPR cable jacket are shown in Figure 5.23. The gel fraction increased linearly with the aging dose. After LOCA, the gel fraction increased from its pre-LOCA values, probably because of cross-linking during the 600-kGy accident irradiation.

U.S. EPR cable—FR-EPDM Insulation

Gel fraction data for the U.S. EPR cable insulation are shown in Figure 5.24. During aging under irradiation, the gel fraction increased slightly with dose. After LOCA, measurements could not be performed because the insulation adhered to the cable conductors.

French EPR cable—Hypalon Jacket

Gel fraction data for the French EPR cable jacket are shown in Figure 5.25. During aging, the gel fraction increased linearly with dose, probably representing the cross-linking of the product. This phenomenon was independent of the dose rate and the test temperature. After LOCA, an increase in the gel fraction was observed. The fact that the gel fraction increased while the density was unchanged during the LOCA indicates that considerable cross-linking occurred during the accident irradiation.

French EPR cable—EPR Insulation

Gel fraction data for the French EPR cable insulation are shown in Figure 5.26. The gel fraction of the unaged insulation was 92.5%; no major variation was observed during aging under irradiation or after LOCA. These high values indicate that the unaged material was already fully cross-linked.

5.3 Electrical Measurement Results

The electrical measurement data presented here are from the complete cable specimens; no electrical measurements were performed on the cut specimens.

5.3.1 Coaxial Cable

Insulation Resistance

Insulation resistance of the coaxial cable (French PE), shown in Figure 5.27, was approximately 10^{12} Ω during aging. It remained fairly constant, even when the cable mechanical characteristics degraded. After the LOCA 600-kGy irradiation, the coaxial cable was significantly degraded and therefore no measurements were possible.

Microbreakdown

No microbreakdown was measured during aging in Kronos at 5, 10, and 20 Gy/hr. The behavior of the aged coaxial cable in Evocable was considerably different; disruption was observed on the unaged cable at a voltage of 600 Vdc. Disruptions were observed during aging irradiation at the following doses and electrical voltages: 3 kGy at 800 Vdc; 46 kGy at 1480 Vdc; 50 kGy at 1230 Vdc; and 56.5 kGy at 1500 Vdc. These disruptions were possibly due to a decrease of electrical insulation resistance of the connectors used in the test setup, not the coaxial cable under test.

Characteristic Impedance

The characteristic impedance was close to 50 Ω during the aging irradiation.

5.3.2 Non-Coaxial Cables

Dielectric Strength

No disruptions were observed during dielectric-strength tests performed during aging and after LOCA in the U.S. EPR cable or in the French EPR cable. However, a disruption was observed for 1 of the 7 test conditions (2 kVac after 30 sec) for the U.S. XLPO cable after the LOCA exposure.

Insulation Resistance

As shown in Figures 5.28–5.30, the IR values measured on the 3 cables (U.S. XLPO, U.S. EPR, and French EPR) remained greater than 5×10^5 MΩ during aging and after LOCA. Because of the extremely high IR values for all the measurements, it is likely that the observed variations in IR are not significant.

5.4 Summary of Experimental Results

Sections 4 and 5 have presented the CEA-sponsored, French test activities performed at the Centre d'Études Nucléaires (Center for Nuclear Studies) in Saclay, France, by CEA and CIS bio international teams as part of a cooperative U.S./French program to investigate the long-term aging of electrical cables. The French test program is summarized here; see Section 3.3 for a summary of the U.S. test program and Section 6.3 for a summary of the comparison between the two test programs.

Of the measurement techniques used in this program, only the elongation at break and gel fraction data were consistent enough to show the effect of the aging exposure on the cables. Mechanical tests during aging revealed gradual degradation of the jackets and insulations on the cables, specifically:

- For the three Hypalon jacket materials tested in this program, degradation due to simultaneous exposure to 5 Gy/hr radiation and 70°C thermal environments was greater than the sum of the degradation due to 5 Gy/hr radiation-only and 70°C thermal-only exposures. This indicates a possible synergism between these thermal and radiation exposures; which is consistent with the results of an earlier study [1].
- The elongation at break data for the U.S. XLPO cable's XLPE insulation material exhibited two distinct types of behavior that might be due to the type of clamp used to hold the specimens during tensile testing. Because of this, no definite conclusions about this material's behavior during the aging exposures can be reached.
- The elongation at break for the French EPR cable's EPR insulation was sensitive only to the dose received, not the dose rate, during the aging except for the 20 Gy/hr, 40°C data which had substantially more degradation than the lower dose rate data at 40°C; the reason for this behavior is unknown.
- Degradation of the FR-EPDM insulation of the U.S. EPR cable and the EPR insulation of the French EPR cable showed greater degradation during the 20 Gy/hr irradiation at 40°C than at 70°C; this behavior is somewhat unusual.

After exposure to the simulated LOCA environment, the elongation at break data for the cables showed considerable degradation from their pre-LOCA values; however, the cables still retained sufficient residual mechanical properties. The gel fraction measurements showed a small increase in the cross-linking of the three Hypalon jackets during the LOCA simulation. In spite of the measurable changes that occurred in the elongation at break values, the density data remained essentially unchanged. The electrical properties of the cables remained very high for all measurements. Note that measurements were made only before and after the LOCA simulation at room temperature, not during the simulation.

Both the jacket and insulation of the French PE cable were quickly degraded to 0% elongation at break by the aging radiation exposures. The effect of dose rate on this degradation was somewhat unusual in that, for a given dose, the degradation increased as the dose rate increased. In spite of the degradation in elongation at break values, the electrical properties were not affected by the aging irradiation up to the maximum aging dose of 84 kGy.

For the French PE (coaxial) cable, which was not qualified for accident conditions, both the PE jacket and insulation were destroyed by the 600 kGy (60 Mrad) accident irradiation.

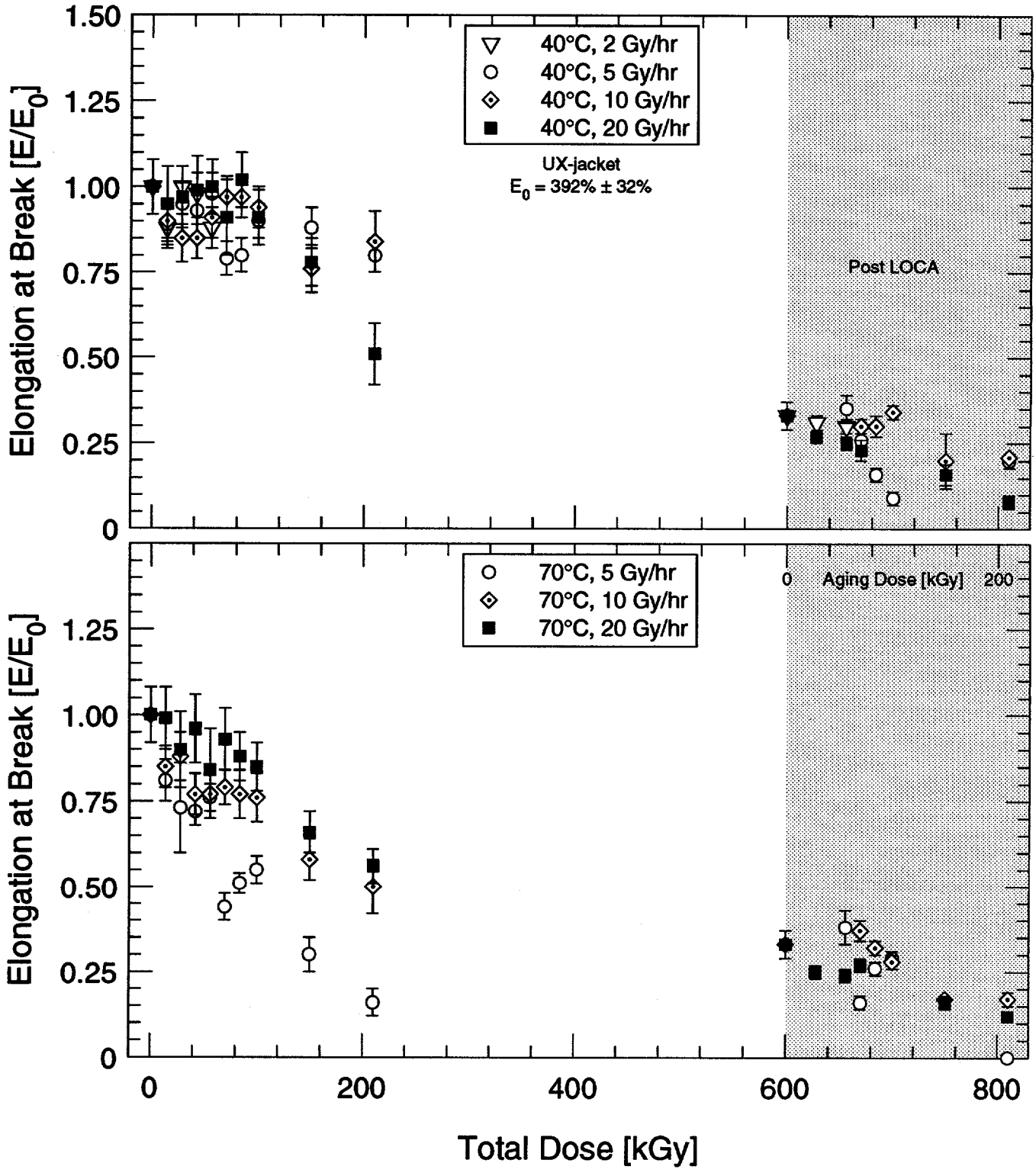

Figure 5.1: Elongation at break during aging and after LOCA simulation versus total dose for U.S. XLPO cable—Hypalon jacket.

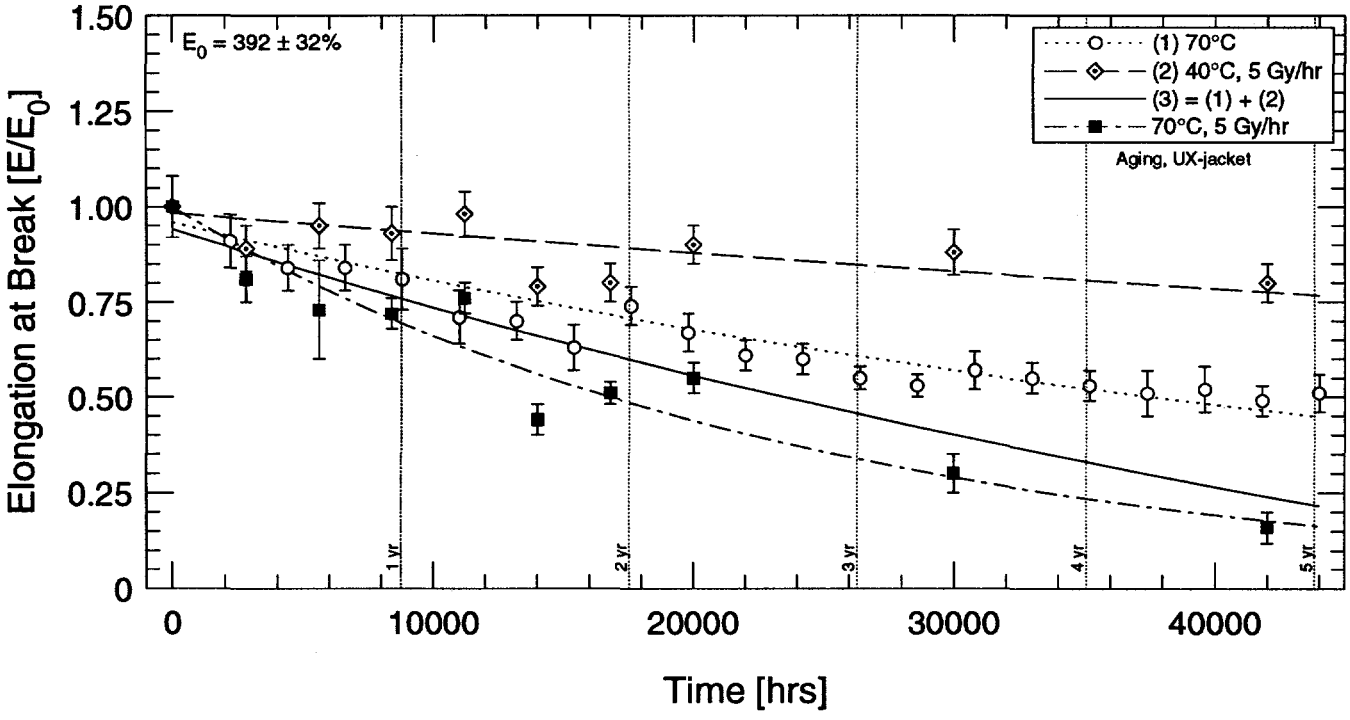

Figure 5.2: Elongation at break versus time for U.S. XLPO cable—Hypalon jacket.

Table 5.1: Elongation at Break versus Dose for U.S. XLPO Cable—XLPE Insulation ($E_0 = 256\% \pm 40\%$).

Dose [kGy]	$T = 40°C$ Total Samples	Fraction of Type A	E/E_0 Type A	E/E_0 Type B	$T = 70°C$ Total Samples	Fraction of Type A	E/E_0 Type A	E/E_0 Type B
Aging at 2 Gy/hr								
14	-	-	-	-	-	-	-	-
28	9	0%	-	0.05±0.01	-	-	-	-
42	9	0%	-	0.05±0.01	-	-	-	-
56	9	78%	1.01±0.16	0.41±0.06	-	-	-	-
Aging at 5 Gy/hr								
14	5	80%	1.14±0.13	0.40	8	88%	1.03±0.29	0.40
28	8	100%	1.13±0.15	-	8	100%	1.13±0.13	-
42	6	100%	1.07±0.11	-	8	88%	1.06±0.12	0.64
56	12	67%	1.09±0.13	0.25±0.17	12	75%	1.00±0.11	0.23±0.09
70	11	55%	1.01±0.19	0.20±0.10	12	50%	0.97±0.17	0.20±0.10
84	10	70%	1.05±0.13	0.16±0.08	11	55%	1.03±0.14	0.29±0.17
100	12	33%	0.99±0.20	0.13±0.05	12	42%	0.96±0.17	0.22±0.12
150	11	0%	-	0.08±0.02	12	33%	0.89±0.14	0.24±0.12
210	11	0%	-	0.10±0.04	12	83%	0.69±0.13	0.31±0.04
Aging at 10 Gy/hr								
14	7	100%	1.14±0.14	-	8	100%	1.08±0.15	-
28	8	100%	1.13±0.13	-	8	88%	1.04±0.15	0.65
42	8	88%	0.98±0.20	0.32	7	100%	1.01±0.13	-
56	7	100%	1.09±0.12	-	8	100%	1.06±0.13	-
70	12	100%	0.89±0.11	-	12	41%	0.94±0.20	0.18±0.07
84	12	42%	1.04±0.13	0.16±0.07	11	73%	0.96±0.15	0.21±0.04
100	12	42%	1.00±0.11	0.17±0.07	12	67%	0.97±0.14	0.30±0.15
150	9	0%	-	0.09±0.04	12	50%	0.83±0.21	0.14±0.05
210	11	0%	-	0.06±0.01	11	9%	0.68	0.12±0.04
Aging at 20 Gy/hr								
14	7	100%	0.91±0.13	-	9	100%	1.00±0.11	-
28	8	100%	1.06±0.12	-	9	100%	1.05±0.12	-
42	7	100%	1.02±0.12	-	7	100%	0.97±0.11	-
56	7	100%	1.02±0.11	-	11	100%	0.98±0.11	-
70	8	100%	0.93±0.12	-	11	100%	0.95±0.11	-
84	9	100%	0.85±0.10	-	9	100%	0.89±0.13	-
100	12	100%	0.84±0.09	-	9	100%	0.85±0.14	-
150	9	0%	-	0.05±0.01	9	0%	-	0.21±0.09
210	7	0%	-	0.04±0.01	9	0%	-	0.09±0.01

Table 5.2: Elongation at Break versus Time for U.S. XLPO Cable—XLPE Insulation, 70°C Thermal-Only Exposure ($E_0 = 256\% \pm 40\%$).

Exposure Time [hr]	Equivalent Dose at 10 Gy/hr [kGy]	Total Samples	Fraction of Type A	E/E_0	
				Type A	Type B
2200	22	10	50%	1.00±0.19	0.30±0.15
4400	44	12	75%	1.07±0.13	0.36±0.18
6600	66	10	80%	1.11±0.13	0.23±0.04
8800	88	11	91%	1.06±0.13	0.22
11000	110	10	100%	1.07±0.13	-
13200	132	12	33%	1.09±0.21	0.18±0.09
15400	154	8	88%	1.10±0.14	0.49
17600	176	12	58%	1.05±0.17	0.21±0.13
19800	198	12	67%	1.07±0.13	0.11±0.04
22000	220	12	83%	1.07±0.13	0.16±0.10
24200	242	10	60%	1.08±0.12	0.20±0.06
26400	264	10	70%	1.07±0.15	0.14±0.05
28600	286	12	58%	1.08±0.13	0.17±0.03
30800	308	12	50%	1.05±0.16	0.18±0.06
33000	330	12	75%	1.08±0.15	0.46±0.17
35200	352	12	83%	1.10±0.13	0.42±0.22
37400	374	12	67%	1.08±0.12	0.46±0.22
39600	396	11	73%	1.04±0.19	0.46±0.07
41800	418	12	83%	1.07±0.18	0.50±0.23
44000	440	12	67%	1.11±0.13	0.50±0.11

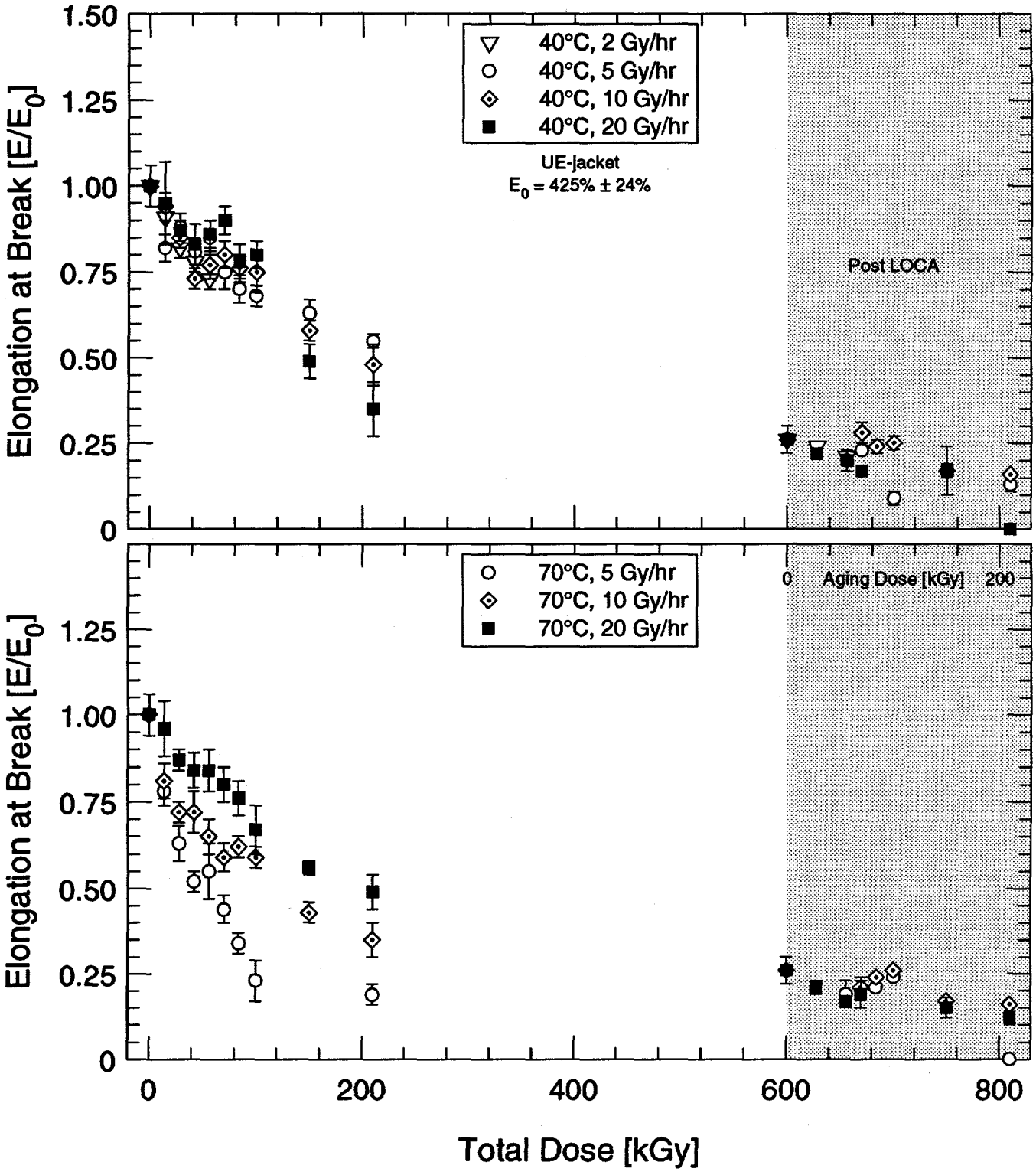

Figure 5.3: Elongation at break during aging and after LOCA simulation versus total dose for U.S. EPR cable—Hypalon jacket.

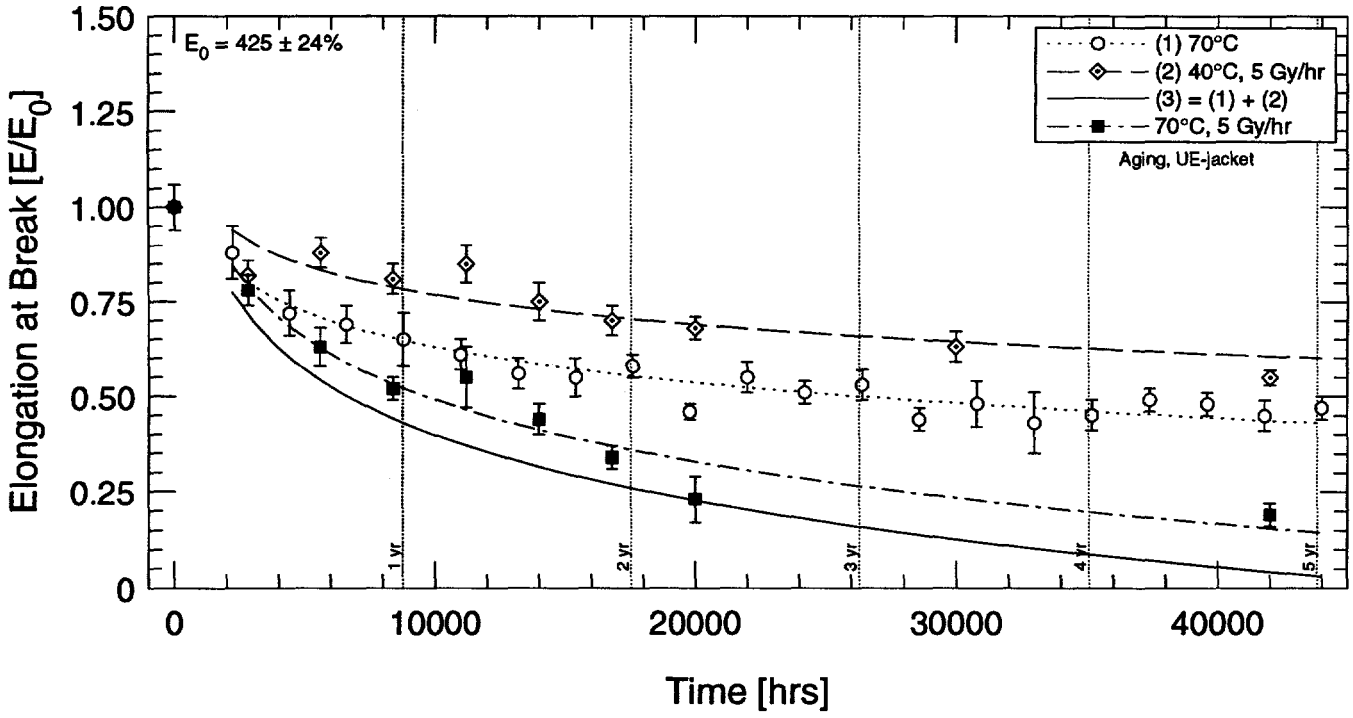

Figure 5.4: Elongation at break versus time for U.S. EPR cable—Hypalon jacket.

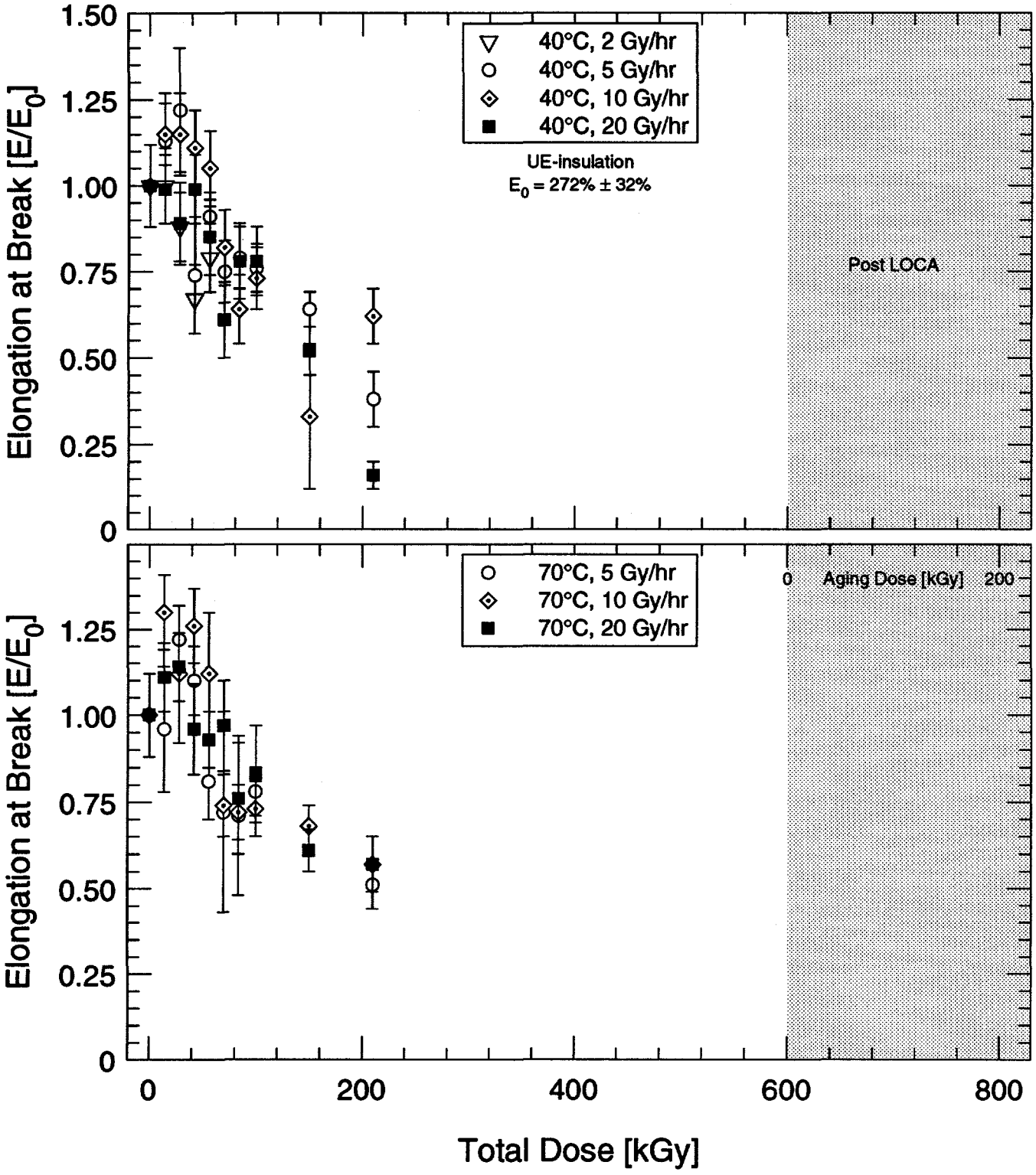

Figure 5.5: Elongation at break during aging versus total dose for U.S. EPR cable—FR-EPDM insulation.

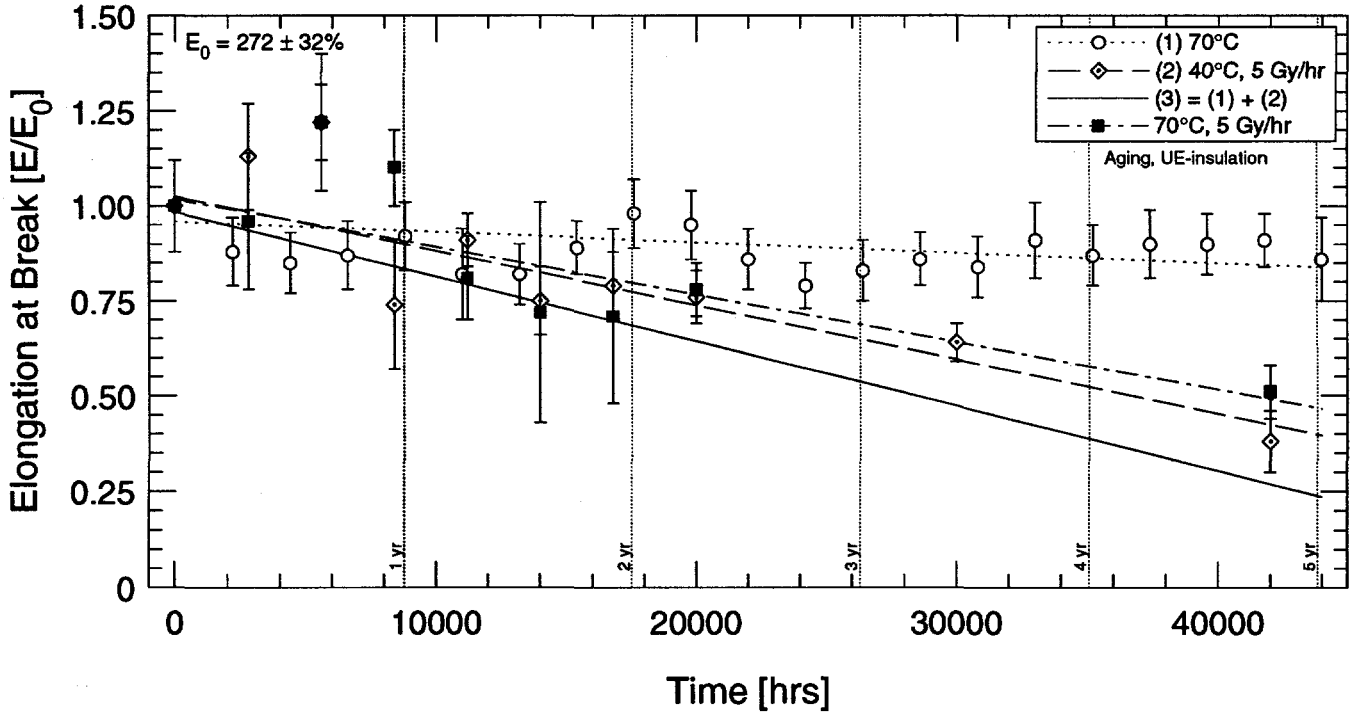

Figure 5.6: Elongation at break versus time for U.S. EPR cable—FR-EPDM insulation.

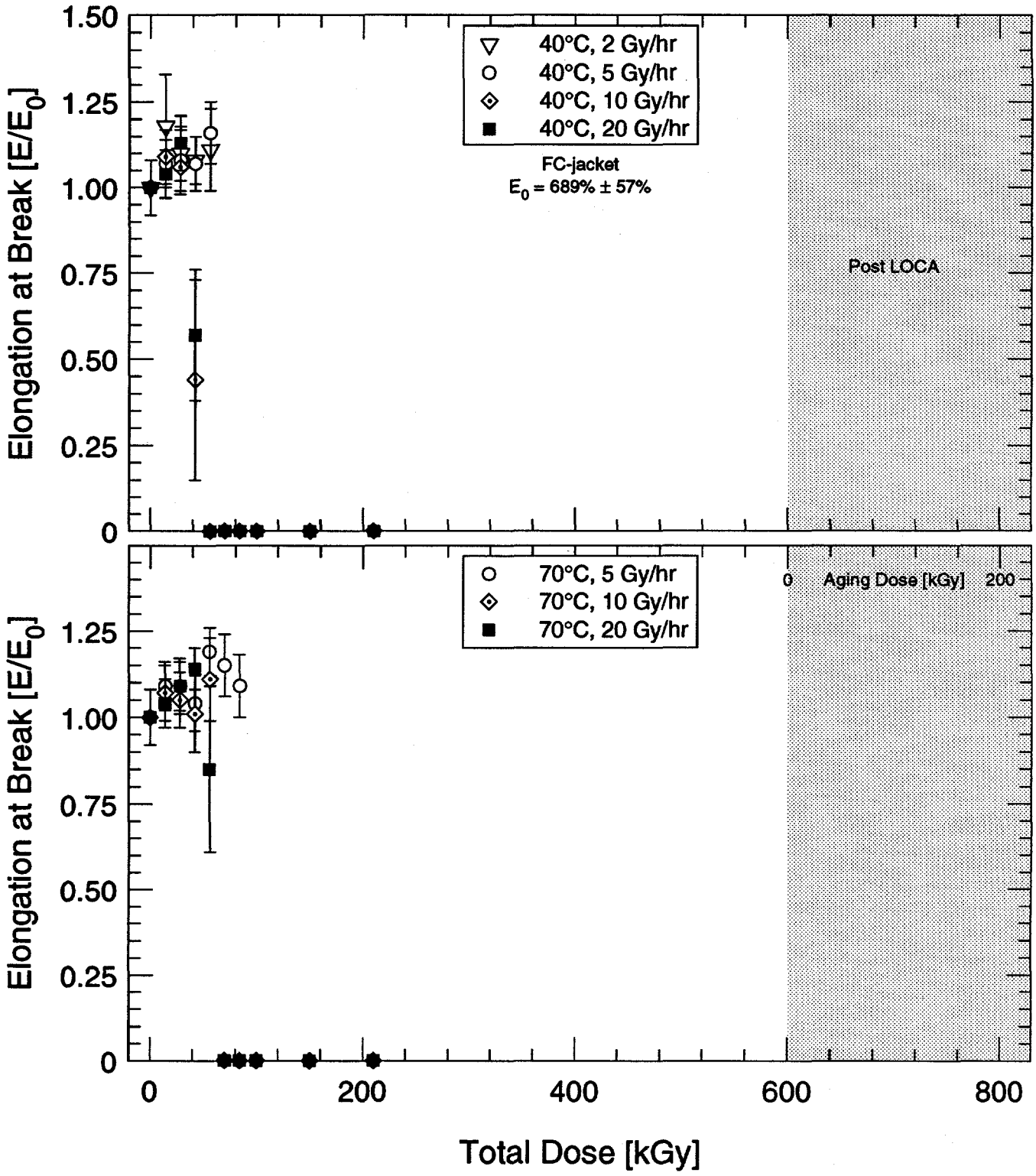

Figure 5.7: Elongation at break during aging versus total dose for French PE cable—PE jacket.

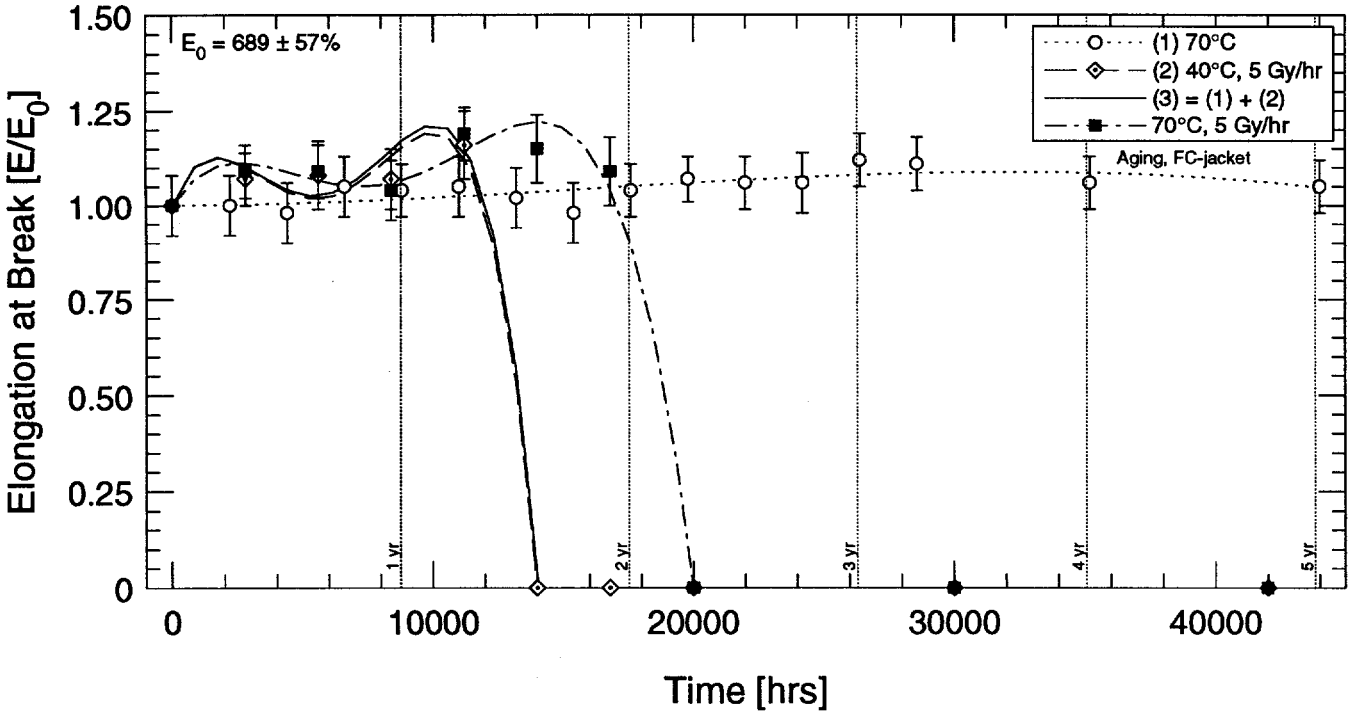

Figure 5.8: Elongation at break versus time for French PE cable—PE jacket.

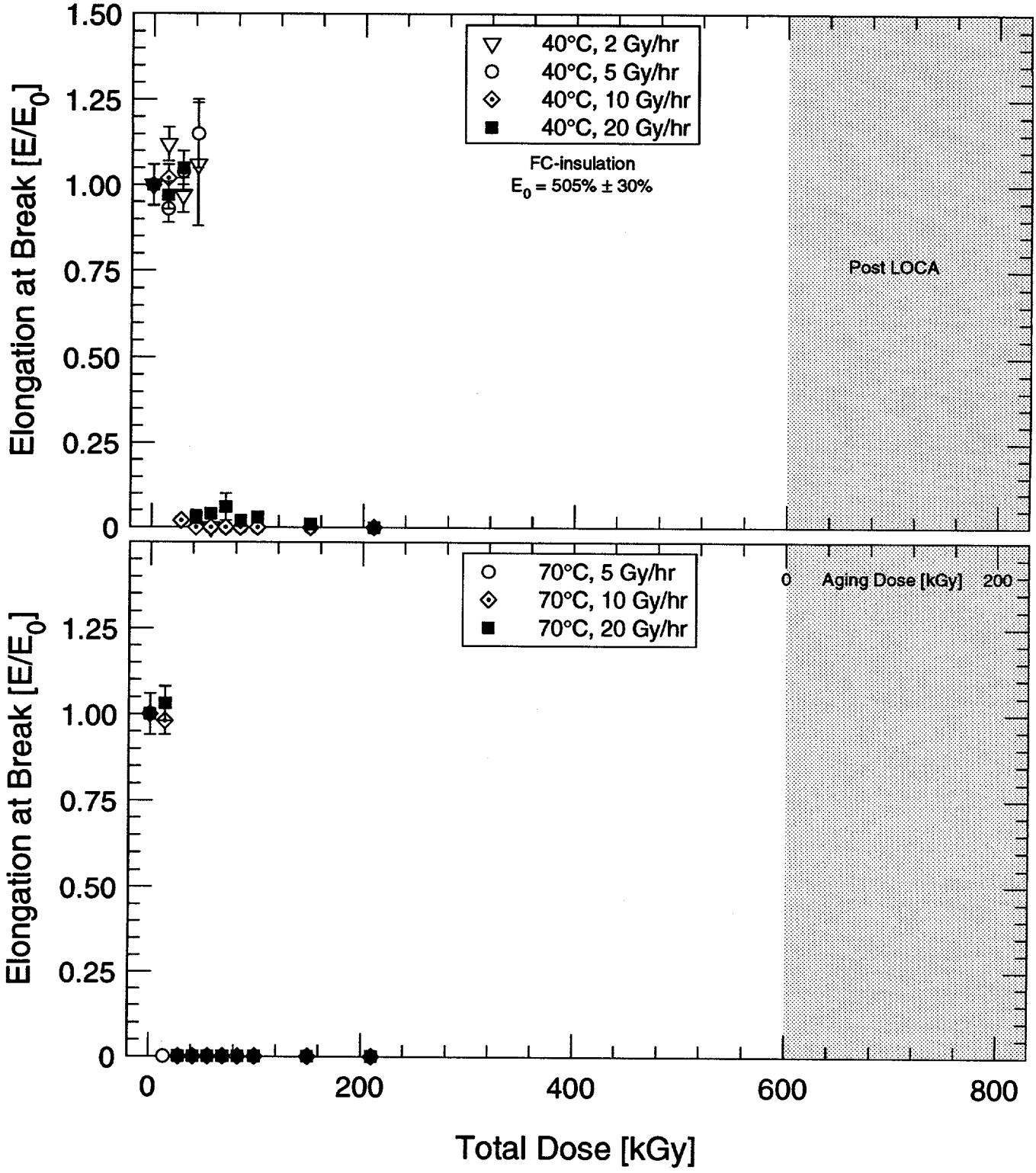

Figure 5.9: Elongation at break during aging versus total dose for French PE cable—PE insulation.

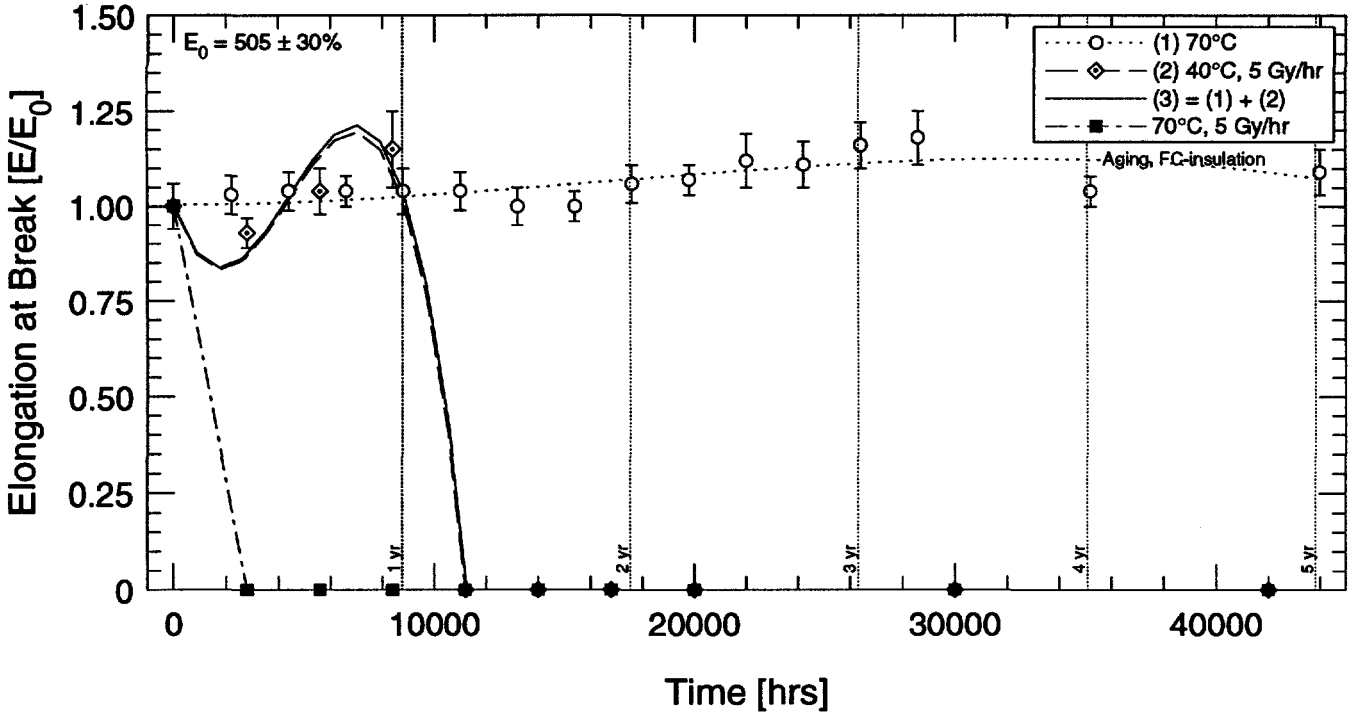

Figure 5.10: Elongation at break versus time for French PE cable—PE insulation.

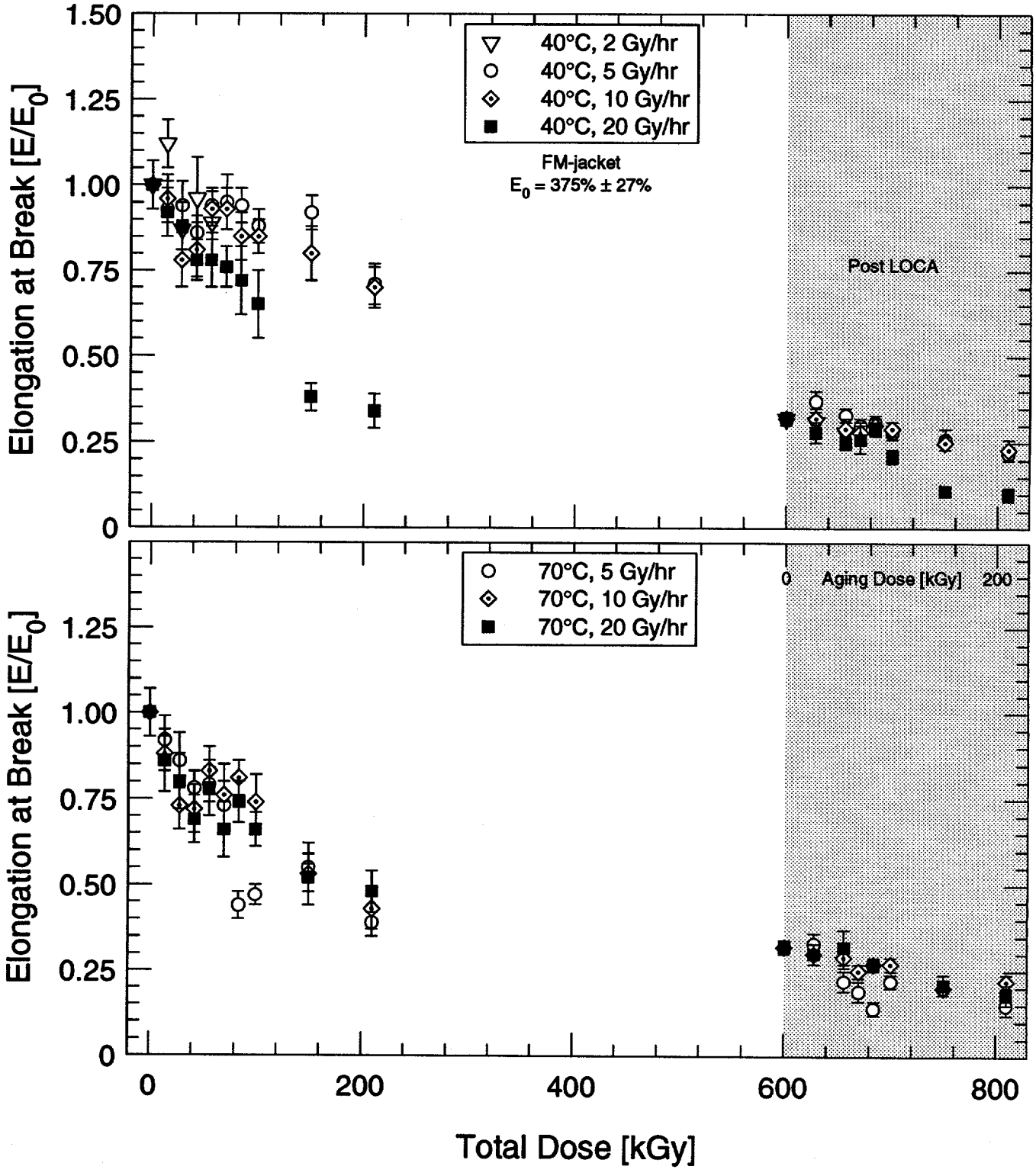

Figure 5.11: Elongation at break during aging and after LOCA simulation versus total dose for French EPR cable—Hypalon jacket.

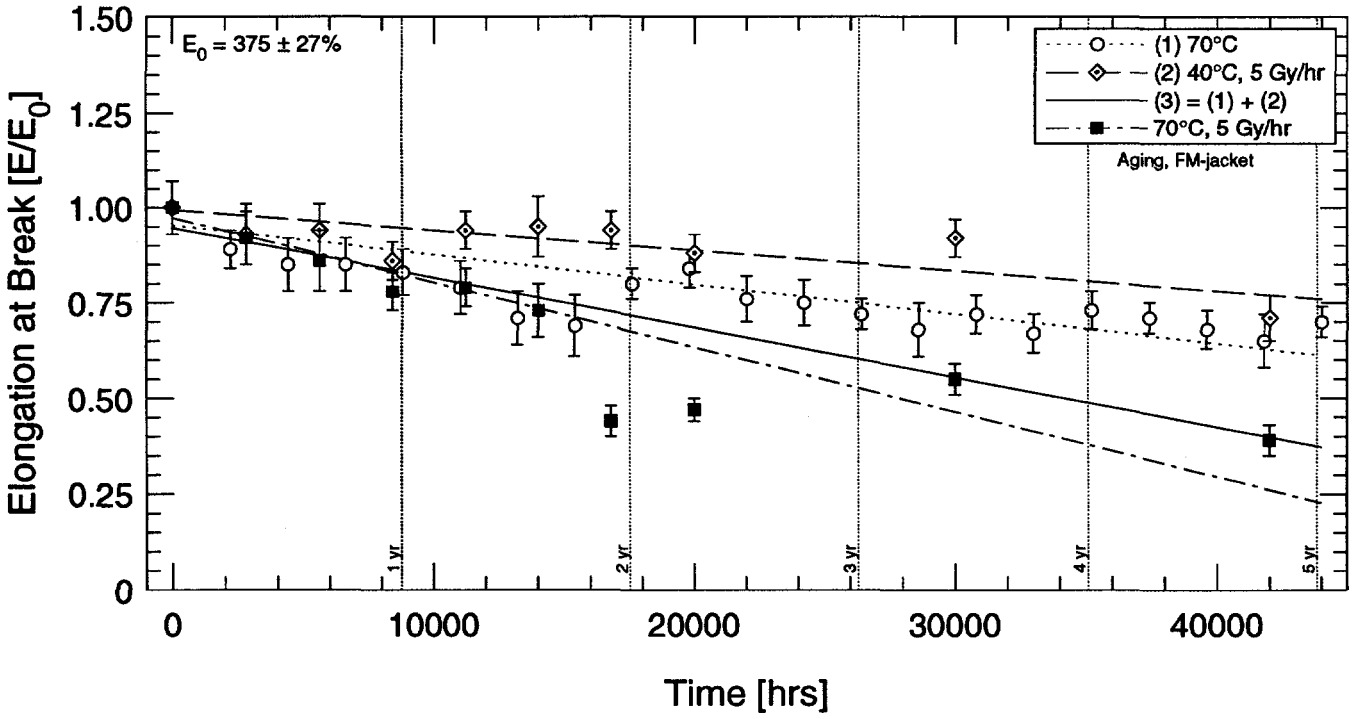

Figure 5.12: Elongation at break versus time for French EPR cable—Hypalon jacket.

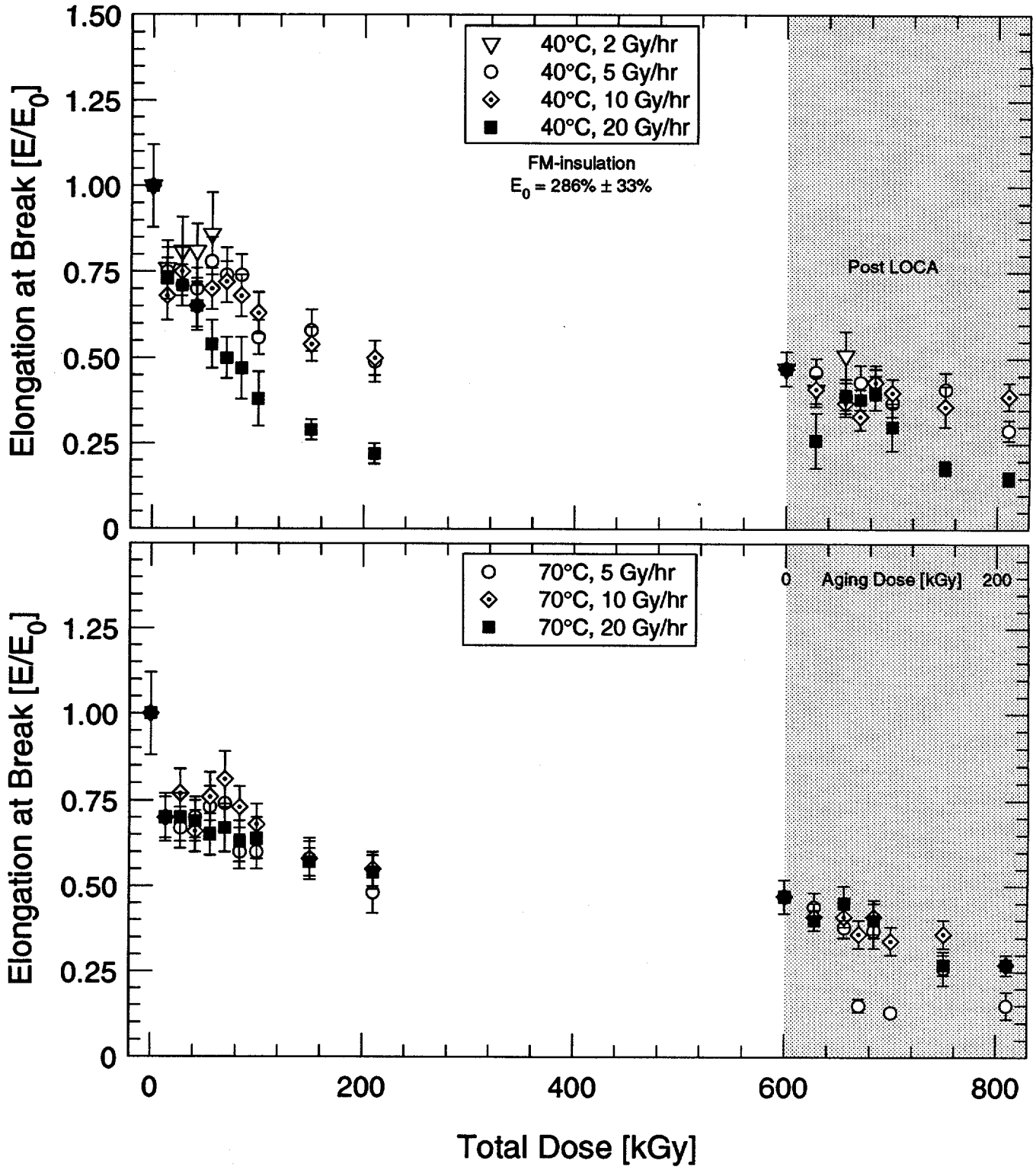

Figure 5.13: Elongation at break during aging and after LOCA simulation versus total dose for French EPR cable—EPR insulation.

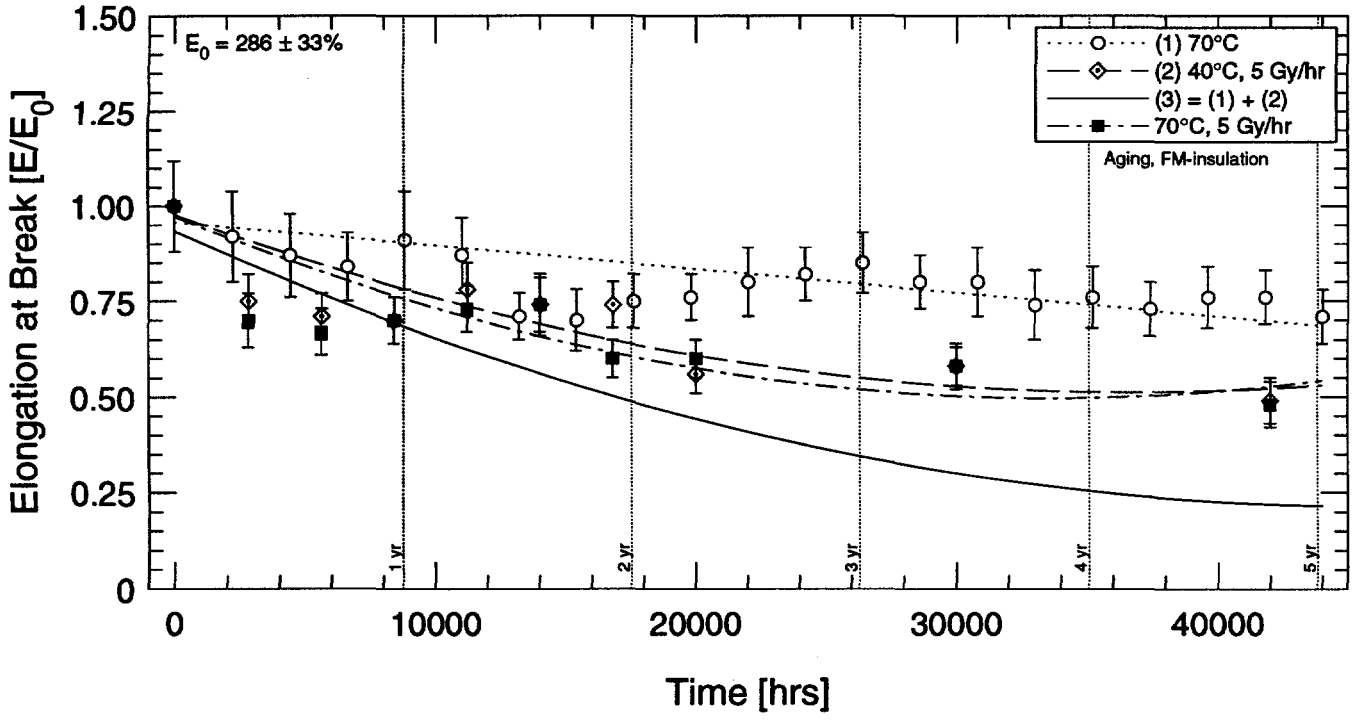

Figure 5.14: Elongation at break versus time for French EPR cable—EPR insulation.

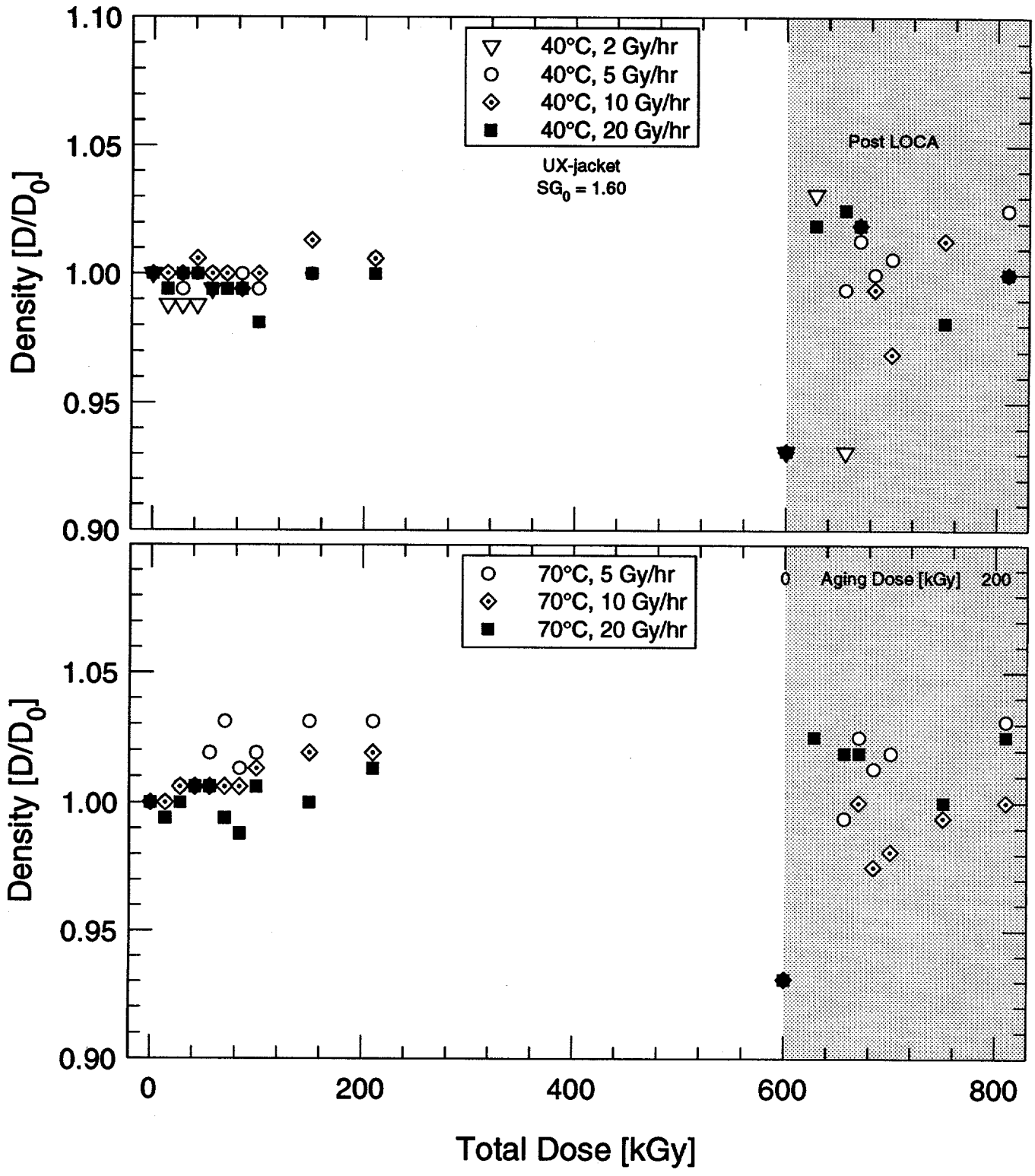

Figure 5.15: Density during aging and after LOCA exposure versus total dose for U.S. XLPO cable—Hypalon jacket.

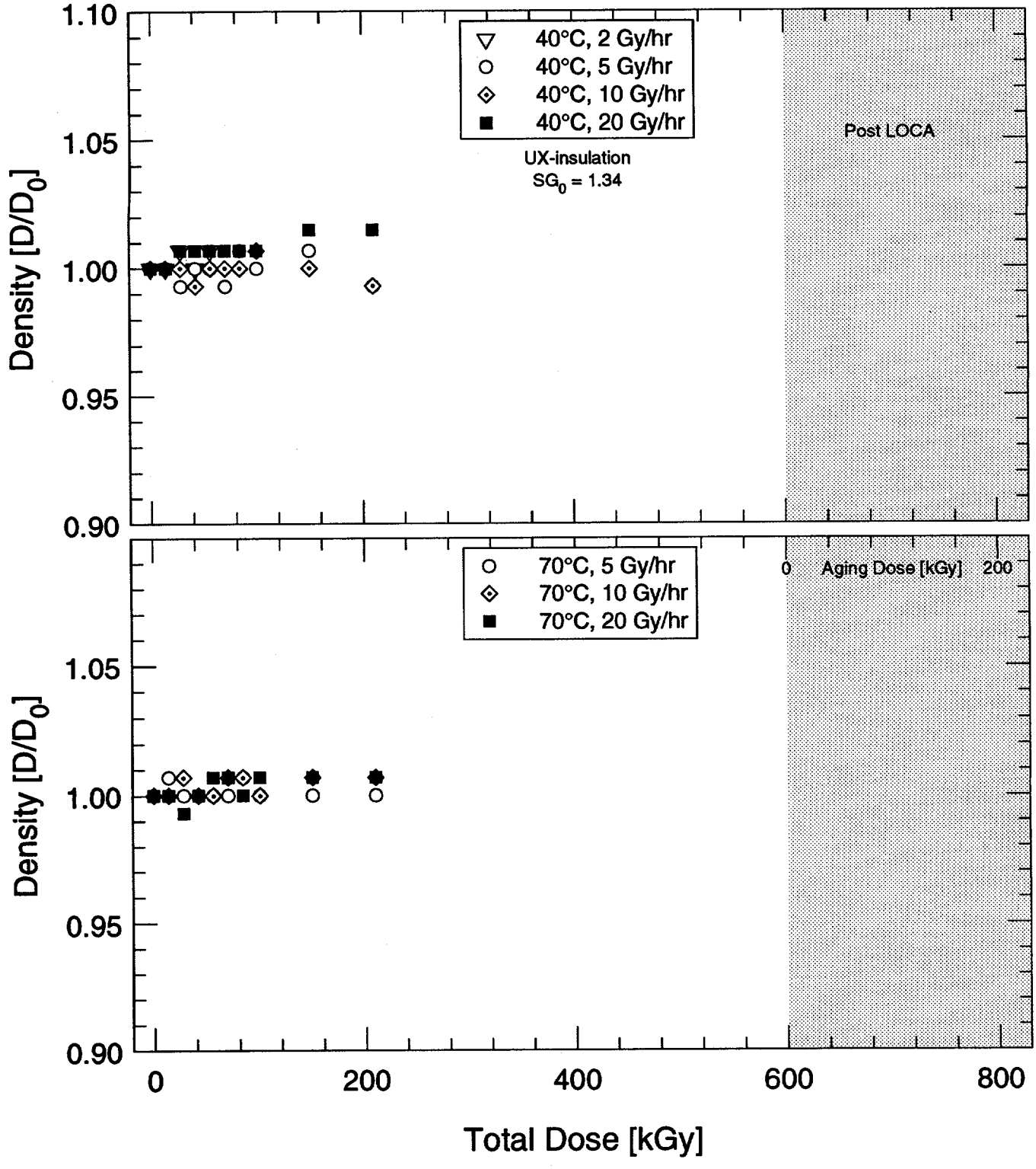

Figure 5.16: Density during aging versus total dose for U.S. XLPO cable—XLPE insulation.

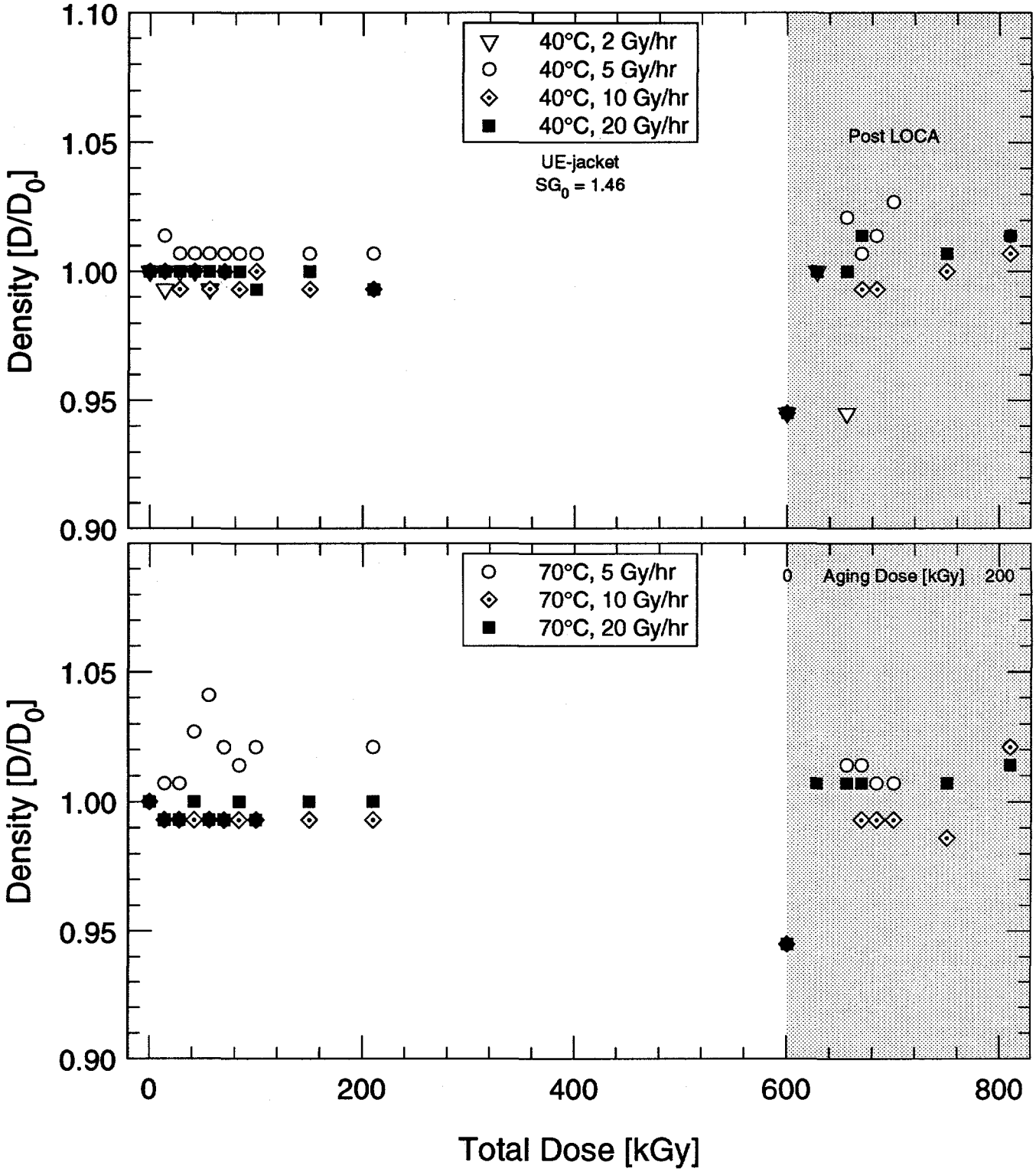

Figure 5.17: Density during aging and after LOCA exposure versus total dose for U.S. EPR cable—Hypalon jacket.

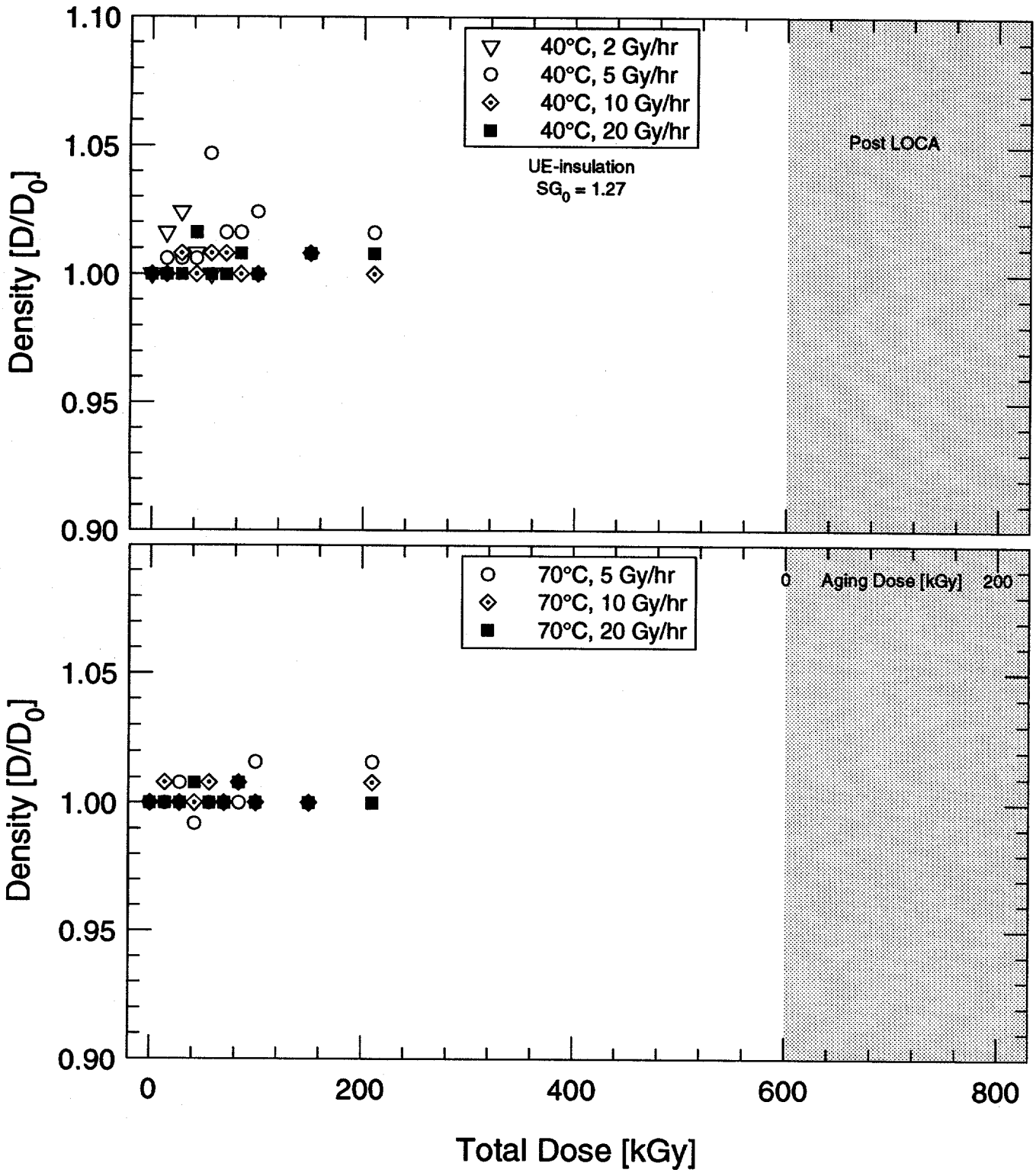

Figure 5.18: Density during aging versus total dose for U.S. EPR cable—FR-EPDM insulation.

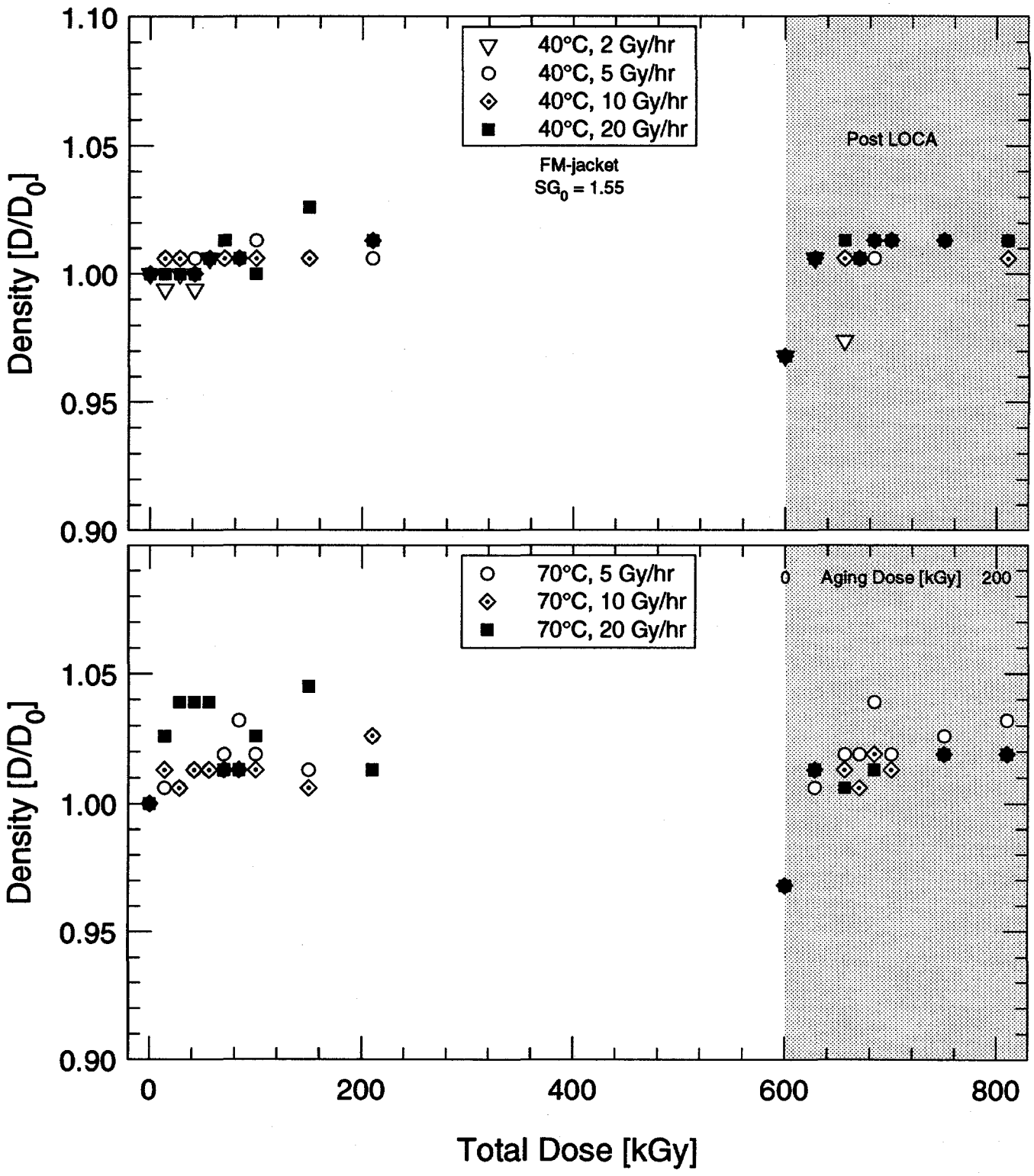

Figure 5.19: Density during aging and after LOCA exposure versus total dose for French EPR cable—Hypalon jacket.

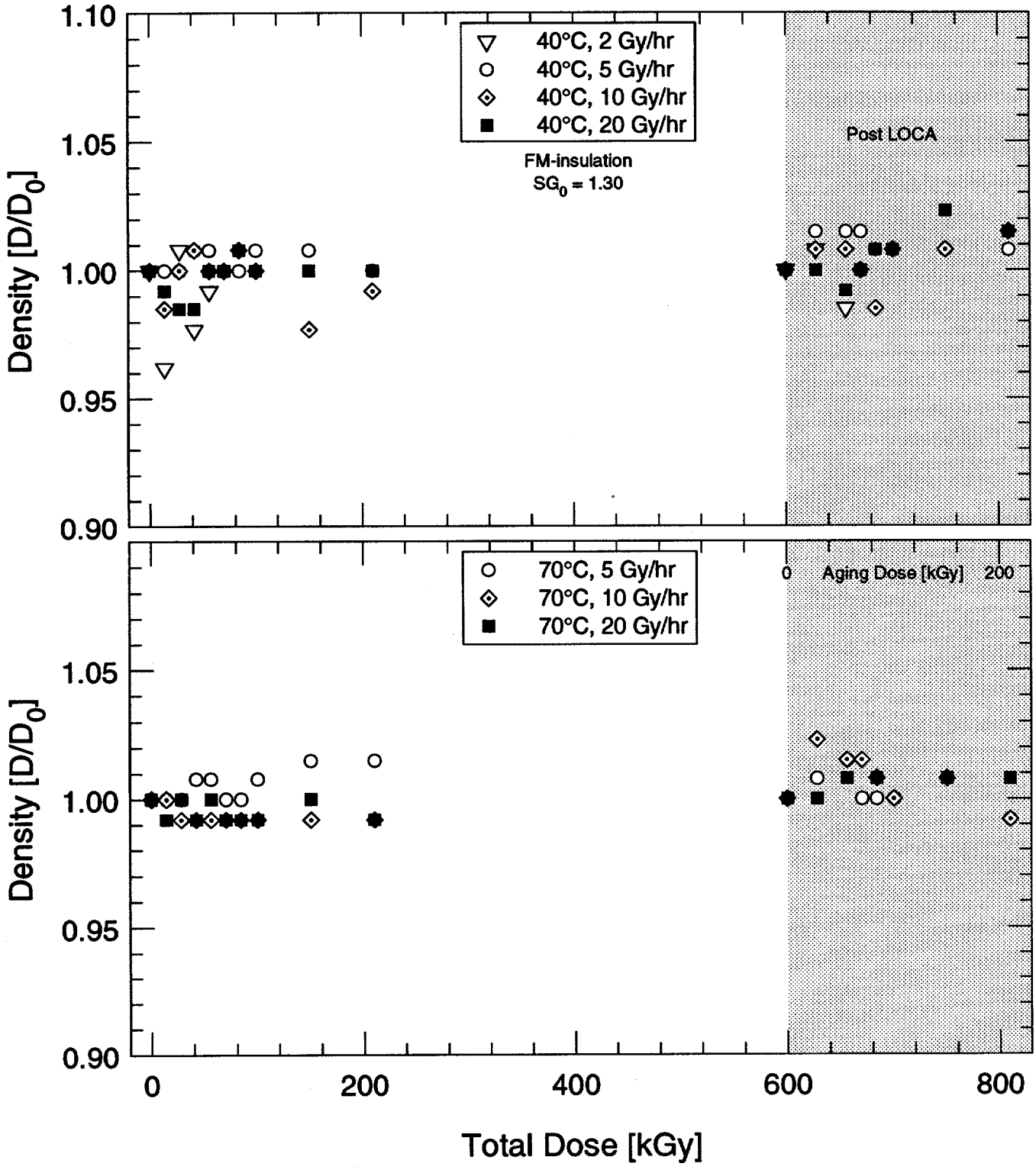

Figure 5.20: Density during aging and after LOCA exposure versus total dose for French EPR cable—EPR insulation.

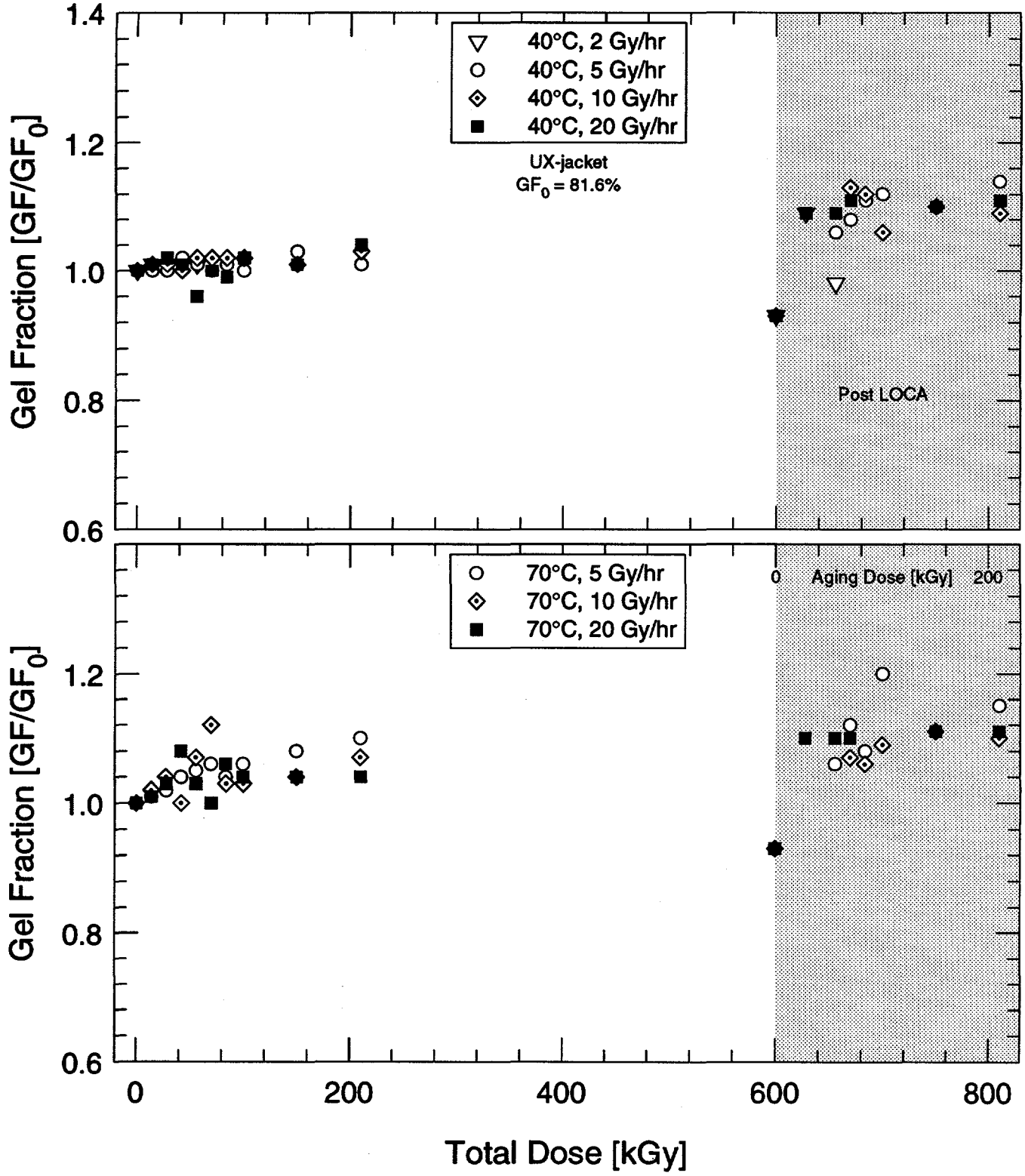

Figure 5.21: Gel fraction during aging and after LOCA exposure versus total dose for U.S. XLPO cable—Hypalon jacket.

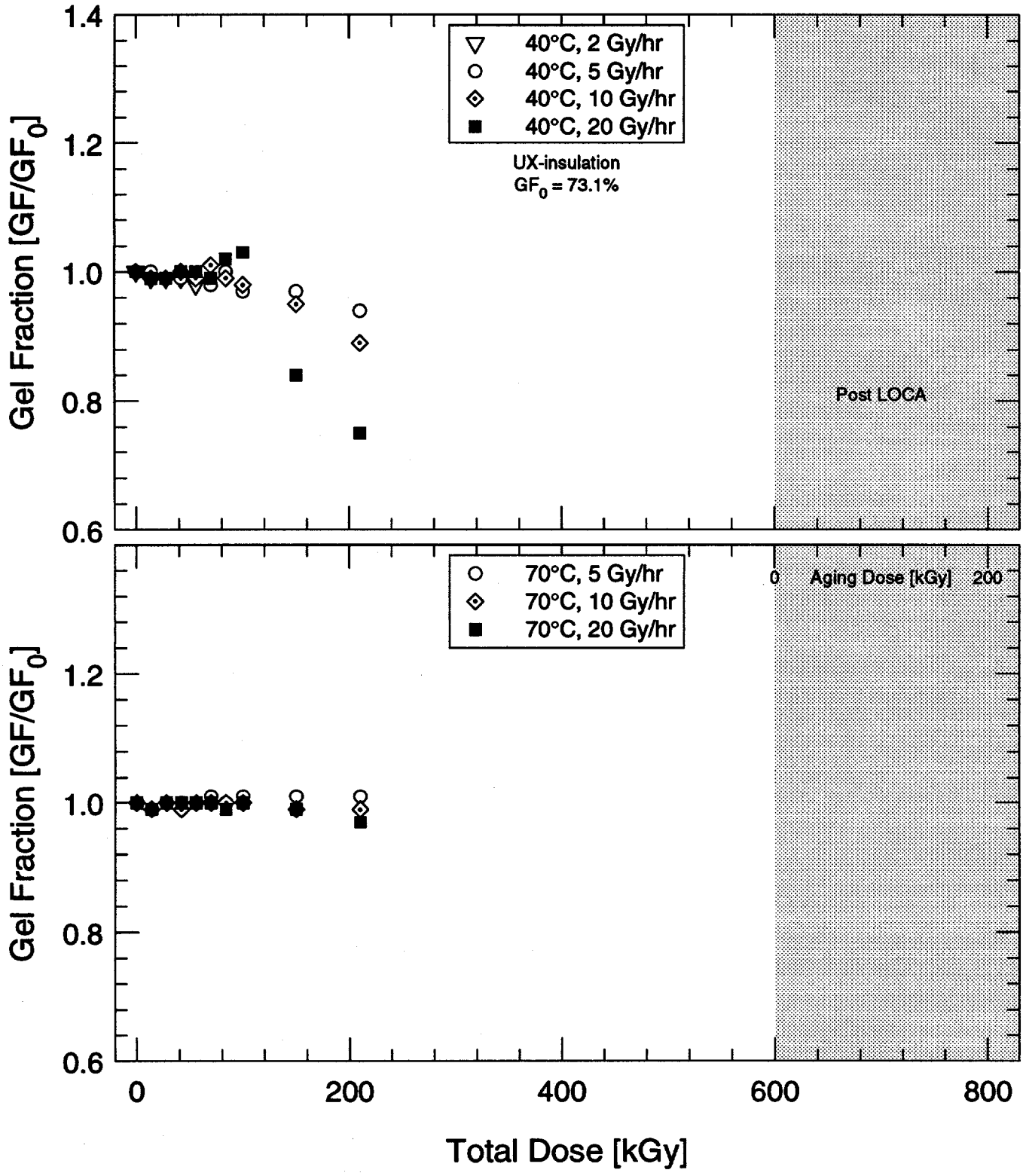

Figure 5.22: Gel fraction during aging versus total dose for U.S. XLPO cable—XLPE insulation.

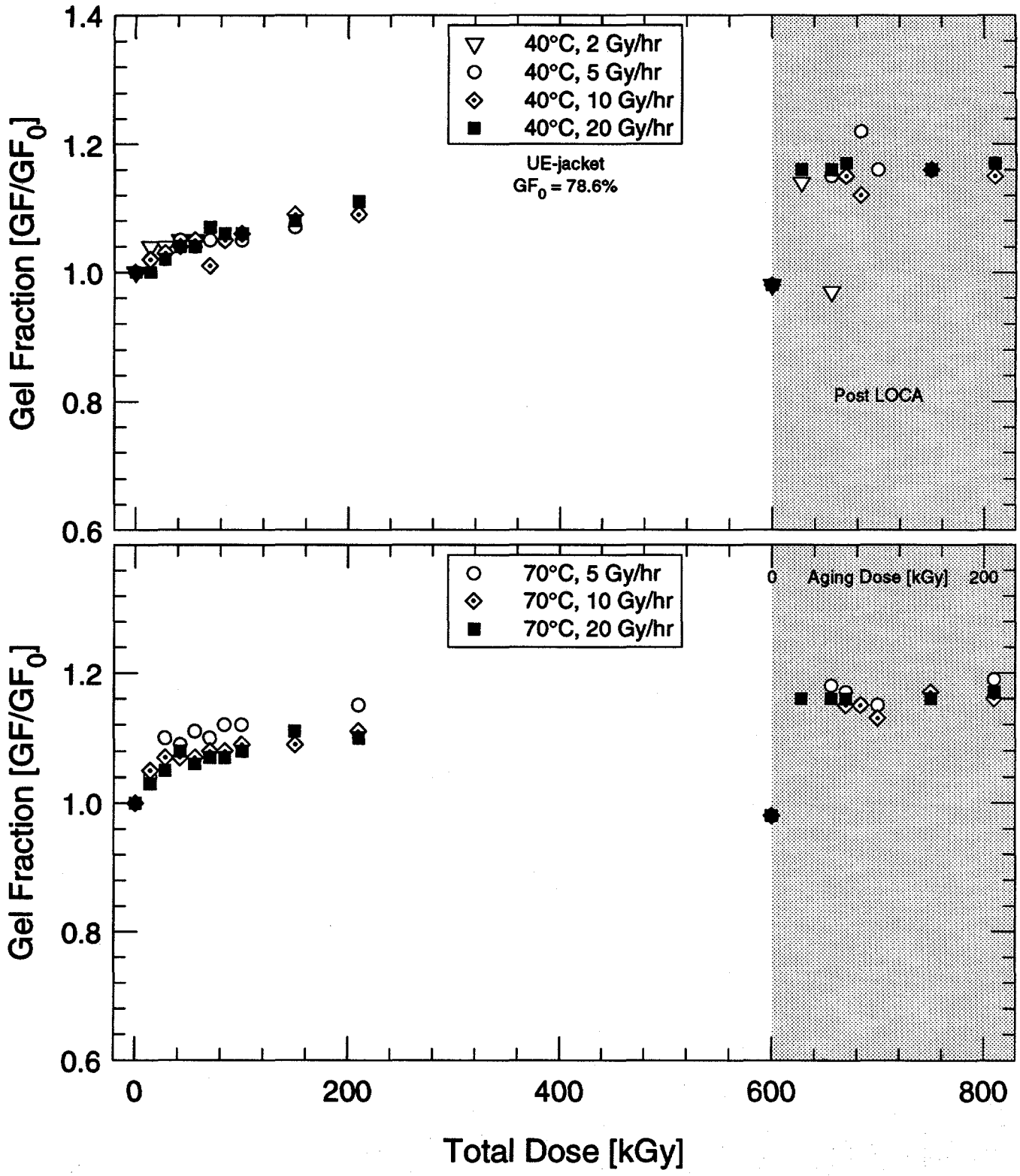

Figure 5.23: Gel fraction during aging and after LOCA exposure versus total dose for U.S. EPR cable—Hypalon jacket.

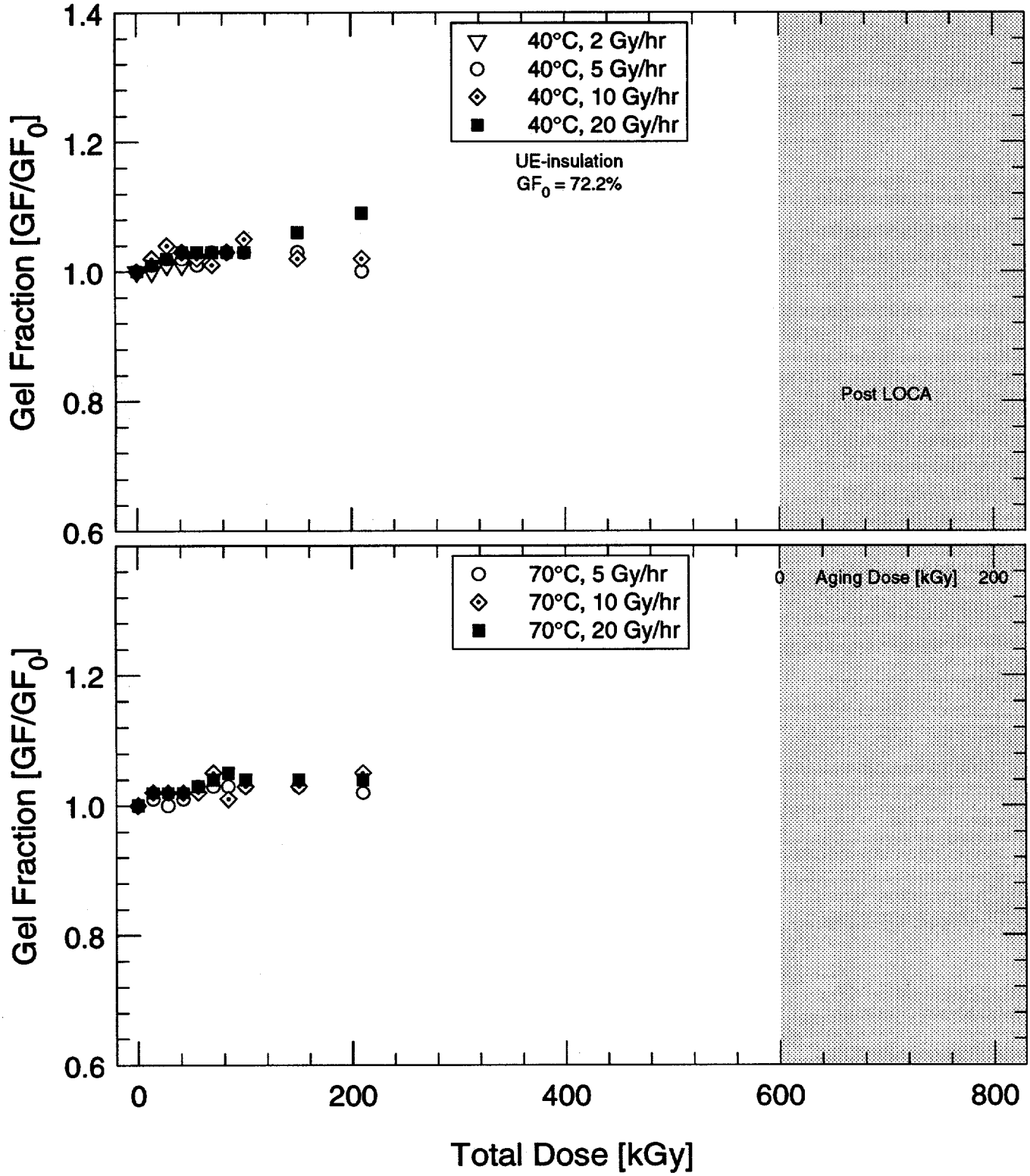

Figure 5.24: Gel fraction during aging versus total dose for U.S. EPR cable—FR-EPDM insulation.

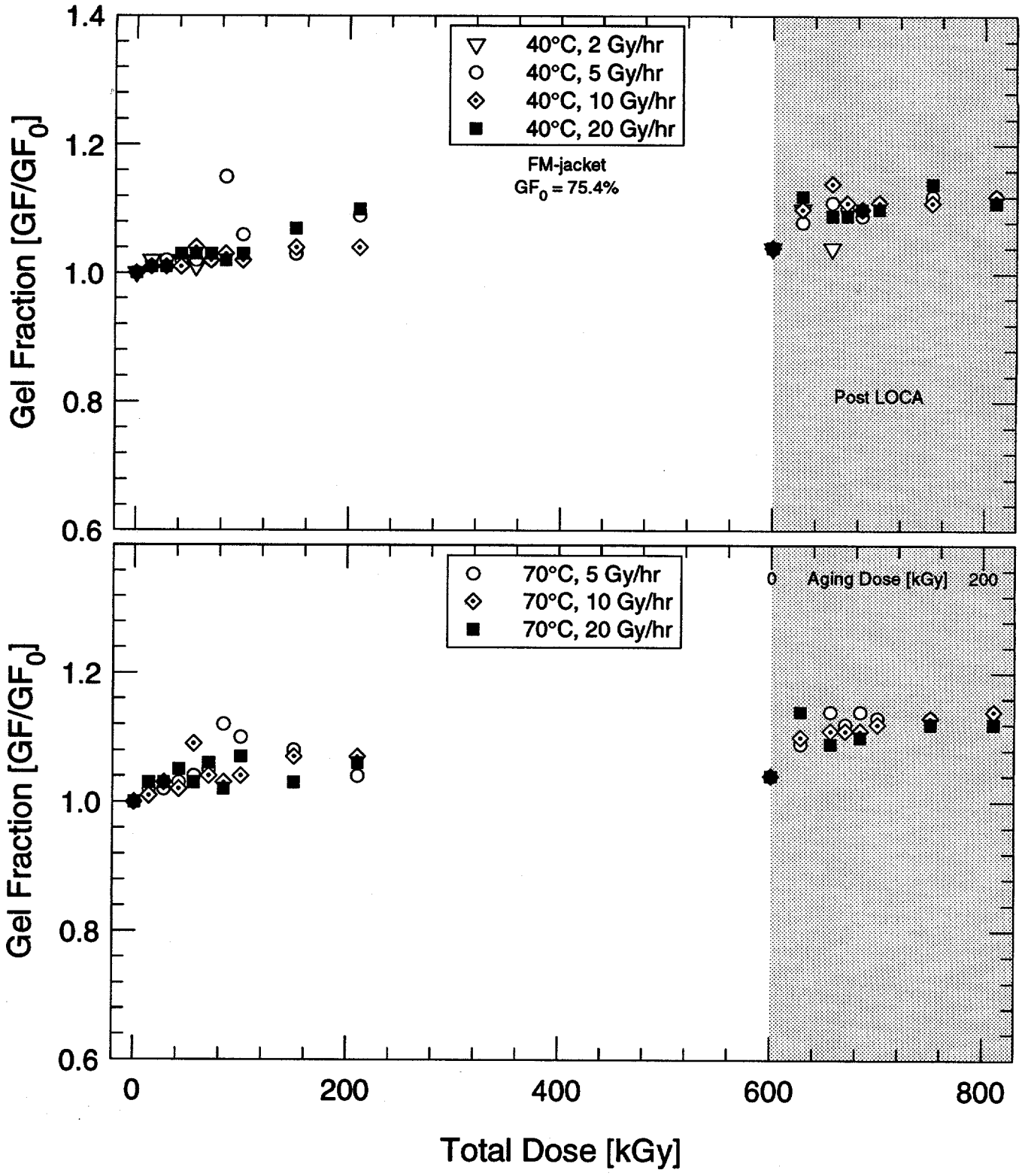

Figure 5.25: Gel fraction during aging and after LOCA exposure versus total dose for French EPR cable—Hypalon jacket.

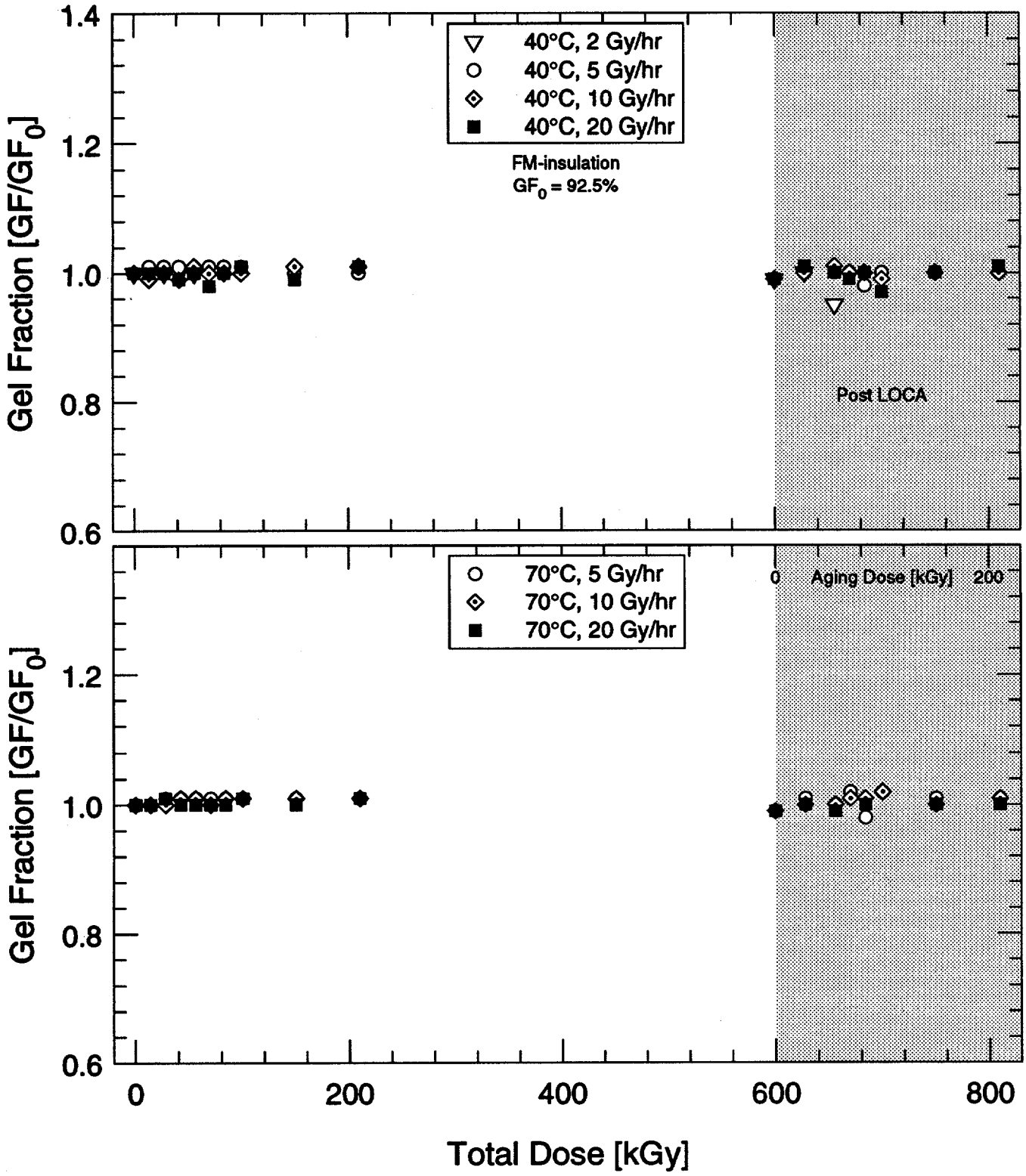

Figure 5.26: Gel fraction during aging and after LOCA exposure versus total dose for French EPR cable—EPR insulation.

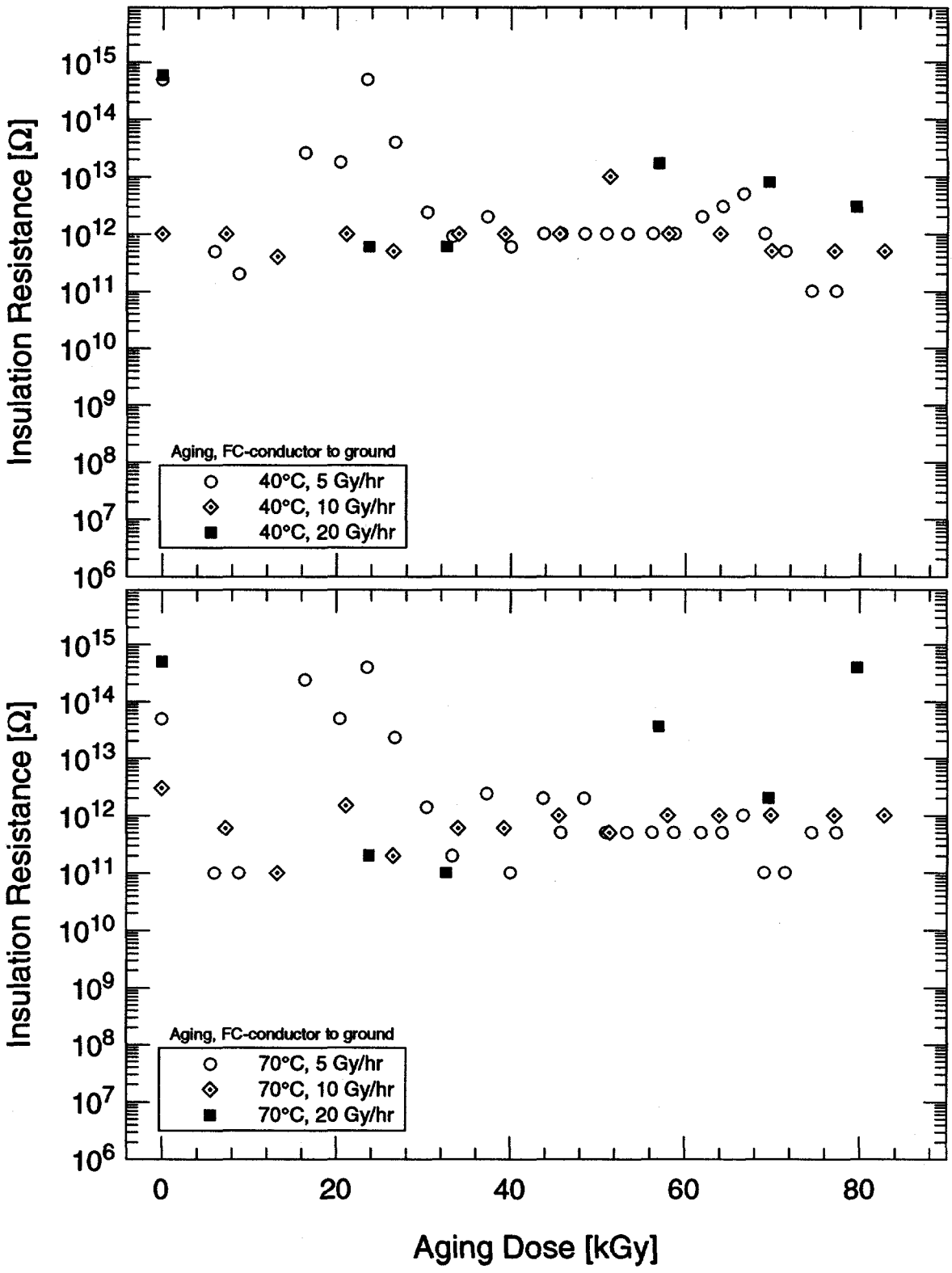

Figure 5.27: French PE cable insulation resistance versus dose.

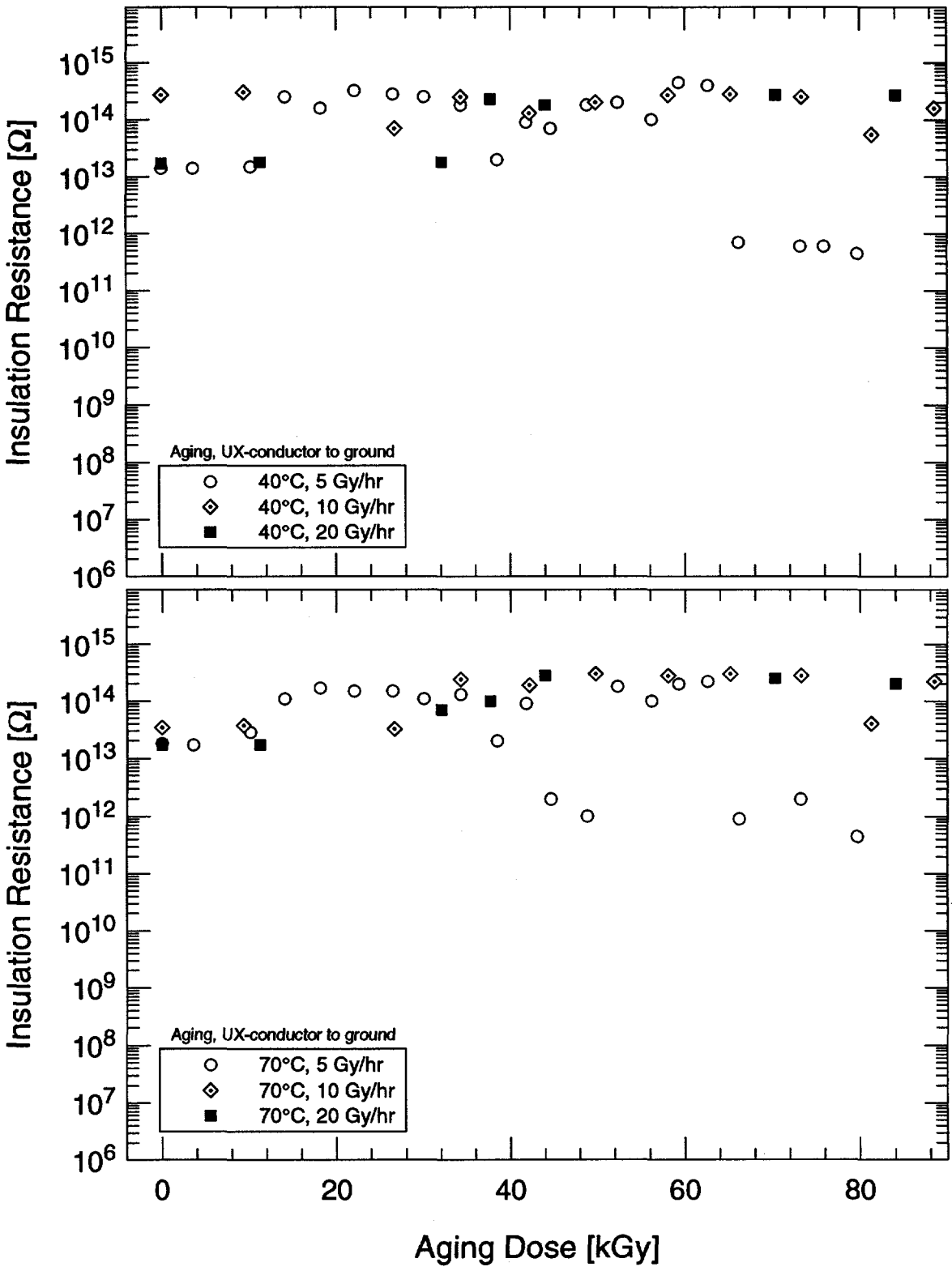

Figure 5.28: U.S. XLPO cable insulation resistance versus dose.

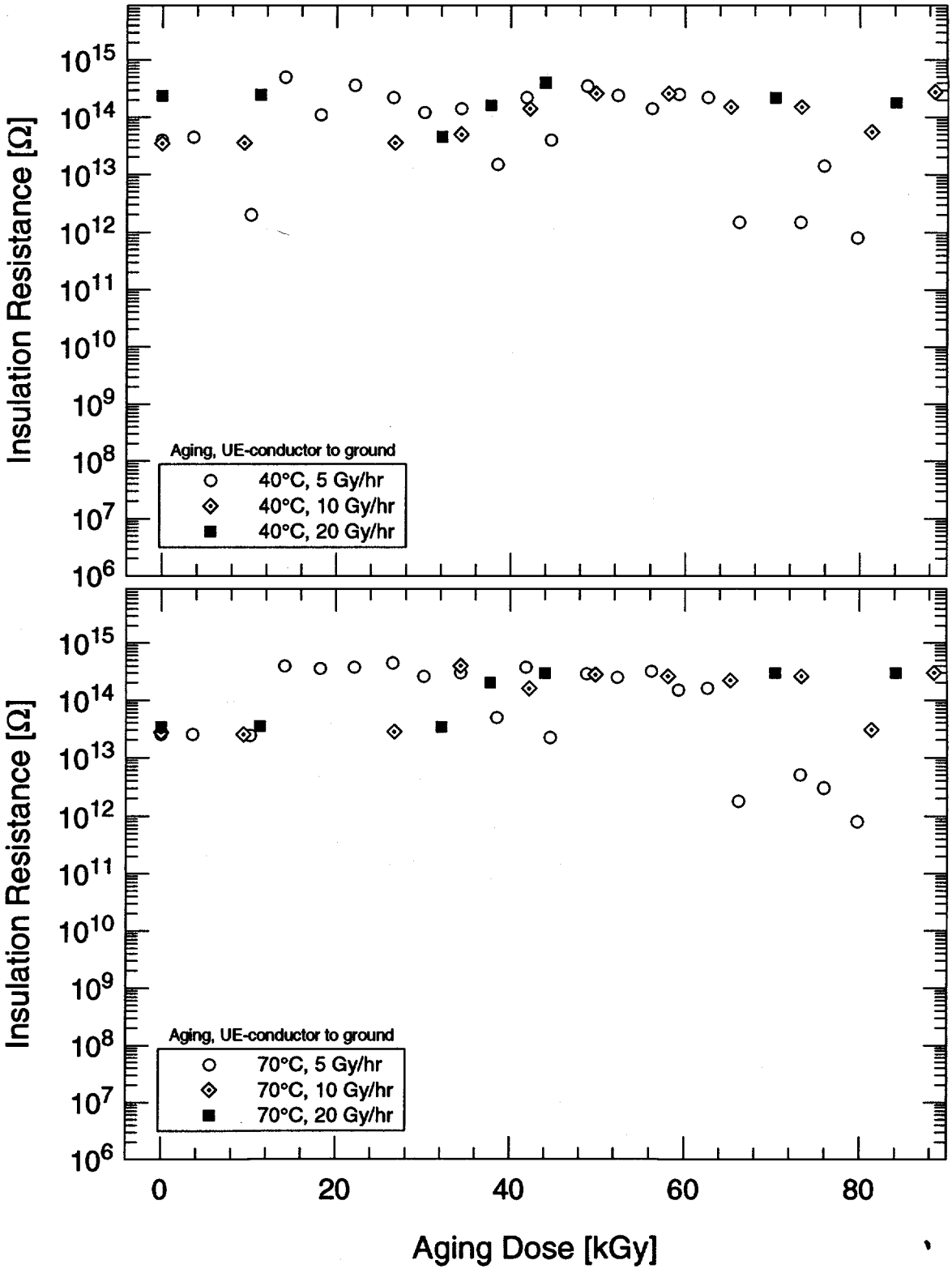

Figure 5.29: U.S. EPR cable insulation resistance versus dose.

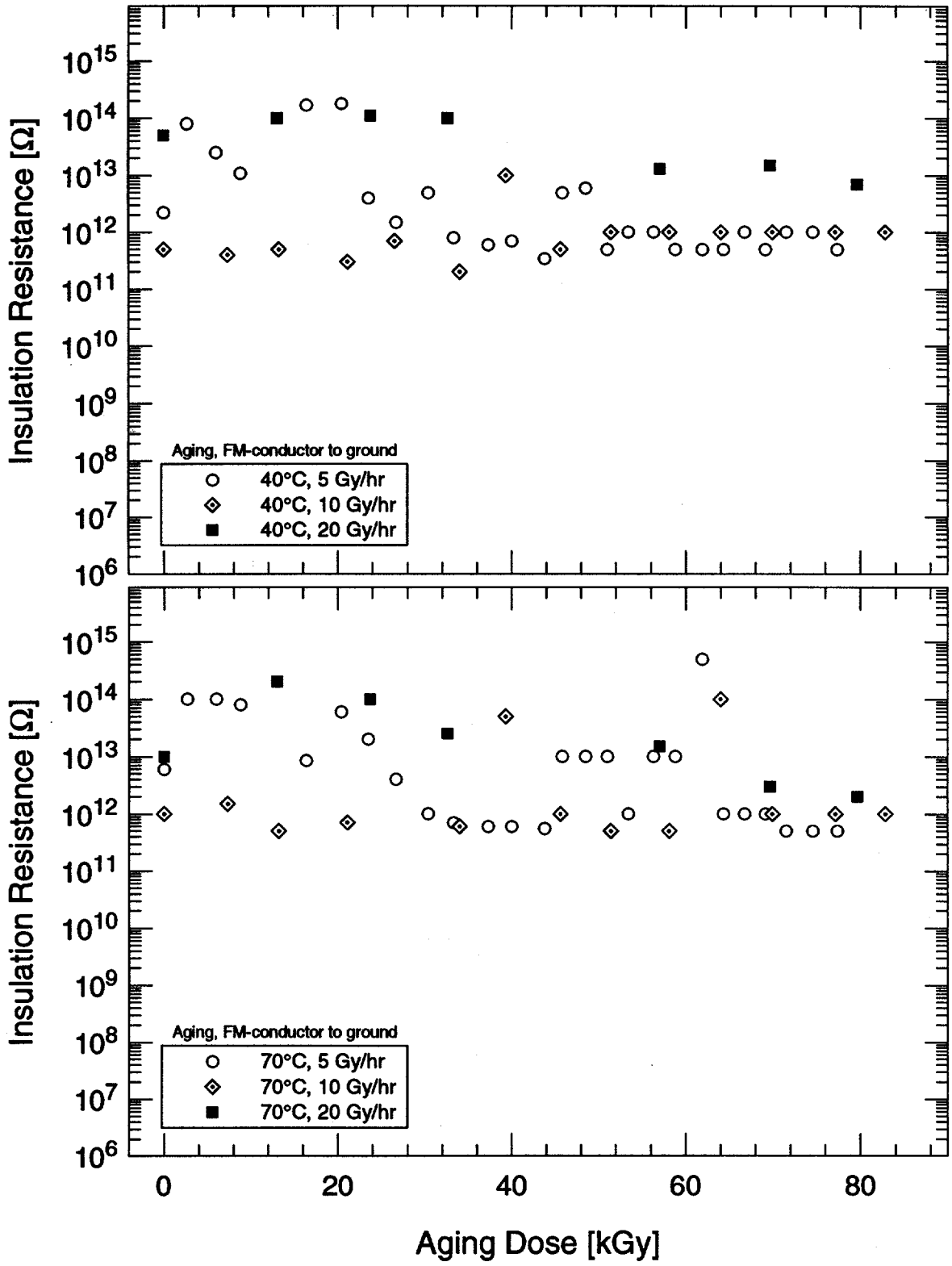

Figure 5.30: French EPR cable insulation resistance versus dose.

Part III
Joint Results

6 Comparison of Results and Conclusions

This section compares the results of the U.S. and French test programs with one another and previous results. Then a summary and conclusions for the cooperative program are presented. See also Section 3.3 for a summary of the U.S. test program and Section 5.4 for a summary of the French test program.

6.1 U.S. and French Results

A summary of test conditions for the U.S. and French programs is given in Table 6.1. Note that only simultaneous thermal and radiation aging degradation was investigated; degradation due to sequential radiation and thermal aging was not part of this program. In France, the lowest dose rate (2 Gy/hr) was obtained using a research reactor to simulate aging at approximately 10 times realistic containment conditions; the higher dose rates (5, 10, and 20 Gy/hr) were simulated using cobalt-60 sources. The French aging exposures were performed at both 40°C and 70°C, except for the 2 Gy/hr irradiation, which was performed at only 40°C. In the United States, the aging was simulated at a high dose rate (100 Gy/hr) at 40°C using cobalt-60 sources. As is evident from Table 6.1, the majority of the testing was performed in France.

The LOCA simulations were similar, but not identical, for the U.S. and French test programs. Differences were:

- The accident irradiation dose rates were 900 Gy/hr and 800 Gy/hr for the U.S. and French test programs respectively. This small difference is considered to be insignificant.
- The target test profiles used for the accident steam exposures were not identical. French Standard NF M 64-001 [15] used for the steam exposure defines minimum and maximum bounds for the test profile; the target profile for the U.S. steam exposure tended to follow the maximum bounds while the French target more closely followed the minimum bounds. However, the measured temperature and pressure for the two steam exposures were very similar to one another.
- Chemical spray was used only in the French steam exposure. It is not clear if chemical spray is conservative or nonconservative because moisture from the spray enhances electrical grounding if the cable is cracked but also tends to improve the cable's elongation at break, which prevents the formation of cracks. In addition, not all areas of a nuclear plant would be exposed to chemical spray during an accident. The cables were in a ground-enhancing, moist environment during the U.S. steam exposure even without the chemical spray because of the saturated steam that was present.
- For the accident irradiation and steam exposures, the complete cables were energized only for the U.S. testing. The energized cables were not exposed to significant stress because of the low applied voltage and current levels and the short duration of the accident irradiation (28 days) and steam (14 days) exposures. Voltage was applied during the accident irradiation solely to help detect if a gross cable short to ground had occurred and during the accident steam exposure to perform continuous IR measurements.

These four differences in the LOCA simulations were all considered to have a negligible effect on the test results. Except for the French PE cable, which failed prior to the accident steam exposure, all of the cables survived the LOCA simulation.

Direct comparison of experimental data from the U.S. and French test programs is possible only for cables that were aged at 40°C. The following subsubsections describe the influence of dose rates ranging from 2 to 100 Gy/hr for these cables. See the French test program summary in Section 5.4 for a comparison of radiation aging data at 40°C and 70°C.

6.1.1 Elongation at Break

In this subsubsection, the 2–20 Gy/hr French elongation at break data are plotted together with the 100 Gy/hr U.S. elongation at break data. Elongation at break data for the U.S. XLPO cable jacket are shown in Figure 6.1, which combines data shown earlier in Figures 3.7 and 5.1. The 100 Gy/hr data show less degradation during aging than the lower dose rates; this could indicate that there is a dose rate effect as the dose rate is increased. The post-LOCA

Table 6.1: Summary of Test Conditions for the U.S. and French Programs.

U.S. Test Program	French Test Program
Aging Exposure (cut specimens)	
Simultaneous 40°C and 100 Gy/hr to 28, 56, 84, 140, and 200 kGy; air flow.	Simultaneous 40°C and 2, 5, 10, 20 Gy/hr to 14, 28, 42, 56, 70, 84, 100, 150, and 210 kGy (56 kGy maximum for 2 Gy/hr); air flow. Simultaneous 70°C and 5, 10, 20 Gy/hr to 14, 28, 42, 56, 70, 84, 100, 150, and 210 kGy; air flow. Thermal-only for 5 years at 70°C, specimens removed for testing every 3 months; air flow.
Aging Exposure (complete specimens)	
Simultaneous 40°C and 100 Gy/hr to 84 kGy; air flow; cables energized.	Simultaneous 40°C and 2, 5, 10, 20 Gy/hr to 84 kGy (56 kGy for 2 Gy/hr); air flow; cables energized. Simultaneous 70°C and 5, 10, 20 Gy/hr to 84 kGy; air flow; cables energized.
Loss-of-Coolant Accident (LOCA) Simulation (both cut and complete specimens)	
Irradiation sequentially followed by a steam exposure.	Irradiation sequentially followed by a steam exposure.
Accident irradiation: 900 Gy/hr at 70°C to 600 kGy, air flow, complete cables energized.	Accident irradiation: 800 Gy/hr at 70°C to 600 kGy, air flow, complete cables not energized.
Accident steam exposure: 14-day duration with single 159°C, 600 kPa peak, gradual drop to 80°C after 4 days, last 10 days at 100°C, air overpressure, no chemical spray, complete cables energized.	Accident steam exposure: 14-day duration with single 156°C, 560 kPa peak, gradual drop to 71.5°C after 4 days, last 10 days at 100°C, air overpressure, chemical spray for first 4 days starting at 200 sec, complete cables not energized.

measurements also show that pre-aging at 100 Gy/hr causes less degradation than pre-aging at lower dose rates.

Elongation at break data for the U.S. EPR cable jacket are shown in Figure 6.2, which combines data shown earlier in Figures 3.6 and 5.3. Again the 100 Gy/hr data show less degradation than the lower dose rates both during aging and for the post-LOCA measurements.

Elongation at break data for the U.S. EPR cable insulation are shown in Figure 6.3, which combines data shown earlier in Figures 3.9 and 5.5. There are no post-LOCA data because the insulation adhered to the conductors and thus only mandrel bend tests were performed. The 100 Gy/hr data show less degradation than the lower dose rates for the higher doses; at low doses (< 100 kGy) this trend does not hold. At low doses, the 100 Gy/hr data show only very slight degradation while the low dose rate exposures actually improved the elongation at break.

Elongation at break data for the French EPR cable jacket are shown in Figure 6.4, which combines data shown earlier in Figures 3.5 and 5.11. There is not much change in elongation at break with dose rate during the aging exposure. However, the post-LOCA measurements show that pre-aging at 100 Gy/hr causes slightly less degradation than pre-aging at lower dose rates.

Elongation at break data for the French EPR cable insulation are shown in Figure 6.5, which combines data shown earlier in Figures 3.8 and 5.13. Again, the 100 Gy/hr data show less degradation than the lower dose rates both during the aging and also, but only slightly if at all, for the post-LOCA measurements.

6.1.2 Density

The results for the different dose rates showed essentially no change with dose rate; any change in the density data is so small that the effect of aging on the results is not possible to determine reliably.

6.1.3 Insulation Resistance

The IR data showed no effect of aging. The IR values for the cables remained very high at all times, thus any changes in value were not considered significant.

6.2 Comparison with Earlier Tests

In this subsection, the current test conditions and data are compared with the results of earlier tests.

6.2.1 Test Conditions

While the test conditions in this report are very similar to those used by Bustard *et al.* [19] for a previous joint U.S.-French experimental program, the radiation doses are substantially less than those used in a typical U.S. cable qualification test program. In earlier U.S. testing by Jacobus [3][4][5], 600 kGy aging (90 Gy/hr for 9 months at 95°C) and 1100 kGy accident irradiation (6 kGy/hr for 183 hr at ambient temperature) were performed. This compares with 200–210 kGy of aging and 600 kGy of accident irradiation in the current report where the aging was performed for exposure times of up to 5 years at temperatures of 40°C and 70°C. Smaller doses were used in the current test program because:

- The current aging exposure was performed over a much longer period, thereby reducing the aging acceleration factor required to extrapolate the results out to typical reactor lifetimes. Because the aging is more representative of actual nuclear plant conditions, the margins on total dose to ensure that such extrapolations are conservative can be reduced.
- Total doses were based on French specifications, not typical U.S. test or qualification programs.
- The current test program was never intended to simulate end-of-life conditions for cables in a nuclear power plant environment using an accelerated aging test. Instead, the goal was to investigate the aging degradation of cables exposed to conditions more representative of actual plant environments than is typically used in accelerated testing.

The accident steam exposure used in the current report was based on the French Standard NF M 64-001 [15, Figure A.3]. This varies from the "generic" accident steam condition profile given in Appendix A of IEEE Std. 323-1974 [11, Figure A1], which is the basis for typical U.S. cable qualification testing. The IEEE profile reaches a higher peak temperature (171.1°C versus 159°C) but a slightly lower peak pressure (583.9 kPa versus 600 kPa) than the French steam profile. A single transient profile with saturated steam conditions was used for the current program, while the IEEE profile has two transients with superheated steam conditions and does not go to saturated steam conditions until 6 hr after the start of the second transient. The French steam exposure profile includes air starting at 3 hr, while the IEEE profile has a pure steam environment at all times.

6.2.2 Cable Material Behavior

Gillen and Clough have published a series of reports [20][21][16] giving a model for the degradation of cable materials under the combined effects of thermal and radiation environments. This "combined environments" methodology is an extension of the Arrhenius technique that has proved to be a good model of the thermal-only degradation behavior of polymer materials. Because Gillen and Clough's results carefully address the effect of dose rate on material degradation, it is useful to compare their results with the current results.

For time-dependent degradation data taken under isothermal conditions, the most commonly observed functional form describing the degradation is the Arrhenius relationship, which can be written as (Ref. [22, Sections 4 and 8.3.2]):

$$\frac{t_2}{t_1} = \exp\left[\frac{E_{a1}}{R}\left(\frac{1}{T_2} - \frac{1}{T_1}\right)\right] = \exp\left[\frac{E_{a2}}{k_b}\left(\frac{1}{T_2} - \frac{1}{T_1}\right)\right],$$

where

Table 6.2: Estimated Elongation after Thermal-Only Aging at 70°C for 5 Years—Hypalon Jackets.

Hypalon Material	E/E_0
U.S. XLPO cable jacket (Figure 5.2)	0.45 ± 0.07
U.S. EPR cable jacket (Figure 5.4)	0.45 ± 0.05
French EPR cable jacket (Figure 5.12)	0.60 ± 0.10

- E_a = activation energy of the material (units of [kcal/mole] for E_{a1}, [eV/molecule] for E_{a2})
- k_b = Boltzmann's constant = gas constant per molecule = 8.6174×10^{-5} eV/(molecule-K)
- R = gas constant = 0.0019858 kcal/(mole-K)
- t_i = aging time
- T_i = aging temperature (absolute temperature)

This equation gives the relationship between two thermal-only (*i.e.*, time-temperature) exposures that produce an equivalent material degradation with the only unknown being the empirically derived activation energy.

The "combined environments" methodology expands the Arrhenius time-temperature technique to include radiation dose rate. This time-temperature-dose rate methodology is based on two assumptions:

1. An Arrhenius expression relates time and temperature for constant dose conditions, and
2. E_a is independent of both the dose value and the degradation level selected.

A complete description of this methodology and its applicability to common nuclear power plant cable materials is described by Gillen and Clough [20, 21, 16].

Hypalon Jackets

Table 6.2 presents thermal-only aging results for the three Hypalon jackets (from the U.S. XLPO, U.S. EPR, and French EPR cables) in the current report. This table gives the estimated remaining elongation at break after 5 years of thermal aging at 70°C. These values, which are estimated from the data in Figures 5.2, 5.4, and 5.12, are in relatively good agreement with one another.

Reference [21] presents aging data for an Anaconda Flameguard cable's Hypalon jacket, which has an activation energy of 25 kcal/mole (1.084 eV/molecule). The current 40°C and 70°C data must be converted to an equivalent 45°C exposure for comparison with Gillen and Clough's data. An Arrhenius calculation shows that a 5-year, 70°C thermal exposure is equivalent to an 89.2-year, 45°C thermal exposure for which Gillen and Clough's data [21, Figure 10] give a remaining elongation of $E/E_0 = 0.62 \pm 0.09$. Within experimental uncertainty, the Hypalon jacket results in Table 6.2 are quite similar.

Similarly, Ref. [20] presents aging data for a Kerite FR cable's Hypalon jacket,[1], which has an activation energy of 24 kcal/mole (1.041 eV/molecule). An Arrhenius calculation shows that a 5-year, 70°C thermal exposure is equivalent to a 79.5-year, 45°C thermal exposure for which Gillen and Clough's data [20, Figure 14] give a remaining elongation of $E/E_0 = 0.47 \pm 0.04$. This again is in excellent agreement to the Hypalon jacket results in Table 6.2.

These two examples demonstrate that the current thermal-only aging data for the Hypalon jackets are consistent with earlier results and thus provide evidence of generic elongation at break behavior for Hypalon materials. Since the previous data were collected using dose rates that were mostly well above 100 Gy/hr, this lends credence to the applicability of the Arrhenius methodology for predicting the degradation of Hypalon in long-term thermal exposures.

For the three current Hypalon jackets, Table 6.3 gives the doses at which the elongation at break falls to 50% and 25% of its initial value; these doses were estimated from the aging data in Figures 5.1, 5.3, and 5.11. In order to compare them with the Kerite Hypalon jacket data, the current dose rates were shifted to equivalent 45°C values, giving:

- 5, 10, and 20 Gy/hr at 40°C are equivalent to 9.17, 18.3, and 36.7 Gy/hr at 45°C
- 5, 10, and 20 Gy/hr at 70°C are equivalent to 0.315, 0.629, and 1.26 Gy/hr at 45°C

Using the shifted dose rates, current data from Table 6.3 have been plotted on top of predicted values for the Kerite Hypalon jacket [20, Figure 13] in

[1] The material is only identified as a Hypalon jacket material in Ref. [20]; however, Ref. [21, Table 1] identifies it as being from a Kerite FR cable jacket.

Table 6.3: Estimated Dose Values for Given Elongation at Break—Hypalon Jackets.

Material	Aging Temperature	Aging Dose Rate [Gy/hr]	Estimated Dose [kGy] for: $E/E_0 = 0.5$	$E/E_0 = 0.25$
U.S. XLPO cable jacket (Figure 5.1)	40°C	5	$\gg$210	$\gg$210
		10	$\gg$210	$\gg$210
		20	210	$\gg$210
	70°C	5	90	180
		10	200	$\gg$210
		20	> 210	$\gg$210
U.S. EPR cable jacket (Figure 5.3)	40°C	5	> 210	$\gg$210
		10	200	$\gg$210
		20	170	$\gg$210
	70°C	5	60	100
		10	120	$\gg$210
		20	200	$\gg$210
French EPR cable jacket (Figure 5.11)	40°C	5	$\gg$210	$\gg$210
		10	$\gg$210	$\gg$210
		20	150	$\gg$210
	70°C	5	120	$\gg$210
		10	180	$\gg$210
		20	180	$\gg$210

Figure 6.6. The 70°C data are in very close agreement with the predictions. For dose rates of 5–20 Gy/hr, the jackets degraded to 50% of their initial elongation at doses of 50–200 kGy, and higher doses were required to reach equivalent degradation as the dose rate was increased. For the 40°C data, the Hypalon jackets degraded faster than predicted; however, the differences are not considered to be significant; the actual and predicted results for the elongation to fall to 50% of its initial value are all in the 100–500 kGy range for dose rates of 5–20 Gy/hr. The predicted curve for the 40°C data is flatter than for the 70°C data, which indicates that less dose rate effect is expected at 40°C.

The elongation at break data in Table 6.3 show that degradation occurs faster at 40°C than 70°C for 20 Gy/hr irradiation. This behavior is strange because the same inverse temperature behavior does not occur for the 5 Gy/hr and 10 Gy/hr data. The 40°C data plotted in Figure 6.6 seem to show an inverse dose rate effect, where less dose is required to reach equivalent degradation as the dose rate is increased. However, no definite conclusion can be reached because these data are essentially the same because of uncertainty in estimating their value.

For the three Hypalon jacket materials tested in this program, degradation due to the simultaneous exposure to 5 Gy/hr radiation and 70°C thermal environments was greater than the sum of the degradation due to 5 Gy/hr radiation-only and 70°C thermal-only exposures. This indicates the presence of a possible synergism between these thermal and radiation exposures, which is consistent with the results of an earlier study by Alba *et al.* [1].

EPR Insulations

When irradiated at 20 Gy/hr, both EPR insulations (U.S. EPR cable's FR-EPDM insulation and the French EPR cable's EPR insulation) were more degraded during irradiation at 40°C than at 70°C. This same behavior was seen in earlier testing by Gillen and Clough [16] on this same material, in which they found faster degradation of mechanical properties at 41°C than 61°C for dose rates of 60–70 Gy/hr. Gillen and Clough also noted that this behavior appeared in even earlier testing of this same material by Bustard *et al.* [17] for 650 Gy/hr exposures at 27°C and 70°C. An explanation of this "inverse temperature effect" has been proposed by Gillen *et al.* [18] based on the semi-crystalline nature of EPR materials and the fact that these materials undergo crystalline melting

Table 6.4: Predicted Time and Dose for the Elongation to Decrease to 100% Absolute for a Low-Density PE.

Aging Temperature	Aging Dose Rate [Gy/hr]	Time [years]	Dose [kGy]
40°C	2	1.95	34
	5	1.05	46
	10	0.68	60
	20	0.43	75
70°C	2	0.90	16
	5	0.50	22
	10	0.31	27
	20	0.21	37

Note: Data from Ref. [21, Figure 28].

and reforming over a broad temperature range from roughly room temperature up to at least 100°C.

XLPE insulation

The accident steam exposure caused a noticeable recovery in elongation for the U.S. XLPO cable insulation (see Figure 3.10); this has been noted previously for more severely aged XLPO cables [3, p. 54].

PE Insulation

Reference [21] gives the results for low-density PE insulation from a General Cable Corp. cable tested in combined environments. Interpolating values from Ref. [21, Figure 28] of when the elongation will decrease to 100% absolute ($E/E_0 = 0.18$) for several aging temperatures and dose rates gives the predicted times (and resulting doses) shown in Table 6.4. The elongation at break for PE materials tends to degrade rapidly once it begins to fall. This is consistent with the French PE cable insulation data in Figure 5.9 in which the elongation goes to zero almost immediately after it begins to drop from its initial value. Thus a value of $E/E_0 = 0.20$ (100% absolute elongation for the French PE cable insulation) is essentially equal to the time at which the cable has no remaining elongation. From Table 6.4, the General Cable PE insulation is predicted to have no remaining elongation for a dose in the range of 34–75 kGy at 40°C and 16–37 kGy at 70°C. These predictions are in good agreement with the French PE cable insulation data in Figure 5.9 where the remaining elongation has dropped to a negligible value in the range of 28–56 kGy at 40°C (the 2 Gy/hr elongation was not yet degraded at 42 kGy, its last measured value) and 14–28 kGy at 70°C.

Thus, for the PE insulation, predictions based on previous results are in good agreement with the current results. The French PE cable insulation is not suitable for environments in which radiation exposure is expected. As shown in Figure 5.10, the PE insulation material is unaffected by a 5-year, 70°C thermal-only exposure but completely degrades in several months if a 5 Gy/hr irradiation is added.

6.3 Summary and Conclusions

6.3.1 Summary

This report has presented the results obtained during a cooperative U.S./French program to investigate the long-term aging degradation and LOCA behavior of electrical cables and cable materials. The objective was to investigate the effect of radiation dose rate on aging degradation and LOCA survivability while also investigating the effect of temperature on the aging and whether there is synergy between the radiation and thermal aging exposures.

The programs exposed the cables to the same aging radiation doses and similar simulated LOCA conditions. However, the dose rate used for the aging irradiation varied over a wide range (2–100 Gy/hr) in the two programs. Radiation aging was accompanied by simultaneous thermal aging at either 40°C or 70°C. The data represent up to 5 calendar years of simultaneous radiation and thermal aging—a 5-year, 70°C thermal exposure is equivalent to 25 years at 55°C or 80 years at 45°C for the Hypalon jacket materials (assuming a 24 kcal/mole activation energy). Following the various aging exposures, the cables were subjected to a simulated LOCA consisting of an accident radiation exposure sequentially followed by an accident steam exposure. Note that the exposures generally followed French qualification procedures, which utilize a lower peak steam temperature and

substantially smaller aging and accident radiation doses than those used in typical U.S. cable test or qualification programs.

This program was originally designed to test control and instrumentation cables that provide safety functions under both normal and LOCA nuclear power plant environment conditions. However, the French PE (coaxial) cable was added to the program even though it is not required to remain operable under accident conditions in French nuclear power plants. Both cut and complete (electrically energized) cable specimens were tested. The four different cable types tested in the U.S. and France were:

1. U.S. 2 conductor with EPR insulation and a Hypalon jacket
2. U.S. 3 conductor with XLPE insulation and a Hypalon jacket
3. French 3 conductor with EPR insulation and a Hypalon jacket
4. French coaxial with PE insulation and a PE jacket

Several condition monitoring techniques were used to investigate degradation behavior. Elongation at break was the most effective technique for monitoring the aging degradation of the polymeric cable materials. Electrical techniques showed very little change in electrical properties with aging. Gel fraction measurements[2] showed that cross-linking of the three Hypalon jacket materials increased during aging and also during the LOCA simulation.

6.3.2 Anomalies

Several anomalies occurred during the test program:

- During the U.S. testing, no elongation at break data were acquired for the French PE cable because it quickly degraded to a state where undamaged tensile specimens could not be created. However, the qualitative data available from bending the cable are comparable to the French test data.
- During the French testing, the elongation at break and tensile strength data for the U.S. XLPO cable's XLPE insulation exhibited two distinct behaviors. It has been hypothesized that these behaviors were due to the type of clamps used to hold the specimens during tensile testing because the same problem was not seen in the U.S. testing, which utilized a different type of clamp.
- During the French testing, the FR-EPDM insulation of the U.S. EPR cable adhered to the copper conductors after the accident steam exposure, thus no elongation at break measurements were performed. The results of the mandrel bend testing that was performed were in qualitative agreement with the U.S. post-LOCA findings that the insulation had sufficient remaining elongation to resist cracking.

[2] Gel fraction measurements were only performed in the French test program.

6.3.3 Conclusions

The conclusions of this cooperative program with regard to the program objectives are addressed below.

Objective: Investigate the effect of radiation dose rate on aging degradation and LOCA behavior.

- All the cables, except for the French PE cable, performed acceptably during the aging and LOCA simulations in both the U.S. and France. The French PE cable is susceptible to radiation damage and is not suitable for accident applications.
- In general, degradation *at a given dose* was highest for the lowest dose rate, and the amount of degradation decreased as the dose rate was increased. While this effect was present, but small relative to scatter in the data, for irradiation at 40°C, the 70°C data from the French test program indicate that this effect is larger at higher temperatures; however, no 100 Gy/hr data at 70°C were available to confirm this[3].
- The elongation at break data for the Hypalon jackets and PE insulation were well predicted by the time-temperature-dose rate methodology of Gillen and Clough [20][21][16].

[3] This effect is expected to be larger at higher temperatures. As the dose rate is decreased, more exposure time is required to achieve the same total dose and thus there will be more thermal aging (a 200 kGy dose requires 4.6 years at 5 Gy/hr, but only 1.1 years at 20 Gy/hr). In addition, the relative contribution of thermal aging to the overall degradation will increase as the temperature is increased.

- The effect of dose rate becomes more pronounced as the aging dose increases.
- At 40°C, the behavior of the cable irradiated at 2 Gy/hr in a research reactor was very similar to the cable irradiated at 5 Gy/hr using cobalt-60 sources.
- All cables that functioned electrically prior to the accident steam exposure remained electrically functional through the accident steam exposure. This held true even for cables that had degraded to low residual elongation prior to the steam exposure.
- The dependence of the post-LOCA measurements on aging dose confirms that pre-aging these cables affects their post-LOCA values.
- Significant degradation in cable materials was observed after aging and the 600 kGy accident irradiation.[4] Prior to the accident steam exposure, the elongation at break (E/E_0) was in the range of 5–15% for the U.S. XLPO cable's XLPE insulation and 20–50% for the U.S. EPR cable's FR-EPDM insulation. The accident steam exposure tended to slightly improve the elongation at break for the EPR and XLPE insulation materials, while the elongation was either unchanged or decreased slightly for the Hypalon jackets.

Objective: Investigate the effect of temperature on the aging and whether there is synergy between the radiation and thermal aging exposures.

- Except for the Hypalon jackets, all insulation and jacket materials had slight degradation or none after being exposed to 5 years of thermal-only aging at 70°C. The Hypalon jackets from the U.S. EPR and U.S. XLPO cables had lost over half of their relative elongation at the end of the 5-year thermal aging; the French EPR cable's Hypalon jacket did slightly better.
- The EPR insulations (from the U.S. EPR and French EPR cables) exhibited unusual behavior; their elongation at break data showed greater degradation at 40°C than at 70°C during the 20 Gy/hr irradiation. This "inverse temperature effect" has been noted by previous researchers and may be caused by a transition in material structure in this temperature range.
- There appears to be synergy between radiation and thermal aging for the three Hypalon jacket materials, which all had substantially more degradation when exposed to simultaneous 70°C thermal and 5 Gy/hr radiation exposures than the individual thermal and radiation exposures. The two EPR insulation materials exhibited no synergistic effect between radiation and thermal aging.

[4] Measurements during and between the accident irradiation and accident steam exposure were performed only in the U.S. test program.

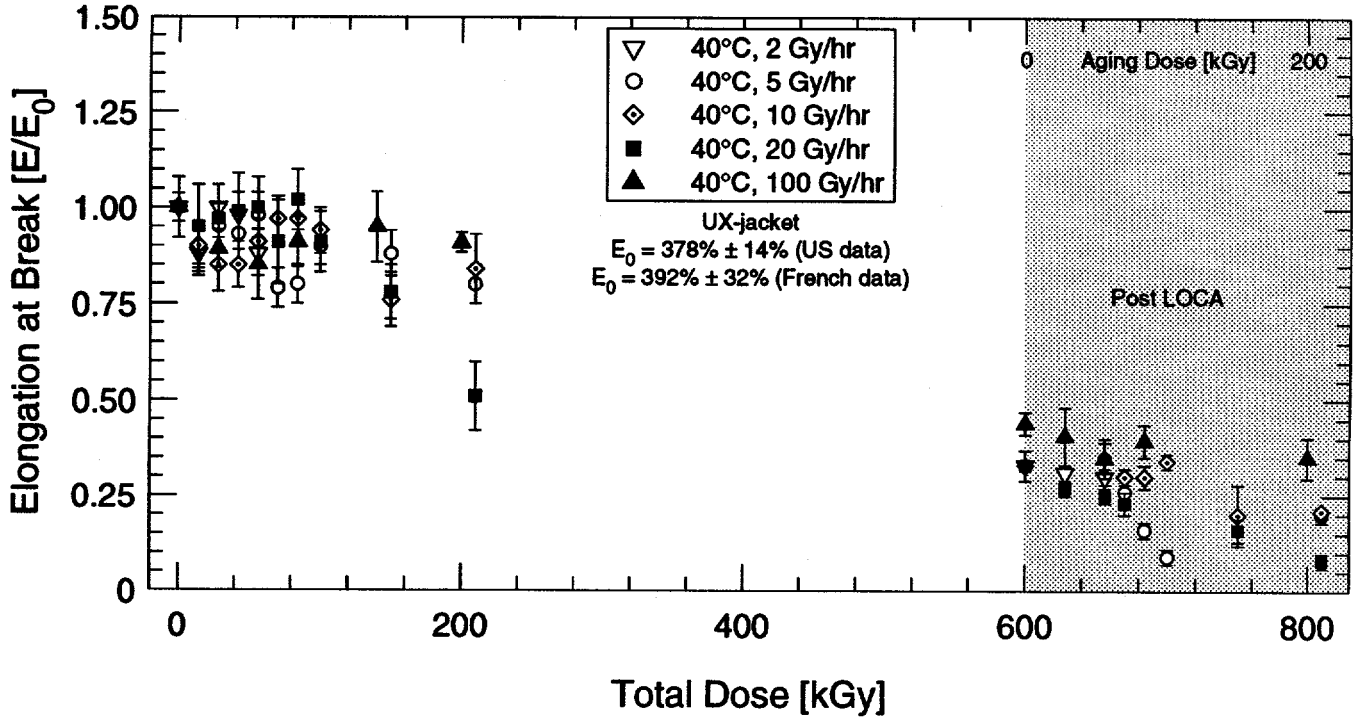

Figure 6.1: Comparison of U.S. and French elongation at break data versus total dose for U.S. XLPO cable—Hypalon jacket.

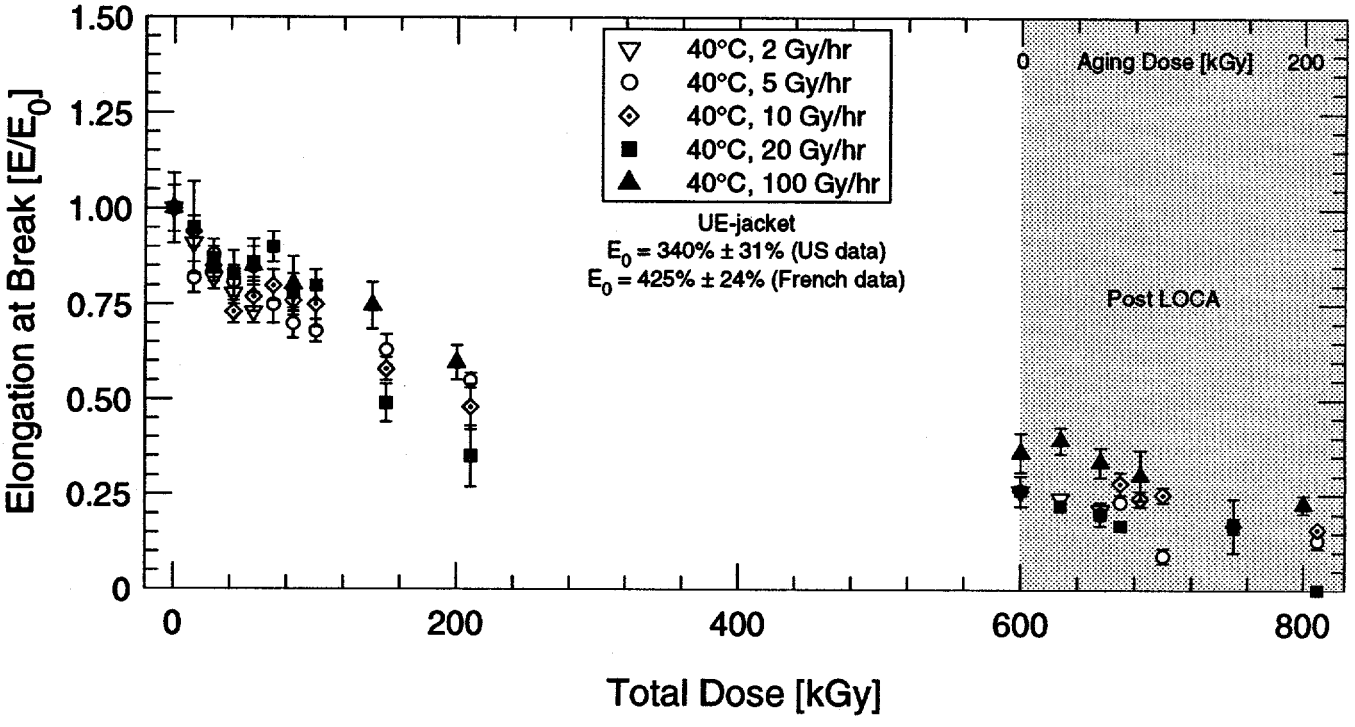

Figure 6.2: Comparison of U.S. and French elongation at break data versus total dose for U.S. EPR cable—Hypalon jacket.

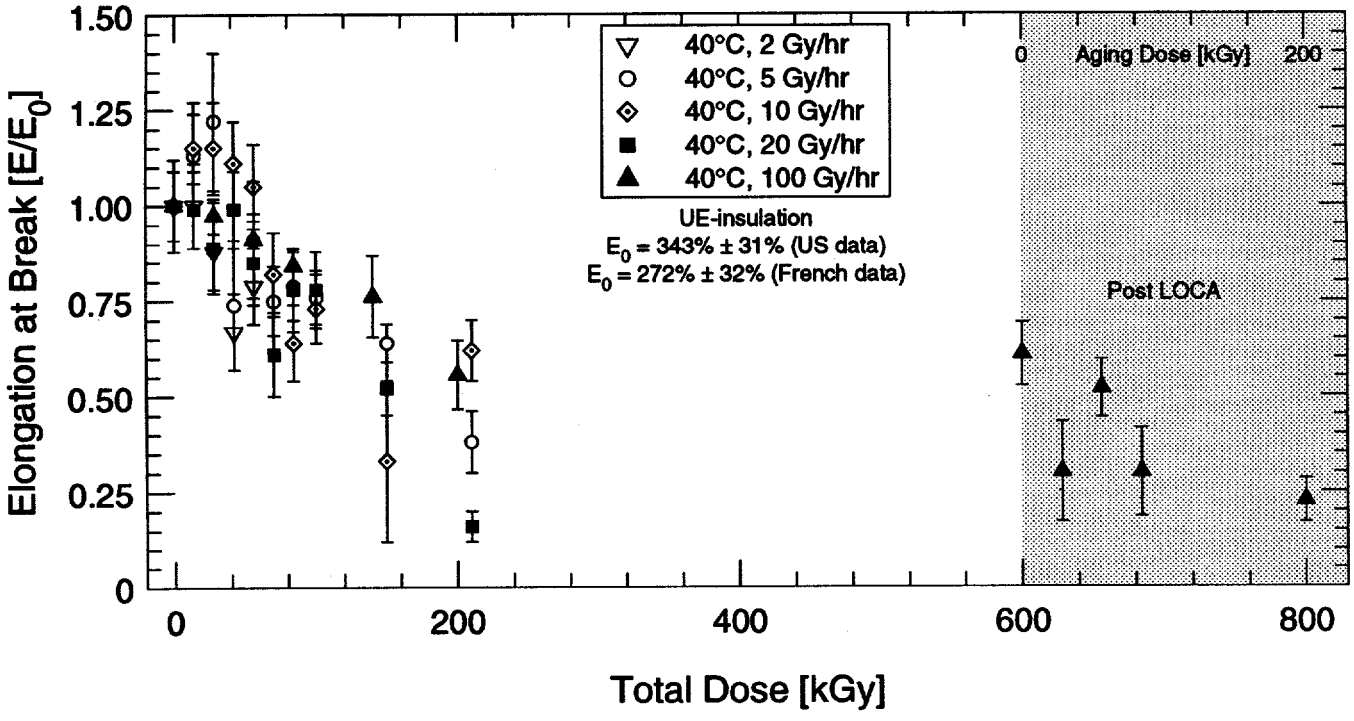

Figure 6.3: Comparison of U.S. and French elongation at break data versus total dose for U.S. EPR cable—FR-EPDM insulation.

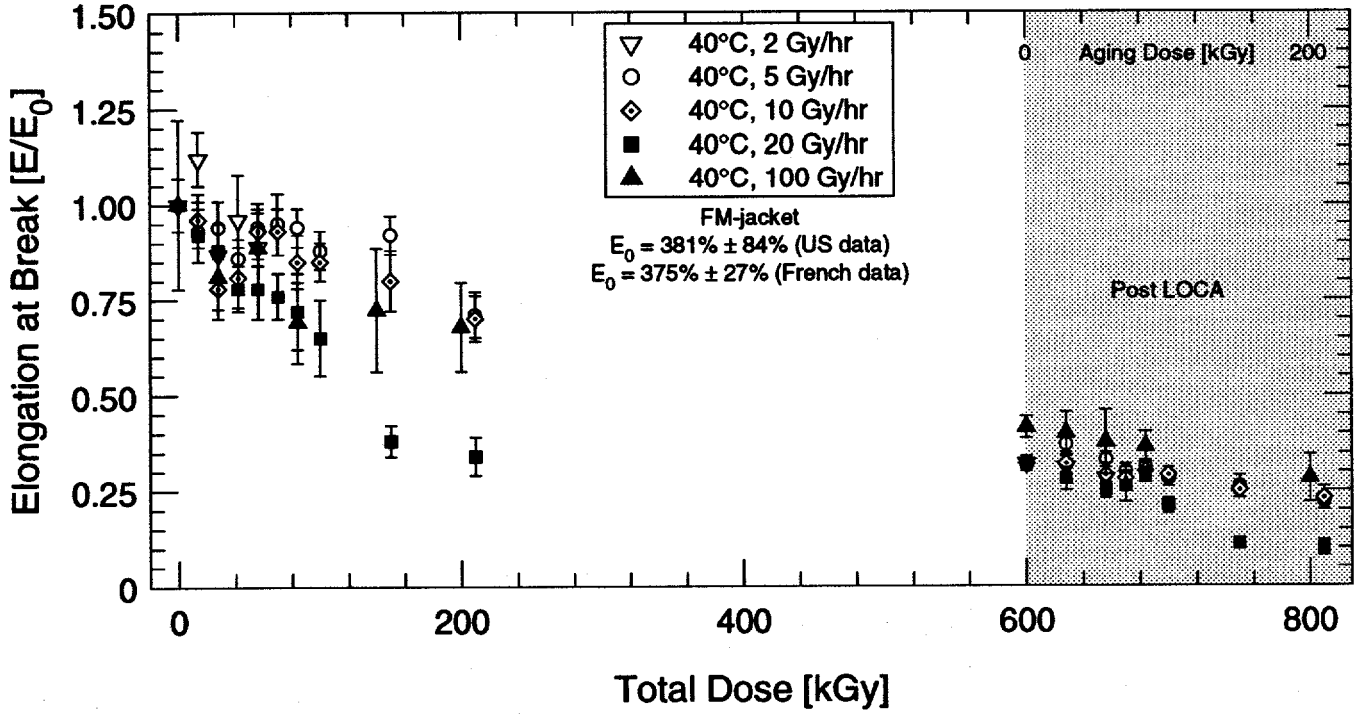

Figure 6.4: Comparison of U.S. and French elongation at break data versus total dose for French EPR cable—Hypalon jacket.

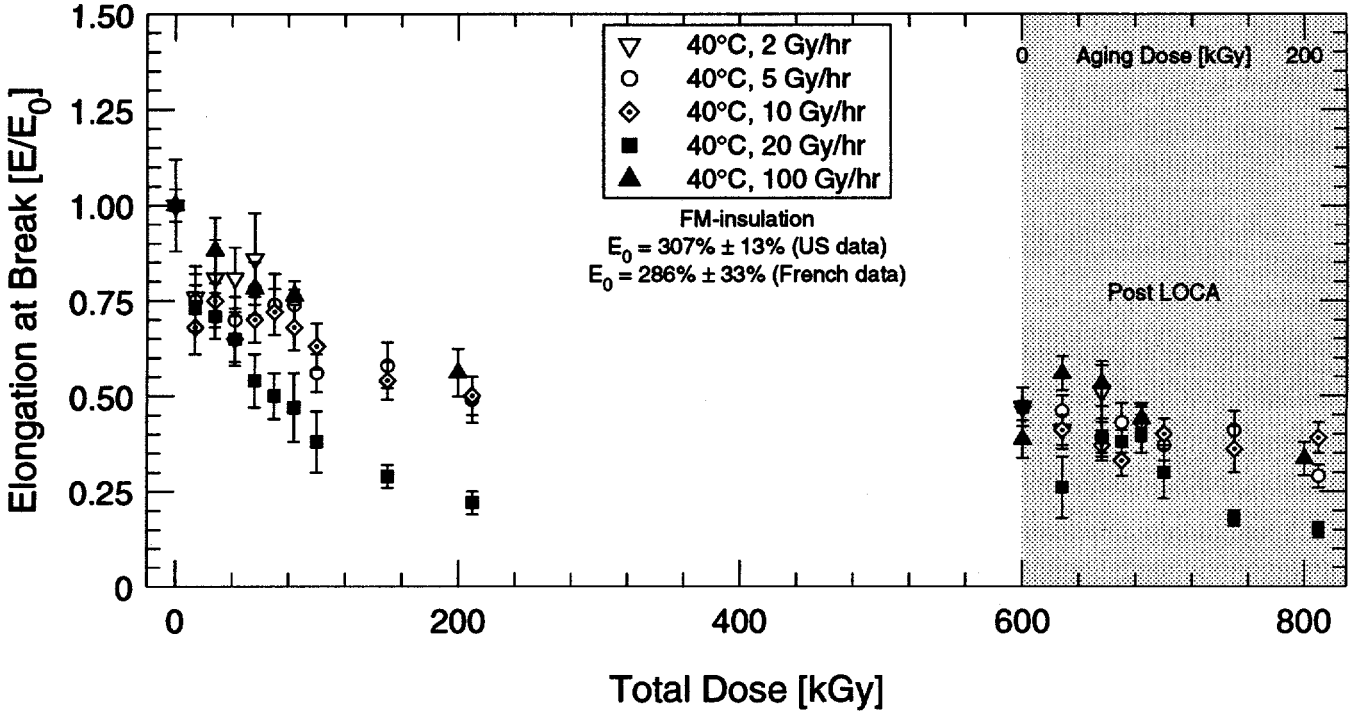

Figure 6.5: Comparison of U.S. and French elongation at break data versus total dose for French EPR cable—EPR insulation.

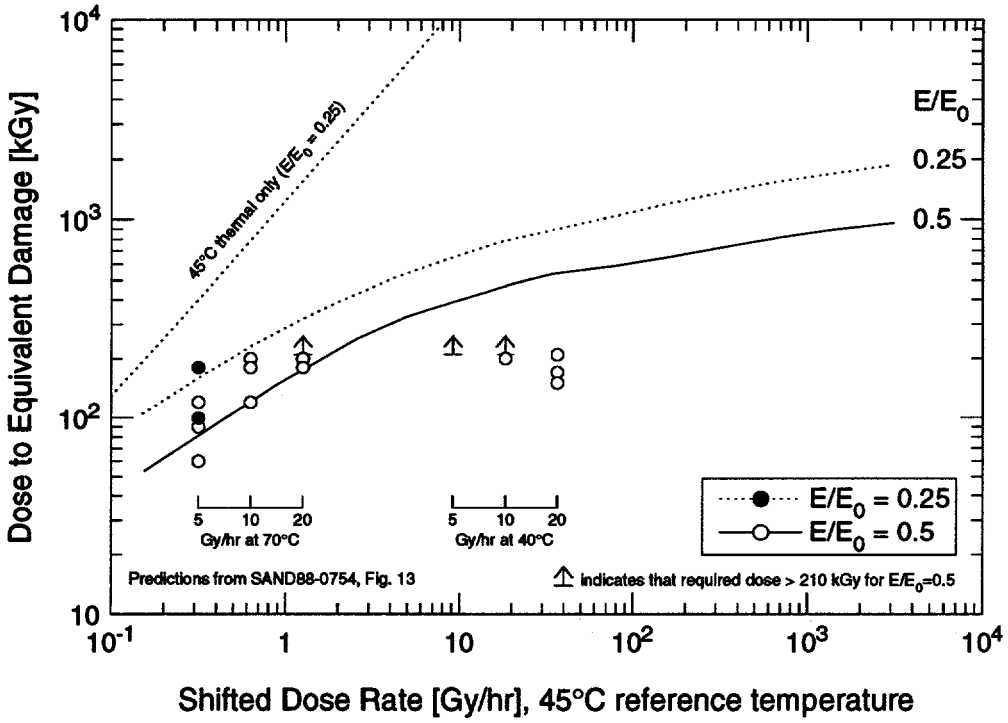

Figure 6.6: Predicted dose (lines) and actual dose (circles) required for the elongation to drop to 50% and 25% of its initial value under combined radiation and thermal aging conditions—Hypalon jackets.

References

[1] C. Alba, F. Carlin, J. Chénion, F. Lemaire, G. Gaussens, and M. LeMeur, "Irradiation de vieillissement des polymères - Influence du débit de dose et des séquences d'essais," (Aging Irradiation of Polymers - Influence of Dose Rate and Test Sequences), Société Française d'Énergie Nucléaire (SFEN), Paris, France, May 1984.

[2] M. Attal, F. Carlin, J. Chenion, G. Gaussens, P. LeTutour, M. LeMeur, "Effect of irradiation dose rate on changes in the properties of polymer materials," International Conference on Operability of Nuclear Systems in Normal and Adverse Environments (OPERA 89), SFEN, Lyon, France, September 1989.

[3] M.J. Jacobus, "Aging, Condition Monitoring, and Loss-of-Coolant Accident (LOCA) Tests of Class 1E Electrical Cables—Crosslinked Polyolefin Cables," NUREG/CR-5772, Vol. 1, SAND91-1766/1, Sandia National Laboratories, Albuquerque, NM, Aug. 1992.

[4] M.J. Jacobus, "Aging, Condition Monitoring, and Loss-of-Coolant Accident (LOCA) Tests of Class 1E Electrical Cables—Ethylene Propylene Rubber Cables," NUREG/CR-5772, Vol. 2, SAND91-1766/2, Sandia National Laboratories, Albuquerque, NM, Nov. 1992.

[5] M.J. Jacobus, "Aging, Condition Monitoring, and Loss-of-Coolant Accident (LOCA) Tests of Class 1E Electrical Cables—Miscellaneous Cable Types," NUREG/CR-5772, Vol. 3, SAND91-1766/3, Sandia National Laboratories, Albuquerque, NM, Nov. 1992.

[6] W.H. Buckalew, "Cobalt-60 Simulation of LOCA Radiation Effects," NUREG/CR-5231, SAND88-1054, Sandia National Laboratories, Albuquerque, NM, July 1989.

[7] National Oceanic and Atmospheric Administration, *U.S. Standard Atmosphere, 1976*, NOAA-S/T 76-1562, Washington, D.C., Oct. 1976.

[8] William C. Reynolds and Henry C. Perkins, *Engineering Thermodynamics*, 2nd. ed., McGraw-Hill, New York, NY, 1977 (ISBN 0-07-052046-1).

[9] K.T. Gillen, R.L. Clough, G. Ganouna-Cohen, J. Chenion, and G. Delmas, "Loss of Coolant Accident (LOCA) Simulation Tests on Polymers: The Importance of Including Oxygen," NUREG/CR-2763, SAND82-1071, Sandia National Laboratories, Albuquerque, NM, July 1982.

[10] K.T. Gillen, R.L. Clough, G. Ganouna-Cohen, J. Chenion, and G. Delmas, "The Importance of Oxygen in LOCA Simulation Tests," *Nuclear Engineering and Design*, Vol. 74, 1982, pp. 271–285.

[11] Institute of Electrical and Electronics Engineers, "IEEE Standard for Qualifying Class 1E Equipment for Nuclear Power Generating Stations," IEEE Std. 323-1974, New York, NY, June 1976 (corrected copy).

[12] K.T. Gillen, R.L. Clough, and N.J. Dhooge, "Density Profiling of Polymers," *Polymer*, Vol. 27, No. 2, Feb. 1986, pp. 225–232.

[13] American Society for Testing and Materials, "Standard Test Method for Density of Plastics by the Density-Gradient Technique," ASTM D1505-85 (Reapproved 1990), Philadelphia, PA.

[14] "Caoutchouc vulcanisé ou caoutchouc thermoplastique: Essai de traction," (Vulcanized or Thermoplastic Rubber — Tensile Test), NF T 46-002, *norme française*, September 1988.

[15] "Procédure de qualification des matériels électriques installés dans l'enceinte de confinement des réacteurs à eau sous pression et soumis aux conditions accidentelles," (Procedure for Qualification of Electric Equipment Installed in Containments for Pressurized Water Reactors Subject to Accident Conditions), NF M 64-001, *norme française*, November 1991.

[16] K.T. Gillen and R.L. Clough, "Aging Predictions in Nuclear Power Plants—Crosslinked Polyolefin and EPR Cable Insulation Materials," SAND91-0822, Sandia National Laboratories, Albuquerque, NM, June 1991.

[17] L.D. Bustard, E. Minor, J. Chenion, F. Carlin, C. Alba, G. Gaussens, and M. LeMeur, "The Effect of Thermal and Irradiation Aging Simulation Procedures on Polymer Properties," NUREG/CR-3629, SAND83-2651, Sandia National Laboratories, Albuquerque, NM, April 1984.

[18] K.T. Gillen, R.L. Clough, J. Wise, and G.M. Malone, "Explanation of Enhanced Mechanical Degradation Rate for Radiation-Aged Polyolefins as the Aging Temperature is Decreased," *Polymer Preprints*, Vol. 35, No. 2, American Chemical Society, Aug. 1994, pp. 911-912.

[19] L.D. Bustard, J. Chenion, F. Carlin, C. Alba, G. Gaussens, and M. LeMeur, "The Effect of Alternative Aging and Accident Simulations on Polymer Properties," NUREG/CR-4091, SAND84-2291, Sandia National Laboratories, Albuquerque, NM, May 1985.

[20] K.T. Gillen and R.L. Clough, "Time-Temperature-Dose Rate Superposition: A Methodology for Predicting Cable Degradation Under Ambient Nuclear Power Plant Aging Conditions," SAND88-0754, Sandia National Laboratories, Albuquerque, NM, Aug. 1988.[1]

[21] K.T. Gillen and R.L. Clough, "Predictive Aging Results for Cable Materials in Nuclear Power Plants," SAND90-2009, Sandia National Laboratories, Albuquerque, NM, Nov. 1990.[2]

[22] Franklin Research Center, "A Review of Equipment Aging Theory and Technology," EPRI NP-1558, Electric Power Research Institute, Palo Alto, CA, Sept. 1980.

[23] American Society for Testing and Materials, "Standard Practice for Application of Thermoluminescence-Dosimetry (TLD) Systems for Determining Absorbed Dose in Radiation-Hardness Testing of Electronic Devices," ASTM E668-93, Philadelphia, PA.

[24] David M. Pozar, *Microwave Engineering*, Addison-Wesley, Reading, MA, 1990 (ISBN 0-201-50418-9).

[1] A refereed version of this report exists, it is K.T. Gillen and R.L. Clough, "Time-Temperature-Dose Rate Superposition: A Methodology for Extrapolating Accelerated Radiation Aging Data to Low Dose Rate Conditions," *Polymer Degradation and Stability*, Vol. 24, 1989, pp. 137–168.

[2] A refereed version of this report exists, it is K.T. Gillen and R.L. Clough, "Predictive Aging Results in Radiation Environments," *Radiation Physics and Chemistry*, Vol. 41, No. 6, 1993, pp. 803–815.

Appendices

A U.S. Dosimetry

In order to describe the location of objects, a coordinate system must be defined. The *fixture coordinate system* is based on the fixture that holds the cobalt sources and the test chamber. Figures A.1 and A.2 show this coordinate system. The z-axis is in the vertical direction, and thus the xy-plane is horizontal. The xy-origin is at the center of the opening into which the test chamber will fit, and the plane $z = 0$ passes through the vertical midpoint of the cobalt sources. The fixture coordinate system is used for all the figures in this appendix—an angle of 0° is along the x-axis and 90° is along the y-axis.

A second coordinate system is the *chamber coordinate system*, which is tied to the test chamber itself. This coordinate system can be rotated in relation to the fixture coordinate system by rotating the test chamber in its fixture (this was done periodically during aging of the complete cables to make the radiation dose more uniform on the test specimens).

A.1 Dosimetry Technique

Thermoluminescent dosimetry was used to quantify the dose rates used in this test program. Dosimetry was performed using the following steps:

1. The cable specimens were installed in the test chamber in their radiation exposure configuration for the ensuing test.
2. Thermoluminescent dosimeters (TLDs) were then placed in the test chamber and on the cable samples at various locations.
3. The test chamber was then sealed and placed in the radiation environment to expose the TLDs to an optimum measurement dose (100–300 Gy was used for the TLD exposures and the 1-σ uncertainty in the measured dose was between 5% and 6%).
4. After the proper exposure time, the test chamber was removed from the radiation field and the TLDs were removed and sent to be read.
5. The test chamber was then resealed and placed back in the radiation field to start the aging or accident radiation exposure of the cable samples.

Dosimetry was performed with the cables in their test configuration to give the most accurate measure of the cable dose rate.

The Radiation Dosimetry Laboratory at Sandia National Laboratories provided the TLDs and also read the TLD exposures. Their equipment and techniques follow ASTM E668 [23], and the resulting values for radiation exposure are traceable to the National Institute of Standards and Technology (NIST). Harshaw TLD 400 dosimeters were used. These are small (approximately 6 mm square by 5 mm thick) calcium fluoride (CaF_2) crystals doped with manganese (Mn). When a TLD is heated, it emits an amount of light that is proportional to its radiation exposure. A Harshaw Atlas hot gas reader was used to heat the TLD and the emitted light was measured using a photomultiplier tube connected to a picoammeter that integrated the amount of emitted light. The picoammeter reading was then converted to a radiation dose using the appropriate calibration.

A.2 Radiation and Thermal Aging

Radiation dosimetry was performed to quantify the aging radiation field to which the test samples were exposed. As shown in Figure A.3, five cobalt-60 sources were used to produce the aging radiation field for the test chamber containing the cut cable samples; the dosimetry was performed using a single TLD at each of 50 different locations. For aging, the cut samples were placed vertically (*i.e.*, parallel with the z-axis) in a long, narrow rectangular basket (see Figure A.4). The long axis of the basket was oriented perpendicular to the x-axis of the large chamber fixture. The resulting aging dose rate at the front of the basket (along the plane $x = 2$ inches) is shown in Figure A.5.

As shown in Figure A.6, five cobalt-60 sources were used to produce the aging radiation field for the test chamber containing the complete cable samples; the dosimetry was performed using a single TLD at each of 100 different locations. The resulting aging dose rate is shown in Figures A.7 and A.8 for the outside and inside of the cable wraps, respectively.

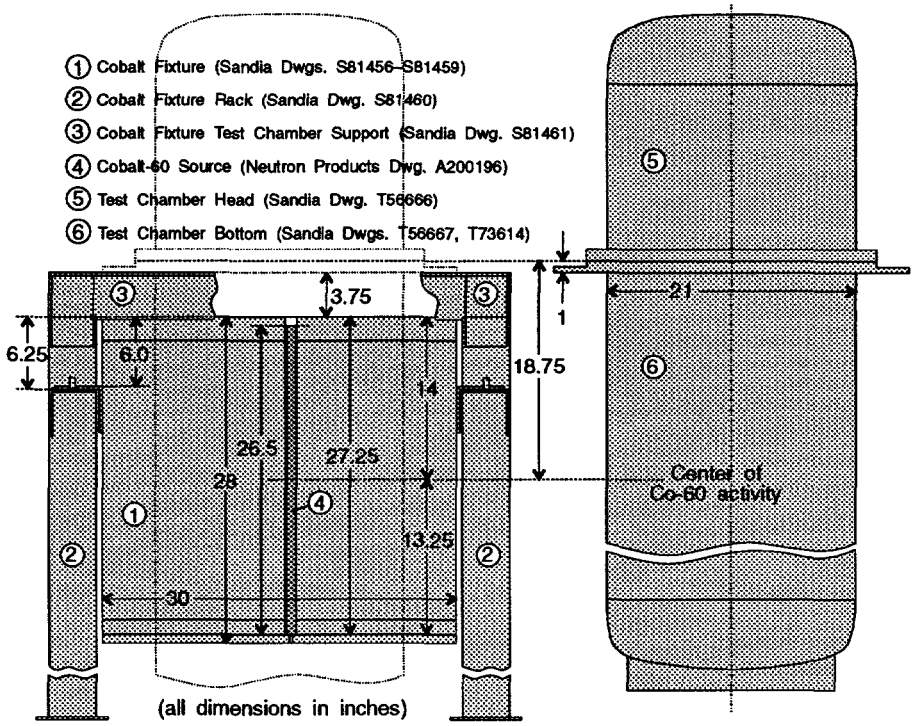

Figure A.1: Sketch of a test chamber and large chamber cobalt fixture.

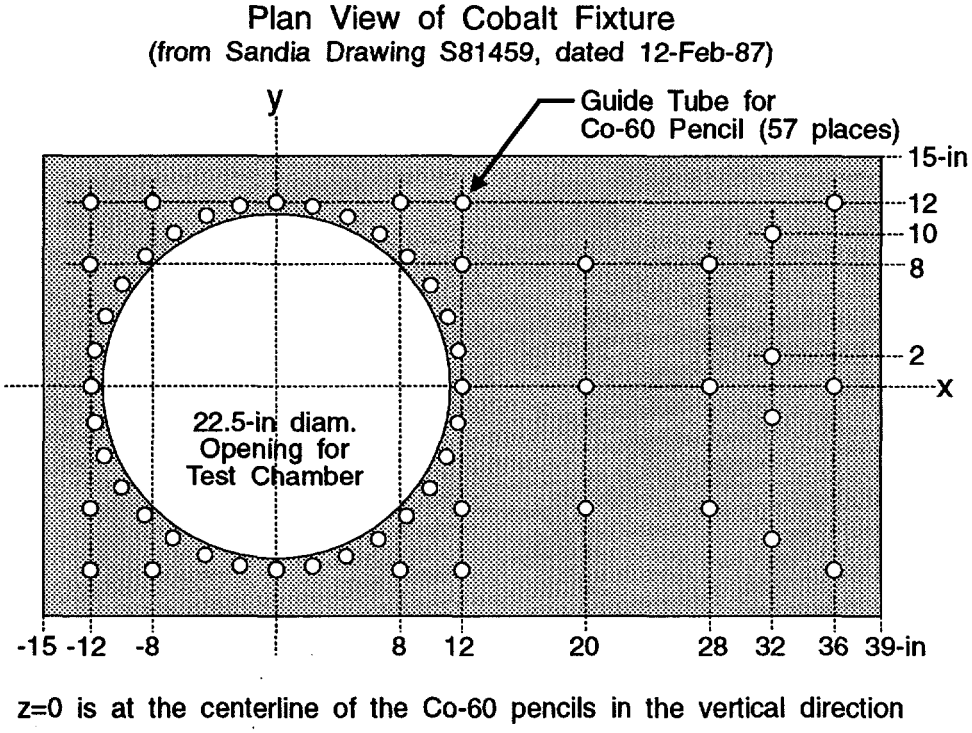

Figure A.2: Plan view of large chamber cobalt fixture showing the fixture coordinate system and possible cobalt source locations.

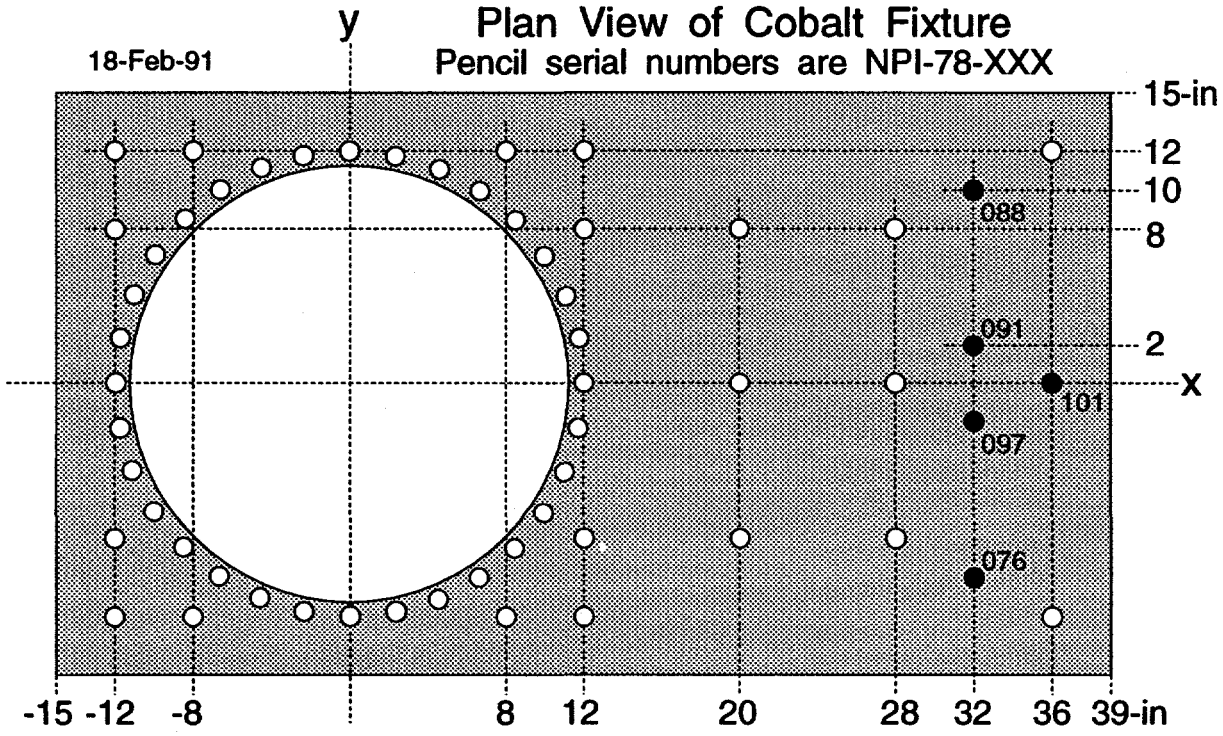

Figure A.3: Cobalt-60 source configuration for aging irradiation of cut cable specimens (black circles are guide tubes filled with a cobalt-60 source and white circles are empty guide tubes).

A.3 Accident Radiation Exposure

Radiation dosimetry was performed to quantify the accident radiation field to which the test samples were exposed. Only one test chamber was used for the accident irradiation instead of the two chambers used for aging. A round basket holding the cut cable specimens (see Figure A.4) was installed into the test chamber with the complete cable specimens, and all the specimens were irradiated at the same time. The round basket of cut specimens was mounted inside the mandrel on which the complete cable specimens were wrapped. As shown in Figure A.9, nine cobalt-60 sources were used to produce the accident radiation field; the dosimetry was performed using a single TLD at each of 49 different locations. The resulting accident dose rate is shown in Figures A.10 and A.11. Figure A.10 shows the dose rate plotted for a 6.5-in. radius from a linear, least-squares polynomial regression fit to the data from all 49 dosimeters. The dose rate plotted in Figure A.11 is from a spline fit based only on data from the 15 dosimeters actually located on the 6.5-in. radius. The spline fit passes through the dosimeter data; this differs from the regression fit, which generally does not pass through the data but only minimizes the error between the data and the fit.

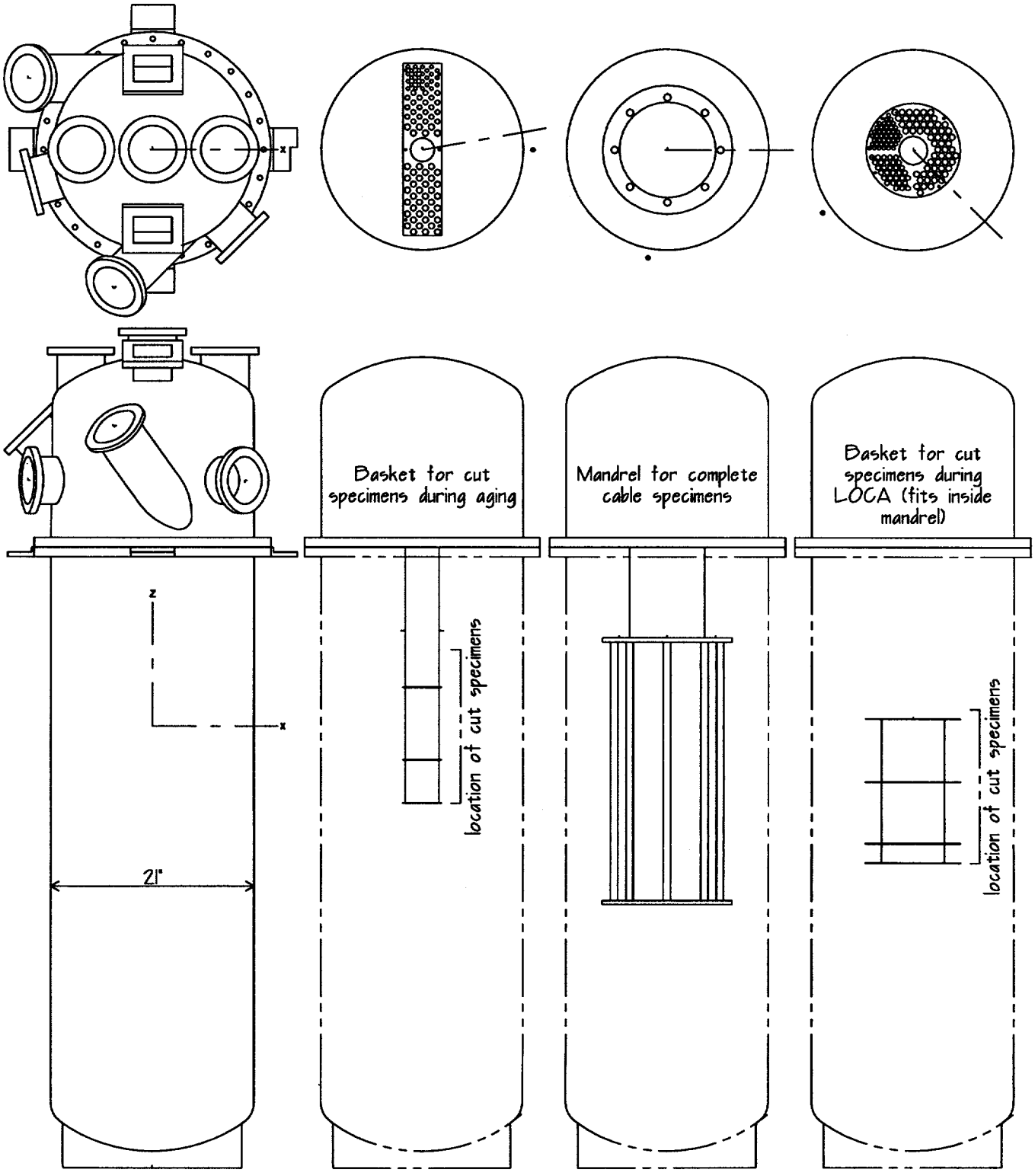

Figure A.4: Detail of the test chamber and sketches of the two baskets used to hold cut specimens and the mandrel on which the complete specimens were mounted—drawn to scale.

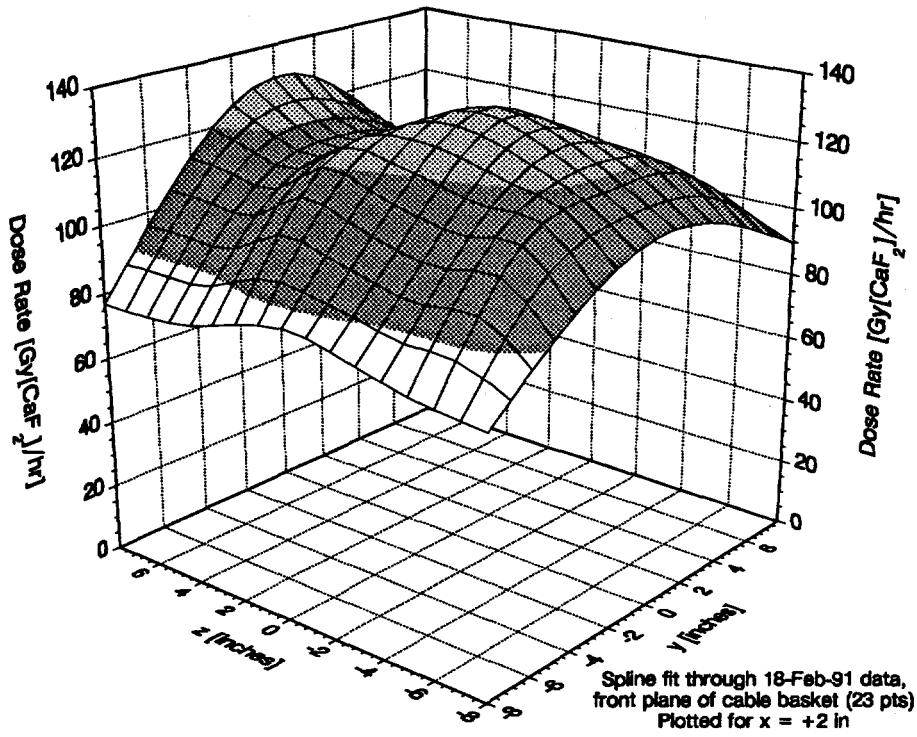

Figure A.5: Aging radiation dose rate for cut cable specimens—front plane of the cable basket.

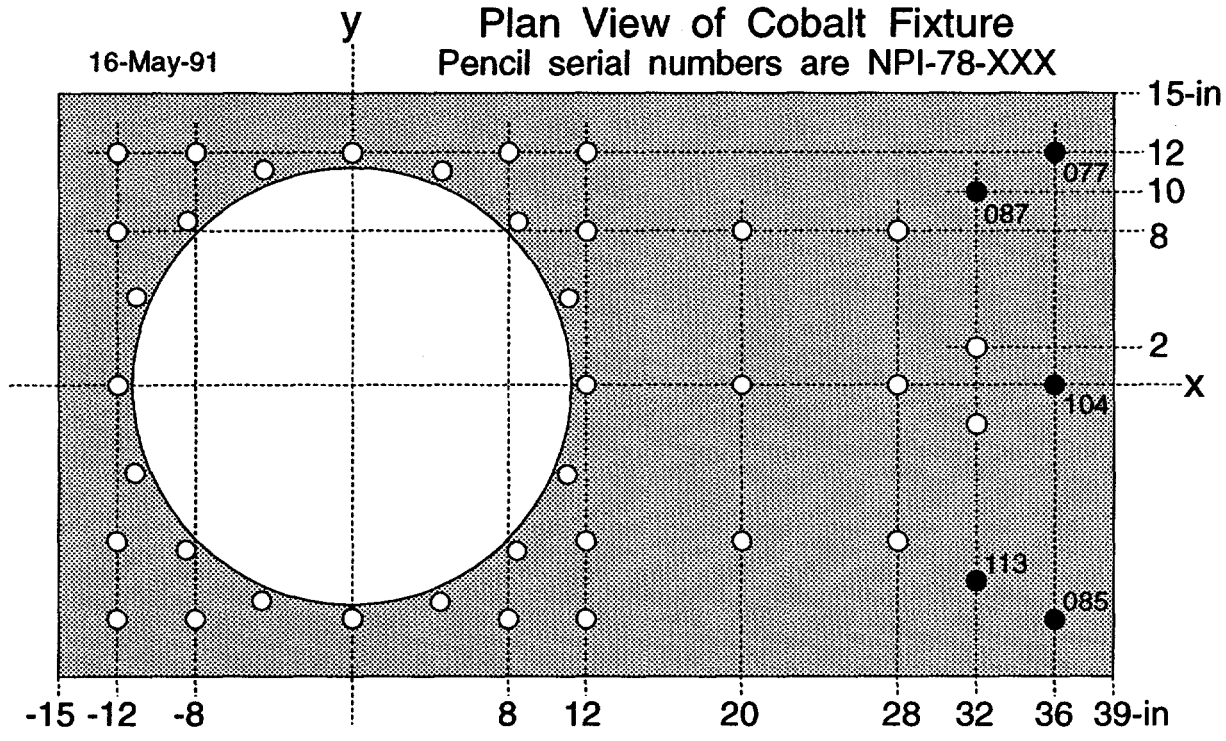

Figure A.6: Cobalt-60 source configuration for aging irradiation of complete cable specimens (black circles are guide tubes filled with a cobalt-60 source and white circles are empty guide tubes).

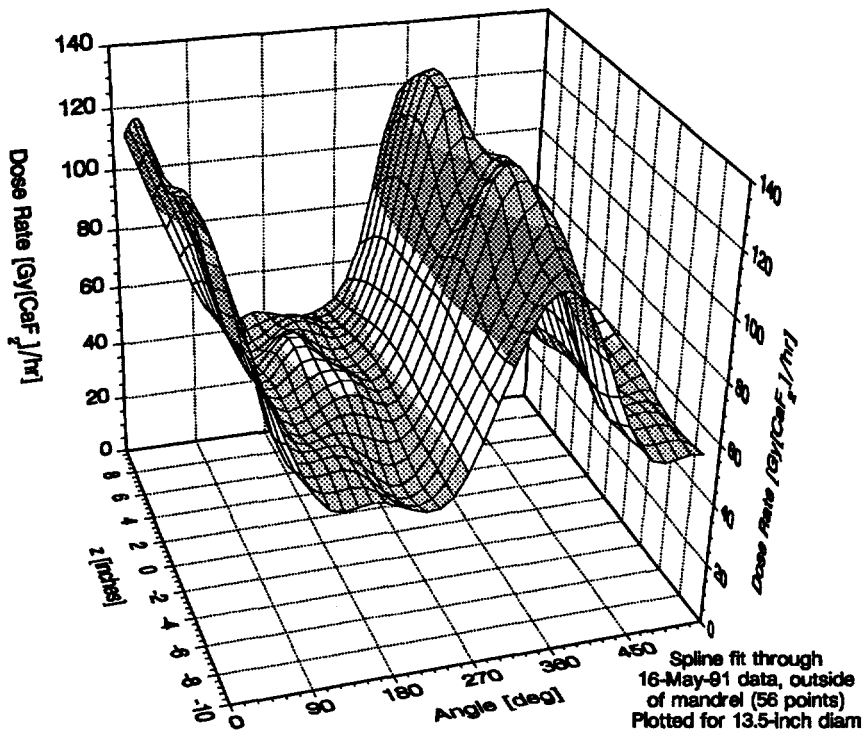

Figure A.7: Aging radiation dose rate for complete cable specimens—outside of cable wraps (0° corresponds to $x = 6.75$ inches, $y = 0$ inches).

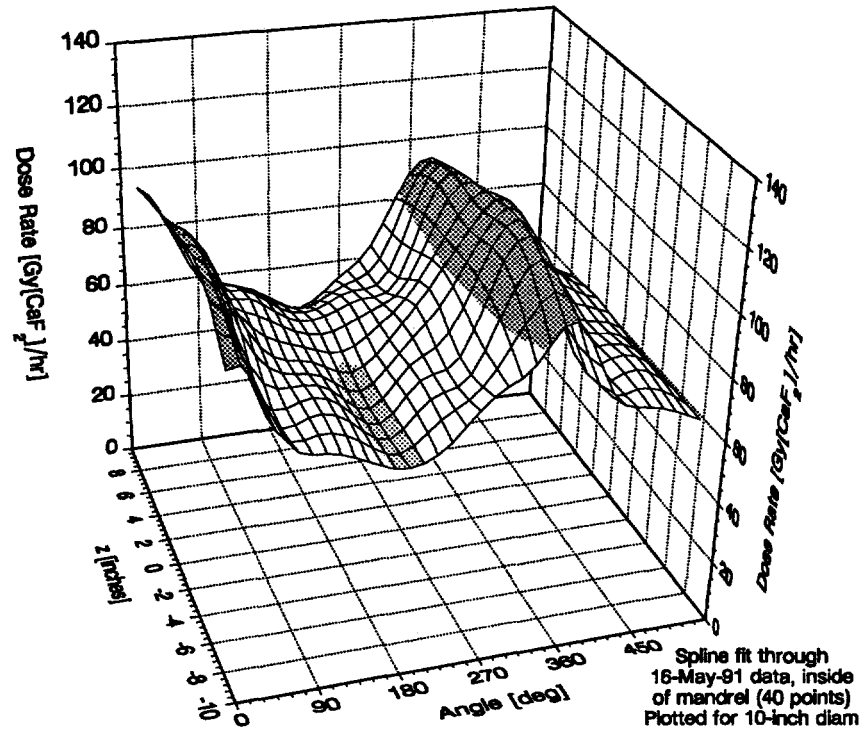

Figure A.8: Aging radiation dose rate for complete cable specimens—inside of cable wraps (0° corresponds to $x = 5$ inches, $y = 0$ inches).

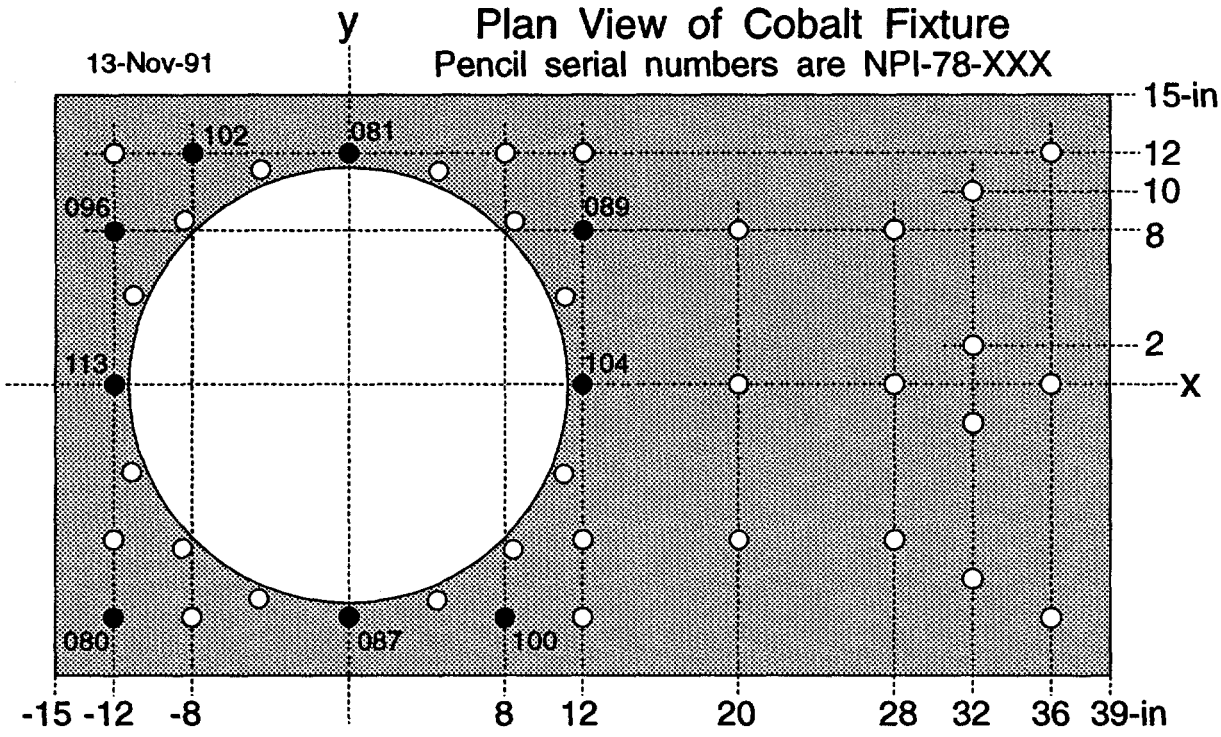

Figure A.9: Cobalt-60 source configuration for accident irradiation (black circles are guide tubes filled with a cobalt-60 source and white circles are empty guide tubes).

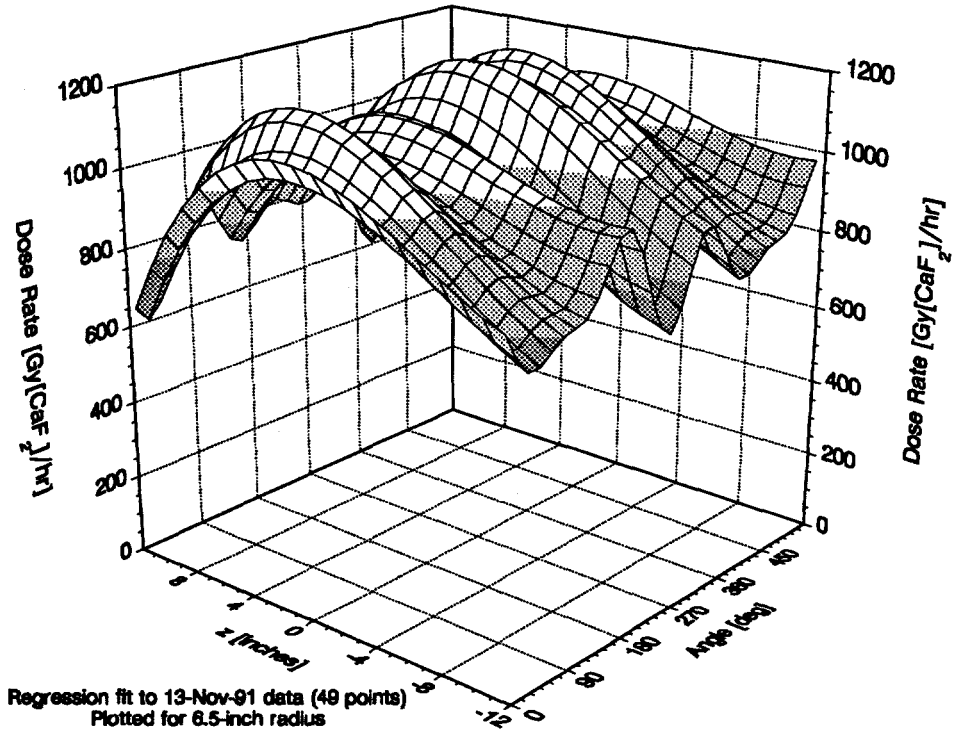

Figure A.10: Accident radiation dose rate—regression fit to data (0° corresponds to $x = 6.5$ inches, $y = 0$ inches).

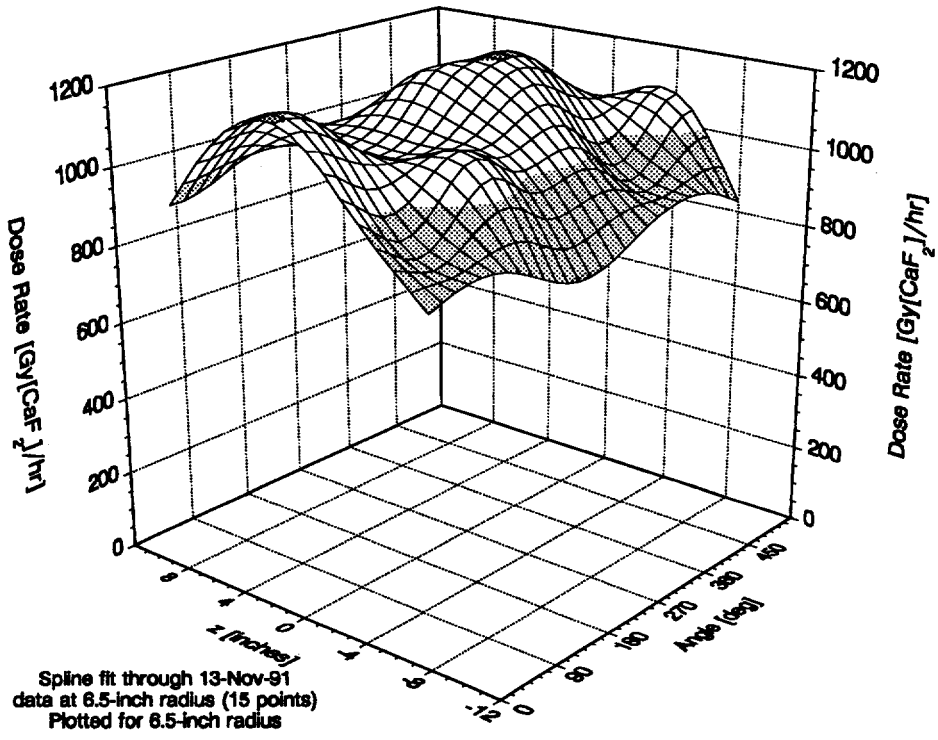

Figure A.11: Accident radiation dose rate—spline fit through data (0° corresponds to $x = 6.5$ inches, $y = 0$ inches).

B Interpretation of Electrical Measurements

Because of the long leads necessary to connect the test chamber to electrical equipment during the radiation portions of the testing, all electrical measurements are influenced by the long leads used. In this section, a conductor is analyzed to develop an understanding of the effect of lead length on electrical measurements.

B.1 Conductor Model

The key difference between circuit theory and transmission line theory is the size of the electrical system. Circuit analysis assumes that the physical dimensions of a network are much smaller than the electrical wavelength, while transmission lines may be a considerable fraction of a wavelength, or many wavelengths, in size. The elements in an ordinary electric circuit can be considered discrete and as such may be described by lumped parameters. It is assumed that currents flowing in lumped-circuit elements do not vary spatially over the elements. A transmission line, on the other hand, is a distributed-parameter network and must be described by circuit parameters that are distributed throughout its length. Thus voltages and currents can vary in magnitude and phase over the length of a transmission line.

The short length Δz of a two-conductor transmission line can be modeled as a lumped-element circuit[1], as shown in Figure B.1, where R, L, G, and C are per unit length quantities defined as follows:

- R = series resistance per unit length, for both conductors, in Ω/m
- L = series inductance per unit length, for both conductors, in H/m
- G = shunt conductance per unit length, in S/m
- C = shunt capacitance per unit length, in F/m

The series inductance L represents the total self-inductance of the two conductors, while the shunt capacitance C is due to the close proximity of the two conductors. The series resistance R represents the resistance due to the finite conductivity of the conductors, while the shunt conductance G is due to dielectric loss in the material between the conductors.

[1] This development follows that found in Ref. [24, Section 3.1].

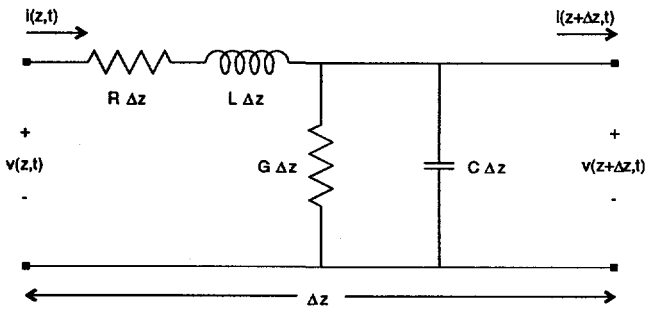

Figure B.1: Lumped-element circuit model for an incremental length of transmission line.

R and G, therefore, represent loss. A finite length of transmission line can be viewed as a cascade of sections of the form of Figure B.1. The top conductor in Figure B.1 represents the actual conductor under test and the bottom conductor represents the ground plane formed by the test chamber, mandrel, and all the other conductors which were grounded.

From the circuit of Figure B.1, Kirchhoff's voltage law can be applied to give

$$v(z,t) - R\Delta z i(z,t) - L\Delta z \frac{\partial i(z,t)}{\partial t} - v(z+\Delta z,t) = 0,$$

while Kirchhoff's current law leads to

$$i(z,t) - G\Delta z v(z+\Delta z,t) - C\Delta z \frac{\partial v(z+\Delta z,t)}{\partial t} - i(z+\Delta z,t) = 0.$$

Dividing these two equations by Δz and taking the limit as $\Delta z \to 0$ gives the following differential equations:

$$\frac{\partial v(z,t)}{\partial z} = -Ri(z,t) - L\frac{\partial i(z,t)}{\partial t},$$
$$\frac{\partial i(z,t)}{\partial z} = -Gv(z,t) - C\frac{\partial v(z,t)}{\partial t}.$$

These equations are the time-domain form of the *transmission line*, or *telegrapher's*, equations.

B.2 Insulation Resistance

Insulation resistance (IR) measures the current leaking from the conductor through the insulation to a ground

outside the insulation when a dc voltage is applied. For dc conditions, there is no time dependence and the transmission line equations simplify to:

$$\begin{aligned} \frac{dv(z)}{dz} &= -Ri(z), \\ \frac{di(z)}{dz} &= -Gv(z). \end{aligned}$$

If we assume that the conductor is perfect (*i.e.*, $R = 0$), then these equations can be solved to give:

$$\begin{aligned} v(z) &= V_0, \\ i(z) &= I_0 - V_0 \int_0^z G dz. \end{aligned}$$

Note that the voltage is constant along the entire conductor.

For dc conditions, the only mechanism by which the current can change as we move down the conductor is due to leakage to ground through the insulation. Thus we will define the dc *leakage current* as the amount of current lost along the conductor. If G is constant along the conductor, then $i(z) = I_0 - GV_0 z$ and a conductor of length l has a leakage current of $I_{\text{leak}} = i(0) - i(l) = GV_0 l$. The IR is the applied voltage divided by the leakage current, namely $\text{IR} = 1/Gl$.

Thus, for an ideal conductor, the IR depends only on the conductive component of dielectric impedance and the conductor length; for a given conductor, the measured IR decreases (and the leakage current increases) as the conductor length is increased. Thus, an IR of 500 kΩ for a 3 m long conductor is equivalent to an IR of 1.5 MΩ for a 1 m long conductor or 15 kΩ for a 100 m long conductor. Comparisons between IR values from different literature references are meaningful only after accounting for the cable length on which the measurement was performed.

The U.S. testing utilized a total cable length of 23 m consisting of 10 m of cable lead, then 3 m wrapped around the mandrel inside the test chamber, then another 10 m of cable lead. The conductivity of the cable outside the test chamber is expected to remain constant while the conductivity of the cable inside the test chamber will be changed by the radiation, thermal, and steam exposures. Thus it will be useful to look at how changes in the conductivity of the cable inside the test chamber impact the measured IR for the entire cable.

Let the shunt conductance to ground per meter be G_0 for the entire cable at the start of the test. Assume that this remains constant during the entire test for the two sections of cable lead, but that the conductance per unit length for the cable section in the test chamber is changed to a different constant, G_0/r, by the environmental exposures.[2] For the 3 m long section of cable in the test chamber,

$$\text{IR}_{3\text{m}} = \frac{1}{Gl} = \frac{r}{3G_0}. \tag{B.1}$$

At the start of the test, there is no difference between the cable inside and outside the test chamber (*i.e.*, $r = 1$), thus the ratio of the IR to the initial IR for the 3-m long section of cable in the test chamber is

$$\left(\frac{\text{IR}}{\text{IR}_0}\right)_{3\text{m}} = r. \tag{B.2}$$

Ideally, we desire to measure only the changes in cable properties for the 3-m long section of cable in the test chamber; however, the IR for the entire 23-m long conductor is what is actually measured. The leakage current for the entire 23-m long conductor is

$$\begin{aligned} I_{\text{leak}} &= i(0) - i(23) \\ &= I_0 - \left(I_0 - V_0 \int_0^{23} G dz\right) \\ &= V_0 \left[\int_0^{10} G_0 dz + \int_{10}^{13} (G_0/r) dz + \int_{13}^{23} G_0 dz\right] \\ &= V_0 G_0 (20 + 3/r) = V_0 G_0 (20r + 3)/r, \end{aligned}$$

and the measured IR is

$$\text{IR}_{\text{meas}} = \frac{V_0}{I_{\text{leak}}} = \frac{r}{G_0(20r + 3)}. \tag{B.3}$$

The initial measured IR is $\text{IR}_0 = 1/23G_0$ (for $r = 1$) and the ratio of the measured IR to the initial IR is

$$\left(\frac{\text{IR}}{\text{IR}_0}\right)_{\text{meas}} = \frac{23r}{20r + 3}. \tag{B.4}$$

The ratio of the measured IR to the IR for the 3 m of cable in the test chamber is

$$\frac{\text{IR}_{\text{meas}}}{\text{IR}_{3m}} = \frac{3}{20r + 3} = \frac{23 - 20(\text{IR}/\text{IR}_0)_{\text{meas}}}{23}. \tag{B.5}$$

This equation is plotted in Figure B.2, which shows that the measured IR quickly approaches the IR for the

[2] Expect $0 < r \leq 1$ because the leakage current typically increases (*i.e.*, conductance increases) for a cable as it degrades.

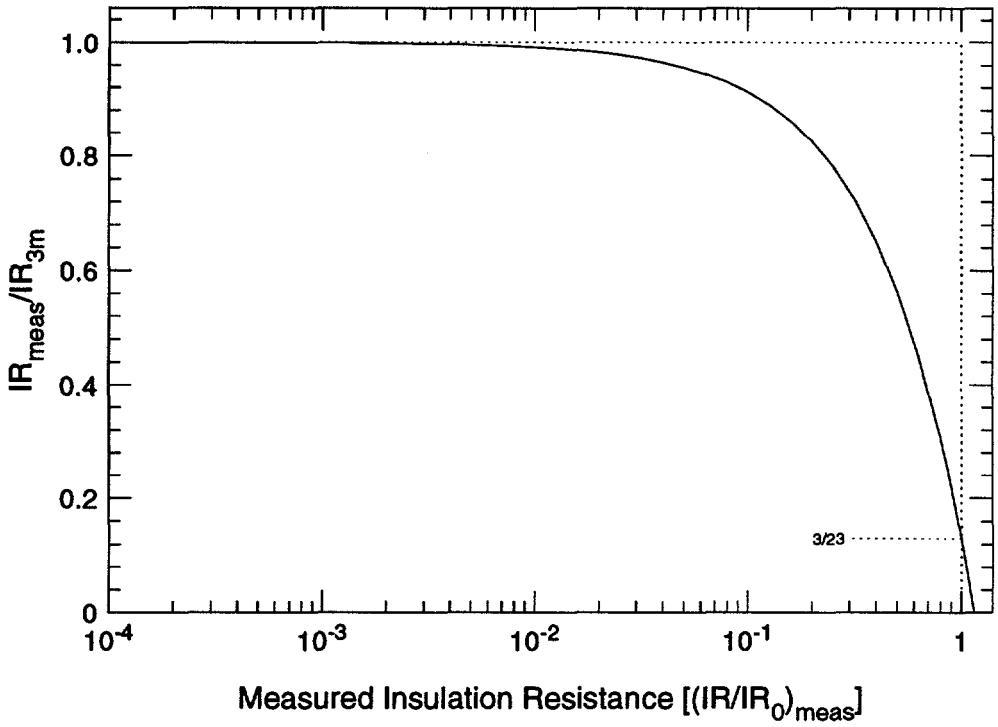

Figure B.2: Ratio of the measured IR to the test chamber IR as a function of the measured IR.

3 m of cable in the test chamber as the measured IR decreases from its initial value. At the start of the test [*i.e.*, $r = (IR/IR_0)_{meas} = 1$], the ratio of measured IR to test chamber IR is 3/23, which is simply due to the difference in cable length; 3 m in the test chamber and 23 m for the measurement. However, as the measured IR decreases due to degradation of the cable in the test chamber, the amount of current leakage for the entire cable becomes dominated by the leakage from the 3 m of cable in the test chamber and the measured IR approaches the test chamber IR. Thus, the effect of the leads becomes less and less important as the cable in the test chamber degrades. The difference between the measured IR and the test chamber IR is less than 10% when the measured IR has decreased by one order of magnitude from its initial value.

Because the measured IR quickly approaches the test chamber IR as the measured IR decreases from its initial value, if an IR of 500 kΩ in Figures 3.21–3.32 is at least an order of magnitude less than the initial IR value, then it should be referred to as an IR of 500 kΩ-3 m.

The initial conductor-to-ground IR values of these cables are so high that some loss in sensitivity due to the long cable leads has no meaningful effect on the results. For instance, a typical initial IR measurement of 10^{11} Ω is not an IR of 10^{11} Ω-3 m for the 3-m section of cable in the test chamber, but is actually an IR of 10^{11} Ω-23 m ($= 7.67 \times 10^{11}$ Ω-3 m) for the entire 23-m long cable. Such initial IR values are all so high that a difference of 7.67 makes no practical difference. Only when the measured IR has decreased significantly does it become meaningful to know the actual IR value; it is precisely under these conditions that the measured IR value is equivalent to the IR of the 3 m of cable wrapped around the mandrel in the test chamber.

C French Dosimetry

C.1 General

Independent dosimetry measurements were performed for the Evocable, Kronos, and Caline devices. These measurements were carried out in collaboration with the Laboratoire de Mesure des Rayonnements (LMRI), which is accredited by the National Metrology Office. Whenever necessary, LMRI used passive dosimeters consisting of L-Alanine powder for compacted analysis, placed in small 11.5 mm (0.45 in.) diameter cylinders measuring 17 mm (0.69 in.) in height. The dose values absorbed in water at the center of the dosimeters were measured from the electronic paramagnetic resonance signal on the detecting element. The system was calibrated in one of LMRI's cobalt-60 reference beams.

C.2 Dosimetry in Evocable

The Evocable system was equipped with a calibrated ionization chamber and L-Alanine chemical dosimeters. Sixteen dosimeters were placed on 4 disks of a model installed in Evocable (see Figure C.1). The disks were identified by the letters A, B, C, and D. Five dosimeters were placed on disks A and D, and three on disks B and C. It was possible to move the ionization chamber from position E to position F of the model. The dosimetry results from the L-Alanine dosimeters and the ionization chambers are compared in Table C.1.

Dosimetry established the correct correlation between the measured dose values on the ionization chambers and the L-Alanine chemical dosimeters. It also demonstrated uniformity of the dose rate over the length of the Evocable tube.

The ionization chamber remained in the Evocable tube at all times during the irradiation of the cables to determine the dose rate integrated during the operation of the reactor for each cycle and the total dose received by the materials. Figure C.2 shows the ionization chamber measurements and the total dose accumulated by the equipment.

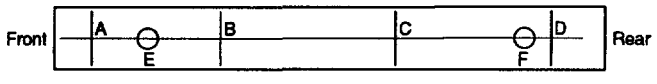

Figure C.1: Sketch of the model used for dosimetry inside the Evocable tube.

C.3 Dosimetry in Kronos

The Kronos installation was symmetrical to a central plane. The activity and position of the sources around housings 1, 2, and 3 on the one side, and 4, 5, and 6 on the other side, were identical. Initial dosimetry was performed in housings 1, 2, and 3 where dose rates of 20, 10, and 5 Gy/hr (2, 1, and 0.5 krad/hr) were desired. The 20 Gy/hr testing lasted for 2.5 years. After completion of the 20 Gy/hr testing, the cobalt-60 sources were replaced and additional dosimetry was performed in the 10 and 5 Gy/hr housings. To perform the dosimetry, five L-Alanine dosimeters were installed in the central plane of the housings in the 4 corners and at the center of the rectangle occupied by the equipment.

The results of the 2 dosimetry measurements are given in Table C.2. They indicate good consistency of the dose rates in the various housings, as well as satisfactory staging of dose values with respect to nominal values. After the sources were replaced, the average dose rate of housing 3 was slightly too high (6.5 Gy/hr instead of the desired 5 Gy/hr). To compensate for this, the equipment was placed at the bottom of the housing where the dose rate was lower. The effect of cobalt-60 decay was taken into consideration when calculating the exposure times needed to achieve desired doses.

C.4 Dosimetry in Caline

Two parallel source planes were arranged either side of the 8 cubic meter housing. On each source plane, 9 source support frames were positioned in 3 columns, each having 3 different positions. The frames were spaced by inserts to irradiate over the entire height of the housing.

Table C.1: Dosimetry inside Evocable.

L-Analine Detector Location	Dose Rate [Gy/hr]			
	Disk A	Disk B	Disk C	Disk D
top east	0.786	—	0.843	0.700
bottom east	0.950	1.107	—	0.750
bottom west	0.964	—	0.936	0.764
top west	0.793	0.957	—	0.721
middle	0.879	1.050	0.886	0.736
Detector Average	0.876	1.041	0.888	0.735
Ionization Chamber Location	in E		in F	
Chamber Dose Rate	1.130 Gy/hr		0.825 Gy/hr	

Table C.2: Dosimetry inside Kronos.

Date of Dosimetry	L-Analine Detector Location	Dose Rate [Gy/hr]		
October 1988	top north	17.1	11.5	5.7
	bottom north	15.6	10.6	5.1
	middle	18.1	9.6	4.6
	top south	17.6	10.0	5.8
	bottom south	16.2	9.4	5.3
	Average	16.9	10.2	5.3
April 1991	top north	—	11.0	8.1
	bottom north	—	7.2	5.0
	middle	—	10.2	6.2
	top south	—	11.3	7.7
	bottom south	—	7.5	5.3
	Average	—	9.4	6.5

Dosimetry in Caline was performed yearly when the sources were relocated and when new sources were added. For instance, a new distribution of the sources was made in October 1990, subsequently 136 cobalt-60 sources having an active length of 42 cm (16.5 in) and overall activity of 226,000 Ci were positioned around the housing.

Isodose contours inside the housing were plotted on the basis of the response of 37 L-Alanine dosimeters and 10 ionization chambers irradiated for 24 hr. The isodoses in the various planes were then plotted in order to arrange the equipment most effectively in the available volume. Figure C.3 shows the isodose contours for the central longitudinal plane of Caline after dosimetry during October 1990. The average dose rate at the center of the housing equalled 891 ± 45 Gy/hr (89.1 ± 4.5 krad/hr).

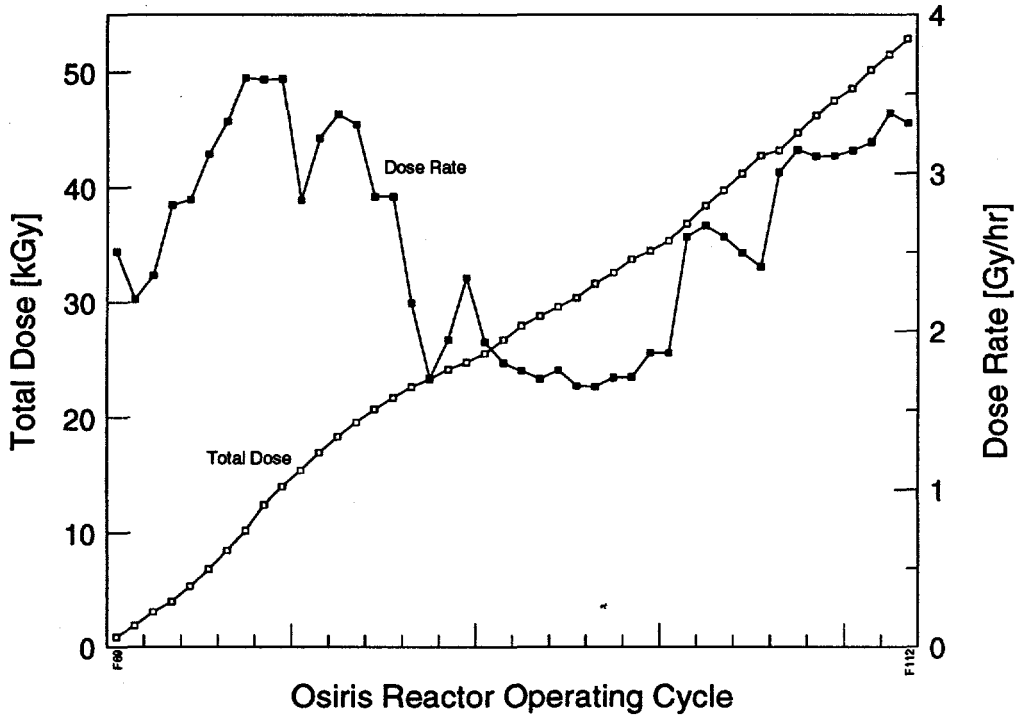

Figure C.2: Dose rate and total dose during irradiation of the Evocable tube.

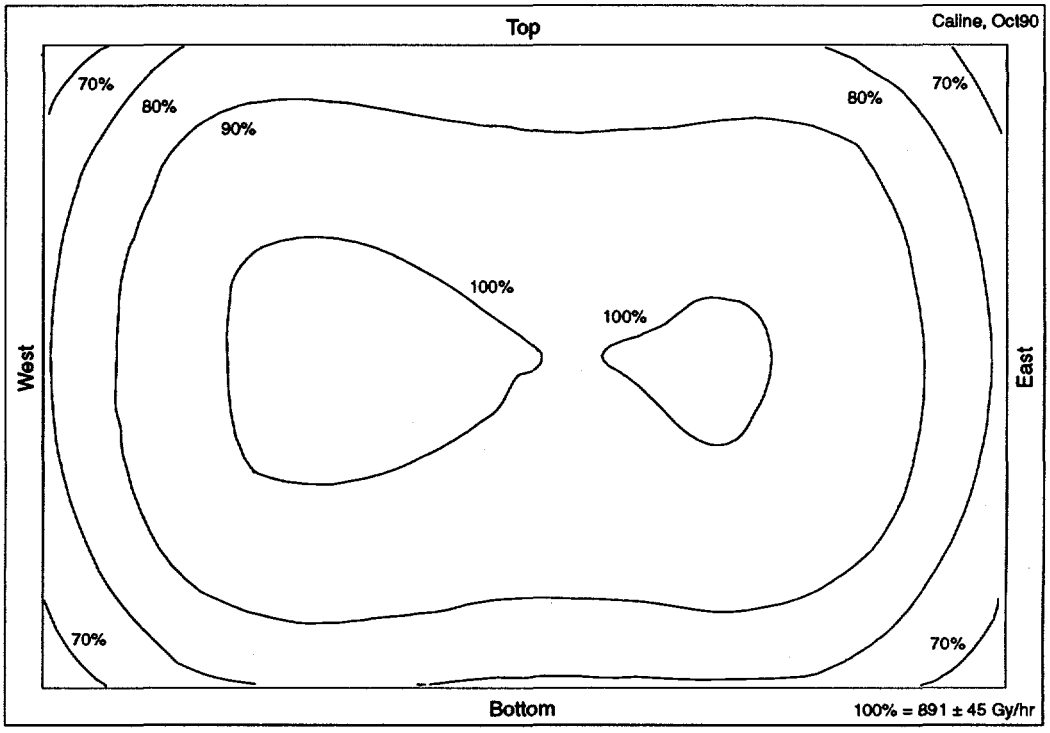

Figure C.3: Caline dosimetry—Isodose contours for the median vertical longitudinal plane (in % of dose measured in the middle of the facility).

NRC FORM 335 (2-89) NRCM 1102, 3201, 3202

U.S. NUCLEAR REGULATORY COMMISSION

BIBLIOGRAPHIC DATA SHEET

(See instructions on the reverse)

1. REPORT NUMBER (Assigned by NRC, Add Vol., Supp., Rev., and Addendum Numbers, if any.)
NUREG/CR-6202
IPSN 94-03
SAND94-0485

2. TITLE AND SUBTITLE
Long-Term Aging and Loss-of-Coolant Accident (LOCA) Testing of Electrical Cables - U.S./French Cooperative Research Program

3. DATE REPORT PUBLISHED
MONTH: October
YEAR: 1996

4. FIN OR GRANT NUMBER
A1841

5. AUTHOR(S)
C. F. Nelson (SNL), G. Gauthier (IPSN-DES-SAMS), F. Carlin, M. Attal, G. Gaussens, P. LeTutour (CEA/ORIS/CIS bio international), C. Morin (CEA/DRE/SRO)

6. TYPE OF REPORT
Technical

7. PERIOD COVERED *(Inclusive Dates)*

8. PERFORMING ORGANIZATION – NAME AND ADDRESS *(If NRC, provide Division, Office or Region, U.S. Nuclear Regulatory Commission, and mailing address; if contractor, provide name and mailing address.)*
Sandia National Laboratories
Albuquerque, NM 87185-0742

Department of Safety Evaluation
Institute of Nuclear Safety and Protection (IPSN)
Commissariat à l'Energie Atomique
Fontenay aux Roses, FRANCE

9. SPONSORING ORGANIZATION – NAME AND ADDRESS *(If NRC, type "Same as above"; if contractor, provide NRC Division, Office or Region, U.S. Nuclear Regulatory Commission, and mailing address.)*
Division of Engineering Technology
Office of Nuclear Regulatory Research
U.S. Nuclear Regulatory Commission
Washington, DC 20555 - 0001

10. SUPPLEMENTARY NOTES
S. Aggarwal, NRC Program Manager

11. ABSTRACT *(200 words or less)*
Experiments were performed to assess the aging degradation and loss-of-coolant accident (LOCA) behavior of electrical cables subjected to long-term aging exposures. Four different cable types were tested in both the U.S. and France.

1. U.S. 2 conductor with ethylene propylene rubber (EPR) insulation and a Hypalon jacket.
2. U.S. 3 conductor with cross-linked polyethylene (XLPE) insulation and a Hypalon jacket.
3. French 3 conductor with EPR insulation and Hypalon jacket.
4. French coaxial with polyethylene (PE) insulation and a PE jacket.

The data represent up to 5 years of simultaneous aging where the cables were exposed to identical aging radiation doses at either 40°C or 70°C; however, the dose rate used for the aging irradiation was varied over a wide range (2-100 Gy/hr). Aging was followed by exposure to simulated French LOCA conditions. Several mechanical, electrical, and physical-chemical condition monitoring techniques were used to investigate the degradation behavior of the cables. All the cables, except for the French PE cable, performed acceptably during the aging and LOCA simulations. In general, cable degradation was highest for the lowest dose rate, and the amount of degradation decreased as the dose rate was increased.

12. KEY WORDS/DESCRIPTORS *(List words or phrases that will assist researchers in locating the report.)*
radiation aging, thermal aging, condition monitoring, loss-of-coolant accident (LOCA), cables, cable properties

13. AVAILABILITY STATEMENT
Unlimited

14. SECURITY CLASSIFICATION
(This Page)
Unclassified
(This Report)
Unclassified

15. NUMBER OF PAGES

16. PRICE